IL-15-based trifunctional antibody-fusion proteins with costimulatory TNF-superfamily ligands for cancer immunotherapy

Von der Fakultät Energie-, Verfahrens- und Biotechnik
der Universität Stuttgart zur Erlangung der Würde eines Doktors der Naturwissenschaften (Dr. rer. nat.) genehmigte Abhandlung

Vorgelegt von

Nadine Beha

aus Villingen-Schwenningen

Hauptberichter: Prof. Dr. Roland E. Kontermann

Mitberichter: Prof. Dr. Thomas Kufer

Tag der mündlichen Prüfung: 14.12.2018

Institut für Zellbiologie und Immunologie

Universität Stuttgart

2018

Für Sascha

Table of content

Abbreviations 1

Abstract 5

Zusammenfassung 6

1 Introduction 8

1.1 Cancer immunotherapy 8

1.2 Common cytokine receptor γ-chain family 11

1.2.1 IL-15 in cancer immunotherapy 14

1.2.2 IL-15 in therapeutic approaches 15

1.3 TNF superfamily-mediated costimulation of T cells 16

1.3.1 4-1BB and 4-1BBL 19

1.3.2 OX40 and OX40L 20

1.3.3 GITR and GITRL 21

1.3.4 Therapeutic strategies involving the TNFSF 22

1.4 Targets for cancer therapy 24

1.4.1 Fibroblast activating protein 24

1.4.2 Epithelial growth factor receptor 25

1.5 Purpose of this study 27

2 Material 29

2.1 General supplies 29

2.2 Antibodies 29

2.3 Bacteria 30

2.4 Buffers and Solutions 31

2.5 Cell lines 33

2.6 Primary human cells 33

2.7 Enzymes 33

2.8 Instruments 33
2.9 Kits and Markers 34
2.10 Mice 35
2.11 Plasmids 35
2.12 Primers for cloning 36
2.13 Recombinant proteins 37
2.14 Reagents and Media for bacterial culture 37
2.15 Reagent and Media for mammalian cell culture 37
2.16 Software 38
2.17 Special implement 39
3 Methods 40
3.1 Cloning strategy of murine homologs of tri-functional fusion proteins 40
3.2 Cloning strategy of fusion proteins targeting EGFR 40
3.3 PCR 41
3.4 Gel electrophoresis 41
3.5 Restriction digestion 41
3.6 Ligation 42
3.7 Transformation 42
3.8 Isolation of plasmid DNA 42
3.9 Sequence analysis 43
3.10 Photometric determination of DNA concentration 43
3.11 Mammalian cell culture 43
3.11.1 General cultivation methods 43
3.11.2 PBMCs 43
3.11.3 Isolation of regulatory T cells 44
3.12 Expression and purification of recombinant proteins 44

3.12.1 Transfection of HEK293-6E 44
3.12.2 Immobilized metal ion affinity chromatography (IMAC) 45
3.13 Biochemical characterization 45
3.13.1 SDS polyacrylamide gel electrophoresis 45
3.13.2 Size exclusion chromatography 46
3.13.3 Thermal stability 46
3.14 Functional characterization 46
3.14.1 ELISA 46
3.14.2 Flow cytometry 47
3.15 Protein stability 53
3.15.1 *In vitro* serum stability 53
3.16 Animal studies 53
3.16.1 B16-FAP lung tumor model 53
3.16.2 B16-FAP solid tumor model 53
3.17 Statistics 54
4 Results 56
4.1 Bifunctional tumor-targeted antibody-fusion proteins 56
4.1.1 Biochemical properties 56
4.1.2 Binding properties 58
4.1.3 Costimulatory activity 59
4.2 Trifunctional tumor-targeted antibody-fusion proteins with IL-15 and 4-1BBL 60
4.2.1 Biochemical characterization 61
4.2.2 Binding properties 63
4.2.3 Activity of trifunctional antibody-fusion proteins 63
4.2.4 Antitumor activity in a syngeneic mouse model 65
4.3 Antibody-fusion proteins incorporating scGITRL and scOX40L 69

4.3.1 Biochemical properties 69
4.3.2 Binding properties 71
4.3.3 Plasma stability 73
4.3.4 Activity of untargeted trifunctional fusion proteins 73
4.3.5 Activity of targeted fusion proteins 74
4.3.6 Activity of targeted bi- and trifunctional fusion proteins on T cells subpopulations 75
4.3.7 Trifunctional versus combination of bifunctional fusion proteins 78
4.3.8 Antitumor activity of RD_IL-15_scFv$_{FAP}$_mscGITRL in syngeneic mouse models 82
4.4 EGFR-directed trifunctional antibody-fusion proteins for the enhancement of ADCC 89
4.4.1 Biochemical properties 90
4.4.2 Binding properties 91
4.4.3 IL-15 activity 92
4.4.4 Targeting-mediated activity on T cells 93
4.4.5 Targeting-mediated activity on NK cells 94
4.4.6 Influence of fusion proteins directed against EGFR on antibody-mediated cellular cytotoxicity (ADCC) 95
5 Discussion 97
5.1 Improving antibody-fusion proteins by introducing the TNFSFL in the single-chain format 97
5.2 Combination of IL-15 and TNF superfamily members 4-1BBL, OX40L and GITRL in trifunctional fusion proteins 100
5.3 Bi- and trifunctional fusion proteins with IL-15 and sc4-1BBL enhance ADCC 105
5.4 Conclusion and outlook 107
6 Publication bibliography 109
7 Sequences 133

7.1 $scFv_{FAP}$_scTNFSFL 133
7.2 RD_IL-15_$scFv_{FAP}$_scTNFSFL 134
7.3 sc4-1BBL 137
7.4 scOX40L 139
7.5 scGITRL 141
7.6 msc4-1BBL 143
7.7 mscGITRL 146
7.8 $scFv_{CEA}$ 147
7.9 $scFv_{EGFR}$ 149
List of Figures 151
List of Tables 153
Declaration 154
Erklärung 154
Danksagung 155
Conference contributions and publications 156

Abbreviations

aa	amino acid
Ab	antibody
ADCC	antibody-dependent-cellular cytotoxicity
Amp	ampicillin
APC	antigen presenting cell
APC	Allophycocyanin
BiTE	bispecific T cell engager
BLAST	basic local alignment search tool
BSA	bovine serum albumin
CAR	chimeric antigen receptor
CD	cluster of differentiation
CFSE	carboxyfluorescein succinimidyl ester
CTL	cytotoxic T lymphocyte
CTLA-4	cytotoxic T lymphocyte-associated protein
Db	diabody
DC	dendritic cell
dd	double distilled
DMEM	Dulbecco's Modified Eagle Medium
DMSO	dimethyl sulfoxide
DNA	deoxyribonucleic acid
dNTP	deoxynucleotide
EC_{50}	half-maximal effective concentration
ECD	extracellular domain
EDTA	ethylenediaminetetraacetic acid
EGFR	epidermal growth factor
ELISA	enzyme-linked immunosorbent assay
EpCAM	epithelial cell adhesion molecule
FAP	fibroblast activation protein
FBS	fetal bovine serum
FC	flow cytometry

Fc	fragment crystallizable
FITC	fluorescein isothiocyanate
FoxP3	forkhead box P3
GITR	glucocorticoid-induced TNFR-related protein
GITRL	ligand of glucocorticoid-induced TNFR-related protein
HEK	human embryonic kidney
HEPES	4-(2-hydroxyethyl)-1-piperazineethanesulfonic acid
His	hexahistidyl-tag
HPLC	high-pressure liquid chromatography
HRP	horseradish peroxidase
hu	human
HVEM	herpes virus entry mediator
IFN	interferon
Ig	immunoglobulin
IL	interleukin
IMAC	immobilized metal ion affinity chromatography
LIGHT	homologous to lymphotoxins, exhibits inducible expression, and competes with HSV glycoprotein D for HVEM, a receptor expressed by T lymphocytes
m/mo	murine/mouse
mAb	monoclonal antibody
MEM	Minimum Essential Medium
MFI	median fluorescence intensity
MHC	major histocompatibility complex
MTT	3-(4,5-dimethylthiazol-2-yl)-2,5-diphenyltetrazolium bromide
NEAA	non-essential amino acids
NK	natural killer
NTA	nitrilotriacetic acid
OD	optical density
PAA	polyacrylamide
PAGE	polyacrylamide gel electrophoresis
PBA	phosphate-buffered saline containing BSA and sodium azide

PBMC	peripheral blood mononuclear cells
PBS	phosphate-buffered saline
PCR	polymerase chain reaction
PD-1	programmed cell death protein 1
PD-L1	programmed cell death 1 ligand 1
PE	phycoerythrin
PEI	polyethylenimine
Pen/Strep	Penicillin/Streptomycin
PerCP	peridinin-chlorophyll-protein
PFA	paraformaldehyde
rh	recombinant
RPMI	Rosswell Park Memorial Institute
sc	singe-chain
scDb	single-chain diabody
scFv	single-chain fragment variable
SDS	sodium dodecyl sulfate
SEC	size exclusion chromatography
TAA	tumor-associated antigen
TAE	tris-acetate-EDTA
taFv	tandem scFv
TCR	T cell receptor
TEMED	tetramethylethylenediamine
THD	TNF homology domain
TMB	3,3’-5,5’-tetramethylbenzidine
TN1	trypton N1
TNF	tumor necrosis factor
TNFSFL	tumor necrosis factor superfamily ligand
TNFSFR	tumor necrosis factor superfamily receptor
TNFSF	tumor necrosis factor superfamily
Treg	regulatory T cell
v/v	volume per volume
V_H	variable domain of the heavy chain

V_L	variable domain of the light chain
w/v	weight per volume
wt	wildtype

Abstract

IL-15 shows great potential to support an antitumor immune response and emerges as a promising agent in cancer immunotherapy. However, the systemic application of IL-15 is associated with toxicity and, as a monotherapy the efficacy of IL-15 is still limited. This study focusses on the development of novel trifunctional fusion proteins enforcing the activity of IL-15 with costimulatory ligands of the TNF superfamily and targeting the therapeutic activity to the tumor site by an antibody moiety. The homotrimeric trifunctional fusion proteins of the first generation was comprised of an antibody moiety (scFv), IL-15 fused to the extended sushi domain of the IL-15Rα chain (RD), and the extracellular domain (ECD) of 4-1BBL. Non-covalent trimerization of the ECD of 4-1BBL led to a homotrimeric fusion protein with three antibody moieties and three RD_IL-15 units. Based on the first generation trifunctional fusion protein, a novel second generation trifunctional fusion protein incorporating the ligand of the TNF superfamily in the single-chain format, i.e. genetic fusion of three extracellular domains by linkers on the same polypeptide chain, was generated, resulting in a monomeric trifunctional fusion protein with only one functional unit of each component. Similar T cell stimulation in a non-targeted setting, even improved capacity to enhance T cell stimulation when target bound and a clear antitumor effect in a mouse model *in vivo* was observed for the novel trifunctional fusion protein in the single-chain format. Furthermore, OX40L and GITRL were successfully incorporated into the novel trifunctional fusion protein in the single-chain format demonstrating stable protein configuration. Advantageous costimulatory properties in comparison to the combination of the respective bifunctional fusion proteins were observed for all trifunctional fusion proteins. Strongest synergistic effects were shown for RD_IL-15_scFv$_{FAP}$_scGITRL in terms of enhancing the cytotoxic potential of $CD8^+$ T cells and enhanced proliferation of $CD4^+$ T cells. Finally, in a syngeneic lung tumor mouse model evaluating the antitumor potential of RD_IL-15_scFv$_{FAP}$_scGITRL revealed a strong, targeting-dependent antitumor response. Additionally, the effect of an EGFR-directed trifunctional fusion protein on Trastuzumab-mediated ADCC was evaluated. Strong enhancement of the ADCC was achieved by the trifunctional fusion protein RD_IL-15_scFv$_{EGFR}$_sc4-1BBL and the bifunctional fusion protein RD_IL-15_scFv$_{EGFR}$. Thus, the trifunctional fusion protein format incorporating the ligand of the TNF superfamily in the single-chain format appears as a promising platform with versatile opportunities for further development.

Zusammenfassung

Im Bereich der Krebsimmuntherapie hat sich die Therapie mit IL-15 zu einem vielversprechenden Ansatz entwickelt und zeigt großes Potential bei der Unterstützung einer antitumoralen Immunantwort. Allerdings ist die systemische Anwendung von IL-15 mit Toxizität verbunden und die Wirksamkeit von IL-15 in einem monotherapeutischen Ansatz begrenzt. Diese Arbeit beschäftigt sich mit der Entwicklung neuartiger trifunktioneller Fusionsproteine, welche die Aktivität von IL-15 mit Hilfe costimulatorischer Liganden der TNF-Superfamilie verstärken und die therapeutische Aktivität durch eine Antikörperkomponente auf den Tumor ausrichten. Das bereits vorhandene homotrimere trifunktionelle Fusionsprotein der ersten Generation besteht aus einer Antikörpereinheit (scFv), IL-15 fusioniert an die erweiterte Sushidomäne des IL-15Rα (RD) und der extrazellulären Domäne (ECD) von 4-1BBL. Die nicht-kovalente Trimerisierung der ECD von 4-1BBL führt zu einem homotrimeren Fusionsprotein mit drei Antikörpereinheiten und drei RD_IL-15 Einheiten. Basierend auf dem trifunktionellen Fusionsprotein der ersten Generation wurde in dieser Arbeit ein neuartiges trifunktionelles Fusionsprotein der zweiten Generation entwickelt, in dem der trimere Ligand der TNF-Superfamilie in einem einzelketten-Format (single-chain) vorliegt. Durch die lineare Verknüpfung von drei extrazellulären Domänen zum single-chain Format entsteht ein monomeres, trifunktionelles Fusionsprotein, mit nur einer Antiköpereinheit und einer RD_IL-15 Einheit. Für das trifunktionelle Fusionsprotein im single-chain Format wurde im Target-ungebundenen Zustand eine ähnliche, im Target-gebundenen Zustand dagegen eine verbesserte Stimulation von T-Zellen *in vitro* gezeigt, sowie ein deutlicher Antitumoreffekt in einem Lungentumor-Mausmodell *in vivo* beobachtet. Darüber hinaus wurden auch OX40L und GITRL erfolgreich in das neue trifunktionelle Fusionsproteinformat eingebracht. Im Hinblick auf die Stimulierung von T-Zellen zeigten alle trifunktionellen Fusionsproteine verbesserte Eigenschaften im Vergleich zur Kombination aus den jeweiligen bifunktionellen Fusionsproteinen. Hinsichtlich der Verstärkung des zytotoxischen Potentials von $CD8^+$ T-Zellen und der Proliferation von $CD4^+$ T-Zellen wurden die stärksten synergistischen Effekte für RD_IL-15_$scFv_{FAP}$_scGITRL beobachtet. Zusätzlich konnte in einem syngenen Lungentumor-Mausmodell eine starke, targeting-abhängige Antitumorantwort für RD_IL-15_$scFv_{FAP}$_scGITRL gezeigt werden. Des Weiteren wurde der Effekt eines gegen EGFR gerichteten, trifunktionellen Fusionsproteins auf Trastuzumab-vermittelte ADCC untersucht.

Die von dem monoklonalen Antikörper vermittelten ADCC wurde durch das trifunktionelle Fusionsprotein RD_IL-15_scFv$_{EGFR}$_sc4-1BBL und das bifunktionelle Fusionsprotein RD_IL-15_scFv$_{EGFR}$ verstärkt. Folglich erscheint das trifunktionelle Fusionsprotein im single-chain Format als eine vielversprechende Plattform mit vielseitigen Möglichkeiten für die weitere Entwicklung.

1 Introduction

It was Rudolf Virchow who first observed immune cell infiltration in human tumors in the mid-nineteenth century (Balkwill and Mantovani 2001). In 1891, William Coley then pioneered in the field of cancer immunotherapy with the development of an early immunotherapy using bacterial toxins. He injected a non-infectious mixture of bacteria into inoperable sarcomas of patients thereby triggering an immune response leading to clearance of cancer in some patients (Coley 1910). Due to the lack of understanding immune mechanisms and severe side effects, progress in the field of cancer immunotherapy stalled for nearly a century. In the 1970s, a number of crucial discoveries like the existence of T cells and their critical role of cellular immune response in adaptive immunity (Miller et al. 1967), the discovery of tumor necrosis factor (TNF) as one key player in the immune response triggered by endotoxins (Carswell et al. 1975) and the manufacturing of monoclonal antibodies (Köhler and Milstein 2005) set stage for the renewed advent of cancer immunotherapy.

1.1 Cancer immunotherapy

The rapid developments in the field of cancer immunotherapy started with the approval of Ipilimumab for the treatment of metastatic melanoma in 2011. Ipilimumab is a monoclonal antibody directed against the cytotoxic T-lymphocyte-associated protein 4 (CTLA-4), an immune checkpoint downregulating the immune response (Hodi et al. 2010). Two other checkpoint inhibitors, Nivolumab (2014) and Pembrolizumab (2015) have been approved for the treatment of metastatic melanoma and non-small lung cancer. Both these antibodies antagonize the programmed cells death protein 1 (PD-1), one of the main regulators of T cell exhaustion and tolerance (Robert et al. 2014). The principle goal of cancer immunotherapy in this case is to unleash the suppressed immune system and launch sustained attacks against tumor cells, resulting in the eradication of cancer. The first approved immunomodulatory cancer therapeutic to treat cancer in patients is the above mentioned anti-CTLA-4-mAb Ipilimumab. This success created interest in evaluating other strategies not only to target checkpoint inhibitors but to investigate costimulatory receptors. To date, more than 30 immunomodulatory antibodies are tested in clinical studies in Phase I to III (Table 1).

Table 1: Immunomodulatory antibodies for cancer therapy either approved or in ongoing clinical trials. Data from https://clinicaltrials.gov/ and https://www.fda.gov, Mai 2018.

Target	Generic name	Indication	Stage of development
Co-inhibitory pathways			
CTLA-4	Ipilimumab	Metastatic melanoma	Approved in 2011
		Sarcoma, Wilm's tumor, Lymphoma, Neuroblastoma	Phase I
	AGEN-1884	Advanced solid cancers	Phase I
	BCD-145	Metastatic melanoma	Phase I
PD-1	Nivolumab	Metastatic melanoma	Approved in 2014
		Metastatic NSCLC, renal cell carcinoma	Approved in 2015
		Lymphoma, head and neck cancer	Approved in 2016
		Liver cancer, colorectal cancer, bladder cancer	Approved in 2017
		Mesithelioma	Phase III
		AML	Phase II
		Oral cavity cancer	Phase II
		Prostate cancer	Phase II
	Pembrolizumab	Metastatic melanoma	Approved in 2014
		NSCLC	Approved in 2015
		head and neck cancer	Approved in 2016
		Stomach and gastroesophageal cancer, bladder cancer, lymphoma, metastatic solid tumors	Approved in 2017
		Inflammatory breast cancer	Phase II
		Metastatic breast cancer	Phase I/II
		Soft tissue sarcoma, bone sarcoma	Phase II
		Recurrent endometrial cancer	Phase II
		Medullary thyroid cancer	Phase II
		Multiple myeloma	Phase II
		Renal cell carcinoma	Phase III
		Neuroendocrine tumors	Phase II
		Meningioma	Phase II
	JS-001	Metastatic melanoma	Phase II
		NSCLC	Phase I
		Lymphoma	Phase I
	Sym021	Metastatic cancer, solid rumors, lymphoma	Phase I
	SHR-1210	Advanced solid tumors	Phase II
		Hodgkin's lymphoma	Phase II
		NK/T cell lymphoma	Phase II
		hepatocellular carcinoma	Phase II
	Pidilizumab	Diffuse pontine glioma	Phase I/II
	Tislelizumab	Metastatic NSCLC/SCLC	Phase II
		Hepatocellular Carcinoma	Phase II
	Cemiplimab	NSCLC	Phase III
		Basal cell carcinoma	Phase II
		Advanced cutaneous squamous cell carcinoma	Phase II

PD-1	IBI308	NK/T cell lymphoma	Phase II
		Hodgkin's Lymphoma	Phase II
	Spartalizumab	Melanoma, NSCLC, TNBC, anaplastic thyroid cancer, solid tumors	Phase I/II
		Nasopharyngeal carcinoma	Phase II
	AGEN2034	Cervical cancer	Phase I/II
	Genolimzumab	Peripheral T cell lymphoma	Phase I
	CK-301	Recurrent or metastatic cancers	Phase I
	BCD-100	Melanoma	Phase II
	INCMGA00012	Metastatic solid tumors	Phase I
	M7824	HPV associated malignancies	Phase II
PD-L1	Atezolizumab	NSCLC, bladder cancer	Approved in 2016
		Hodgkin's lymphoma	Phase II
		TNBC	Phase II
	Avelumab	Bladder cancer, Merkel cell carcinoma	Approved in 2017
		Ovarian cancer	Phase II
		Hepatocellular carcinoma	Phase II
		Nasopharyngeal cancer	Phase II
		Testicular germ cell cancer	Phase II
		Neuroendocrine tumors	Phase I/II
		Metastatic colorectal cancer	Phase II
	Durvalumab	Bladder cancer	Approved in 2017
		NSCLC	Phase II
		Esophageal cancer	Phase II
Costimulatory pathways			
4-1BB	PF-05082566	Solid tumors, B cell lymphoma	Phase I
OX40	MEDI0562	Advanced solid tumors	Phase I
		Melanoma, head and neck cancer	Phase I
	MEDI6469	Colorectal cancer	Phase I
		head and neck cancer	Phase I
OX40	MEDI6469	Metastatic breast cancer	Phase I
	PF-04518600	Metastatic cancer	Phase I
GITR	INCAGN01876	Metastatic cancer	Phase I/II
	OMP-336B11	Metastatic cancer	Phase I
	MEDI-1873	Metastatic cancer	Phase I
	GWN323	Solid tumors, lymphomas	Phase I
	TRX518	Melanoma, solid tumors	Phase I
ICOS	MEDI-570	Lymphoma	Phase I

Cancer immunotherapy not only focuses on immunomodulatory antibodies but also other approaches. Significant progress in understanding the function of molecular pathways has led to the development of a number of new immunotherapies like cancer vaccination (Butterfield 2015), small molecules (Adams et al. 2015), CAR T cells (Maude et al. 2018), cytokines (Waldmann 2017), bispecific T cell engagers (Krishnamurthy and Jimeno 2018) and antibody-fusion proteins (Müller 2015) which are also evaluated in terms of their effectiveness against numerous types of cancers and their clinical use. One promising approach is Blinatumomab, a bispecific T cell engager binding to CD19 on the tumor cell and

CD3 on the T cell (Goebeler et al. 2016). Blinatumomab has been approved by the FDA for relapsed or refractory B cell precursor ALL in 2017. In the context of destruction of cancer cells by the immune system, cytokines have been explored for the treatment of cancer. Cytokines are the major regulators of the innate and adaptive immune system and control proliferation, differentiation, effector functions and survival of leucocytes. Preclinical models using IL-2, IL-12, IL-15, IL-21 and granulocyte macrophage colony-stimulating factor (GM-CSF) have shown efficacy in the treatment of murine cancer (Floros and Tarhini 2015; Kaufman et al. 2014). IL-2 for example has been studied intensively, with recombinant IL-2 (rhIL-2) (Lafreniere and Rosenberg 1985) being one broadly used agent in cancer immunotherapy which received approval for the treatment of renal cell carcinoma in 1992 and metastatic melanoma in 1998 (Rosenberg 2014). Although IL-2 has shown capability of mediating tumor regression, monotherapy with IL-2 has shown to be associated with severe adverse effects in high dose. Despite the success of some concepts in cancer immunotherapy as monotherapy, the future of cancer immunotherapy lies in the combinatory treatment of different approaches. Meaningful synergistic effects are anticipated with combinatory strategies, for example combining checkpoint inhibitors with conventional therapies (Robert et al. 2011) or targeted therapies (Stagg et al. 2011), the combination of two different checkpoint inhibitors (e.g. Ipilimumab and Nivolumab (Callahan et al. 2018)) or the combination with cellular therapies (Cherkassky et al. 2016). On the heel of these studies, combinations of IL-2 with targeted therapy (Bersanelli et al. 2014) or peptide vaccines (Schwartzentruber et al. 2011) have shown potent anti-tumor effects with high overall response rates in patients. This demonstrates that combinations with cytokines gain increasing interest especially when it comes to finding new combinations with other immunotherapeutic agents. Therefore, the role of cytokines in cancer immunotherapy will be further addressed here.

1.2 Common cytokine receptor γ-chain family

Cytokines, such as interferons, interleukins, chemokines, and growths factors are modulators of immunity and inflammation secreted by numerous cell types such as lymphocytes, monocytes and macrophages. Cytokines are the main coordinators of the innate as well as the adaptive immune response. The coordination of these responses is achieved by a network of cytokines that induce maturation of immune cells, control effector functions and turn the immune response off when control of the pathogen is achieved. Crucial members of

this coordinating network belong to the type I cytokines. One important family of type I cytokines consists of interleukin-2 (IL-2), IL-4, IL-7, IL-9, IL-15 and IL-21 that bind to the receptors of the common γ-chain receptor family, named after the shared receptor-γ-chain γ_c (Leonard 2001) (Figure 1). The receptor-γ-chain was first discovered as a component of the receptor for IL-2, which is the most extensively studied member of this family. The IL-2 receptor consists of three chains, namely IL-2Rα (Leonard et al. 1984), IL-2Rβ (Sharon et al. 1986) and γ_c (Takeshita et al. 1992) which together form the high affinity IL-2 receptor (Wang et al. 2005). The αβγ heterotrimer, βγ dimer and α chain monomer have high, intermediate and low affinities to IL-2, respectively (Dhupkar and Gordon 2017). Upon binding of the binary complex of IL-2 and IL-2Rα to IL-2Rβ and IL-2Rγ, Janus kinases (JAK) 1 and JAK3 which are associated with the β- and γ-chain, respectively are activated (Nelson and Willerford 1998). One of the members of the signal transducers and activators of transcription family (STAT), STAT1, STAT3 and STAT5 in T cells or STAT4 in NK cells, are recruited and bind to the phosphorylated IL-2 receptor, resulting in dissociation and dimerization of these transcription factors. The formed STAT dimers are then translocated to the nucleus leading to the transcription of target gens (Gaffen 2001). IL-2 binding to its receptor can also lead to the activation of the PI_3K-Akt pathway (Lin and Leonard 2000; Malek and Castro 2010), which promotes cell growth and survival (Franke et al. 1997). JAK kinase activation and phosphorylation of IL-2Rβ can also lead to association of the SHC adaptor protein which provides a platform for the Ras-MAPK activation promoting cell growth (Friedmann et al. 1996). Interestingly, IL-2, IL-7, IL-9 and IL-15 mainly activate STAT5 whereas IL-4 activates STAT6 and IL-21 activates STAT3. This differences in activation of STAT proteins explain the different effects of these cytokines (Leonard and Spolski 2005). As already mentioned, cytokines can directly enhance or suppress the antitumor response of T cells which is why cytokines like IL-2 were among the first approaches in cancer immunotherapy (Atkins et al. 1999).

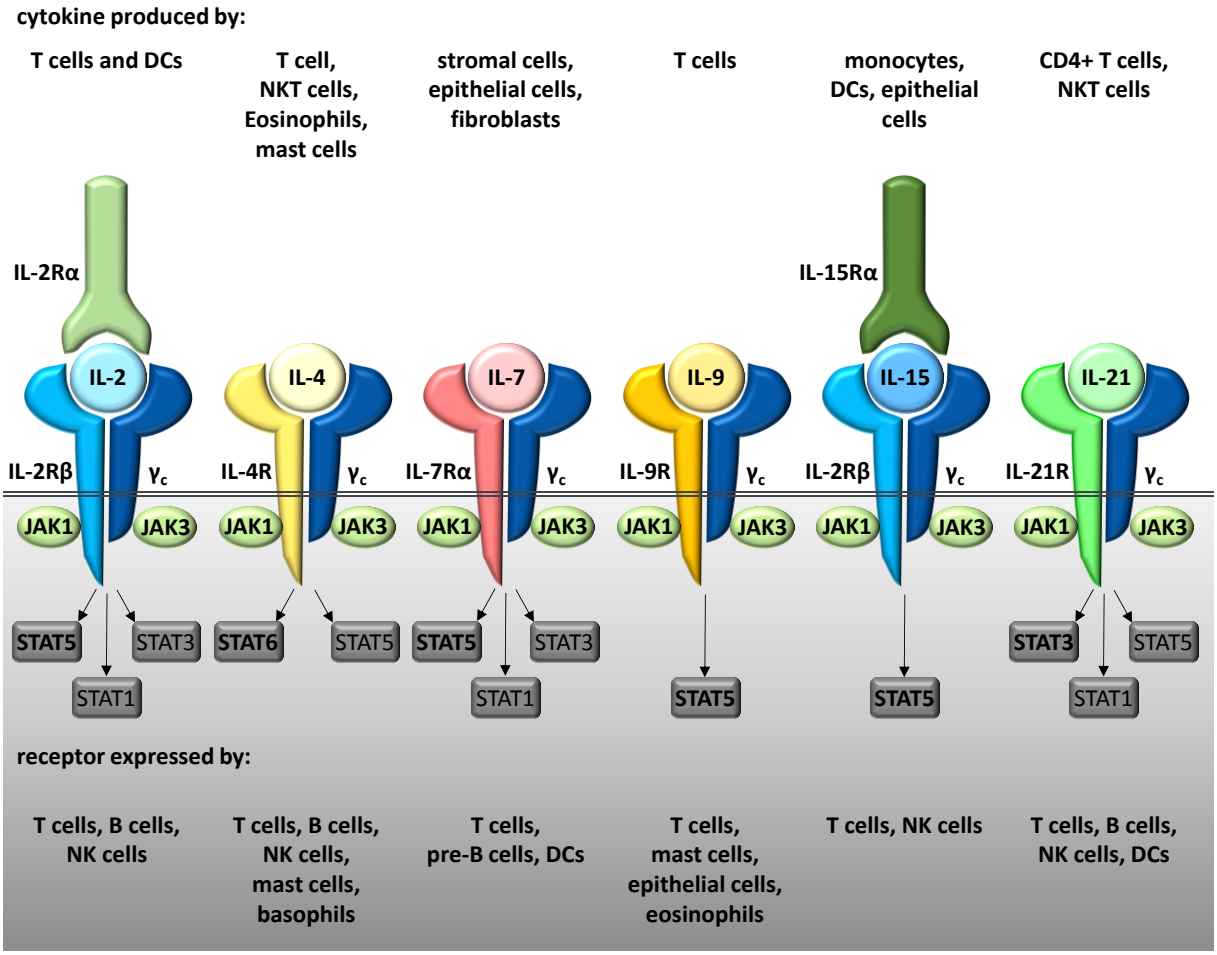

Figure 1: Common γ-chain receptor family. All cytokines share the common γ-chain (γ_c), IL-2 and IL-15 additionally share the IL-2Rβ chain and both have three receptor chains. The receptor for each cytokine activates Janus kinase 1 (JAK1) and JAK3. The main signal transducer and activator of transcription (STAT) proteins that are activated by these cytokines are shown in bold. Figure adapted from Rochman et al. (2009).

First discovered as a lymphocyte stimulating factor in 1965 (Gordon and MacLean 1965), IL-2 is a T cell growth factor which can augment NK cell cytolytic activity and promotes immunoglobulin production of B cells (Kim et al. 2006). Additionally, IL-2 contributes to the development of regulatory T cells hence peripheral T cell tolerance (Sakaguchi et al. 2008) and regulates the proliferation and survival of activated T cells (D'Souza and Lefrançois 2003). Recombinant IL-2 (rhIL-2) (Lafreniere and Rosenberg 1985) received approval for the treatment of renal cell carcinoma in 1992 and metastatic melanoma in 1998 (Rosenberg 2014). Although IL-2 has been shown to mediate tumor regression, severe adverse effects in high dose monotherapy with IL-2 have been observed. While IL-2 has been thoroughly studied and used for cancer treatment, other cytokines like IL-15 are being investigated for their use in cancer immunotherapy.

1.2.1 IL-15 in cancer immunotherapy

IL-15 was first identified in 1994 as a T lymphocyte growth factor that shares ~19% sequence homology and many biological properties of IL-2 (Grabstein et al. 1994). IL-15, in contrast to IL-2, is mostly trans-presented by the high affinity IL-15 receptor α-chain (Castillo and Schluns 2012). IL-15 receptor α (IL-15Rα) and IL-15 are coexpressed by macrophages and dendritic cells, where IL-15Rα chaperones IL-15 through the cell and shuttles it to the cell surface, where it is presented to NK, NK-T and memory $CD8^+$ T cells expressing the IL-15 receptor β- and the common γ-chain (Dubois et al. 2002). Trans-presented IL-15/IL-15Rα signals through IL-15Rβγ, leading to the recruitment and activation of the Janus kinases JAK1 and JAK3. Activated JAK1 and JAK3 phosphorylate the signal transducer STAT5 leading to transcription of effector gens (Lodolce et al. 2002). Soluble IL-15 can also bind to the receptor β- and γ-chain with intermediate affinity (Jakobisiak et al. 2011). IL-15 signaling promotes the antigen presentation and production of IL-12 and IFN-γ by DCs and macrophages (Ohteki et al. 2001), intensifies NK cell proliferation and cytotoxicity (Becknell and Caligiuri 2005) and provides a potent stimulus for memory $CD8^+$ T cells *in vivo* (Zhang et al. 1998). In contrast to IL-2, IL-15 has shown to be less efficient in expanding regulatory T cells although both share the γ_c and the IL-2Rβ chain (Vang et al. 2008). Additionally, trans-presentation of IL-15 plays an important role in the homeostasis of IL-15-dependent cell lineages, i.e. NK cells and NK-T cells, regulation of their biological functions (Lucas et al. 2007; Lodolce et al. 2002) and appears to regulate homeostasis and acquisition of memory functions in naïve $CD4^+$ T cells (Chen et al. 2014). Cancer therapy with IL-2 had showed severe side effects when administered in high dose. In contrast to IL-2, IL-15 preferentially induced proliferation of $CD8^+$ T cells rather than T_{regs} (Rochman et al. 2009), IL-15 treatment does not stimulate activation-induced cell death of T cells (Marks-Konczalik et al. 2000) and contributes to the proliferation and differentiation of activated $CD8^+$ T cells and NK cells (Morishima et al. 2015) as well as the maintenance of long-term $CD8^+$ memory T cells (Zhang et al. 1998). Therefore, IL-15 has been extensively studied as an alternative to IL-2. Safety and tolerability is tested for recombinant IL-15 as a monotherapy in treatment of metastatic cancer (NCT01572493), for the ex vivo expansion of NK cells (NCT02123836) or for the expansion of CAR T cells (NCT02992834). Furthermore, combinations of rhIL-15 with monoclonal antibodies like Alemtuzumab (anti-CD52) (NCT02689453), mAbs targeting checkpoint inhibitors like Nivolumab (anti-PD-1) and Ipilimumab (anti-CTLA-4)

(NCT03388632) or combinations of the IL-15/IL-15Rα with the checkpoint inhibitor Spartalizumab (anti-PD-1) (NCT02452268) are evaluated in phase I clinical trials.

1.2.2 IL-15 in therapeutic approaches

With the fusion of IL-15 to the high affinity IL-15 binding domain (extended sushi domain) of the human IL-15Rα, a novel strategy to improve the activity of IL-15 has evolved (Mortier et al. 2006). The extracellular part at the N-terminus of IL-15Rα has been shown to hold the structural elements responsible for IL-15 binding. This particular structure, the so called extended sushi domain, has been shown to enhance the biological effects of IL-15. Fusion of IL-15 to the extended sushi domain of the IL-15Rα chain has shown enhanced activation and survival of NK cells and $CD8^+$ T cells (Huntington et al. 2009). Additionally, decreased tumor burden and long-term survival could be shown in different mouse models (Bessard et al. 2009). Based on this, a new format of cytokine fusion protein, a so called IL-15 superagonistic antibody constituting of IL-15 and a IL-15Rα-Fc chimera has been developed (Rubinstein et al. 2006). Immunostimulatory effects especially on NK cells but also on NK-T cells and $CD8^+$ T cells in spleen, liver, peripheral blood and bone marrow have been shown for the superagonistic antibody containing two IL-15 and two effective IL-15Rα sushi domains per unit (Guo et al. 2015; Wu and Xu 2010; Dubois et al. 2008; Stoklasek et al. 2006). Furthermore, the IL-15/IL-15Rα-Fc fusion protein (ALT-803) has been extensively studied in various murine *in vivo* models showing antitumor efficacy either in a monotherapeutic approach (Xu et al. 2013) or in combination with mAbs targeting CD20 or PD-1 (Rosario et al. 2016; Mathios et al. 2016). Safety and tolerability of the IL-15/IL-15Rα-Fc fusion protein ALT-803 in clinical phase I studies has been shown for different cancer types either in a monotherapeutic approach (NCT01946789; NCT02099539; NCT01885897; NCT02384954) or in combination with standard chemotherapy (NCT02559674; NCT03054909), the immunomodulatory monoclonal antibodies Nivolimab (NCT02523469; NCT03228667) or Pembrolizumab (NCT03228667), NK cell transfer (NCT03050216; NCT02890758; NCT02465957) or in combination with a vaccination strategy (NCT03127098). All human clinical trials are still in the process of collecting safety information, but so far there is no evidence for adverse events in patients receiving ALT-803 treatment. However, monotherapy with rhIL-15, as the primary effective component of ALT-803, has shown cytotoxic side effects like hypotension, thrombocytopenia, liver injury, fever and rigors in

patients with metastatic malignancies (Conlon et al. 2015). Potential cytotoxic side effects could be circumvented by targeting the IL-15/IL-15Rα complex directly to the tumor side while half-live and immunomodulatory effects of the cytokines could be improved. Furthermore, antibody cytokine fusion proteins with their capability to accumulate at the tumor site could potentially mediate the enrichment of favorable tumor-infiltrating immune cells like cytotoxic T cells and NK cells. Targeting cytokine delivery to the tumor site could be achieved by fusion of the cytokine to a targeting moiety e.g. an antibody. The format of the antibody moiety responsible for selective targeting to the tumor site is crucial as pharmacokinetic properties of the fusion protein directly influence performance (Kontermann 2012). Different formats can be used from small fusion proteins based on antibody fragments like scFvs, to bispecific antibodies (Müller and Kontermann 2010) or whole antibodies targeting tumor-associated antigens (Kontermann 2012). Fusion of the IL-15/IL-15Rα to an scFv as a targeting moiety has been shown to mimicking trans-presentation of IL-15, mediated T cell activation *in vitro* and reduction of tumor burden *in vivo* (Kermer et al. 2012). Additionally, it has been shown that fusion of IL-15/IL-15Rα sushi domain to an anti-GD2 antibody targeting disialoganglioside did not only retain the immunostimulatory potential of IL-15 but additionally combined it with antibody-dependent cell mediated cytotoxicity (ADCC) (Vincent et al. 2013).

The combination of cytokines with an immunomodulatory antibody has shown to augment tumor immunotherapy against multiple tumor types and was able to restore anergic tumor-reactive $CD8^+$ T cells (Redmond et al. 2012). This shows that targeting costimulatory pathways gains increasing interest especially when it comes to finding new combinations with other immunotherapeutic agents. Therefore, mechanisms and interactions of costimulatory molecules in T cell stimulation will be further addressed here.

1.3 TNF superfamily-mediated costimulation of T cells

For complete activation of a T cell resulting in clonal expansion and the acquisition of effector functions, multiple signals are mandatory. The first signal is mediated by the recognition of a peptide being displayed on the major histocompatibility complex (MHC) class I/II of antigen presenting cells (APCs) by the T cell receptor leading to the formation of the immunological synapse (Dustin 2014). Peptide-MHC class II complexes are only recognized by $CD4^+$ T cells whereas Peptide-MHC class I complexes are exclusively recognized by $CD8^+$ T cells (König et al. 1992). The second signal, also called the

costimulatory signal, is necessary to stimulate T cells in conjunction with the first signal and is provided by ligands on the surface of APCs that engage costimulatory receptors on the T cell (Lafferty et al. 1983). T cells that recognize the antigen in absence of a costimulatory signal either fail to respond and undergo apoptosis or enter a state of unresponsiveness known as anergy (Quill and Schwartz 1987). Thus, costimulation plays a key role in the activation of T cells (Mueller et al. 1989). The best characterized T cell costimulatory pathway involves the CD28 receptor (Jenkins et al. 1991), which binds to the two costimulatory ligands B7-1 and B7-2 (Linsley et al. 1990). With the identification of the co-inhibitory receptor cytotoxic T lymphocyte antigen 4 (CTLA-4) which also binds to B7-1 and B7-2, the two signal model begun to evolve into a more complex regulatory system (Linsley et al. 1991). Since then, T cell cosignaling receptors have been defined as surface molecules transducing signals into T cells to positively or negatively modulate T cell receptor signaling. Costimulatory signaling represents a complex network of receptor ligand interactions qualitatively and quantitatively influencing the immune response. The expression of costimulatory or co-inhibitory molecules on the T cell surface is induced upon activation whereby cell surface interaction and intracellular signaling continuously vary in response to dynamic tissue environmental conditions (Saito et al. 2010). Accordingly, in the early phase of T cell activation upregulation of costimulatory receptors leads to functional responsiveness. Subsequently, inhibitory receptors become upregulated till the expression of co-inhibitory dominates the expression of costimulatory receptors, leading to the termination of the T cell response (Zhu et al. 2011). Diverse expression of cosignaling molecules additionally allows differential control of T cell subsets leading to the assumption of an intrinsic difference in responding to costimulation (Zhu et al. 2011).

Based on structural features, the wide range of known costimulatory and co-inhibitory receptors can be grouped into those belonging to the immunoglobulin (Ig) superfamily (e.g. CD28) or the tumor necrosis factor receptor superfamily (TNFSF) including CD27, OX40, 4-1BB, and GITR.

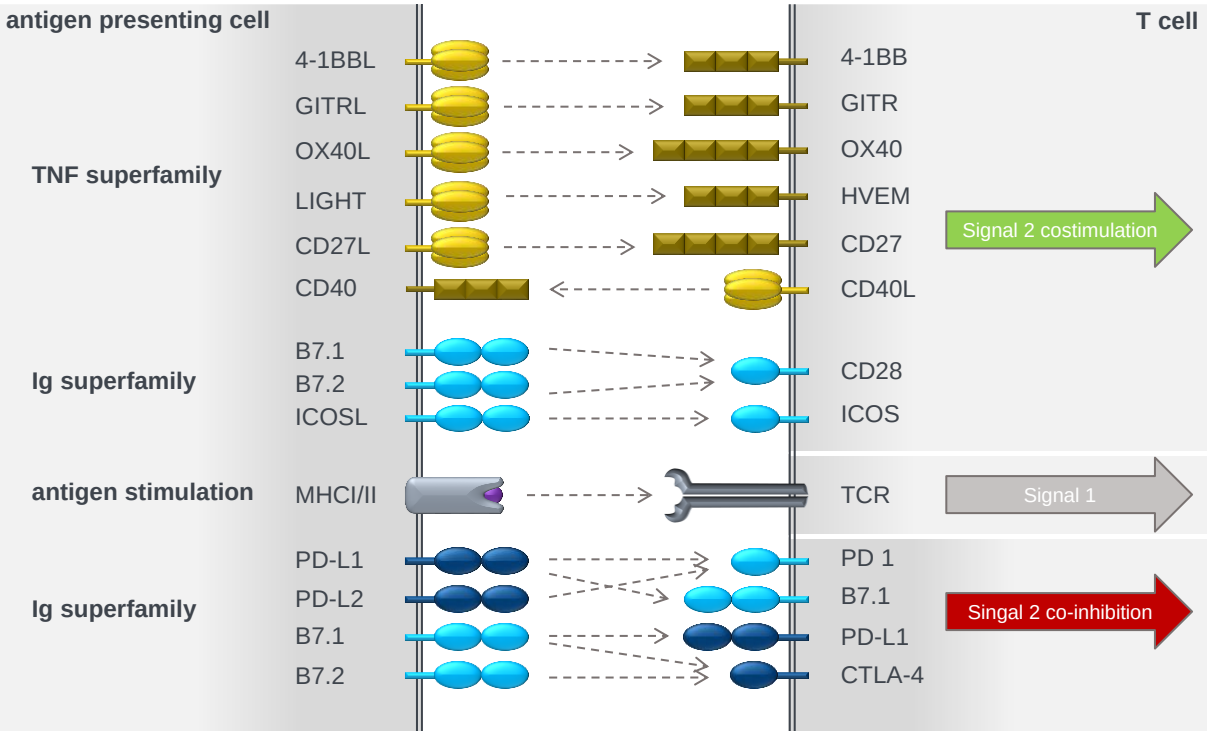

Figure 2: Costimulatory and co-inhibitory signaling at the immune synapse. The first signal is mediated by the interaction of the antigen presented on MHC and the T cell receptor followed by the interaction of costimulatory or co-inhibitory receptor-ligand interaction. Only the most common receptor-ligand pairs are depicted including the TNFSFR (brown) and their ligands (yellow), the Ig superfamily (light blue) and the inhibitory members of the Ig superfamily (dark blue). Adapted from Chen and Flies (2013).

At present 19 different ligands and 29 corresponding receptors that belong to the TNF superfamily (TNFSF) have been identified (Figure 2). The receptors of the TNFSF can be divided into three major groups. The first group includes the receptors comprising a death domain. Secondly, the group of non-signaling decoy receptors and the third group of TRAF interacting receptors where the costimulatory receptors belong to. The TNFSF receptors are type I transmembrane proteins (i.e. extracellular N-terminus and intracellular C-terminus) and are characterized by the presence of one or more extracellular cysteine-rich domains (CRDs) which typically contain six cysteine residues forming a ladder-like structure stabilized by disulfide bonds (Chattopadhyay et al. 2009). The trimeric TNF homology domain of the ligand is responsible for highly efficient receptor clustering and signal initiating mechanisms. The TRAF interacting receptors directly interact with one of the six TRAF family members to initiate canonical or non-canonical nuclear factor κB (NFκB) activation (Silke and Brink 2010). The TNFSF ligands are type II transmembrane proteins (i.e. intracellular N-terminus and extracellular C-terminus) characterized by a conserved C terminal domain, the TNF homology domain (THD) (Magis et al. 2012).The THD is a beta-sandwich structure that is responsible for the characteristic formation of non-covalent homotrimers (Bodmer et al.

2002). Although most ligands are synthesized in a membrane-bound form, soluble forms can be generated by cleavage of membrane ligands into soluble proteins. This study focuses on the costimulatory members 4-1BB, OX40 and GITR of the TNFSF, which are important for the formation of an immune response and the activation of T lymphocytes.

1.3.1 4-1BB and 4-1BBL

4-1BB (CD137) was originally discovered on activated T lymphocytes (Kwon and Weissman 1989) and found to favor proliferation and IL-2 secretion in those cells (Pollok et al. 1993). 24 hours after initial antigen-mediated activation, 4-1BB expression can be observed on $CD4^+$ and $CD8^+$ T cells, reaching peak expression after 40 to 64 hours (Vinay and Kwon 1998). 4-1BB is additionally expressed on activated NK cells, B cells and myeloid cells (Vinay and Kwon 2011). Experiments in 4-1BB knockout mice have indicated that 4-1BB plays an important role in anti-viral and alloreactive CTL responses (DeBenedette et al. 1999) and in the induction of persistent formation of memory T cells (Willoughby et al. 2014). Only one transmembrane ligand for 4-1BB, namely 4-1BBL, has been identified (Alderson et al. 1994). Expression of 4-1BB ligand is found on APC such as mature DCs, activated B cells and activated macrophages (DeBenedette et al. 1997). The interaction of 4-1BB with its ligand leads to a costimulatory signal that protects tumor antigen specific cells from cell death (Watts 2005). Although the stimulatory effect of 4-1BB/4-1BBL in T cell response addresses both $CD4^+$ and $CD8^+$ T cells, $CD8^+$ T cells are mainly activated (Tan et al. 1999). Due to its important costimulatory properties, 4-1BB gained strong interest as a target in cancer immunotherapy. *In vitro*, stimulation of 4-1BB by agonistic monoclonal antibodies results in enhancement of proliferation, survival and effector functions such as cytotoxicity and cytokine secretion (Melero et al. 1997). The therapeutic effect of agonistic mAbs targeting 4-1BB has been reported to be mostly driven by a strong CTL response but also an effect on NK cells (Kohrt et al. 2011) as well as on regulatory T cells (Akhmetzyanova et al. 2016) has been observed. On human as well as mouse NK cells, 4-1BB becomes expressed upon exposure to IgG-coated target cells subjected to antibody-dependent cellular cytotoxicity (ADCC) (Kohrt et al. 2011). This upregulation is mediated by the CD16 Fc_γ receptor. Once 4-1BB is expressed on the NK cell surface, stimulation via 4-1BB can strongly enhance the capability of the NK cell to mediate ADCC in subsequent encounters. This synergistic effect of ADCC with 4-1BB stimulation has been shown for several mAb like Rituximab (Kohrt et al.

2011), Trastuzumab (Kohrt et al. 2012) and Cetuximab (Kohrt et al. 2014). In addition to agonistic mAbs various approaches targeting 4-1BB have been pursued like RNA-dimerized aptamers (McNamara et al. 2008) or second and third generation CAR T cells comprising the intracellular signaling domain of 4-1BB (Maude et al. 2018). Two monoclonal antibodies, Utomilumab (PF-05082566) and Urelumab, targeting 4-1BB are undergoing clinical evaluation in phase I trials. Safety and tolerability of Utomilumab in combination with PF-04518600 (OX40 agonist) (NCT02315066), Rituximab (anti-CD20) (NCT01307267), Trastuzumab (anti-ErbB2) (NCT03364348) and Avelumab (anti-PD-L1) (NCT02554812) are currently under clinical investigation. In 2009, a Phase II study of Urelumab was terminated due to two hepatotoxicity-related deaths (Segal et al. 2017). Therefore, a reduced dose of Urelumab in combination with Nivolumab (anti-PD-1) (NCT02845323, NCT02253992, NCT02534506) in different cancer types is being tested in phase I/II clinical trials. Since systemic delivery of anti-4-1BB mAb has shown severe adverse events, strategies to target and limit the 4-1BB signaling to the tumor side become of increasing interest.

1.3.2 OX40 and OX40L

OX40 was first discovered in 1987 on the surface of activated $CD4^+$ T cells in rats (Paterson et al. 1987). Expression pattern of OX40 on T cells depend on the activation status, differentiation state and population subset. $CD4^+$ T cells as well as $CD8^+$ T cells, albeit at low levels, express OX40 24 to 72 hours following TCR engagement (Mallett et al. 1990). Thus, activation of $CD4^+$ as well as $CD8^+$ T cells can potentially be achieved by immunotherapeutic agents directed against OX40. Furthermore, studies have shown that regulatory T cells express a high amount of OX40 upon activation (Lai et al. 2016). OX40 is predominantly expressed on T cells, although expression has also been described on NK, NK-T cells and neutrophils (Baumann et al. 2004). Stimulation of these cells via OX40 has shown a pro-inflammatory and pro-survival effect suggesting that OX40-targeting also contributes to the innate immune response (Karulf et al. 2010).The expression of the unique ligand of OX40 (OX40L) is induced on human DCs upon exposure to thymic stromal lymphopoietin (Ito et al. 2005) or tolllike receptor (TLR) agonists (Ohshima et al. 1997). Additionally, human monocytes, neutrophils (Karulf et al. 2010) and mast cells (Fujita et al. 2006) can express OX40L. *In vitro* studies have shown that stimulation of T cells with OX40L enhances proliferation, expression of effector molecules and cytokine release (Baum et al. 1994). The

effects on $CD8^+$ T cells are most likely mediated via enhanced helper function of the $CD4^+$ T cell population (Serghides et al. 2005). In preclinical tumor models, targeting OX40 has been intensively studied but only showed effectiveness in eradicating primarily immunogenic tumors (Redmond et al. 2009; Kjaergaard et al. 2000; Weinberg et al. 2000). Therefore, combinatorial approaches with OX40 agonistic monoclonal antibodies are pursued. For example combinations of OX40 agonists with chemotherapy (Hirschhorn-Cymerman et al. 2009) or cancer vaccines (Murata et al. 2006) have shown an improvement in control of established tumors and enhance the expansion and prolonged survival of tumor-specific T cells. Additionally, anti-OX40 antibodies have been combined with other immunostimulatory approaches like mAbs targeting 4-1BB (Lee et al. 2004) or CTLA-4 (Redmond et al. 2014) and cytokines such as IL-2 (Redmond et al. 2012). Currently, two monoclonal antibodies targeting OX40 are undergoing clinical evaluation. The murine antibody MEDI6469 is being evaluated in phase I or phase I/II studies as monotherapy in patients with colorectal cancer metastasis (NCT02559024) and in head and neck cancer (NCT02274155) as well as in combination with stereotactic body radiation in breast cancer (NCT01862900). To circumvent immunogenicity and allow repeated dosing, fully human OX40 agonists are being developed. Safety and feasibility of the humanized Ab MEDI0562 either in a monotherapeutic approach (NCT03336606) or in combination with Tremelimumab (anti-CTLA-4) or Darvilimab (anti-PD-L1) (NCT02705482) as well as the combination of the fully human anti-OX40 monoclonal antibody PF-04518600 with PF-05082566 (anti-4-1BB) (NCT02315066) is currently under evaluation.

1.3.3 GITR and GITRL

Glucocorticoid-induced TNFR-related protein (GITR) was originally discovered in murine T cell hybridoma cells treated with dexamethasone (Nocentini et al. 1997). GITR is expressed at low levels on resting $CD4^+$ and $CD8^+$ T cells (Gurney et al. 1999) and is upregulated 27 to 72 hours after TCR engagement and remains expressed on the cell surface for several days (Ronchetti et al. 2004). In contrast, GITR is constitutively and brightly expressed on regulatory T cells where it is thought to have an inhibitory effect on T_{reg} activity (McHugh et al. 2002). In addition, GITR expression has been found on cells of the innate immune system like NK cells, eosinophils, basophils, macrophages, and upon activation on B cells (Suvas et al. 2005). The ligand of GITR (GITRL) is highly expressed on activated APCs and endothelial

cells (Krausz et al. 2007). Costimulation via GITR/GITRL was shown to enhance T cell proliferation and effector functions. Ligation of GITR protected T cells from activation induced cells death leading to an increase in memory T cells (Ronchetti et al. 2004). Modulation of GITR with agonistic mAbs in preclinical models has shown promising antitumor activity via the significant increase in effector T cells, depletion and inhibition of T_{regs} as well as suppression of MDSCs and IL-10 secretion (Zhu et al. 2015). It has been shown that the combination of GITR agonists with other immune modulating agents, i.e. a PD-1 antagonist leads to additive antitumor effects (Lu et al. 2014). A number of approaches targeting GITR have entered clinical evaluation. For example, TRX518, a humanized non-depleting mAb, was the first antibody to enter clinical trials for metastatic melanoma. In this phase I study little toxicity but also little efficacy was observed (Koon et al. 2016). A multi dose study of TRX518 is still ongoing (NCT01239134).

1.3.4 Therapeutic strategies involving the TNFSF

Monoclonal antibodies for the stimulation of the TNFSF receptors showed promising antitumor response, but due to antigen-independent activation of memory T cells bear the risk of severe side effects like cytokine release syndrome and hepatotoxicity (Niu et al. 2007). Therefore, targeting the TNFSF receptors using their naturally occurring ligands could potentially give rise to an advantageous therapeutic approach. However, challenges evolve from using costimulatory ligands in their natural homotrimeric form, i.e. soluble TNFSF ligands are only active in an oligomerized form (Rabu et al. 2005). Therefore, different strategies like addition of a trimerization domain (Harbury et al. 1993) or an oligomerization domain linking trimers together (Schabowsky et al. 2009) have evolved. Incorporating a fusion partner like the Fc domain of an IgG has been shown to mediate oligomerization of TNFSF ligands (Meseck et al. 2011; Hu et al. 2008; Morris et al. 2007). Different GITRL-Fc fusion proteins have been shown to mediate the expansion of $CD4^+$ and $CD8^+$ T cells, the generation of a $CD8^+$ T cell memory, depletion of regulatory T cells and thereby an antitumor effect *in vivo* (Durham et al. 2017; Leyland et al. 2017; Tigue et al. 2017; Hu et al. 2008). The recombinant fusion protein MEDI1873, a hexameric GITRL molecule with a human IgG1 Fc has shown to be a potent T cell agonist *in vivo*, enhancing the proliferative response of T cells against protein antigens (Tigue et al. 2017) leading to the initiation of a phase I clinical study in patients with advanced solid tumors (NCT02583165). Additionally, the combination

of a murine version of GITRL-Fc and a recombinant poxvirus-based vaccine has been reported to mediate a robust antitumor response, tumor regression and durable tumor-free survival (Morillon et al. 2017). Furthermore, OX40L-Fc in combination with vaccination strategies has been reported to enhance the antitumor response mediated by T cells (Murphy et al. 2012) and an allogenic cell-based vaccine secreting Fc-OX40L mediating superior priming of antigen-specific $CD8^+$ T cells compared to the agonistic mAb (Fromm et al. 2016). Strong activation of T cells *in vivo* and *in vitro* was reported for the human OX40L-IgG4P Fc fusion protein MEDI6383 which mediates proliferation of effector and memory T cells and protection from T_{reg}-mediated suppression (Oberst et al. 2018). MEDI6383 is currently undergoing clinical evaluation in patients with advanced solid malignancies both as monotherapy and in combination with the anti-PD-L1 blocking mAb Darvalumab (NCT02221960). Theses design may provide the opportunity to maximize multimerisation of TNFSF ligands and thereby enhance the costimulatory function on effector T cells. Under physiological conditions, crosslinking of the costimulatory ligands is achieved by cell surface expression which can be mimicked by fusion of the TNFSF ligand to a targeting moiety in form of a recombinant antibody. Fusion to a targeting moiety is not only beneficial for mimicking cell surface expression but additionally is expected to reduces systemic side effects by targeting the stimulatory effect of the TNFSF ligand to the tumor site (Müller 2015). The smallest, most commonly used antigen-binding fragment is the monovalent single chain fragment variable (scFv) in which the variable domains of the heavy (VH) and the light chain (VL) are fused by a short, flexible linker (~15 amino acids) that allows folding into one binding site (Bird et al. 1988). Moreover, to preserve the biological activity of the antibody fragment and the linked effector moiety, structural features have to be taken into account. Immunomodulatory cytokines can either occur in a monomeric (e.g. IL-2, IL-15), homodimeric (e.g. IL-10, IFN-γ) or homotrimeric (e.g. 4-1BBL, OX40L, GITRL) form thereby additionally influencing the size and valency of the fusion protein (Kontermann 2012). Antibody-fusion proteins incorporating TNFSF ligands like 4-1BBL, OX40L and GITRL were generated by connecting one scFv to one extracellular domain of the ligand, resulting in a large molecule comprising one functional homotrimeric ligand and three antibody moieties. Costimulatory activity and antitumor effects of such molecules have been extensively studied (Hornig et al. 2013; Hornig et al. 2012; Müller et al. 2008a). The costimulatory fusion protein itself is not able to introduce T cell activation, hence a primary T cell stimulus is

necessary. This first T cell signal can be mediated artificially using bispecific antibodies directed against a tumor associated antigen and CD3 retargeting T cells to the tumor cells or via a cross-linked anti-CD3 monoclonal antibody (Dixon et al. 1989). Based on the promising results of the scFv_TNFSFL fusion proteins, Fellermeier et al. (2016) generated novel fusion proteins of simpler configuration and smaller size by introducing the TNFSFL in a single-chain format i.e. genetic fusion of three extracellular domains by linkers on the same polypeptide chain.

1.4 Targets for cancer therapy

Targeting tumor cells requires precise discrimination between healthy and malignant cells. For antibody-mediated strategies target antigens are usually tumor associated antigens (TAA) that are highly over expressed on cancer cells and only present at low levels on healthy tissue (Nestle et al. 1998). TAAs can be further categorized into cancer testis antigens (van der Bruggen et al. 1991), oncofetal antigens (Shively and Beatty 1985), differentiation antigens (Vigneron 2015), lineage-specific antigens (Manzo et al. 2015), oncovial antigens (Linē et al. 2002), and overexpressed antigens (van der Bruggen et al. 1991). The antigens targeted by antibody-fusion proteins characterized in this study belong to the group of overexpressed antigens (EGFR) and a target not directly expressed by tumor cells but by fibroblasts in the tumor microenvironment (FAP). In contrast to cancer therapy using antibodies, the main goal for antibody-fusion proteins incorporating members of the TNFSF and cytokines is to deliver the fusion protein to the tumor site, concentrating its effect at the tumor site and thereby minimalizing systemical effects. Therefore, clinically validated targets, i.e. EGFR and FAP are suitable candidates to mediate the accumulation of antibody-fusion proteins at the tumor site.

1.4.1 Fibroblast activating protein

Dependent on tumor type and stage of tumor progression, tumors and their microenvironment compose of a heterogeneous population of cells including infiltration immune cells, endothelial cells, mesenchymal cells and tumor associated fibroblasts (TAF). TAFs are a heterogeneous population that can be phenotypically distinguished from normal fibroblasts. One marker of reactive fibroblasts in tumors is the fibroblast activation protein (FAP), a type II transmembrane cell surface protein belonging to the post-proline dipeptidyl aminopeptidase family. FAP is expressed selectively by TAFs and pericytes in more than 90%

of human epithelial cancers (Cohen et al. 2008; Goscinski et al. 2008; Garin-Chesa et al. 1990), during embryonic development (Niedermeyer et al. 2000), in tissue of healing wounds (Mathew et al. 1995) and in chronic inflammation (Wang et al. 2008; Acharya et al. 2006). However, FAP expression is not detected in benign lesions or healthy adult tissue (Huber et al. 2003; Aertgeerts et al. 2005). Targeting FAP presents as a promising concept for cancer therapy. F19 is a mouse monoclonal antibody, targeting FAP on activated tumor stromal fibroblasts. In a biodistribution study, the F19 mAb has accumulated at the tumor site with minimal localization to healthy tissue (Welt et al. 1994) and phase I clinical trial revealed a safe and tolerable profile using the humanized F19 antibody Sibrotuzumab (Scott et al. 2003). In a phase II clinical trial, the treatment of 25 cancer patients with Sibrotuzumab was found to be safe and well tolerated, but unfortunately no responses were observed (Hofheinz et al. 2003). More recently, FAP is being explored as a target for antibody strategies delivering effector molecules like chemical drugs, radioisotopes and cytokines. FAP5-DM1, a maytansinoid conjugated monoclonal antibody mediated inhibition of tumor growth and even complete regressions in xenograft models of lung, pancreas, and head and neck cancer (Ostermann et al. 2008). Also two FAP-directed monoclonal antibodies, ESC11 and ESC14, labeled with the radiolanthanide ^{177}Lu have shown to accumulate in xenograft models of FAP-positive human melanoma and delay tumor growth *in vivo* (Fischer et al. 2012). FAP-directed fusion proteins of scFvmo36 with IL-15 showed antitumor effects in a lung tumor mouse model (Kermer et al. 2012). The targeting moiety directed against FAP (scFvmo36) used in this study was isolated by phage display by Brocks and colleagues (Brocks et al. 2001).

1.4.2 Epithelial growth factor receptor

Malignant transformation of cells and therefore tumor progression can be mediated by genetic alterations in the expression of growth regulating genes giving them a selective growth and/or metastatic advantage compared to other cells. Cancer cells generally exhibit a reduced requirement for exogenous supply of growth factors to maintain their high proliferation rate. Thereby, different mechanisms contribute to the amplification of signals, e.g. the upregulation of receptor expression on the cell surface (Aaronson 1991). Different families of growth factors and their receptors have been shown to contribute to the autonomous growth of cancer cells. The human epidermal growth factor receptor family

which comprises of four members, EGFR (HER1, ERBB1), HER2 (NEU, ERBB2), HER3 (ERBB3) and HER4 (ERBB4), plays a central role in the pathogenesis and progression of different cancer types. All receptors consist of an extracellular part, a transmembrane domain and a cytoplasmic membrane. The four extracellular domains of the receptor are responsible for ligand binding and in an unbound state adopt a tethered conformation that is characterized by the interaction of domain II and IV. Upon ligand binding, the dimerization interface of domain II is exposed allowing receptor homo- or heterodimerization, thereby activation of the tyrosine-kinase domain in the cytoplasmic region. Subsequently, phosphorylation of the tyrosine residue in the cytoplasmic tail leads to activation of downstream signaling including the MAPK and PI_3K/AKT pathway. Physiologically, the receptors of the EGF family are essential for normal tissue development and are expressed on epithelial, mesenchymal and neuronal cells where their activation is tightly controlled by restriction of ligand expression. However, abnormal expression or function of the receptors results in an imbalance between cell proliferation and differentiation leading to carcinogenesis. Overexpression of the EGF receptors has been observed in numerous malignancies (Uberall et al. 2008). EGFR is involved in different processes during tumor progression e.g. motility, adhesion, invasion, survival and angiogenesis (Verbeek et al. 1998; Hazan and Norton 1998; Turnert et al. 1996; Grotendorst et al. 1989). Several approaches have been investigated targeting EGFR, whereby monoclonal antibodies and small molecule inhibitors have shown the most promising results. In 2004, Cetuximab, as one of the first monoclonal antibodies targeting EGFR, was approved by the FDA for the treatment of colorectal and head and neck cancer. Cetuximab is a chimeric IgG1 antagonistic monoclonal antibody binding to domain III of EGFR in the inactive form, thus blocking ligand-receptor interaction and formation of the active receptor (Sato et al. 1983). In preclinical studies, EGFR has also shown to be a suitable target to redirect T cells to tumor cells using bispecific antibodies targeting CD3 on the T cell and EGFR on the tumor cell (Gedeon et al. 2018; Mølgaard et al. 2018; Zhu et al. 2018; Harwood et al. 2017; Lutterbuese et al. 2010; Reusch et al. 2006). The bispecific antibody anti-CD3xanti-EGFR (EGFRBi) has been shown to increase cytotoxic activity of EGFRBi-armed cytokine-induced killer cells (CIK). Furthermore, in glioblastoma xenograft mice, infusion of EGFRBi-armed CIK cells inhibited glioblastoma tumor growth (Ma et al. 2015). In a first clinical study, patient derived activated T cells were generated which were then armed with the bispecific antibody EGFRBi creating EGFR bispecific antibody armed activated T cells

(EGFR BATs). So far, multiple injections of EGFR BATs did not show any dose limiting toxicities (Lum et al. 2015). EGFRBi armed activated T cells in combination with chemotherapy is currently under clinical investigation (NCT03269526) in phase I/II studies. Several other antibody-based approaches, e.g. CAR-engineered NK cells and anti-EGFR immunoliposomes directed against $EGFR^+$ tumors are in clinical or preclinical investigation (Han et al. 2015; Hsu et al. 2015; Mamot et al. 2012), highlighting the great potential of such therapeutic concepts. The EGFR-targeting moiety used in this study derived from a humanized version of the approved monoclonal antibody Cetuximab.

1.5 Purpose of this study

Supporting the activation of the immune system using members of the TNF superfamily and thereby unleashing an antitumor immune response is a rapidly evolving branch of cancer immunotherapy. This study focuses on trifunctional antibody-fusion proteins incorporating costimulatory ligands of the TNF superfamily in the single-chain format. The trifunctional antibody-fusion protein RD_IL-15_scFv_4-1BBL comprised of the homotrimeric TNFSF ligand, three targeting moieties directed against FAP ($scFv_{FAP}$) and three IL-15 fused to the extended sushi domain of the IL-15Rα chain (RD_IL-15), has already shown promising results *in vitro* and *in vivo* (Kermer et al. 2014). According to the concept, IL-15 is directed to the tumor site, where the cytokine activity is further enhanced by the costimulatory activity of 4-1BBL in a targeting-dependent manner. Thus, improved immune stimulation is expected to be achieved at lower cytokine dosage with reduced risk of systemic toxicity. The purpose of this study was to further develop this strategy by improving the fusion protein format, extending the concept to other costimulatory TNFSF members and direct it to a clinical relevant tumor target. A novel monomeric trifunctional antibody-fusion protein with a single-chain version of 4-1BBL was created (RD_IL-15_$scFv_{FAP}$_sc4-1BBL). Comparison of the homotrimeric antibody-fusion proteins and the novel monomeric antibody-fusion protein was performed regarding target and receptor binding, costimulatory activity, thermal stability and antitumor activity. Furthermore, other costimulatory members of the TNFSF namely OX40L and GITRL were incorporated into the novel trifunctional fusion protein single-chain format and evaluated in terms of protein assembly and stability, target and receptor binding and immunostimulatory activity on various immune cell subtypes. Additionally, two *in vivo* studies were performed using syngeneic tumor models with immunocompetent mice. Due to the distinct effect of IL-15 on NK cells, an additional set of bi- and trifunctional fusion

proteins targeting the tumor-associated antigen EGFR was implemented in order to combine them with a clinically approved monoclonal antibody to enhance the ADCC, thus exploring a further application option for this fusion protein.

2 Material

2.1 General supplies

All chemicals were purchased in p.a. quality by Merck (Darmstadt, Germany), Roche (Basel, Switzerland), Roth (Karlsruhe, Germany), Sigma-Aldrich (Taufkirchen, Germany) or VWR International (Fontenay-sous-Bois, France). Laboratory plastic was obtained from Greiner Bio-One (Frickenhausen, Germany). Any different sources are clearly stated.

2.2 Antibodies

All antibodies were purchased from Biolegend (San Diego, USA), Immunotools (Friesoythe, Germany), KPL (Gaithersburg, USA), Miltenyi Biotech (Bergisch-Gladbach, Germany), Merck (Darmstadt, Germany) or R&D Systems (Minneapolis, USA).

Table 2: Antibodies used in this study.

Antibody	clone	Isotype	Application	Source
PE anti-human CD3	OKT3	mouse IgG2a, κ	FC (1:100)	Biolegend
anti-human CD4 VioBlue©	M-T466	mouse IgG1,κ	FC (1:100)	Miltenyi Biotech
anti-human CD8 PE-Vio770™	BW135/80	mouse IgG2a,κ	FC (1:100)	Miltenyi Biotech
APC anti-human CD56	5.1H11	mouse IgG1,κ	FC (1:100)	Biolegend
FITC anti-human CD107a	H4A3	mouse IgG1,κ	FC (1:100)	Biolegend
PerCP/Cy5.5 anti-human CD3	OKT3	mouse IgG2a,κ	FC (1:100)	Biolegend
PE anti-human CCR7	G043H7	mouse IgG2a, κ	FC (1:100)	Biolegend
APC anti-human CD45RA	HI100	mouse IgG2b, κ	FC (1:100)	Biolegend
anti-human CD25 FITC	4E3	mouse IgG2b,κ	FC (1:100)	Miltenyi Biotech
anti-mouse and human FoxP3 PE	3G3	mouse IgG1,κ	FC (1:100)	Miltenyi Biotech
PE anti-human CD69	FN50	mouse IgG1,κ	FC (1:100)	Biolegend
anti-His PE	GG11-8F3.5.1	mouse IgG1	FC (1:200)	Miltenyi Biotech
Anti-human IgG (γ-chain specific)-PE		goat polyclonal	FC (1:500)	Merck
anti-human CD3ε Antibody	UCHT1	mouse IgG1	functional assays	R&D Systems
anti-mouse IgG (H+L)		goat polyclonal	functional assays	KPL
anti-mouse CD45 PE-Vio770™	30F11	rat IgG2b,κ	FC (1:100)	Miltenyi Biotech
FITC anti-mouse CD3	17A2	rat IgG2b,κ	FC (1:100)	Biolegend

anti-mouse CD4 VioBlue©	GK1.5	rat IgG2b,κ	FC (1:100)	Miltenyi Biotech
PE anti-mouse CD8a	53-6.7	rat IgG2a,κ	FC (1:100)	Biolegend
APC anti-mouse CD94	18d3	rat IgG2a,κ	FC (1:100)	Miltenyi Biotech
anti-mouse MHC class II PE	M5/114.15.2	rat IgG2b,κ	FC (1:100)	Miltenyi Biotech
anti-mouse CD11c FITC	N418	hamster IgG	FC (1:100)	Miltenyi Biotech
anti-human and mouse CD11b VioBlue©	M1/70.15.11.5	rat IgG2b,κ	FC (1:100)	Miltenyi Biotech
APC anti-mouse CD25	PC61	rat IgG1, λ	FC (1:100)	Biolegend
Mouse IgG1-PE	IS5-21F5	mouse IgG1	FC (1:100)	Miltenyi Biotech
Mouse IgG1-VioBlue©	X-56	mouse IgG1	FC (1:100)	Miltenyi Biotech
APC Mouse IgG1,κ Isotype Ctrl	MOPC-21	mouse IgG1,κ	FC (1:100)	Biolegend
FITC Mouse IgG1,κ Isotype Ctrl	MOPC-21	mouse IgG1	FC (1:100)	Biolegend
Mouse IgG2a-PE-Vio770™	S43.10	mouse IgG2a	FC (1:100)	Miltenyi Biotech
mouse IgG2a control PE	PPV-04	mouse IgG2a	FC (1:100)	Immunotools
PerCP/Cy5.5 Mouse IgG2a, κ Isotype Ctrl	MOPC-173	mouse IgG2a, κ	FC (1:100)	Biolegend
APC Mouse IgG2b, κ Isotype Ctrl	MPC-11	mouse IgG2b, κ	FC (1:100)	Biolegend
FITC Mouse IgG2b, κ Isotype Ctrl	MPC-11	mouse IgG2b, κ	FC (1:100)	Biolegend
PE Rat IgG2a, κ Isotype Ctrl	RTK2758	rat IgG2a, κ	FC (1:100)	Biolegend
APC Rat IgG2a, κ Isotype Ctrl	RTK2758	rat IgG2a, κ	FC (1:100)	Biolegend
Rat IgG2b-FITC	RG7/11.1	rat IgG2b	FC (1:100)	Miltenyi Biotech
Rat IgG2b-VioBlue©	RG7/11.1	rat IgG2b	FC (1:100)	Miltenyi Biotech
Rat IgG2b-PE-Vio770™	RG7/11.1	rat IgG2b	FC (1:100)	Miltenyi Biotech
PE Rat IgG2b, κ Isotype Ctrl	RTK4530	rat IgG2b, κ	FC (1:100)	Biolegend
APC Rat IgG1, λ Isotype Ctrl	G0114F7	rat IgG1, λ	FC (1:100)	Biolegend
FITC Armenian Hamster IgG Isotype Ctrl	HKT888	ah IgG	FC (1:100)	Biolegend
Anti-human IgG (F specific)-HRP		goat polyclonal	ELISA (1:5000)	Sigma-Aldrich

2.3 Bacteria

Escherichia coli TG1 supE thi-1 Δ(lac-proAB) Δ(mcrB-hsdSM)5 (rk- mK-) [F' traD36 proAB laclqZΔM15] (Stratagene, La Jolla, USA)

2.4 Buffers and Solutions

For all solutions water was used as a solvent, unless stated otherwise.

Bradford solution	Bio-Rad Protein Assay (Bio-Rad, Munich, Germany)
Buffers for cloning	restriction enzyme dependent (Thermo Fisher Scientific, Waltham, USA)
Coomassie solution	0.008% (w/v) Coomassie Brilliant Blue G-250, 35 nM HCl
DNA loading buffer, 5x	250 µg/ml xylenecyanol blue, 250 µg/ml bromphenol blue, 50 mM EDTA, 80% glycerol
DPBS	Dulbecco's phosphate-buffered saline (Thermo Fisher Scientific, Waltham, USA)
ELISA blocking solution (BSA)	1% (w/v) BSA in 1x PBS
ELISA blocking solution (MPBS)	2% (w/v) non-fat dry milk powder in 1xPBS
ELISA developing solution	100 mM sodium acetate pH 6.0, 100 µg/ml TMB in DMSO, 0.006% (v/v) H_2O_2
ELISA wash buffer (PBST)	0.1% (v/v) Tween in PBS
Fekete's solution	63.4% (v/v) ethanol absolute, 8.7% (v/v) formaldehyde (37%), 4.3% (v/v) glacial acetic acid
Fixation buffer	4% (v/v) PFA
FoxP3 Perm Buffer (10x)	(BioLegend, San Diego, USA)
HPLC buffer	0.1 M Na_2HPO_4, 0.1 M NaH_2PO_4, 0.1 M Na_2SO_4, pH 6.7
IMAC elution buffer	20% (v/v) 5x Sodium phosphate buffer, 250 mM imidazole
IMAC sodium phosphate buffer, 5x (low salt)	250 mM Na-phospohate (37.38 g Na_2HPO_4 + 6.24 g NaH_2PO_4 ad 1l H_2O), 1.25 M NaCl, pH 7.5
IMAC wash buffer	20% (v/v) 5x sodium phosphate buffer, 25 mM imidazole

Laemmli loading buffer, 5x	25% (v/v) glycerol, 10% (w/v) SDS, 0.05% (w/v) bromphenol blue, in 313 mM Tris, pH 6.8; reducing conditions: + 12,5% (v/v) β-mercaptoethanol
Brefeldin A (1000x)	(Biolegend San Diego, USA)
erythrocyte lysis buffer	55 mM NH_4Cl, 10 mM $KHCO_3$, 0.1 mM EDTA, 0.4 mM NaOH, pH 8.0
MTT	5 g/l MTT (Thiazol Blue Tetrazolium Bromide, approx. 98% TLC)
MTT lysis buffer	15% SDS (w/v) in Dimethylformamide/H_2O (1:1) with 80% acetic acid, pH 4.5-5
PBA	2% FCS, 0.2% NaN_3 in PBS
PBS	2.67 mM KCl, 1.47 mM KH_2PO_4, 137.93 mM NaCl, 8.06 mM Na_2HPO_4, pH 7.5
reagent diluent	0.1% (w/v) BSA, 0.05% (v/v) Tween20, 20 mM Tris, 150 mM NaCl, pH 7.2
SDS-PAGE running buffer, 5x	1.92 M glycine, 0.25 M Tris, 1% (w/v) SDS, pH 6.8
streptavidin Poly HRP	(Thermo Fisher Scientific, Waltham, USA)
TAE buffer 50x	2 M Tris, 0.95 M glacial acetic acid, 50 mM EDTA, pH 8

2.5 Cell lines

Table 3: Cell lines used in this study.

cell line	origin	stably transfected	media
B16	mouse melanoma		RPMI 1640, 5% FBS
B16-FAP	mouse melanoma	human FAP	RPMI 1640, 5% FBS, 200 µg/ml Zeocin
HT1080	human fibrosarcoma		RPMI 1640, 5% FBS
HT1080#33	human fibrosarcoma	human FAP	RPMI 1640, 5% FBS, 200 µg/ml G418
HEK293-6E	human embryonic kidney		FreeStyle Medium F17, 4 nM GlutaMAX-I, 0.1% (v/v) Kolliphor P188
SKBR-3	human breast adenocarcinoma		DMEM, 10% FBS
CTLL-2	mouse cytotoxic T lymphocytes		RPMI 1640, 20% FBS, 10 mM HEPES, 1x MEM-NEAA, 0.05 mM β-Mercaptoethanol, 1 mM natriumpyruvate, 400 IU/ml rhIL-2

2.6 Primary human cells

PBMCs	from healthy donors (Blutzentrale, Kinikum Stuttgart)

2.7 Enzymes

FastAP alkaline Phosphatase	1 U/µl (Thermo Fisher Scientific, Waltham, USA)
Pfu DNA-Polymerase	2.5 U/µl (Thermo Fisher Scientific, Waltham, USA)
Restriction enzymes	BamHI, EcoRI,NotI, SfiI, XbaI, XhoI (Thermo Fisher Scientific, Waltham, USA)
T4 DNA Ligase	5 U/µl (Thermo Fisher Scientific, Waltham, USA)

2.8 Instruments

balance	440-39N and 440-33N (Kern, Balingen, Germany)
centrifuge	Eppendorf 5804R (Eppendorf, Hamburg, Germany) AvantiJ301, rotors: JA14, JA30.5 (Beckman Coulter, Krefeld, Germany) Rotana 460 RF (Hettich Zentrifugen, Tuttlingen, Germany)
CO_2 incubator for cell culture	Varocell 140 (varolab GmbH, Giesen, Germany)

electrophoresis system	Mini PROTEAN© TetraCell, Mini-Sub© Cell GT and PowerPac™ Basic (Bio-Rad, Munich, Germany)
flow cytometer	MACSQuant Analyzer 10, MACSQuant VYB (Miltenyi Biotec GmbH, Bergisch-Gladbach, Germany)
gel documentation	Transilluminator, Gel documentation system Felix (Biostep, Jahnsdorf, Germany)
heat block	HBT1-131 (HLCHeap Labor Consult, Bovenden, Germany)
HPLC	Waters 2695 Separation Module, Waters 2489 UV/Visible Detector (Waters, Milford, USA)
incubator for bacteria	InforsHAT Multitron 2 (Infors AG, Basel, Swizerland)
laminar flow cabinet	Variolab Mobilien W90 (Waldner-Laboreinrichtung, Wangen, Germany)
magnetic stirrer	MR 3001K 800W (Heidolph Instruments, Nürnberg, Germany)
microplate reader	Tecan Spark® (Tecan, Crailsheim, Germany)
microscope	Olympus CKX41SF (Olympus, Tokyo, Japan)
PCR cycler	Eppendorf Mastercycler (Eppendorf, Hamburg, Germany)
pH-meter	PH 522 (Schütt Labortechnik, Göttingen, Germany)
spectrophotometer	Nanodrop® ND-1000 (pEQLab, Biotechnology, Erlangen, Germany)
Vortex	Vortex-Genie 2 (Scientific Industries Inc., Bohemia, New York, USA)
ZetaSizer	ZetaSizer Nano Z3 (Malvern, Herrenberg, Germany)

2.9 Kits and Markers

CellTrace™ CFSE Proliferation Kit	(Thermo Fisher Scientific, Waltham, USA)
GeneRuler™ DNA Ladder Mix	(Thermo Fisher Scientific, Waltham, USA)
human IFN-γ DuoSet ELISA	(R&D Systems Inc., Minneapolis, USA)

NucleoBond® Xtra Midi	(Macherey-Nagel, Düren, Germany)
NucleoSpin® Gel and PCR Clean-up	(Macherey-Nagel, Düren, Germany)
PageRuler™ prestained protein ladder	(Thermo Fisher Scientific, Waltham, USA)
REDTaq® ReadyMix™ PCR Reaction Mix	(Sigma-Aldrich, St. Louis, USA)
Tumor Dissociation Kit, mouse	(Miltenyi Biotec GmbH, Bergisch-Gladbach, Germany)
MACS Comp Bead Kit anti-mouse Igk	(Miltenyi Biotec GmbH, Bergisch-Gladbach, Germany)

2.10 Mice

C57BL/6	C57BL/6NCrl (Charles River, Wilmington, USA)

2.11 Plasmids

pIRESpuro3_msc4-1BBL-mscCD40L	Sina Fellermeier, 2015, Institute of Cell Biology and Immunology
pSecTagA_scFv36_hscOX40L	Sarah Ring, 2014, Institute of Cell Biology and Immunology
pSecTagA_RD_IL-15_scFv36_hscOX40L	Sarah Ring, 2014, Institute of Cell Biology and Immunology
pSecTagA_scFvhu225co_his_4-1BBL	Nadine Beha, 2014, Institute of Cell Biology and Immunology
pSecTagA(-XbaI)_RD_IL-15_scFv36_His_sc4-1BBL	Sarah Ring, 2014, Institute of Cell Biology and Immunology
pSecTagAHis_RD_IL-15_scFv36	Vanessa Kermer, 2012, Institute of Cell Biology and Immunology
pSecTAgA(-XbaI)_scFv36_his_sc4-1BBL	Sarah Ring, 2014, Institute of Cell Biology and Immunology

pAB1_scFvCEA	2006, Institute of Cell Biology and Immunology
pSecTagA_scFv36_hscGITRL	Sarah Ring, 2014, Institute of Cell Biology and Immunology
pSecTagA_RD_IL-15_scFv36_hscGITRL	Sarah Ring, 2014, Institute of Cell Biology and Immunology

2.12 Primers for cloning

Primers were synthesized by Sigma Aldrich (St. Louis, USA) and dissolved in H_2O to a concentration of 50 µM and stored at -20°C.

Table 4: Primers for cloning.

Name	Application	Sequence (5'-3')
msc4-1BBL-Stop-EcoRI-for	cloning: pSecTagA_scFv36_msc4-1BBL pSecTagA_RD_IL-15_scFv36_msc4-1BBL	CCGGAATTCTTACTCCCAAGGGTTGT CGGGCTTGAC
BamHI-msc4-1BBL-back	cloning: pSecTagA_scFv36_msc4-1BBL pSecTagA_RD_IL-15_scFv36_msc4-1BBL	CGCGGATCCTCTAGAAGGACCGAGC CACGGCCCGCCCTC
CEA(VL)-NotI-for	cloning: pSecTagA_RD_IL-15_scFvCEA_mscGITRL	ATAGTTTAGCGGCCGCCCGTTTCAG CTCCAGCTTGGTGCC
CEA(VH)-XhoI-back.	cloning: pSecTagA_RD_IL-15_scFvCEA_mscGITRL	AC CGGTCG ACC GGA GGC GGT TCA CAG GTG AAA CTG CAG CAG TCT GGG
hu225co-NotI-for	cloning: pSecTagA_scFvhu225co_sc4-1BBL pSecTagA_RD_IL-15_scFvhu225co_sc4-1BBL	ATAGTTAGCGGCCGCTCTCTTGATTT CCAGCTTGGTGCC
hu225co-XhoI-back	cloning: pSecTagA_scFvhu225co_sc4-1BBL pSecTagA_RD_IL-15_scFvhu225co_sc4-1BBL	AACCGCTCGAGCGGAGGCGGTTCA GAGGTGCAGCTGGTCGAGTCTGGC
pSec-Seq2	reverse Primer for pSecTag	TAGAAGGCACAGTCGAGG
pET-Seq1	forward Primer for pSecTag	TAATACGACTCACTATAGG
leikr-back	reverse Primer for msc-4-1BBL	AAGCTGGAAATAAAACGG
pweggggs-back	reverse Primer for msc-4-1BBL	CCCTGGGAGGGCGGCGGAGGAAGC

2.13 Recombinant proteins

4-1BB-Fc	extracellular domain of human 4-1BB (aa 24-186) fused to human Fcγ1
OX40-Fc	extracellular domain of human OX40 (aa 29-214) fused to human Fcγ1
GITR-Fc	extracellular domain of human GITR (aa 26-161) fused to human Fcγ1 (R&D Systems, Minneapolis, USA)
m4-1BB-Fc	extracellular domain of mouse 4-1BB (aa 24-187) fused to human Fcγ1 (R&D Systems, Minneapolis, USA)
mGITR-Fc	extracellular domain of mouse GITR (aa 22-153) fused to human Fcγ1 (R&D Systems, Minneapolis, USA)
scDb33xCD3	single chain diabody targeting FAP and CD3 (Institute of Cell Biology and Immunology, Hornig et al. (2012))
Cetuximab	Erbitux®, kindly provided by Dr. Thomas Mürdter (Robert-Bosch-Krankenhaus, Stuttgart, IKP, Germany)
Trastuzumab	Herceptin®, kindly provided by Prof. Hans-Heinrich Heidtmann (St. Joseph Hospital, Bremerhaven, Germany)

2.14 Reagents and Media for bacterial culture

Ampicillin (1000x)	100 mg/ml
LB medium (w/v)	1% peptone, 0.5% yeast extract, 0.5% NaCl
$LB_{Amp, Glc}$ agar plates	LB medium, 2% (w/v) agar; after autoclaving addition of ampicillin to 100 µg/ml and 1% (w/v) D-glucose

2.15 Reagent and Media for mammalian cell culture

DMEM	(Thermo Fisher Scientific, Waltham, USA)
Eosin	0.4% Eosin, 10% FBS, 0.02% NaN_3, in PBS
FBS	FBS Premium (PAN Biotech, Aidenbach, Germany)

Freestyle F17-medium	Supplemented with 4 mM GlutaMAX-I (Thermo Fisher Scientific, Waltham, USA), 0.1% Kolliphor P188 (Sigma-Aldrich, Taufkirchen, Germany)
G418 disulfate salt	Merck KGaA, Darmstadt, Germany
human Plasma	from healthy donors (Blutzentrale, Kinikum Stuttgart)
Lymphocyte Separation Medium	(PromoCell, Heidelberg, Germany)
PEI	Polyethylenimin, linear, 25 kDa (Sigma-Aldrich, Taufkirchen, Germany)
Penicillin/Streptomycin (Pen/Strep)	100x (Thermo Fisher Scientific, Waltham, USA)
RPMI 1640	supplemented with L-Glutamine (Thermo Fisher Scientific, Waltham, USA)
TN1	20% (w/v) Trypton N1 in Freestyle F17 Medium+GlutaMAX-I+Kolliphor P188
Trypsin (10x)	0.5% Trypsin Glutamine (Thermo Fisher Scientific, Waltham, USA)
Zeocin™	100 mg/ml (Thermo Fisher Scientific, Waltham, USA)
HEPES (1 M)	(Thermo Fisher Scientific, Waltham, USA)
MEM NEAA (100x)	(Thermo Fisher Scientific, Waltham, USA)
β-Mercaptoethanol (50 mM)	(Thermo Fisher Scientific, Waltham, USA)
rhIL-2	Recombinant Human Interleukin-2 (Immunotools, Friesoythe, Germany)

2.16 Software

Graphic analysis	GraphPad Prism© (GraphPad Software, La Jolla, USA)
	Microsoft Excel 2010 (Microsoft, Redmond, USA)
Flow cytometry analysis	FlowJo 10.4 (tree Star Inc, Ashland, USA)

Sequence analysis	Clone Manager 9 (Scientific & Educational Software, Cary, USA) NCBI Blast (http://blast.ncbi.nim.nih.gov/Blast.cgi)
Protein database	UniProt (http://www.uniprot.org/)
Literature research	NCBI PubMed (https://www.ncbi.nlm.nih.gov/pubmed)

2.17 Special implement

Dialysis chamber	Slide-A-Lyzer© Dialysis Cassettes, 0.5-3 ml capacity, MWCO 10000 (Thermo Fisher Scientific, Waltham, USA)
cell strainer	Falcon™ Cell Strainers, 70 µm, nylon
Dialysis membrane	ZelluTrans, MWCO 6,000-8,000, 40 mm (Carl Roth, Karlsruhe, Germany)
ELISA plates	MICROLON 96-well high binding capacity
Hemocytometer	Neubauer improved (PlanOptik, Elsoff, Germany)
HPLC column	Yarra™ SEC-3000 (Phenomenex, Aschaffenburg, Germany) TSKgel Supra SW3000 (Tosoh Bioscience LLC, King of Prussia, USA)
IMAC affinity matrix	Ni-NTA-Agarose (Qiagen, Hilden, Germany)
Microtiter plates	Microtiter plate Cellstar© 96-well
polycarbonate membrane cell culture inserts	Corning® Transwell® 24 mm with 5 µm pores
Poly-Prep Chromatograpy columns	(Bio-Rad, Munich, Germany)
Reaction tubes	1.5 ml, 2 ml Safe-lock (Eppendorf AG, Hamburg, Germany)
Syringe filters	Acrodisc© 13 mm with 0.2 µm HT Tuffym© membrane (Pall Corporation, Dreieich, Germany)

3 Methods

3.1 Cloning strategy of murine homologs of tri-functional fusion proteins

For the generation of pSecTagA_scFv36_msc4-1BBL and pSecTagA_RD_IL-15_scFv36_msc4-1BBL, the DNA fragment encoding for the msc4-1BBL was amplified from pIRESpuro3_msc4-1BBL-mscCD40L using the primers msc4-1BBL-Stop-EcoRI-for and BamHI-msc4-1BBL-back. After restriction digestion with BamHI and EcoRI, msc4-1BBL was inserted into pSecTagA_scFv36_hscOX40L or pSecTagA_RD_IL-15_scFv36_hscOX40L, respectively replacing hscOX40L.

To generate pSecTagA(-XbaI)_scFv36_mscGITRL and pSecTagA(-XbaI)_RD_IL-15_scFv36_mscGITRL, the DNA fragment encoding for mscGITRL was synthesized by GeneArt including an XbaI and EcoRI restriction site flanking mscGITRL. After restriction digestion with XbaI and EcoRI, mscGITRL was inserted into pSecTagA(-XbaI)_scFv36_msc4-1BBL and pSecTagA(-XbaI)_RD_IL-15_scFv36_msc4-1BBL, respectively replacing msc4-1BBL.

The CEA-targeting tri-functional fusion protein was cloned by amplification of the DNA fragment encoding for $scFv_{CEA}$ from pAB1_scFvCEA using the primers CEA(VL)-NotI-for and CEA(VH)-XhoI-back. The DNA fragment was introduced into pSecTagA(-XbaI)_RD_IL-15_scFv36_mscGITRL via the restriction sites for NotI and XhoI replacing scFv36.

3.2 Cloning strategy of fusion proteins targeting EGFR

The fusion proteins targeting EGFR pSecTagA(-XbaI)_RD_IL-15_scFvhu225co_His_sc4-1BBL and pSecTagAHis_RD_IL-15_scFvhu225co were generated by the amplification of scFvhu225co from pSecTagA_scFvhu225co_his_4-1BBL using the primers hu225co-NotI-for and hu225co-XhoI-back followed by restriction digestion with NotI and XbaI and the insertion of the DNA fragment into pSecTAgA(-XbaI)_RD_IL-15_scFv36_His_sc4-1BBL and pSecTagAHis_RD_IL-15_scFv36 respectively, replacing scFv36.

For the generation of the bi-functional fusion protein targeting EGFR, restriction digestion of pSecTagA_scFvhu225co_his_4-1BBL with SfiI and NotI was performed and the DNA fragment corresponding for scFvhu225co was inserted into pSecTAgA(-XbaI)_scFv36_his_sc4-1BBL resulting in pSecTAgA(-XbaI)_scFvhu225co_his_sc4-1BBL.

3.3 PCR

Polymerase chain reaction was used for the amplification of desired DNA fragments and the introduction of restriction sites for cloning. The reaction was prepared as follows:

10 ng	Template DNA
2.5 µl	dNTPS (each sNTP 50 mM, 200 mM total)
1 µl	Forward and reverse Primer (10 pmol/µl)
0.5 µl	Pfu Polymerase 1 U/µl
Ad to 50 µl	ddH_2O

The following PCR program with 30 cycles of denaturation, annealing and elongation was used for the amplification of DNA fragments. The elongation time differed depending on the expected length of the desired DNA fragment (Pfu Polymerase: 500 bp/min).

	Temperature [°C]	Duration [min]
Pre cycle	94	5
Denaturation	94	1
Annealing	52	1
Elongation	72	1 min/500 bp
Post cycle	72	5

The obtained DNA was purified by preparative agarose gel electrophoresis.

3.4 Gel electrophoresis

After amplification and after digestion, DNA was analyzed using gel electrophoresis. DNA samples were mixed with 5x DNA loading buffer to a final concentration of 1x DNA loading buffer and together with PageRuler™ Prestained Protein Ladder separated on a 1% (w/v) agarose gel with 1 µg/ml ethidium bromide in TAE buffer for 50 minutes and applied voltage of 80 V. The desired DNA fragments were excised under UV light and purified using NucleoSpin© Gel and PCR clean up kit according to the manufacturer's instructions. DNA was eluted from the columns using 30 µl ddH_2O.

3.5 Restriction digestion

Depending on the experiment, either 10 µg of plasmid DNA or the purified PCR product was used for restriction digestion. The buffer and the temperature at which the restriction digestion is optimal were chosen according to manufacturer's instructions. If different

reaction conditions were required for restriction enzymes, consecutive digestion was performed with puffer exchange in between using the NucleoSpin® Gel and PCR clean up Kit according to the manufacturer's instructions. To avoid relegation, vector DNA was dephosphorylated using 1 µl Fast AP thermos-sensitive alkaline phosphatase [1 U/µl] at 37°C for 20 minutes. After restriction digestion vector and insert fragments were separated using agarose gel electrophoresis. The desired DNA fragments were excised under UV light and isolated using NucleoSpin® Gel and PCR clean up Kit according to the manufacturers' instructions.

3.6 Ligation

For ligation of linearized and dephosphorylated vector and insert, molar ratios of 1:1, 1:3 and 1:5 with a fixed quantity of 20 ng vector was used. Linearized and dephosphorylated vector without addition of insert served as control. The ligation was performed using 1 µl of T4 DNA ligase [5 U/µl] in a total volume of 20 µl for 1 h at room temperature.

3.7 Transformation

For transformation 100 µl of freshly thawed chemical competent TG1 E.coli were gently mixed with 10 µl of the ligation mix. After Incubation for 15 minutes on ice, heat shock was performed for 2 minutes at 42°C followed by 1 minute incubation on ice. Then 1 ml of LB medium was added and after incubation at 37°C for 30-90 minutes, TG1 cells were harvested by centrifugation [1500g, 1 min] and plated on LB agar plates containing ampicillin and glucose. Plates were incubated o/n at 37°C.

3.8 Isolation of plasmid DNA

Overnight cultures of LB medium with 1% (v/v) glucose and 100 µg/ml ampicillin were inoculated from a single colony (5 ml for Mini Preparation or 100 ml for Midi preparation) and incubated at 37°C, 170 rpm. Cells were harvested the next day by centrifugation (3500 g, 15 min) and plasmid DNA was isolated using NucleoSpin® Plasmid kit (Mini) or NucleoBond Xtra® Midi kit (Midi) according to manufacturer's instructions. In the case of Midi preparation, DNA was air dried and dissolved in 100 µl ddH_2O, for Mini preparation, DNA was eluted in 30 µl ddH_2O and till further use stored at -20°C. Plasmid identity was confirmed by sequencing.

3.9 Sequence analysis

Sanger sequencing of plasmid DNA was performed using the LIGHTRUN tube system of GATC Biotech (GATC Biotech AG, Konstanz). For further analysis, Clone Manager 9 Basic Edition and Nucleotide BLAST® algorithm was used.

3.10 Photometric determination of DNA concentration

The DNA concentration was determined photometrically at 260 nm using Nanodrop 1000 3.8.1.

3.11 Mammalian cell culture

3.11.1 General cultivation methods

Mammalian cells were cultivated at 37°C in a humidified atmosphere with 5% CO_2. Adherent cells were grown in tissue culture flasks and passaged every 2-3 days using 1x Trypsin-EDTA for detachment. For long time storage cells were detached at 80% confluency, resuspended in FBS with 10% DMSO (v/v) aliquoted into cryo vials and frozen gradually to - 80°C in a cryo box filled with isopropanol. For thawing the cells cryo vials were shortly incubated in a water bath at 37°C and added to 10 ml of the appropriate culture medium. Cells were harvested by centrifugation (500 g, 5 minutes) and transferred into a tissue culture flask with the respective culture medium.

3.11.2 PBMCs

PBMCs were isolated from buffy coats of anonymous healthy donors provided by the blood bank of the Klinikum Stuttgart. All steps during PBMC isolation were performed at room temperature. The buffy coat (approximately 80 ml) was diluted with RPMI 1640 to a total volume of 240 ml. In order to separate the erythrocytes and granulocytes from the lymphocytes, 10 ml lymphocyte separation medium was carefully overlaid with 30 ml of the diluted buffy coat followed by centrifugation (800 g, 20 minutes without break). Most of the supernatant containing plasma and platelets was removed before the white interphase that formed due to the gradient centrifugation containing the PBMCs was carefully collected, transferred into a new tube, diluted with RPMI to a total volume of 50 ml and centrifuged at 650 g for 15 minutes. To remove remaining platelets, the pellet was washed twice using 50 ml RPMI 1640. In the last step PBMCs were pooled, counted and resuspended in FBS +

10% DMSO (v/v), aliquoted into cryo vials and gradually frozen to - 80°C in a cryo box filled with isopropanol.

3.11.3 Isolation of regulatory T cells

Regulatory T cells were separated from freshly isolated PBMCs using human $CD4^+$ $CD25^+$ Regulatory T Cell isolation kit according to the manufacturers' instructions. In brief first, negative selection was performed where all non-$CD4^+$ cells were removed using an antibody cocktail directly coupled to magnetic beads. In the second step, positive selection for $CD4^+$ $CD25^+$ cells was performed using an anti-CD25-biotin antibody followed by the incubation with streptavidin coupled magnetic beads. Purity of the isolated $CD4^+CD25^+$ and $CD4^+CD25^-$ T cells fraction was determined using flow cytometry (anti-CD3-PerCP/Cy5.5, anti-CD4-VioBlue and anti-FoxP3-PE staining).

3.12 Expression and purification of recombinant proteins

3.12.1 Transfection of HEK293-6E

HEK293-6E cells were cultured in an orbital shaker at 37°C with 5% CO_2, 70% humidity and 115 rpm. All fusion proteins were produced using the HEK293-6E system. Plasmid DNA and PEI were mixed in a ratio of 1:2. Depending on the total volume of HEK293-6E cell culture, the amount of DNA and PEI was adjusted according as follows:

Volume of HEK293-6E cell culture	50 ml	100 ml	200 ml
Plasmid DNA [µg]	50	100	200
PEI [µg]	100	200	400

The day of transfection cell count of HEK293-6E cells was adjusted to 1.7 x 10^6 cells/ml and two transfection solutions were prepared. Solution A consisted of F17-medium++ (5% of volume of HEK293-6E cell culture) with plasmid DNA and solution B consisted of F17-medium++ (5% of volume of HEK293-6E cell culture) mixed with PEI (1 mg/ml for solution). Both solutions were incubated for 2 min before they were combined, incubated for additional 15 minutes at room temperature before being carefully added to the cells. After 24 h incubation in the orbital shaker, 0.5% (v/v) TN1 was added. Supernatants were harvested by centrifugation (650 g for 15 minutes) 96 hours post transfection and dialyzed (MWCO 6,000-8,000) against PBS overnight at 4°C.

3.12.2 Immobilized metal ion affinity chromatography (IMAC)

All fusion proteins were purified via their His-tag by IMAC using affinity matrix Ni^{2+}-Nitrilo-Triacetic-Acid-Agarose (Ni-NTA Agarose). Dialyzed HEK293-6E supernatants were incubated overnight with 1 ml Ni-NTA beads at 4°C under rotation. The next day Ni^{2+}-NTA-Protein-suspension was applied to a chromatography column where beads were retained and the flow through was collected. Unspecifically bound proteins were removed by applying IMAC wash buffer to the column (10-20 ml). Subsequently, Ni^{2+}-NTA bound protein was eluted in 4-6 500 µl fractions using IMAC elution buffer. To quantify the amount of protein in the wash fraction as well as in the elution fractions qualitative Bradford assay (10 µl of sample + 90 µl of 1x Bradford reagent) was used. Protein-containing fractions of similar blue coloration were pooled and dialyzed (MWCO 10,000) against 5 l of PBS overnight at 4°C.

3.13 Biochemical characterization

3.13.1 SDS polyacrylamide gel electrophoresis

To determine the molecular mass and purity of the recombinant proteins SDS-PAGE (12%) was performed. Therefore, protein samples (3 µg) were mixed with reducing or non-reducing 5x Laemmli loading buffer to a final concentration of 1x, denaturated at 95°C for 5 minutes and separated at 40 mA/gel in SDS-PAGE running buffer using polyacrylamide gels prepared the following:

	Stacking gel (5%)	Separating gel (12%)
ddH_2O	4.1 ml	4.9 ml
30% PAA	1.0 ml	7.5 ml
1.5 M Tris-HCl pH 8.0	-	3.8 ml
1 M Tris-HCl pH 6.8	0.75 ml	-
10% SDS	0.06 ml	0.15 ml
10% APS	0.06 ml	0.15 ml
TEMED	0.006 ml	0.006 ml

After separation, residual salt and detergent were removed by boiling the polyacrylamide gel three times in H_2O. Proteins were stained using Coomassie staining solution for at least 1 h and destaining was performed using hot water for several hours.

3.13.2 Size exclusion chromatography

Size exclusion chromatography was performed to determine the oligomerization state of the proteins under native conditions. 40 µl of purified protein at a concentration of 0.2-0.6 mg/ml was loaded on a Yarra™ SEC-3000 column at a flow rate of 0.5 ml/min with 0.1 M Na_2HPO_4/NaH_2PO_4, 0.1 M Na_2SO_4, pH 6.7 as mobile phase. As reference molecules, the proteins thyroglobulin (669 kDa), β-Amylase (200 kDa), bovine serum albumin (67 kDa) and carbonic anhydrase (29 kDa) were used. To determine the size of the proteins, the retention time was interpolated in the standard curve using GraphPad Prism.

3.13.3 Thermal stability

Zetasizer Nano ZS was used to analyze the thermal stability of the proteins by dynamic light scattering. A glass cuvette was filled with 100 µg sterile filtered protein in 1 ml PBS and temperature increased in a range of 35°C to 85°C in 1°C intervals. After equilibration of the sample for 2 minutes, two measurements were performed at each temperature. The temperature showing a clear increase in the detected mean count rate indicating variation in particle size was defined as the melting point.

3.14 Functional characterization

Fusion proteins were diluted in the respective solvent (MPBS in ELISA, PBA for flow cytometry, RPMI + 10% FCS for cell based assay and DPBS for animal experiments) in all experiments.

3.14.1 ELISA

Enzyme-linked immunosorbent assay (ELISA) was used to determine the simultaneous binding of the fusion proteins to the target (FAP) via the antibody moiety and the respective receptor via the ligand part. FAP-Flag (1 µg/ml) was immobilized on a 96-well high binding plate overnight at 4°C in 100 µl PBS followed by washing with PBS and blocking of the residual binding sites with 2% MPBS (200 µl/well) for 1h at RT. After another washing step with PBS, samples diluted in 2% MPBS were added in duplicates (100 µl/well) and incubated for 1h at RT. After two washing steps with PBST (0.005% Tween 20) and one with PBS, respective TNFSF-receptor-Fc fusion protein (100 ng/well) was applied. Two washing steps with PBST and one with PBS were performed before addition of anti-huFc-HRP (1:5000) for

1 h. The afore mentioned washing procedure was repeated before 100 µl/well substrate solution (100 mM sodium acetate pH 6.0, 0.1 mg/ml TMB, 0.006% (v/v) H_2O_2) was added. Enzymatic reaction was stopped with 50 µl 1 M H_2SO_4 after distinct blue coloration. Absorbance was measured at 450 nm using the Tecan Spark®.

3.14.2 Flow cytometry

3.14.2.1 Identification of immune cell subsets and their functional characterization

The expression of cell surface and intracellular markers (CD3, CD4, CD8, CD56, CD69, CD107a, CD45RA, CCR7, FoxP3) was used to identify T cell subsets and NK cells and analyze their functional properties using flow cytometry. Cells were seeded into a U bottom microtiter plate and incubated (1 h at 4°C) with directly labeled mAb against the respective marker. After a three times washing step with PBA, cells were analyzed using MACSQuant Analyzer 10. If multicolor staining was used, spectral overlap was compensated using MACS Comp Bead Kit anti-mouse Igk according to manufacturers' instructions. Fluorochrome-conjugated antibody combinations for the determination of leucocyte subpopulations are shown in Table 5.

Table 5: Identification of leucocyte subpopulations.

leucocyte subpopulations	fluorochrome-conjugated mAbs
CD4/CD8 T cells	αCD3-PE, αCD4-VioBlue, αCD8-PE-Vio770
NK cells	αCD3-PE, αCD56-APC
T cell subtypes (naïve, central memory, effector and effector memory)	αCD3-PerCP, αCD4-VioBlue, αCD8-PE-Vio770, αCD4-VioBlue, αCD8-PE-Vio770, αCD45RA-APC, αCCR7-PE
regulatory T cells	αCD3-PerCP, αCD4-VioBlue, αCD25-APC, αFoxP3-PE
Cytotoxicity of T cells	αCD3-PE, αCD4-VioBlue, αCD8-PE-Vio770, αCD107a-FITC

3.14.2.2 Binding analysis

Binding of fusion proteins to targets on the cell surface was determined using flow cytometry. $2x10^5$ target cells per well were seeded into a U-well plate and incubated (1 h, 4°C) with 100 µl of a serial dilution of the respective recombinant protein. After centrifugation (500 g, 5 min, 4°C) and washing three times with PBA cells were incubated for 1 h at 4°C with the respective detection system. For direct detection of the His-tagged fusion proteins a PE conjugated anti-His mAb was used. To verify simultaneous binding of a surface

antigen and respective receptor of the TNF superfamily ligand, cells with bound recombinant fusion protein was incubated with the respective TNFSFR-huFc fusion protein (5 µg/ml, 1 h at 4°C). After washing three times with PBA a PE conjugated anti-human Fc antibody was added for 1 h at 4°C. After three washing steps with 150 µl PBA, cells were resuspended in 150 µl PBA and analyzed using MACSQuant Analyzer 10 or MACSQuant VYB. Data analysis was performed using FlowJo Version 8.8.6 and 10.2. The relative MFI was calculated using the following formula:

$$relative\ MFI = \frac{MFI_{sample} - (MFI_{detection} - MFI_{cells})}{MFI_{cells}}$$

Following a method published by Benedict et al. 1997 the concentration corresponding to half-maximal binding (EC_{50}) was calculated from the relative MFI using Graphpad Prism 6.

3.14.2.3 Stimulatory activity of recombinant fusion proteins

To assess the stimulatory effects of fusion proteins on PBMCs in a targeted setting, target cells were seeded in a concentration of $2x10^4$ cells/well in a 96-well F-bottom microtiter plate and incubated o/n at 37°C with 5% CO_2. PBMCs were thawed and cultivated at 37°C with 5% CO_2 for 2 h in a concentration of about $10\text{-}15x10^6$ cells/10 ml in an Ø 10 cm petri dish to allow the monocytes to adhere. Thereafter, the cells were transferred into a new Ø 10 cm petri dish and cultivated at 37°C with 5% CO_2 o/n. All assays were carried out in a total volume of 200 µl using RPMI supplemented with 10% FCS. The next day, the supernatant on the target cells was removed and 50 µl of the titrated fusion proteins or 50 µl medium as control was added. After incubation for 1 h at RT to ensure target cell binding, unbound fusion protein was removed by washing three times with RPMI supplemented with 10% FCS before 100 µl of $2x10^5$ PBMCs/well were added. To support the activation of PBMCs in the coculture setting, 100 µl of a αCD3 mAb (previously cross-linked for 30 min with an anti-mouse IgG (H+L) mAb at a molar ratio of 1:3) in a suboptimal concentration (PBMC batch dependent) was added. In the non-targeted setting, a dilution series of the fusion proteins was prepared in a 96-well microtiter plate (100 µl/well) and 100 µl of $2x10^5$ PBMCs/well were added. The targeted as well as the non-targeted assays were incubated at 37°C with 5% CO_2 for 1-6 days, according to the read out to be analyzed.

3.14.2.4 IFN-γ ELISA

Stimulation of T cells by the recombinant fusion proteins was determined measuring the concentration of IFN-γ in the supernatants by sandwich ELISA (DuoSet Human IFN-γ # DY285, R&D Systems). Therefore, the coculture setting described in 3.14.2.3 was incubated for 48 h (5% CO_2, 37 °C) followed by centrifugation (500 g, 5 min). Cell-free supernatants were harvested and aliquots stored at-20°C.

A mouse anti-human IFN-γ Ab was immobilized on a 96-well high binding plate overnight at 4°C in 100 µl PBS followed by blocking of the residual binding sites with 200 µl 10% BSA in PBS for 1 h. In the meantime, cell-free supernatants harvested from the coculture assay were diluted 5- to 20-fold in RPMI. For the standard a serial dilution (1:2, RPMI) starting at a concentration of 1000 µg/ml was prepared. After blocking, 100 µl standard/supernatant were transferred into the plate and incubated for 2 h followed by washing and the addition of the detection antibody (biotinylated goat anti-human-IFN-γ Ab) provided by the kit (concentration Lot dependent, diluted in reagent diluent). For detection, streptavidin Poly-HRP (0.5 mg/ml) was added in a dilution of 1:5000 in reagent diluent and incubated for 20 min. After each incubation step, the ELISA plate was washed three times using 0.005% PBS-tween followed by one time washing with PBS. In the last step, substrate solution (100 mM sodium acetate buffer pH 6.0, 0.1 mg/ml TMB, 0.006% H_2O_2) was added and the enzymatic reaction was stopped with 50 µl 1M H_2SO_4 after distinct blue coloration. Absorbance was measured at 450 nm using the Tecan Spark®. IFN-γ concentration was determined via the interpolated standard curve.

3.14.2.5 Interleukin-10 release assay

IL-10 release by regulatory and effector cells upon stimulation with the targeted trifunctional fusion proteins was measured in sandwich ELISA (DuoSet Human IL-10 # DY217B, R&D Systems). Therefore, target cells were incubated with 90 nM of the respective fusion protein, unbound fusion protein was removed by three times washing with RPMI supplemented with 10% FCS and $2x10^4$ T_{regs}/well or T_{eff}/well as well as a cross-linked anti-CD3 antibody (0.5 µg/ml) were added. After incubation for 24 hours at 37°C with 5% CO_2, cell-free supernatants were harvested and aliquots stored at -20°C.

A mouse anti-human IL-10 Ab was immobilized on a 96-well high binding plate overnight at 4°C in 100 µl PBS followed by blocking of the residual binding sites with 200 µl 10% BSA in

PBS. In the meantime, cell-free supernatants harvested from the assay stated above were diluted 5- to 20-fold in RPMI. For the standard a serial dilution (1:2, RPMI) starting at a concentration of 2000 µg/ml was prepared. After 1 h of blocking, 100 µl standard and supernatant were transferred into the plate to incubate for 2h followed the addition of the detection antibody (biotinylated goat anti-human-IL-10 Ab) provided by the kit (concentration Lot dependent, diluted in reagent diluent). For detection, streptavidin Poly-HRP (0.5 mg/ml) was added in a dilution of 1:5000 in reagent diluent and incubated for 20 min. After each incubation step, the ELISA plate was washed three times using 0.005% PBS-tween followed by one time washing with PBS. In the last step, substrate solution (100 mM sodium acetate buffer pH 6.0, 0.1 mg/ml TMB, 0.006% H_2O_2) was added and the enzymatic reaction was stopped with 50 µl 1M H_2SO_4 after distinct blue coloration. Absorbance was measured at 450 nm using the Tecan Spark®.

3.14.2.6 Proliferation

To analyze the proliferative effect, PBMCs were labeled using the CellTrace™ CFSE Cell Proliferation Kit. Therefore, PBMCs were resuspended in PBS with 0.1% BSA at a cell count $1x10^6$ cells/ml and CFSE with final concentration of 625 nM was added. After incubation at 37°C for 15 minutes, internalization of CFSE was stopped by incubation on ice for 5 minutes and addition of double the volume of cold RPMI 1640 + 10% FBS. Cell count was determined and adjusted to meet the conditions of the respective assay. Every isolated PBMC batch was tested for its proliferative response upon stimulation with a cross-linked anti-human CD3 mAb [100-0.001 ng/ml]. To this end, a mouse anti-human CD3 mAb and a goat anti-mouse IgG (H+L) were mixed in a molar ratio of 1:3, incubated for 30 minutes at room temperature followed by serial dilution and the addition to B16-FAP cells with PBMCs. A suboptimal cross-linked anti-CD3 antibody concentration inducing 20-40% of the maximal proliferation capacity was implemented for further proliferation assays measuring the activity of targeted fusion proteins. CFSE labeled PBMCs ($2x10^5$ cells/well) were added to target cells preincubated with the respective targeted fusion protein and cross-linked anti-CD3 antibody in a suboptimal concentration as indicated in 3.14.2.3. For the non-targeted setting CFSE labeled PBMCs were added to a serial dilution of the respective fusion protein only. After 6 days the cells were harvested, transferred into a U bottom plate and resuspended in PBA. In order to analyze the proliferation of T cells, NK cells or T cell subtypes, additional antibody staining of corresponding cell surface markers was performed. Harvested PBMCs were

incubated with anti-CD3-PE, anti-CD4-VioBlue, anti-CD8-PEVio770 and anti-CD56-APC for 1h at 4°C and washed three times with 150 µl PBA before analysis of the proliferation of T cells and NK cells. Proliferation was determined by CFSE dilution through cell division analyzed by flow cytometry using MACSQuant Analyzer 10 or MACSQuant VYB.

3.14.2.7 PBMC subsets

Proliferation response and changes in composition of naïve (T_N, CD45RA$^+$ CCR7$^+$), central memory (T_{CM}, CD45RA$^-$ CCR7$^+$), effector memory (T_{EM}, CD45RA$^-$ CCR7$^-$) and effector (T_E, CD45RA$^+$ CCR7$^-$) T cells upon fusion protein stimulation was analyzed by flow cytometry. CFSE labeled PBMCs ($2x10^5$ cells/well) were added to target cells ($2x10^4$ cells/well) preincubated with the respective targeted fusion protein in presence of a cross-linked anti-CD3 antibody in a suboptimal concentration. After 6 d of incubation at 37°C with 5% CO_2 PBMCs were harvested, resuspended in PBA and stained with anti-CD3-PerCP, anti-CD4-VioBlue, anti-CD8-PEVio770, anti-CCR7-PE and anti-CD45RA-APC. After 1 h incubation and three times washing with 150 µl PBA, analysis of proliferation and composition of the indicated T cell subsets was performed using MACSQuant Analyser10.

3.14.2.8 Cytotoxicity assay

ADCC by NK cells was assessed using MTT assay. For this purpose, $2x10^4$ SKBR-3 cells/well were seeded in a 96-well plate. The next day the target cells were preincubated with the respective fusion proteins (100 nM) for 1h at RT. After washing three times with medium, targeted fusion proteins were incubated in presence of a serial dilution of Trastuzumab (1 nM-0,06 pM) with PBMCs, applied at a concentration of $2x10^4$ NK cells/well (equals target-to-effector ratio of 1:1). After 24 h incubation at 37°C with 5% CO_2 PBMCs were carefully removed and CD107a cell surface levels analyzed by flow cytometry using anti-CD3-PE, anti-CD56-APC and anti-CD107a-FITC antibody staining in presence of Brefeldin A solution. To analyze tumor cells viability, MTT (10 µl MTT + 100 µl RPMI 1640 +10% FBS each well) was added to the remaining target cells. After incubation at 37°C for 2h, MTT lysis buffer (90 µl) was added. Formazan formation was determined after incubation for 4 h at 37°C by measuring the absorption at 595 nm with reference wavelength 655 nm in the Tecan reader.

3.14.2.9 CTLL-2 Proliferation assay

The activity of IL-15 was determined in a cytokine-growth-dependent proliferation assay. Therefore, $2x10^4$ CTLL-2 cells/well were seeded in a F bottom plate, starved in IL-2 free medium for 4 h at 37°C with 5% CO_2. Fusion proteins were added in a serial dilution. After incubation for 72 h at 37°C with 5% CO_2 proliferation of CTLL-2 cells was determined by adding 10 µl MTT to each well. After incubation at 37°C for 2 h, MTT lysis buffer (120 µl) was added. Released formazan was determined after incubation for 3 d at RT by measuring the absorption at 595 nm with reference wavelength 655 nm.

3.14.2.10 Cytotoxic potential of T cells

The cytotoxic potential of T cells was determined by measuring the level of CD107a on the cell surface of degranulating T cells. Therefore, $2x10^5$ PBMCs/well were added to previously seeded target cells ($2x10^4$ cells/well) preincubated with a serial dilution of the respective fusion protein and the crosslinked anti-CD3 antibody at a suboptimal concentration. After incubation for 5 days, the prestimulated PBMCs were transferred to fresh target cells ($2x10^4$ cells/well, seeded the day before) previously preincubated with scDbFAPxCD3 [30 pM] for 1h. The bispecific antibody retargets the T cells to the tumor cells, triggering T cell-mediated cytotoxicity involving the release of cytolytic proteins by degranulation. After 6 h of incubation at 37°C with 5% CO_2 PBMCs were harvested and staining was performed using anti-CD3-PE, anti-CD4-VioBlue, anti-CD8-PEVio770 and anti-CD107a-FITC in presence of Brefeldin A solution. After 1 h incubation and three times washing with 150 µl PBA, flow cytometric analysis was performed using MACSQuant Analyser10.

3.14.2.11 Expression of CD69 activation marker

The activation of regulatory T cells ($CD4^+$ $CD25^+$) or effector T cells ($CD4^+$ $CD25^-$) mediated by the trifunctional fusion proteins was determined by CD69 cell surface expression analysis by flow cytometry. Thus, target cells were incubated for 1h at RT with 90 nM of the respective fusion protein. Unbound fusion protein was removed by three times washing with RPMI supplemented with 10% FCS. $2x10^4$ T_{regs}/well or T_{eff}/well as well as a cross-linked anti-CD3 antibody (0.5 µg/ml) were added. After incubation for 24 hours at 37°C with 5% CO_2, the T cells were harvested, resuspended in PBA and staining with anti-CD3-PerCP, anti-CD4-VioBlue, anti-CD25-FITC and anti-CD69-PE was performed. After 1 h incubation and three times washing with 150 µl PBA, analysis of the early activation marker ($CD69^+$) on regulatory

T cells ($CD4^+$ $CD25^+$) and effector T cells ($CD4^+$ $CD25^-$) was performed using MACSQuant Analyser10.

3.15 Protein stability

3.15.1 *In vitro* serum stability

Serum stability of the fusion proteins was determined by dilution the fusion proteins to a final concentration of 200 nM in 50% human plasma. The samples were either directly stored at - 20°C (day 0 value) or incubated at 37°C for 1, 3 or 7 days prior to storage at-20°C. Levels of intact protein was determined in ELISA via binding of the antibody moiety to recombinant FAP and detection via the respective receptor-Fc fusion protein and anti huFc-HRP. ELISA with the diluted samples (1:2 in MPBS) was performed as described in 3.14.1. Protein concentrations in the diluted samples were interpolated from a standard curve of purified fusion protein and normalized to the value of day 0.

3.16 Animal studies

Animal care and experiments were performed in accordance with federal guidelines and were approved by the university and state authorities. All intravenous injections were performed by Dr. Oliver Seifert.

3.16.1 B16-FAP lung tumor model

To determine the therapeutic potential of the trifunctional fusion proteins a syngeneic lung tumor mouse model was used (Hornig et al. 2013; Kermer et al. 2012; Kermer et al. 2014). Groups of six female C57BL6/N at the age of 8 months received one injection with $8.5x10^5$ B16-FAP cells in 100 µl DPBS per mouse on day 0. On day 1,2 and 10 mice were treated with intraperitoneal injections (100 µl) of fusion proteins or DPBS as a control. Mice were sacrificed on day 21 by CO_2 inhalation. Lunges were removed, fixed and bleached in Fekete's solution and metastasis were counted.

3.16.2 B16-FAP solid tumor model

A syngeneic solid tumor model was used to analyze the *in vivo* antitumor activity of the trifunctional fusion proteins. $5x10^5$ B16-FAP cells (in 100 µl DPBS) were injected subcutaneously into each flank of female C57BL6/N mice at the age of 6 months. Tumor growth was monitored by measuring the length (a) and the width (b) of the tumors using a

caliper. Tumor volume was calculated using the formula: V = a x b^2 /2. Mice were treated intraperitoneal with 0.2 nmol RD_IL-15_scFv, RD_IL-15_scFv_mscGITRL or PBS on days 1,2,10,11,12,13 and 14. On day 15 and 18 mice received a higher dose of 0.4 nmol of the respective fusion proteins. Tumor volume was measured on a daily basis. Tumors and spleen were analyzed for infiltrated immune cell on day 21 when mice were sacrificed.

3.16.2.1 Tumor dissociation and analysis of tumor infiltration lymphocytes

Tumors of each treatment group were pooled according to their size (3-4 pooled tumor samples, 1-3 tumors each sample) and the weight of each tumor sample was determined. Tumors bigger than 1000 mm^3 were cut and only ¼ was used for further analysis. For isolation of immune cells from the tumors Tumor Dissociation Kit, mouse (Miltenyi Biotec GmbH, Bergisch-Gladbach, Germany) was used according to the manufacturer's instructions. Dissociated tumors were analyzed for infiltrating immune cells by flow cytometry using anti-mouse CD45-PEVio770, anti-mouse CD3-FITC, anti-mouse CD4-VioBlue, anti-mouse CD8-PE and anti-mouse CD94-APC.

3.16.2.2 Isolation and analysis of spleenocytes

For harvesting immune cells from the spleen, spleens were extracted and a homogeneous cell suspension was prepared by mashing the spleen through a 70 µm cell strainer. After a washing step with RPMI1640 + 10% FBS, cells were resuspended in 10 ml erythrocyte lysis buffer and incubated for 2 minutes at 37°C. To stop the reaction, 40 ml RPMI 1640 + 10% FCS were added. The erythrocyte lysis step was repeated till total lysis was achieved. Isolated spleenocyte were analysed by flow cytometry using anti-mouse CD3-FITC, anti-mouse CD4-VioBlue, anti-mouse CD8-PE and anti-mouse CD94-APC.

3.17 Statistics

Unless stated otherwise, all data are represented as mean with the corresponding standard deviation of at least three independent experiments. If necessary, daily variability of effector and target cells was compensated using blockshift correction according to

$$X'_n = X_n - (Y_n - \bar{Y})$$

with X'_n is the corrected value of X from the experiment n, $\bar{Y}$ is the average of the X values from all experiments performed and Y_n is the average of the duplicate values of X from

experiment n. Significances were calculated using one-way ANOVA followed by Tukey's post test or unpaired t-test (GraphPad Prism 6). P values below 0.05 were considered statistically significant (*** P <0.001, ** P <0.01, * P <0.05).

4 Results

4.1 Bifunctional tumor-targeted antibody-fusion proteins

Previous studies of homotrimeric antibody-fusion proteins with non-covalent trimerization via the TNF superfamily ligand have demonstrated targeting-dependent costimulatory activity and antitumor potential (Kermer et al. 2014; Hornig et al. 2013; Müller et al. 2008a). For further development, novel fusion proteins of simpler configuration and smaller size have been generated by introducing the TNFSFL in a single chain format, i.e. genetic fusion of three extracellular domains of the TNFSF ligand by linkers on the same polypeptide chain (Figure 3A). Hence, a monomeric costimulatory fusion protein (scFv_scTNFSFL) with a single-chain version of 4-1BBL was generated targeting the fibroblast activation protein (FAP).

The bifunctional antibody-fusion proteins were composed of a FAP-directed scFv ($scFv_{FAP}$) antibody moiety and the extracellular domain (ECD) of the TNFSF member 4-1BBL (aa 71-254). They were generated in two different formats (Figure 3A). In the homotrimeric format, the scFv was linked to the N-terminus of the ECD of 4-1BBL and noncovalent trimerization of the ligand led to the formation of a homotrimeric fusion protein, composed of three antibody units and one functional 4-1BBL unit ($scFv_{FAP}$_4-1BBL) (Müller et al. 2008a). In the novel single-chain format, the scFv was fused to the first of three consecutive linked ECDs of 4-1BBL, leading to a monomeric single-chain fusion protein where intramolecular trimerization 4-1BBL takes place, resulting in a molecule with only one antibody unit and one functional ligand unit, respectively ($scFv_{FAP}$_sc4-1BBL) (Fellermeier et al. 2016). The linker connecting the scFv and 4-1BBL was 15 amino acids long and contained a hexahistidine-tag. The linkers between the ECDs in sc4-1BBL were identical and composed of $(GGGGS)_4$. Both antibody-fusion proteins were provided with an Ig_κ-chain leader sequence for cell secretion and a hexahistidine-tag between the scFv and the ECD of the TNFSF ligand for purification and detection.

4.1.1 Biochemical properties

$ScFv_{FAP}$_4-1BBL and $scFv_{FAP}$_sc4-1BBL were transiently produced in HEK293-6E cells and purified by immobilized metal affinity chromatography (IMAC) with yields of 3.0 mg/l ($scFv_{FAP}$_4-1BBL) and 7.4 mg/l ($scFv_{FAP}$_sc4-1BBL). Protein purity was confirmed by SDS-PAGE analysis under reducing (R) and non-reducing (NR) conditions revealing single bands

corresponding to the respective monomer of the two antibody-fusion proteins (Figure 3B). The determined apparent molecular masses for $scFv_{FAP}$_4-1BBL (approximately 50 kDa) and $scFv_{FAP}$_sc4-1BBL (approximately 89 kDa) correlated to the calculated molecular masses of 47.7 kDa and 89.2 kDa, respectively.

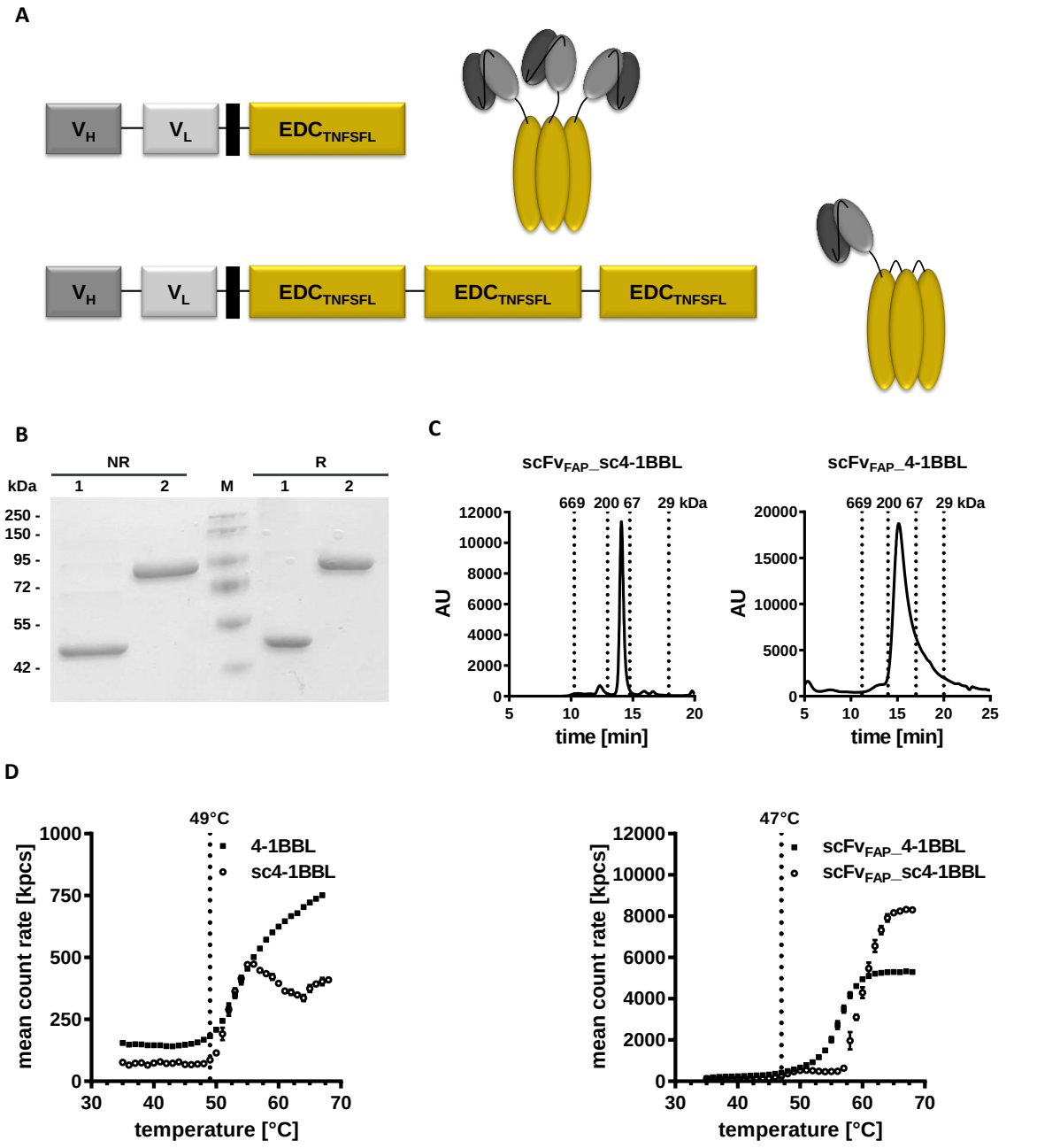

Figure 3: Biochemical characterization of bifunctional antibody-fusion proteins. A Molecular composition and schematic assembly of $scFv_{FAP}$_4-1BBL and $scFv_{FAP}$_sc4-1BBL. **B** SDS-PAGE analysis (12% PAA; 3 µg/lane; Coomassie Brilliant Blue staining) of $scFv_{FAP}$_4-1BBL (1) and $scFv_{FAP}$_sc4-1BBL (2) was performed under non-reducing (NR) and reducing (R) conditions. M, protein marker. **C** Size exclusion chromatography was used to investigate the proteins under native conditions. Elution times of standard proteins and their corresponding molecular mass [kDa] are indicated as dashed lines. **D** Dynamic light scattering was used to determine thermal stability. The melting point is indicated as a dotted line.

Size exclusion chromatography showed one major peak corresponding to the correct assembled trimeric (scFv$_{FAP}$_4-1BBL) or monomeric (scFv$_{FAP}$_sc4-1BBL) molecules under native conditions, respectively (Figure 3C). For scFv$_{FAP}$_sc4-1BBL only a minor peak of high molecular weight species was observed (Figure 3C). Thermal stability of 4-1BBL, sc4-1BBL, scFv$_{FAP}$_4-1BBL and scFv$_{FAP}$_sc4-1BBL was analyzed by dynamic light scattering revealing a melting point of 49°C for both, 4-1BBL and sc4-1BBL. Likewise, the two antibody-fusion proteins scFv$_{FAP}$_4-1BBL and scFv$_{FAP}$_sc4-1BBL exhibited similar stability with a melting point of 47°C (Figure 3D). All evaluated biochemical characterizations are summarized in Table 6. In summary, scFv$_{FAP}$_4-1BBL and scFv$_{FAP}$_sc4-1BBL could be expressed and purified to a high degree, showing correct apparent size and assembly. Fusion of the antibody moiety to 4-1BBL in both formats did not alter thermal stability.

Table 6: Biochemical characterization of the bifunctional antibody-fusion proteins with 4-1BBL.

Fusion protein	MW_{calc}* (kDa, monomer)	MW_{PAGE} (kDa, monomer)	MW_{SEC} (kDa)	Yield (mg/l)
scFv$_{FAP}$_4-1BBL	47.7	50	134	3.0
scFv$_{FAP}$_sc4-1BBL	89.2	89	97	7.4

* the calculated molecular mass (MW_{calc}) is based on the amino acid sequence.

4.1.2 Binding properties

Binding of scFv$_{FAP}$_4-1BBL and scFv$_{FAP}$_sc4-1BBL to FAP expressing cells (B16-FAP) was determined by flow cytometry (Figure 4A). As expected, the antibody-fusion proteins only bound to target expressing cells (B16-FAP) whereas no binding was detected on the FAP negative cells (B16). Bound fusion protein was detected with 4-1BB-Fc and anti-Fc-PE, thus confirming simultaneous binding of the fusion proteins to the antigen (FAP) and the recombinant 4-1BB receptor (Figure 4A). Binding capacity of scFv$_{FAP}$_4-1BBL and scFv$_{FAP}$_sc4-1BBL was compared (Figure 4B). While the homotrimeric fusion protein scFv$_{FAP}$_4-1BBL showed strong binding (EC_{50} 0.15±0.1 nM), the monomeric fusion protein scFv$_{FAP}$_sc4-1BBL showed factor 30 weaker binding (EC_{50} 4.6±1.8 nM) that was similar to the binding observed for scFv$_{FAP}$ only (EC_{50} 3.3±0.17 nM). Thus, the lower antibody valency of scFv$_{FAP}$_sc4-1BBL led to a reduced binding capacity in comparison to the scFv$_{FAP}$_4-1BBL.

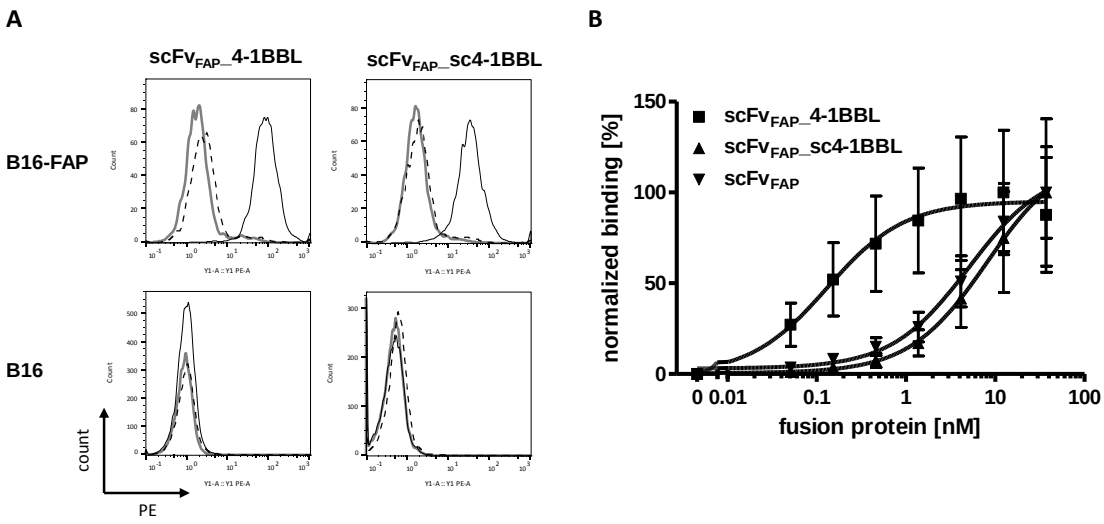

Figure 4: Binding properties of antibody-fusion proteins with 4-1BBL analyzed in flow cytometry. A Bifunctional binding scFv-ligand fusion proteins (40 nM) were incubated either on FAP^+ (B16-FAP) or FAP^- (B16) cells. Antibody-mediated binding was detected via ligand-receptor interaction, using recombinant 4-1BB-Fc (5 µg/ml). Detection of the receptor was performed by anti-human Fc-PE mAb. Thick grey line, cells only; dashed black line, detection system; black line, fusion protein. **B** Comparison of the antibody binding capacity. HT1080-FAP cells were incubated with scFv or scFv-ligand fusion proteins in a serial dilution followed by detection via anti-His-PE mAb. Mean ± SD, n=3.

4.1.3 Costimulatory activity

According to the concept of tumor-targeted costimulation of T cells, it was analyzed how the antigen-binding properties of the bifunctional scFv-ligand fusion proteins would translate into target-mediated costimulatory activity. Hence, a co-culture assay with tumor target cells and human PBMCs in presence of a suboptimal concentration of a cross-linked anti-CD3 mAb and the bifunctional fusion proteins was performed, whereby costimulatory activity was measured in terms of PBMC proliferation. ScFv$_{FAP}$_4-1BBL as well as scFv$_{FAP}$_sc4-1BBL showed to be costimulatory active, enhancing the anti-CD3 mAb-induced T cell proliferation (Figure 5A), whereupon scFv$_{FAP}$_sc4-1BBL was more potent at lower concentrations (0.1-3 nM) compared to scFv$_{FAP}$_4-1BBL. In line with the costimulatory nature of 4-1BBL, no PBMC activation was induced by the fusion proteins themselves, i.e. without CD3-mediated primary stimulus. Furthermore, it was analyzed if the costimulatory effect of the single-chain fusion proteins was also target-dependent. In the absence of target cells scFv$_{FAP}$_sc4-1BBL showed some enhancement of PBMC proliferation compared to scFv$_{FAP}$_4-1BBL that did not (Figure 5B). Thus, scFv$_{FAP}$_sc4-1BBL showed apparently stronger, but less targeting-restrictive costimulatory activity than scFv$_{FAP}$_4-1BBL.

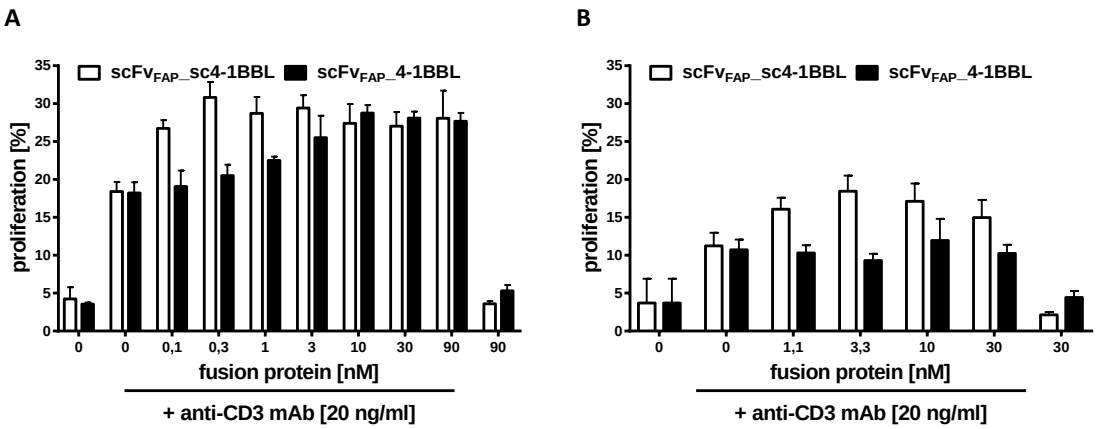

Figure 5: Costimulatory activity of scFv-ligand fusion proteins in target-bound (A) or non-target bound (B) form. PBMCs were incubated with a suboptimal concentration of cross-linked anti-CD3 mAb and scFv-ligand fusion proteins either in **A** presence of HT1080-FAP target cells or **B** without target cells. Mean ± SD, Blockshift, n=3.

4.2 Trifunctional tumor-targeted antibody-fusion proteins with IL-15 and 4-1BBL

Next, the TNFSF ligand 4-1BBL in the single-chain format was introduced in the trifunctional, homotrimeric antibody-fusion protein RD_IL-15_scFv$_{FAP}$_4-1BBL (Kermer et al. 2014), in order to develop a novel fusion protein version of simpler configuration and smaller size that supports this concept.

Trifunctional tumor-targeted antibody-fusion proteins were composed of IL-15 fused to the extended sushi domain of the IL-15Rα chain (aa 31-107) (RD_IL-15), a FAP-directed antibody moiety (scFv) and one or three units of the extracellular domain (ECD) of the TNFSF member 4-1BBL (aa 71-254) (Figure 6A). In the homotrimeric format, RD_IL-15 is fused to the N-terminus of the scFv and the scFv is linked to the N-terminus of one ECD of 4-1BBL. Non-covalent trimerization of 4-1BBL leads to the formation of a homotrimeric molecule composed of one functional 4-1BBL unit, three antibody units and three RD_IL-15 units (RD_IL-15_scFv_4-1BBL). In the novel single-chain format, RD_IL-15_scFv$_{FAP}$ was fused to the N-terminus of the first of the three consecutive ECDs of 4-1BBL (sc4-1BBL), leading to a monomeric single-chain fusion protein with one functional unit of each component (RD_IL-15_scFv_sc4-1BBL). The glycine-serine linker connecting the extracellular domain of the IL-15Rα and IL-15 had a length of 20 amino acids, the linker between scFv and TNFSF ligand was 15 amino acids long, while the linkers between the ECDs of sc4-1BBL was composed of $(GGGGS)_4$. The homotrimeric as well as the single-chain fusion protein were provided with

an Ig_{κ}-chain leader sequence for cell secretion and a His-tag between the scFv and the ECD of the TNFSF ligand for purification and detection.

4.2.1 Biochemical characterization

The trifunctional fusion proteins were transiently produced in HEK293-6E cells and purified by immobilized metal affinity chromatography (IMAC) with yields of 15.0 mg/l (RD_IL-15_scFv$_{FAP}$_4-1BBL) and 21 mg/l (RD_IL-15_scFv$_{FAP}$_sc4-1BBL). Protein purity and integrity was confirmed in SDS-PAGE analysis under reducing (R) and non-reducing (NR) conditions revealing bands corresponding to the monomer of the two antibody-fusion proteins (Figure 6B). The slight double band observed for RD_IL-15_scFv$_{FAP}$_4-1BBL under reducing conditions could be explained by the six potential N-glycosylation sites provided by the three IL-15 moieties (Thaysen-Andersen et al. 2016). The molecular mass determined from the SDS-PAGE for RD_IL-15_scFv$_{FAP}$_4-1BBL (~63 kDa) and RD_IL-15_scFv$_{FAP}$_sc4-1BBL (~105 kDa) correlated to the calculated molecular masses of 71.2 and 112.6 kDa, respectively. Assembly into trimeric (RD_IL-15_scFv$_{FAP}$_4-1BBL) or monomeric (RD_IL-15_scFv$_{FAP}$_sc4-1BBL) molecules under native condition was confirmed by one major peak in size exclusion chromatography, respectively (Figure 6C). RD_IL-15_scFv$_{FAP}$_sc4-1BBL showed in addition two minor peaks corresponding probably to dimers (~259 kDa, 17%) and higher oligomers (~414 kDa, 37%). Dynamic light scattering was used to determine thermal stability of the two trifunctional fusion proteins, revealing a melting point of 47°C which is identical to the melting point of the corresponding bifunctional antibody-fusion proteins (Figure 6D). Hence, fusion of RD_IL-15 to scFv$_{FAP}$_sc4-1BBL or scFv$_{FAP}$_4-1BBL, respectively did not influence thermal stability. Thus, both trifunctional antibody-fusion proteins were obtained at high purity and correctly assembled with similar thermal stability. Biochemical properties are outlined in Table 7.

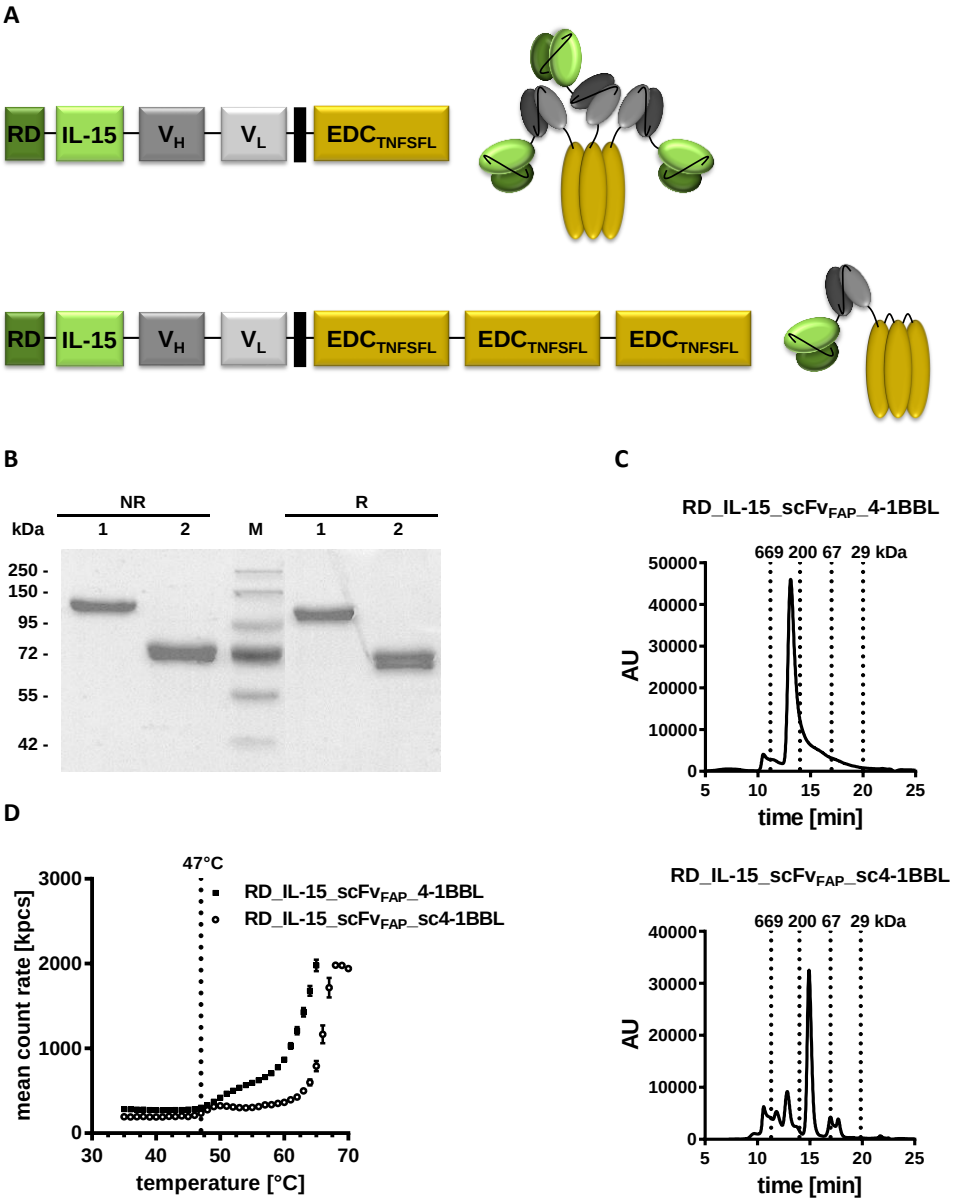

Figure 6: Biochemical characterization of trifunctional fusion proteins. A Molecular composition and schematic assembly of RD_IL-15_scFv$_{FAP}$_4-1BBL and RD_IL-15_scFv$_{FAP}$_sc4-1BBL. **B** SDS-PAGE analysis (12% PAA; 3 µg/lane; Coomassie Brilliant Blue staining) of RD_IL-15_scFv$_{FAP}$_sc4-1BBL (1) and RD_IL-15_scFv$_{FAP}$_4-1BBL (2) was performed under non-reducing (NR) and reducing (R) conditions. M, protein marker. **C** Size exclusion chromatography was used to investigate the proteins under native conditions. Elution times of standard proteins and their corresponding molecular mass [kDa] are indicated as dashed lines. **D** Thermal stability was determined using dynamic light scattering. Dotted line indicates the melting point.

Table 7: Biochemical characterization of the trifunctional antibody-fusion proteins.

Fusion protein	MW_{calc}* (kDa, monomer)	MW_{PAGE} (kDa, monomer)	MW_{SEC} (kDa)	Yield (mg/l)
RD_IL-15_scFv$_{FAP}$_4-1BBL	71.2	63	233	15.0
RD_IL-15_scFv$_{FAP}$_sc4-1BBL	112.6	105	141	21.0

* the calculated molecular mass (MW_{calc}) is based on the amino acid sequence.

4.2.2 Binding properties

Simultaneous binding to FAP expressing cells (B16-FAP) and to the receptor 4-1BB of the trifunctional antibody-fusion proteins was determined using flow cytometry with 4-1BB-Fc and anti-Fc-PE as a detection system (Figure 7A). Antibody-mediated binding could only be observed to target expressing cells (B16-FAP) while no binding could be detected to the FAP negative cell line (B16). The homotrimeric fusion protein RD_IL-15_scFv$_{FAP}$_4-1BBL showed three-fold stronger binding (EC_{50} 0.3±0.3 nM) than the monomeric fusion protein RD_IL-15_scFv$_{FAP}$_sc4-1BBL (EC_{50} 0.92±0.5 nM) (Figure 7B). Thus, lower antibody valency of the RD_IL-15_scFv$_{FAP}$_sc4-1BBL fusion protein manifested in reduced target-binding compared to RD_IL-15_scFv$_{FAP}$_4-1BBL. However, both trifunctional fusion proteins showed the capability to bind simultaneously target-expressing tumor cells and the recombinant receptor 4-1BB, confirming functionality of the antibody moiety and the TNFSF ligand.

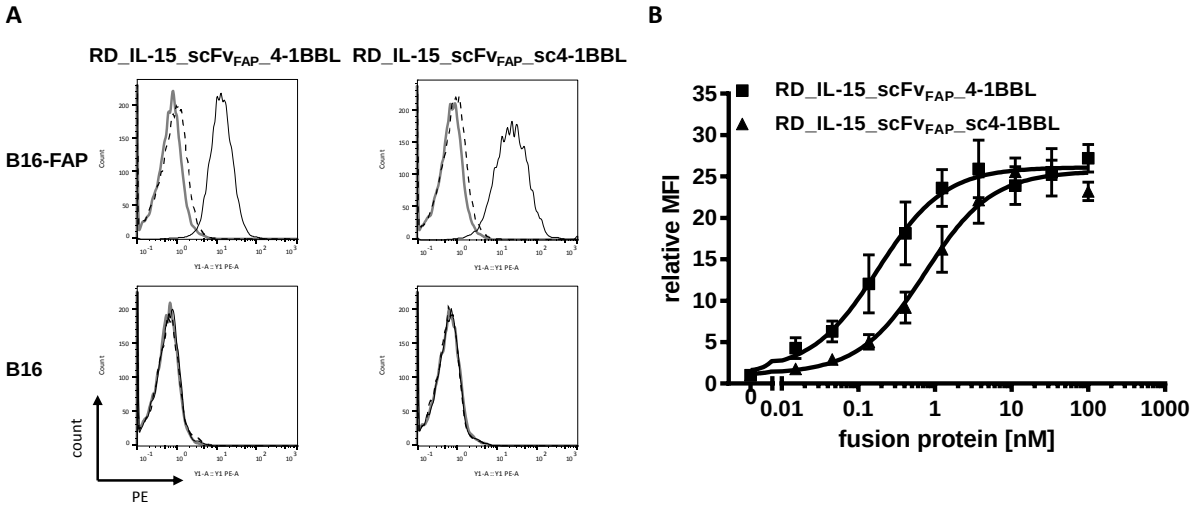

Figure 7: Binding properties of trifunctional fusion proteins. Flow cytometry was used to determine binding to target cells. **A** Dual binding to FAP and the 4-1BB receptor. Trifunctional fusion proteins (40 nM) were incubated either on FAP^+ (B16-FAP) or FAP^- (B16) cells. Antibody-mediated binding was detected via ligand-receptor interaction, using recombinant 4-1BB-Fc (5 µg/ml). Detection was performed by anti-human Fc-PE mAb. Thick grey line, cells only; dashed black line, detection system; black line, fusion protein. **B** Comparison of the antibody-binding capacity. B16-FAP cells were incubated with a serial dilution of the trifunctional fusion proteins followed by detection via anti-4-1BBL-PE mAb. Mean ± SD, n=3.

4.2.3 Activity of trifunctional antibody-fusion proteins

RD_IL-15 is active in a target bound as well as in a soluble form. First, the IL-15 activity of the non-targeted trifunctional fusion proteins was assessed. Therefore, PBMCs were incubated with the trifunctional fusion proteins in absence of target cells. RD_IL-15 scFv$_{FAP}$_4-1BBL as well as RD_IL-15_scFv$_{FAP}$_sc4-1BBL showed similar activity with EC_{50} 1.14±0.07 nM and

EC_{50} 1.8±0.23 nM, respectively. Compared to RD_IL-15_scFv$_{FAP}$ (EC_{50} 0.28±0.05 nM), both trifunctional fusion proteins showed reduced proliferative activity, suggesting that proliferation of PBMCs is driven by stimulation via RD_IL-15 (Figure 8B). Lower RD_IL-15 valency in RD_IL-15_scFv$_{FAP}$_sc4-1BBL did not translate into lower IL-15 activity in the non-targeted setting.

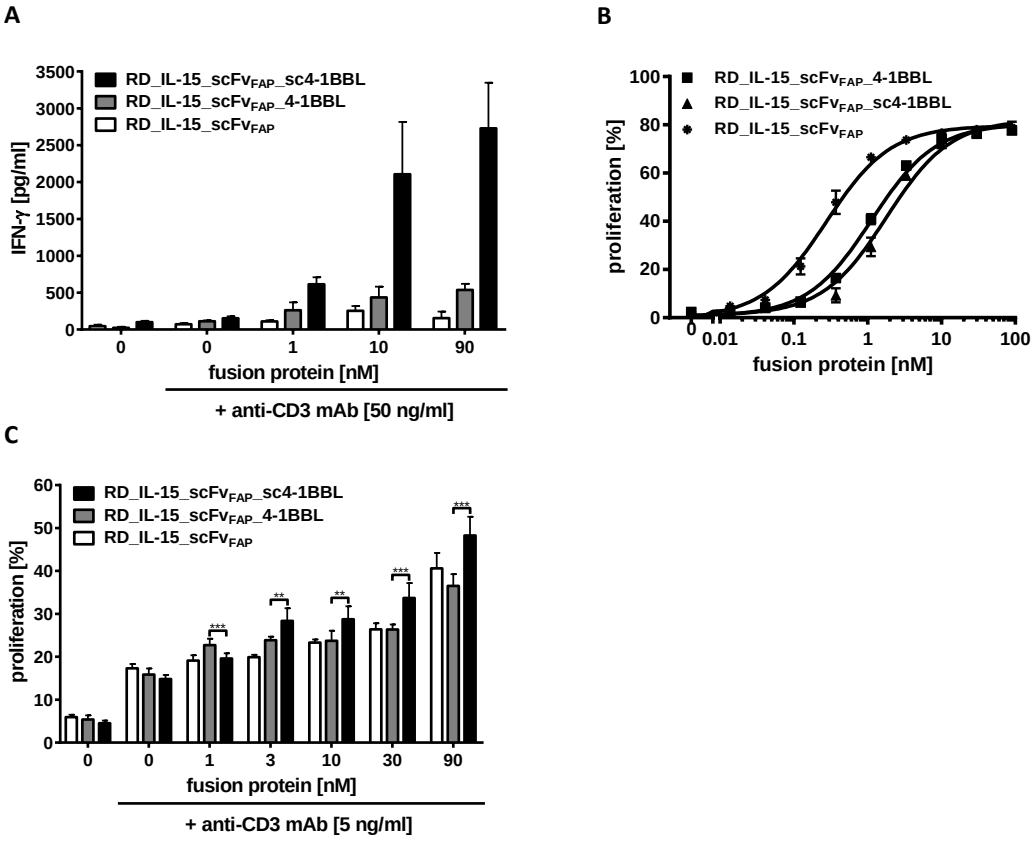

Figure 8: Activity of trifunctional fusion protein in target bound (A and C) or non-target bound (B) form on PBMC proliferation and cytokine release. A B16-FAP cells were co-cultured with PBMCs, a suboptimal concentration of a cross-linked anti-CD3 mAb and fusion proteins. IFN-γ release was measured after 48 h via Sandwich-ELISA. **B** PBMCs were incubated with a serial dilution of fusion proteins in absence of target cells. The proliferation of CFSE-labeled PBMCs was determined after 6 days via flow cytometry. **C** B16-FAP cells were co-cultured with PBMCs, a suboptimal concentration of a cross-linked anti-CD3 mAb and targeted fusion proteins. After 6 days, proliferation of PBMCs was measured by CFSE dilution in flow cytometry. Mean ± SD, Blockshift, n=3, one-way ANOVA, Tukey's post hoc test, ***p<0.001, **p<0.01.

In the targeted setting, PBMCs were incubated with the trifunctional fusion proteins in presence of target cells and a suboptimal concentration of a cross-linked anti-CD3 mAb. To assure the presence of target-bound fusion protein only, unbound fusion protein was removed by washing before addition of PBMCs and the cross-linked anti-CD3 mAb to the co-culture assay. Costimulatory activity, enhancing the anti-CD3 mAb-induced stimulation was measured in terms of proliferation and IFN-γ release. The trifunctional fusion protein in the single chain format (RD_IL-15_scFv$_{FAP}$_sc4-1BBL) was more potent compared to RD_IL-

15_scFv$_{FAP}$_4-1BBL not only in terms of proliferation (Figure 8C), but also in terms of IFN-γ release (up to 5-fold) (Figure 8A). In summary, introduction of the TNFSF ligand 4-1BBL in the single-chain format manifested in higher costimulatory activity of the antibody-fusion protein in the targeted approach.

4.2.4 Antitumor activity in a syngeneic mouse model

Therapeutic antitumor potential of the trifunctional antibody-fusion proteins was investigated *in vivo* using a syngeneic B16-FAP lung metastases tumor model in C57BL/6 mice, previously established in the laboratory (Kermer et al. 2012; Hornig et al. 2013; Kermer et al. 2014). Since inter-species cross-reactivity is not given for human and mouse 4-1BBL (Bossen et al. 2006), in the trifunctional fusion protein the human 4-1BBL was substituted by mouse 4-1BBL (aa 104-309). Thus, RD_IL-15_scFv$_{FAP}$_msc4-1BBL was generated and compared to the corresponding RD_IL-15_scFv$_{FAP}$_m4-1BBL variant (Kermer et al. 2014).

4.2.4.1 Characterization of the trifunctional fusion proteins for the *in vivo* mouse model

RD_IL-15_scFv$_{FAP}$_msc4-1BBL and RD_IL-15_scFv$_{FAP}$_m4-1BBL were produced in transiently transfected HEK293-6E cells and purified via IMAC. In SDS-PAGE analysis under reducing conditions, the two trifunctional fusion proteins showed single bands corresponding to the respective monomer. However, due to an uneven number of cysteine in murine 4-1BBL (position 137, 160, 246), apparently additional disulfide bonds form and both RD_IL-15_scFv$_{FAP}$_m4-1BBL and RD_IL-15_scFv$_{FAP}$_msc4-1BBL appear as multimers under non-reducing conditions (Figure 9A). In addition, m4-1BBL other than human 4-1BBL is expected to be strongly glycosylated (positon 139, 161, 293). Size exclusion chromatography revealed one major peak for RD_IL-15_scFv$_{FAP}$_msc4-1BBL, indicating the apparent molecular mass (279 kDa) clearly above the calculated size of 123.4 kDa. In contrast, RD_IL-15_scFv$_{FAP}$_m4-1BBL (calculated size 223.8 kDa) showed one major peak at 79 kDa and two additional smaller peaks at 130 kDa and 208 kDa, indicating a rather heterogenic, multimeric configuration. (Figure 9B). Functional characterization demonstrated simultaneous binding of the trifunctional fusion proteins to the B16-FAP tumor cells and to the corresponding recombinant receptor m4-1BB-Fc by flow cytometry (Figure 9C). Here, also expression of m4-1BBL was detected on B16-FAP and B16 cells.

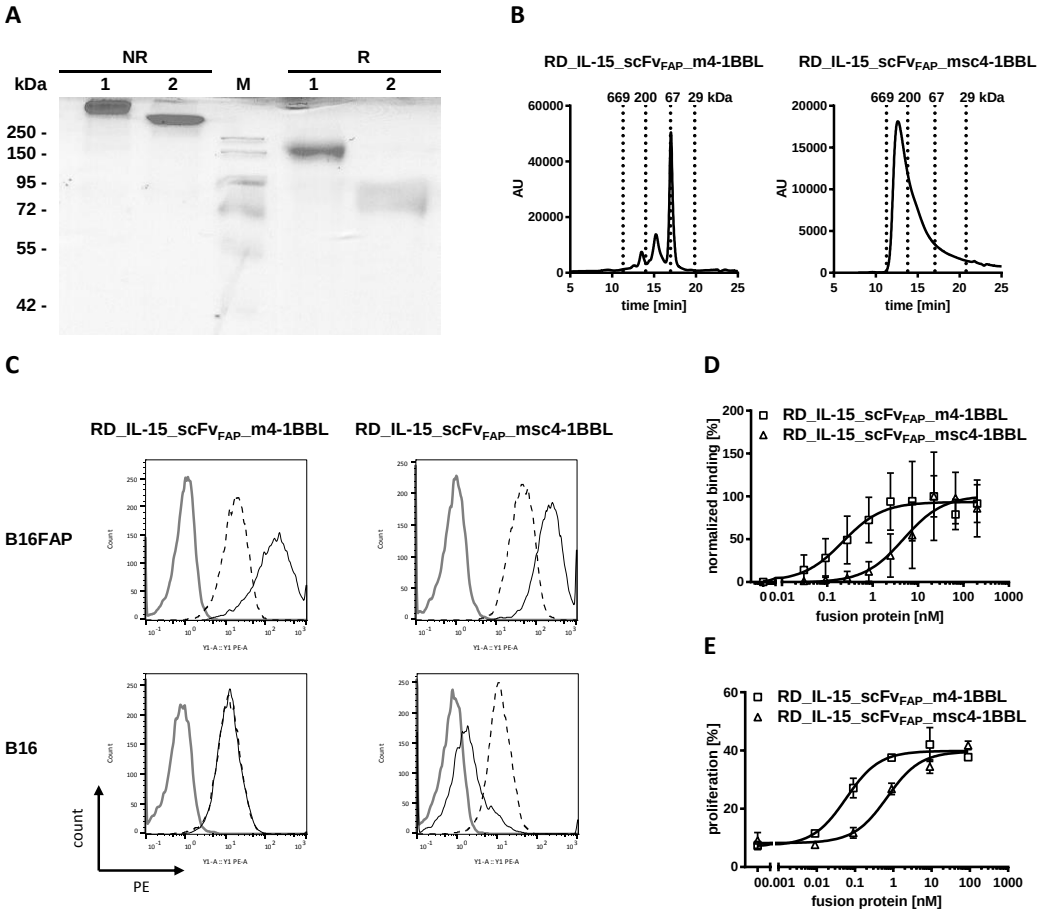

Figure 9: Characterization of the trifunctional fusion proteins applied in the *in vivo* mouse model. A SDS-PAGE analysis (12% PAA; 3 µg/lane, Coomassie Brilliant blue staining) of RD_IL-15_scFv$_{FAP}$_msc4-1BBL (1) and RD_IL-15_scFv$_{FAP}$_m4-1BBL (2) was performed under non-reducing (NR) and reducing (R) conditions. M, protein marker **B** Size exclusion chromatography was used to investigate the proteins under native conditions. Elution times of standard proteins and their corresponding molecular mass [kDa] are indicated as dashed lines. **C** Flow cytometry was used to analyze bifunctional binding. Trifunctional fusion proteins (40 nM) were incubated either on FAP$^+$ (B16-FAP) or FAP$^-$ (B16) cells. Antibody-mediated binding was detected via ligand-receptor interaction, using recombinant m4-1BB-Fc. Detection was performed by anti-human Fc-PE mAb. Thick grey line, cells; dashed black line, detection; black line, fusion protein. **D** Antibody-mediated binding analyzed by flow cytometry. B16-FAP cells were incubated with a serial dilution of fusion proteins followed by detection via anti-His-PE mAb. Mean ± SD, n=3. **E** Cytokine activity on PBMC proliferation. CFSE-labeled PBMCs were incubated with fusion proteins in absence of target cells. After 6 days, the IL-15 activity of non-targeted fusion proteins determined via flow cytometry. Mean ± SD, n=3.

Antibody-mediated binding of the trifunctional fusion proteins was compared by flow cytometry analysis (detection via anti-His-PE mAb) (Figure 9D). RD_IL-15_scFv$_{FAP}$_msc4-1BBL (EC_{50} 4.2±1.1 nM) showed lower binding capacity than RD_IL-15_scFv$_{FAP}$_m4-1BBL (EC_{50} 0.29±0.2 nM). Thus, a pattern similar to that of the corresponding human trifunctional fusion proteins was observed. IL-15 activity was assessed for the trifunctional fusion proteins in a proliferation assay with human PBMCs in a non-targeted setting. RD_IL-15_scFv$_{FAP}$_m4-1BBL induced an approximately 10-fold higher proliferative response (EC_{50} 0.06±0.01 nM) compared to RD_IL-15_scFv$_{FAP}$_msc4-1BBL (EC_{50} 0.7±0.18 nM) (Figure 9E). Results are summarized in Table 8. In summary, although differences in structural features of human

and mouse 4-1BBL are limiting direct molecular translation, the trifunctional fusion proteins with the murine homolog of 4-1BBL showed to be functional for all components and were therefore used as surrogated in the *in vivo* mouse model.

Table 8: Characterization of trifunctional fusion proteins for *in vivo* study.

	RD_IL-15_scFv$_{FAP}$_m4-1BBL	RD_IL-15_scFv$_{FAP}$_msc4-1BBL
MW_{calc} (kDa, monomer) *	74.6	123.4
MW_{PAGE} (kDa, monomer) #	76	159
MW_{SEC} (kDa, main peak)	79	279
EC_{50} (nM, binding in FC)	0.29±0.2	4.2±1.1
EC_{50} (nM, proliferation)	0.06±0.01	0.7±0.18
Yield (mg/l)	15.9	8.8

* The calculated molecular mass (MW) is based on the amino acid sequence.
# The molecular mass calculated from the SDS-PAGE was only determined from reducing conditions.

4.2.4.2 Therapeutic evaluation of the trifunctional fusion proteins in an *in vivo* tumor mouse model

The antitumor potential of RD_IL-15_scFv$_{FAP}$_msc4-1BBL and RD_IL-15_scFv$_{FAP}$_m4-1BBL was evaluated in a syngeneic B16-FAP lung metastases tumor model. Groups of six C57BL/6 mice were challenged with B16-FAP (i.v.) on day 0 and treated with 0.02 nmol of the respective fusion protein or PBS at two early (day 1 and 2) and one late (day 10) time points. On day 21, mice were sacrificed, lungs removed (Figure 10A) and tumor burden evaluated by counting the tumors on the lungs (Figure 10B). Compared to the group of mice treated with PBS, tumor formation was significantly reduced by approximately 70% when mice were treated with RD_IL-15_scFv$_{FAP}$_msc4-1BBL and 54% when treated with RD_IL-15_scFv$_{FAP}$_m4-1BBL, respectively. The difference between the treatment effects of the trifunctional fusion proteins was not statistically significant. In summary, this *in vivo* study indicated strong antitumor potential for both trifunctional fusion proteins.

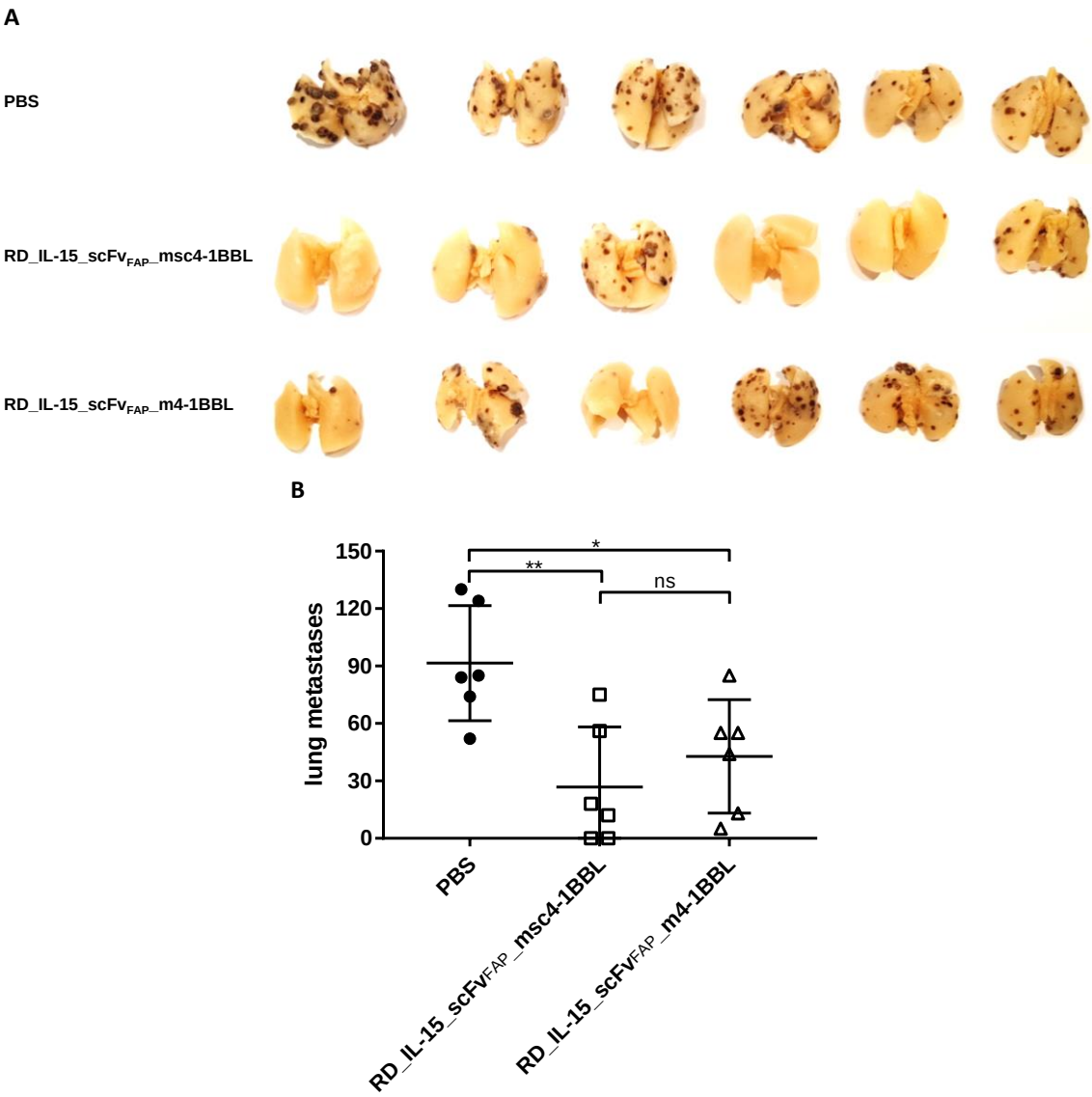

Figure 10: Antitumoral activity of trifunctional fusion protein *in vivo*. $8.5x10^5$ B16-FAP cells were injected i.v. into female C57BL/6 mice. Treatment with 0.02 nmol/day RD_IL-15_scFv$_{FAP}$_msc4-1BBL, RD_IL-15_scFv$_{FAP}$_m4-1BBL or PBS was performed on day 1, 2 and 10 post tumor cell injection. After sacrificing the mice on day 21 **A** lungs were removed, fixed and **B** tumors on the lung counted. Mean ± SD, n=6 mice/group, one-way ANOVA, Tukey's post hoc test, **p<0.01, *p<0.05.

4.3 Antibody-fusion proteins incorporating scGITRL and scOX40L

Trifunctional fusion proteins incorporating sc4-1BBL showed promising effects regarding *in vitro* and *in vivo* activity. Consequently, the repertoire of trifunctional antibody-fusion proteins was extended by the TNFSFL members OX40L and GITRL in the single-chain format.

4.3.1 Biochemical properties

Bifunctional fusion proteins comprised of a targeting moiety (scFv) fused to the ECD of the TNFSF members OX40L (aa 51-183) and GITRL (aa 72-199), both in the single chain format. Similarly, the new trifunctional tumor-targeted antibody-fusion proteins incorporated RD_IL-15, a $scFv_{FAP}$ as an antibody moiety and the extracellular domain (ECD) of the TNFSF member OX40L and GITRL in the single chain format. The linkers between the ECDs of scOX40L was composed of GGGSGGG while a $(GGSGG)_2$ linker was used for the ECDs of scGITRL.

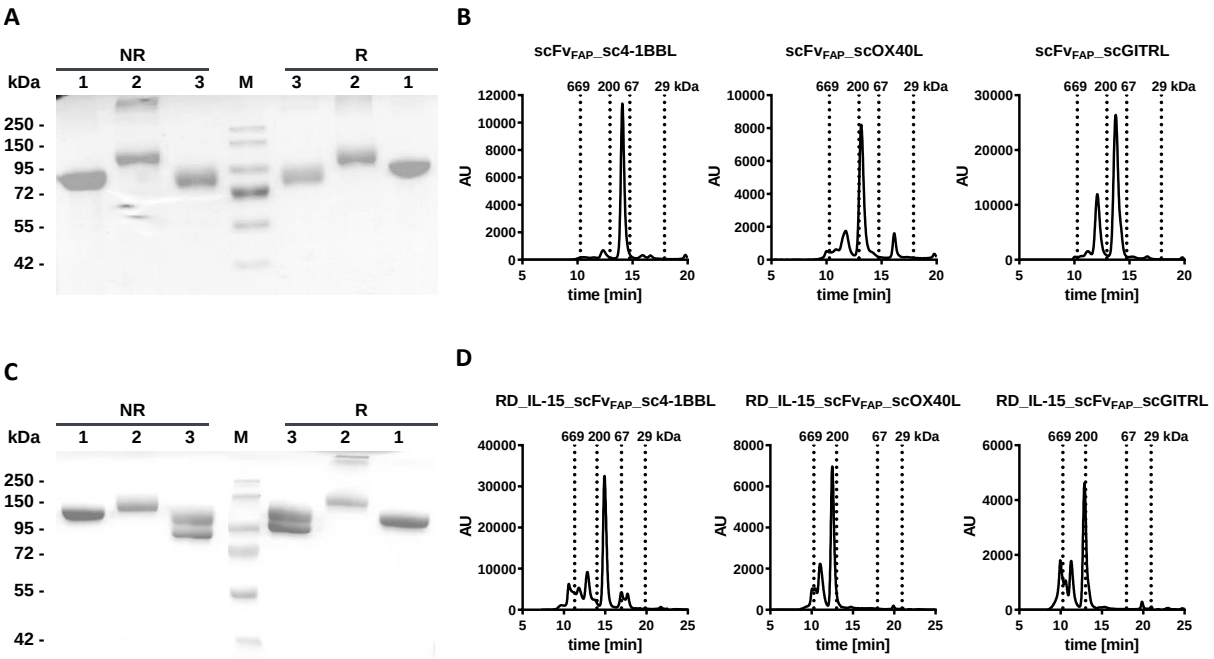

Figure 11: Biochemical characterization of bi- and trifunctional fusion proteins with different scTNFSF ligands. SDS-PAGE analysis (12% PAA; 3 µg/lane, Coomassie Brilliant Blue staining) of **A** $scFv_{FAP}$_sc4-1BBL (1), $scFv_{FAP}$_scOX40L (2) and $scFv_{FAP}$_scGITRL (3) and **C** RD_IL-15_$scFv_{FAP}$_sc4-1BBL (1), RD_IL-15_$scFv_{FAP}$_scOX40L (2) and RD_IL-15_$scFv_{FAP}$_scGITRL (3) was performed under non-reducing (NR) and reducing (R) conditions. M, protein marker. Size exclusion chromatography was used to investigate the bifunctional **B** and trifunctional **D** fusion proteins under native conditions. Elution times of standard proteins and their corresponding molecular mass [kDa] are indicated as dashed lines.

Both the bi- and trifunctional fusion proteins were transiently produced in HEK293-6E cells and purified by immobilized metal affinity chromatography (IMAC) with yields of 3-9 mg/l (bifunctional fusion proteins) and 2-21 mg/l (trifunctional fusion proteins). SDS-PAGE analysis under reducing (R) and non-reducing (NR) conditions was used to confirm protein

purity revealing single bands for the bifunctional fusion proteins (Figure 11A). The apparent molecular mass determined from the SDS-PAGE for scFv$_{FAP}$_sc4-1BBL (approximately 82 kDa) and scFv$_{FAP}$_scGITRL (approximately 76 kDa) correlated to the calculated molecular mass of 89.2 kDa and 73.3 kDa, respectively. However, scFv$_{FAP}$_scOX40L with a calculated molecular mass of 75.6 kDa shows a single band at approximately 110 kDa in the SDS-PAGE, which could be attributed to glycosylation, since OX40L comprises four potential N-glycosylation sites. For the trifunctional fusion proteins, SDS-PAGE revealed single bands for RD_IL-15_scFv$_{FAP}$_sc4-1BBL and RD_IL-15_scFv$_{FAP}$_scOX40L (Figure 11C). While the MW determined from the SDS-PAGE (approximately 103 kDa) corresponded to the calculated molecular mass of 112.6 kDa for RD_IL-15_scFv$_{FAP}$_sc4-1BBL, the trifunctional fusion protein RD_IL-15_scFv$_{FAP}$_scOX40L showed a single band at a higher molecular weight (approximately 124 kDa) than the calculated molecular mass of 99.1 kDa which could again be explained by glycosylation. For the trifunctional fusion protein incorporating scGITRL a double band was observed (approximately 78 and 103 kDa) which could be explained by the two potential N-glycosylation sites provided by GITRL. Deglycosylation of RD_IL-15_scFv$_{FAP}$_scGITRL lead to a single band corresponding to the calculated molecular weight (data not shown). Size exclusion chromatography of scFv$_{FAP}$_sc4-1BBL revealed one major peak at 97 kDa corresponding to the calculated molecular mass of 89.2 kDa (Figure 11B). In comparison, the two novel bifunctional showed one additional minor peak at a higher molecular weight corresponding to dimer formation which is more dominant for scFv$_{FAP}$_scGITRL than for scFv$_{FAP}$_scOX40L. Thus, all bifunctional antibody-fusion proteins showed one dominant peak for the correctly assembled monomer and scFv$_{FAP}$_scOX40L and scFv$_{FAP}$_scGITRL additionally show a small fraction of dimers. Correct assembly into trifunctional monomeric molecules under native condition was confirmed by one major peak in size exclusion chromatography (Figure 11D). RD_IL-15_scFv$_{FAP}$_sc4-1BBL additionally showed two minor peaks of higher molecular weight corresponding to dimer-formation (17%, ~259 kDa) and higher oligomer formation (37%, ~414 kDa). Similar results could be obtained for the two trifunctional fusion proteins with scOX40L and scGITRL, whereby RD_IL-15_scFv$_{FAP}$_scOX40L showed 24% of dimers (~372 kDa) and 15% of trimers (>669 kDa) and the composition of RD_IL-15_scFv$_{FAP}$_scGITRL revealed 17% dimer formation (~283 kDa) and 30% trimer formation (>669 kDa). All evaluated characteristics of the bi-and trifunctional antibody-fusion proteins are summarized in Table 9. In summary, for all trifunctional fusion proteins one major peak

presumably corresponding to monomer formation was observed, with additional minor fractions corresponding to dimer and higher oligomer formation.

Table 9: Characterization of bi- and trifunctional fusion proteins with sc4-1BBL, scOX40L and scGITRL.

Fusion protein	MW_{calc}* (kDa, monomer)	MW_{PAGE}# (kDa, monomer)	MW_{SEC} (kDa)	Yield (mg/l)
$scFv_{FAP}$_sc4-1BBL	89.2	82	97	7
$scFv_{FAP}$_scOX40L	75.6	110	127	3
$scFv_{FAP}$_scGITRL	73.3	76	107	9
RD_IL-15_$scFv_{FAP}$_sc4-1BBL	112.6	103	180	21
RD_IL-15_$scFv_{FAP}$_scOX40L	99.1	124	197	2
RD_IL-15_$scFv_{FAP}$_scGITRL	96.7	93/105	174	18

* The calculated molecular mass (MW) is based on the amino acid sequence.
# The molecular mass calculated from the SDS-PAGE was only determined from reducing conditions.

4.3.2 Binding properties

Flow cytometry was used to determine simultaneous binding of the bi- and trifunctional antibody-fusion proteins to B16-FAP cells and the respective recombinant costimulatory receptors (4-1BB, OX40 and GITR). For analyzing simultaneous binding to target and respective receptor, 4-1BB-Fc, OX40-Fc or GITR-Fc combined with anti-Fc-PE was used as a detection system. All bi- (Figure 12A) and trifunctional (Figure 12B) antibody-fusion proteins showed binding to the target expressing B16-FAP cells, whereas no binding was detected to the FAP negative cell line B16. Bi- (Figure 12C) and trifunctional (Figure 12D) antibody-fusion proteins showed concentration dependent binding to the FAP expressing target cells. While $scFv_{FAP}$_sc4-1BBL (EC_{50} 3.01±0.9 nM) and $scFv_{FAP}$_scGITRL (EC_{50} 4.5±1.7 nM) show similar binding, $scFv_{FAP}$_scOX40L showed a slightly weaker binding (EC_{50} 8.4±1.9 nM). Similar results could be obtained for the trifunctional fusion proteins. Here, similar binding of RD_IL-15_$scFv_{FAP}$_scGITRL (EC_{50} 4.2±0.5 nM) and RD_IL-15_$scFv_{FAP}$_sc4-1BBL (EC_{50} 7.3±3.3 nM) compared to the control RD_IL-15_$scFv_{FAP}$ (EC_{50} 4.3±0.5 nM) could be detected, whereas RD_IL-15_$scFv_{FAP}$_scOX40L showed weaker binding (EC_{50} 11.8±4.3 nM). In summary, all bi- and trifunctional fusion proteins showed the capability to simultaneously bind to target-expressing tumor cells (B16-FAP) and their respective receptor. Fusion of OX40L to $scFv_{FAP}$ or RD_IL-15_$scFv_{FAP}$ seemed to slightly hamper antibody-mediated binding of the antibody-fusion protein.

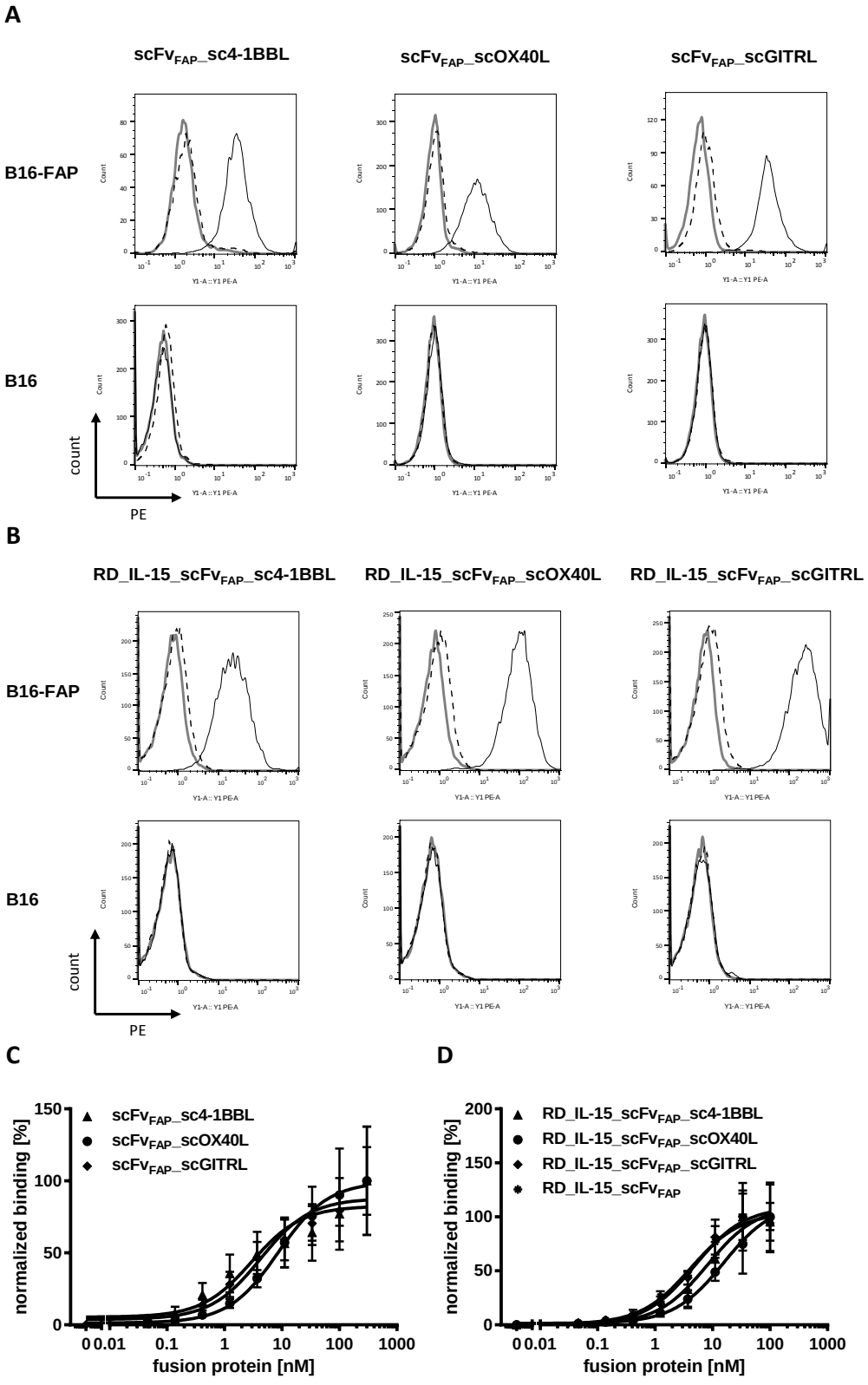

Figure 12: Binding properties of bi- and trifunctional antibody-fusion proteins. Targeting specificity of bifunctional **A** and trifunctional **B** antibody-fusion proteins was determined by flow cytometry. Antibody-fusion proteins (40 nM) were incubated either on FAP$^+$ (B16-FAP) or FAP$^-$ (B16) cells. Antibody-mediated binding was detected via ligand-receptor interaction, using recombinant 4-1BB-Fc, OX40-Fc and GITR-Fc (5 µg/ml), respectively. Detection was performed by anti-human Fc-PE mAb. Thick grey line, cells; dashed black line, detection; black line, fusion protein. Binding properties of bifunctional **C** and trifunctional **D** antibody-fusion proteins was compared by flow cytometry. B16-FAP cells were incubated with a serial dilution of fusion proteins followed by detection via anti-His-PE mAb. Mean ± SD, n=3.

4.3.3 Plasma stability

All bi- and trifunctional fusion proteins were evaluated for their *in vitro* stability in human plasma at 37°C. For all bifunctional fusion proteins, no drop in intact protein level could be detected during the analyzed time of 7 days (Figure 13A). Thus, antibody and TNFSF ligand-receptor binding capacity was preserved over the entire analyzed time period. This was also observed for all analyzed trifunctional fusion proteins, except for RD_IL-15_scFv$_{FAP}$_scGITRL, where the intact protein level dropped to 84% on day 7 (Figure 13B). In summary, the bi- and trifunctional antibody-fusion proteins showed sustained plasma stability *in vitro*.

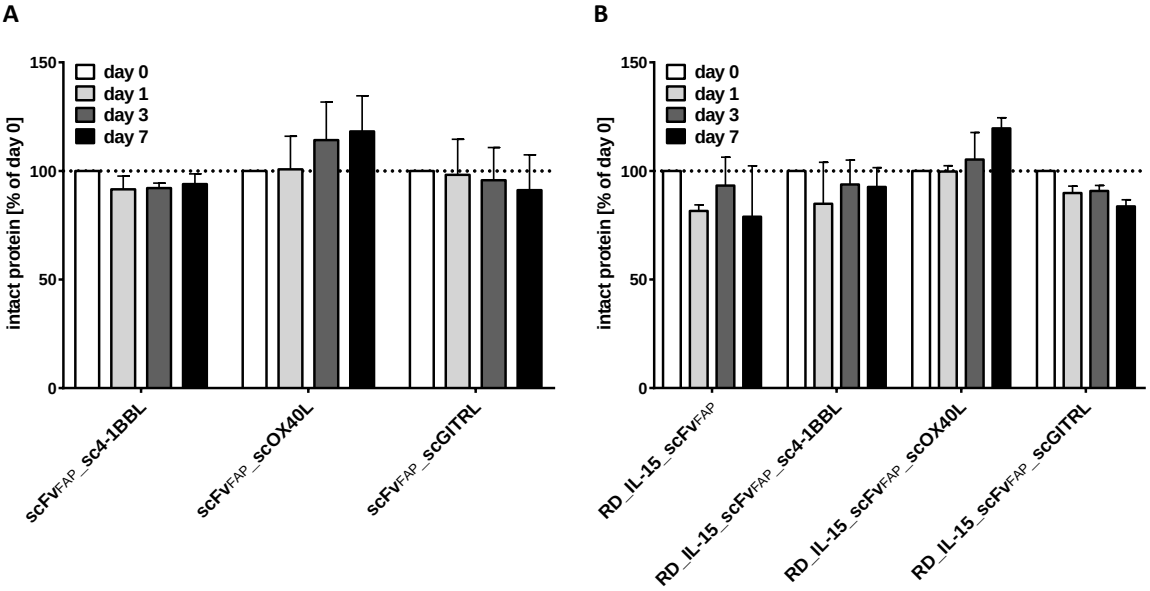

Figure 13: Plasma stability of fusion proteins. A bifunctional and **B** trifunctional fusion proteins (200 nM) were incubated in 50% human plasma over 7 days. Stability of the fusion proteins was determined by ELISA measuring binding to immobilized FAP and detecting bound protein via the respective TNFSFR-Fc / anti-huFc-HRP. Data was normalized to the binding of the fusion protein without serum incubation (day 0). Mean ± SD, n=3.

4.3.4 Activity of untargeted trifunctional fusion proteins

Activity of IL-15 in the trifunctional fusion proteins was determined via proliferation of PBMCs (Figure 14A) and CTLL-2 cells (Figure 14B). CTLL-2 is a murine cytotoxic T lymphocyte cell line which is growth dependent upon IL-2/IL-15. The human and mouse scTNFSFL ligands 4-1BBL, OX40L and GITRL are not cross reactive, thus no activation of corresponding mouse receptors an CTLL-2 cells can be expected. Proliferative activity on CTLL-2 cells could be demonstrated for all three antibody-fusion proteins, reflecting the activity of IL-15. Similar proliferative effects compared to the control RD_IL-15_scFv$_{FAP}$ (EC_{50} 1.0±0.1 nM) were observed for RD_IL-15_scFv$_{FAP}$_scGITRL (EC_{50} 0.4±0.05 nM) and RD_IL-15_scFv$_{FAP}$_sc4-1BBL

(EC_{50} 2.8±0.6 nM), while RD_IL-15_scFv$_{FAP}$_scOX40L (EC_{50} 7.1±3.0 nM) showed slightly reduced activity. Comparison of the proliferation of human PBMCs mediated by RD_IL-15_scFv$_{FAP}$_sc4-1BBL (EC_{50} 7.1±3.8 nM), RD_IL-15_scFv$_{FAP}$_scOX40L (EC_{50} 6.2±2.1 nM) and RD_IL-15_scFv$_{FAP}$_scGITRL (EC_{50} 2.1±1.2 nM) did not reveal significant differences, and was reduced compared to the control RD_IL-15_scFv$_{FAP}$ (EC_{50} 0.8±0.3 nM), suggesting that the TNFSF ligands are not active in a soluble form of the fusion protein. In summary, in untargeted form, all three trifunctional antibody-fusion proteins showed RD_IL-15 activity that was not further enhanced by the TNFSF ligand.

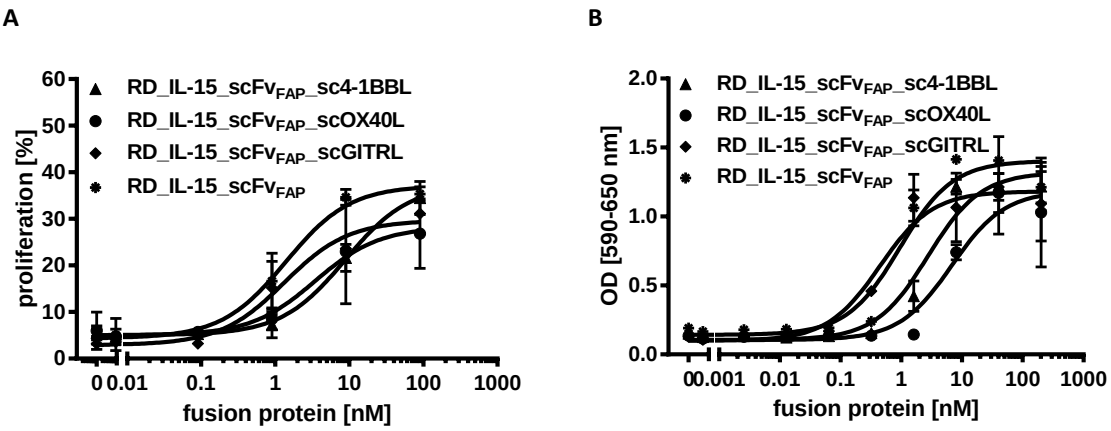

Figure 14: Effect of non-targeted trifunctional fusion proteins on proliferation of PBMCs and proliferation of CTLL-2 cells. A PBMCs were incubated with fusion proteins in absence of target cells. Proliferation of CFSE-labeled PBMCs was determined after 6 days via flow cytometry. **B** Previously starved CTLL-2 cells were incubated with fusion proteins. After 72 h, proliferation was assessed in MTT assay. Mean ± SD, n=3.

4.3.5 Activity of targeted fusion proteins

In a coculture setting of B16-FAP tumor cells and PBMCs, costimulatory activity of targeted bi-and trifunctional antibody-fusion proteins was determined by measuring the enhancement of T cell proliferation above the levels induced by suboptimal anti-CD3 mAb stimulation (Figure 14). In this setting, targeted presentation of the fusion proteins was achieved by removing the unbound fusion proteins from the target cells after 1 hour of incubation before adding the PBMCs and the anti-CD3 mAb in a suboptimal concentration. In presence of target cells and anti-CD3 mAb, all bi-and trifunctional antibody cytokine fusion proteins proved to be costimulatory active. The bifunctional fusion protein with sc4-1BBL showed the highest proliferative enhancement on $CD3^+$ (Figure 14A), $CD4^+$ (Figure 14B) and $CD8^+$ T cells (Figure 14C) compared to scFv$_{FAP}$_scOX40L and scFv$_{FAP}$_scGITRL.

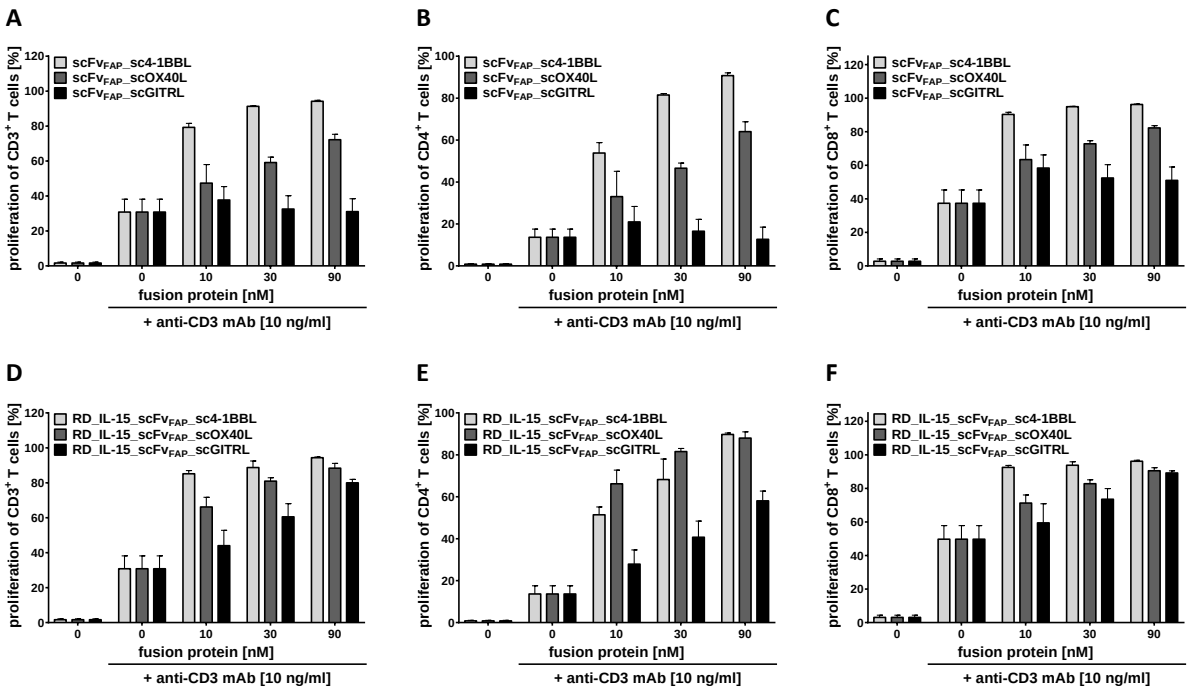

Figure 15: Activity of target-bound bi- and trifunctional fusion proteins. B16-FAP cells were cocultured with PBMCs, a suboptimal concentration of a cross-linked anti-CD3 mAb and targeted **A-C** bifunctional and **D-E** trifunctional fusion proteins. After 6 days the proliferation of **A and D** $CD3^+$ T cells, **B and E** $CD4^+$ T cells ($CD3^+CD4^+$ T cells) and **C and F** $CD8^+$ T cells ($CD3^+CD8^+$ T cells) was determined by CFSE dilution in flow cytometry. Mean ± SD, Blockshift, n=3.

Similar to the bifunctional setting, the trifunctional fusion protein incorporating 4-1BBL showed highest effects on proliferation of $CD3^+$ (Figure 15D) and $CD8^+$T cells (Figure 15F). Regarding proliferation of $CD4^+$ T cells, RD_IL-15_scFv$_{FAP}$_scOX40L showed highest effects. Interestingly, the trifunctional fusion protein with scGITRL was less effective than the trifunctional fusion protein with sc4-1BBL and scOX40L, respectively and the bifunctional fusion protein with scGITRL was only effective on $CD8^+$ T cells. In general, the scTNFSFL members showed costimulatory activity regarding the enhancement of anti-CD3 mAb-induced proliferation.

4.3.6 Activity of targeted bi- and trifunctional fusion proteins on T cells subpopulations

Activity of the bi- and trifunctional fusion proteins was not only examined for proliferation induction of $CD4^+$ and $CD8^+$ T cells (Figure 15), but also for their subpopulations (Figure 16, Figure 17). Proliferation of naïve, central memory, effector memory and effector $CD4^+$ and $CD8^+$ T cells were induced by the anti-CD3 mAb and could be further enhanced by scFv$_{FAP}$_sc4-1BBL, scFv$_{FAP}$_scOX40L (Figure 16) and all trifunctional fusion proteins (Figure 17).

For the bifunctional fusion proteins, strongest proliferation of $CD4^+$ T cell subpopulations, especially effector and effector memory cells, was observed for $scFv_{FAP}$_sc4-1BBL (Figure 16A). In terms of proliferation of $CD8^+$ T cell subpopulations, particularly the memory phenotypes benefited from costimulation with $scFv_{FAP}$_sc4-1BBL (Figure 16C). While all three bifunctional fusion proteins show a similar pattern regarding the composition of the $CD4^+$ T cell subpopulation after costimulation, i.e. shifting towards $CD4^+$ effector memory T cells compared to the anti-CD3 mAb alone (Figure 16B), differences between the bifunctional fusion proteins could be observed regarding the composition of $CD8^+$ T cell subpopulations. Here, treatment with $scFv_{FAP}$_sc4-1BBL led to a clear proportional increase of the effector memory subpopulation, whereas an increased percentage of effector $CD8^+$ T cells was observed for the treatment with $scFv_{FAP}$_scGITRL (Figure 16D).

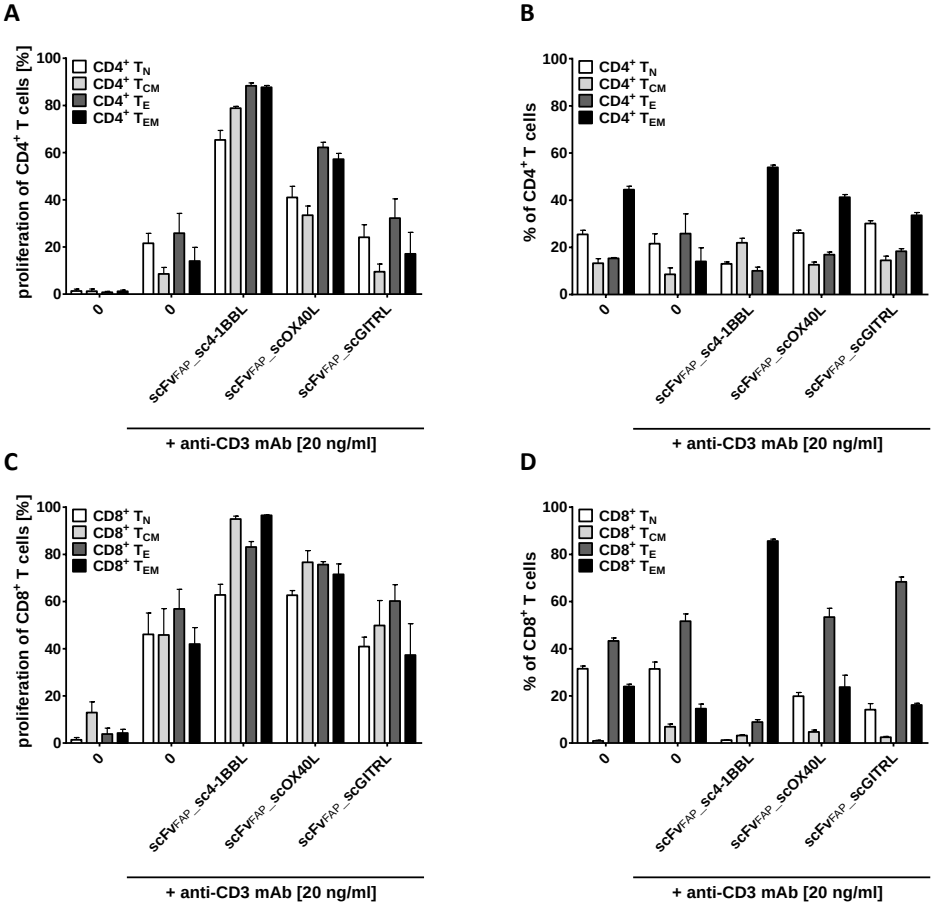

Figure 16: Bifunctional fusion protein mediated effect on proliferation and composition of T cell subpopulations. Proliferation (**A and C**) and composition (**B and D**) of $CD4^+$ T cells (**A and B**) and $CD8^+$ T cells (**C and D**) was determined by flow cytometry. B16-FAP cells were cocultured with CFSE-labeled PBMCs and a suboptimal concentration of a cross-linked anti-CD3 mAb and target-bound bifunctional fusion proteins (30 nM). After 6 days, proliferation and composition of naïve (T_N; $CD45RA^+$, $CCR7^+$), central memory (T_{CM}; $CD45RA^-$, $CCR7^+$), effector (T_E; $CD45RA^+$, $CCR7^-$) and effector memory (T_{EM}; $CD45RA^-$, $CCR7^-$) subpopulations of $CD4^+$ T cells and $CD8^+$ T cells were identified. Mean ± SD, Blockshift, n=3.

Regarding the stimulatory activity of the trifunctional fusion proteins on subpopulations of $CD4^+$ T cells, RD_IL-15_scFv$_{FAP}$_sc4-1BBL and the control protein RD_IL-15_scFv$_{FAP}$ showed rather similar proliferative effects, while RD_IL-15_scFv$_{FAP}$_scOX40L demonstrated the highest effect on the effector memory phenotype (Figure 17A). Additionally, in terms of composition, RD_IL-15_scFv$_{FAP}$_scOX40L showed a mild shift in favor of the effector memory $CD4^+$ T cells (Figure 17B). Concerning the effect of the trifunctional fusion proteins on the proliferation of the subpopulations of $CD8^+$ T cells, treatment with all trifunctional fusion proteins and RD_IL-15_scFv$_{FAP}$ resulted in a proliferative effect on all T cell subpopulations (Figure 17C).

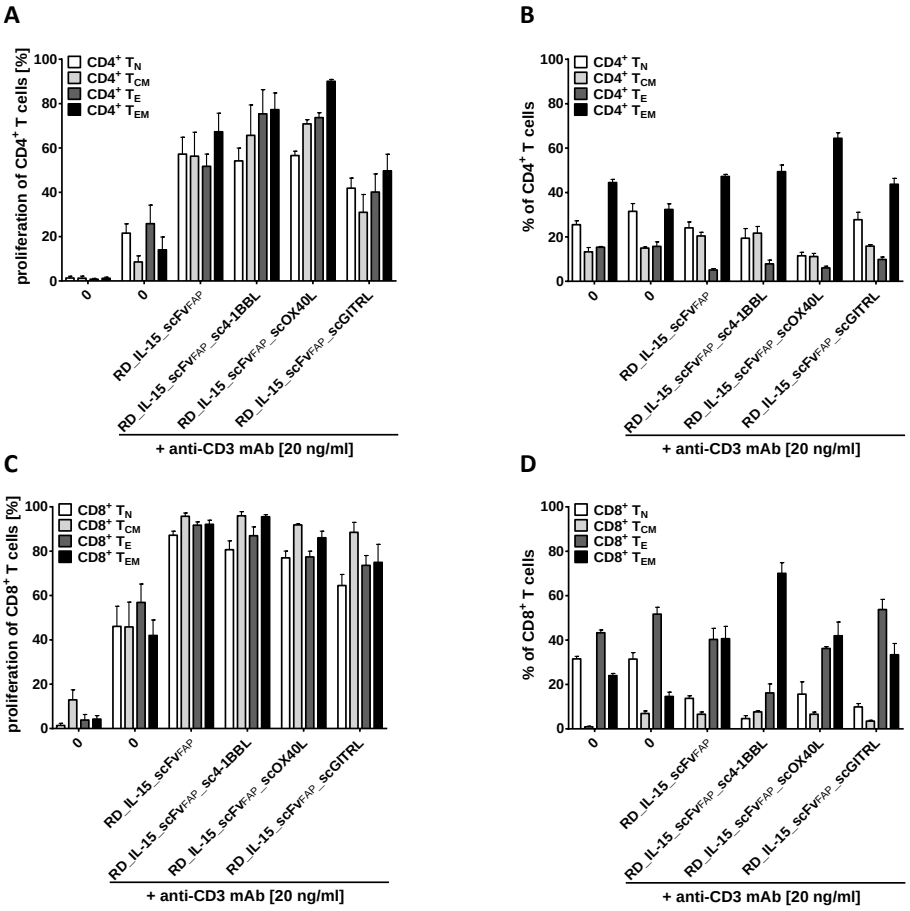

Figure 17: Trifunctional fusion protein induced effect on proliferation and composition of T cell subpopulations. Proliferation (**A and C**) and composition (**B and D**) of $CD4^+$ T cells (**A and B**) and $CD8^+$ T cells (**C and D**) was determined by flow cytometry. B16-FAP cells were cocultured with CFSE-labeled PBMCs and a suboptimal concentration of a cross-linked anti-CD3 mAb and target-bound trifunctional fusion proteins (30 nM). After 6 days, proliferation and composition of naïve (T_N; $CD45RA^+$, $CCR7^+$), central memory (T_{CM}; $CD45RA^-$, $CCR7^+$), effector (T_E; $CD45RA^+$, $CCR7^-$) and effector memory (T_{EM}; $CD45RA^-$, $CCR7^-$) subpopulations of $CD4^+$ T cells and $CD8^+$ T cells were identified. Mean ± SD, Blockshift, n=3.

Interestingly, differences could be observed in terms of composition of the subpopulations. While RD_IL-15_scFv$_{FAP}$ and RD_IL-15_scFv$_{FAP}$_scOX40L equally shifted the composition in favor of effector and effector memory $CD8^+$ T cells, treatment with RD_IL-15_scFv$_{FAP}$_sc4-

1BBL clearly manifested in a shift towards effector memory $CD8^+$ T cells, while RD_IL-15_scFv$_{FAP}$_scGITRL favoured the effector memory phenotype of the $CD8^+$ T cells (Figure 17D). Thus, the different influence on T cell subsets by antibody-fusion proteins in the bi- and trifunctional format was shown, highlighting the role of sc4-1BBL especially in the context of $CD8^+$ T cells and the benefit of combination of RD_IL-15 with scOX40L.

4.3.7 Trifunctional versus combination of bifunctional fusion proteins

Furthermore, the combination of RD_IL-15 and the TNF-superfamily ligands 4-1BBL, OX40L and GITRL were evaluated as trifunctional antibody-fusion protein in comparison to the combination of the respective bifunctional fusion proteins. Bifunctional and trifunctional fusion proteins presented the same antibody moiety and orientation of the fusion partner. Equimolar amounts of cytokine and costimulatory ligand were applied and immunomodulatory effects on proliferation and cytotoxicity of T cells was analyzed.

4.3.7.1 Proliferative effect on T cells and NK cells

Fusion proteins were targeted to B16-FAP cells cocultured with PBMCs in presence of a suboptimal concentration of anti-CD3 mAb. At lower concentrations (1, 10 nM), all trifunctional fusion proteins achieved stronger proliferative effects on T cells compared to the combination of the corresponding bifunctional fusion proteins. The trifunctional fusion proteins with scOX40L and scGITRL (Figure 18B and C) showed the strongest signal enhancement on $CD4^+$ T cells. In contrast, the $CD8^+$ T cells already showed high responsiveness to RD_IL-15 and trifunctional fusion proteins only showed a minor enhancement on the proliferation of $CD8^+$ T cells (Figure 18D-F). Proliferation of NK cells was mainly triggered by RD_IL-15, however this effect could be further enhanced by the trifunctional fusion proteins with scGITRL, especially at lower concentrations (Figure 18I).

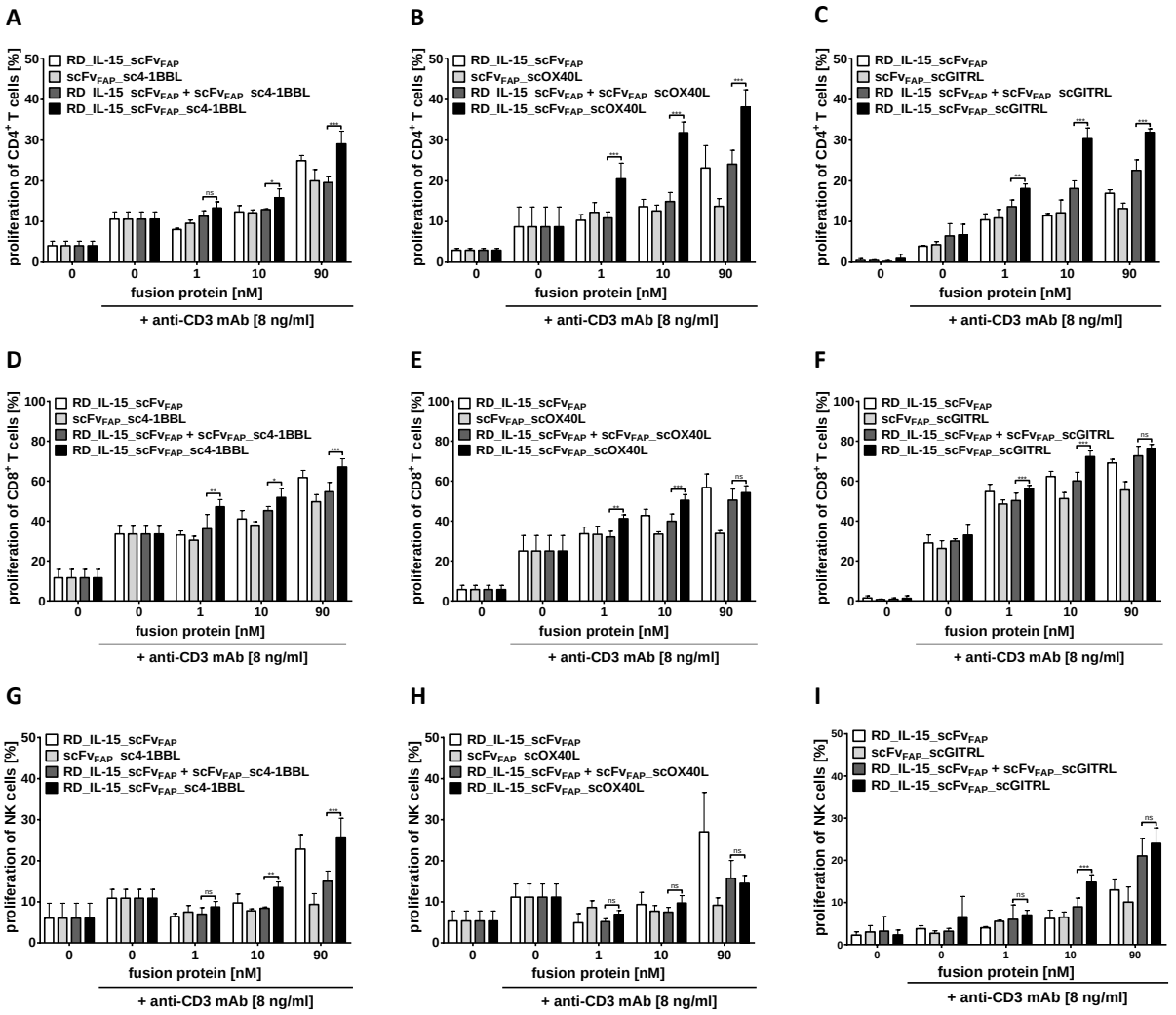

Figure 18: Activity of targeted combined bi- and trifunctional antibody-fusion proteins on the proliferation of T cells and NK cells. B16-FAP cells were cocultured with PBMCs, a suboptimal concentration of a cross-linked anti-CD3 mAb and target-bound antibody-fusion proteins. After 6 days the proliferation of **A-C** CD3$^+$ T cells, **D-F** CD4$^+$ T cells (CD3$^+$CD4$^+$ T cells), **G-I** CD8$^+$ T cells (CD3$^+$ CD8$^+$ T cells) and **J-L** NK cells (CD3$^-$CD56$^+$ cells) was determined by CFSE dilution in flow cytometry. Graphic shows mean ± SD, n=3, one-way ANOVA, Tukey's post hoc test, ***p<0.001, **p<0.01, *p<0.05.

4.3.7.2 Effect of trifunctional fusion proteins on the cytotoxic potential of T cells

The influence of trifunctional fusion proteins in comparison to the combination of the respective bifunctional fusion proteins on the cytotoxicity of T cells was analyzed. Therefore, unstimulated PBMCs were incubated for 5 days with targeted trifunctional fusion proteins or a combination of bifunctional fusion proteins in presence of a suboptimal concentration of the anti-CD3 mAb. Subsequently, PBMCs were transferred to a fresh plate and T cells retargeted to B16-FAP cells via a bispecific antibody (scDbFAPxCD3). Thereby, T cells were triggered and their cytotoxic potential was determined by measuring degranulation of T cells.

Regarding the cytotoxic potential of $CD8^+$ T cells, all trifunctional proteins appeared to strongly enhanced the cytotoxic potential (Figure 19A-C), whereby the strongest enhancement compared to the combination of the respective bifunctional fusion proteins or RD_IL-15_$scFv_{FAP}$ was achieved by RD_IL-15_$scFv_{FAP}$_scGITRL (Figure 19C). Similar degranulation of T cells was observed for RD_IL-15_$scFv_{FAP}$_sc4-1BBL, however, here the effect clearly is driven by sc4-1BBL as similar effects were obtained for the bifunctional fusion protein $scFv_{FAP}$_sc4-1BBL (Figure 19A). Interestingly, RD_IL-15_$scFv_{FAP}$_sc4-1BBL was also effective in enhancing the degranulation capacity of $CD4^+$ T cells, which could not be observed for RD_IL-15_$scFv_{FAP}$_scOX40L or RD_IL-15_$scFv_{FAP}$_scGITRL (Figure 19D-F). In most cases, the combination of RD_IL-15 and members of the TNFSF ligands in trifunctional fusion proteins has shown to be advantageous compared to the individual bifunctional fusion proteins. Moreover, the trifunctional fusion proteins were more effective compared to the combination of two bifunctional fusion proteins and in some cases, the single bifunctional fusion proteins showed higher stimulatory activity than the combination of two bifunctional fusion proteins.

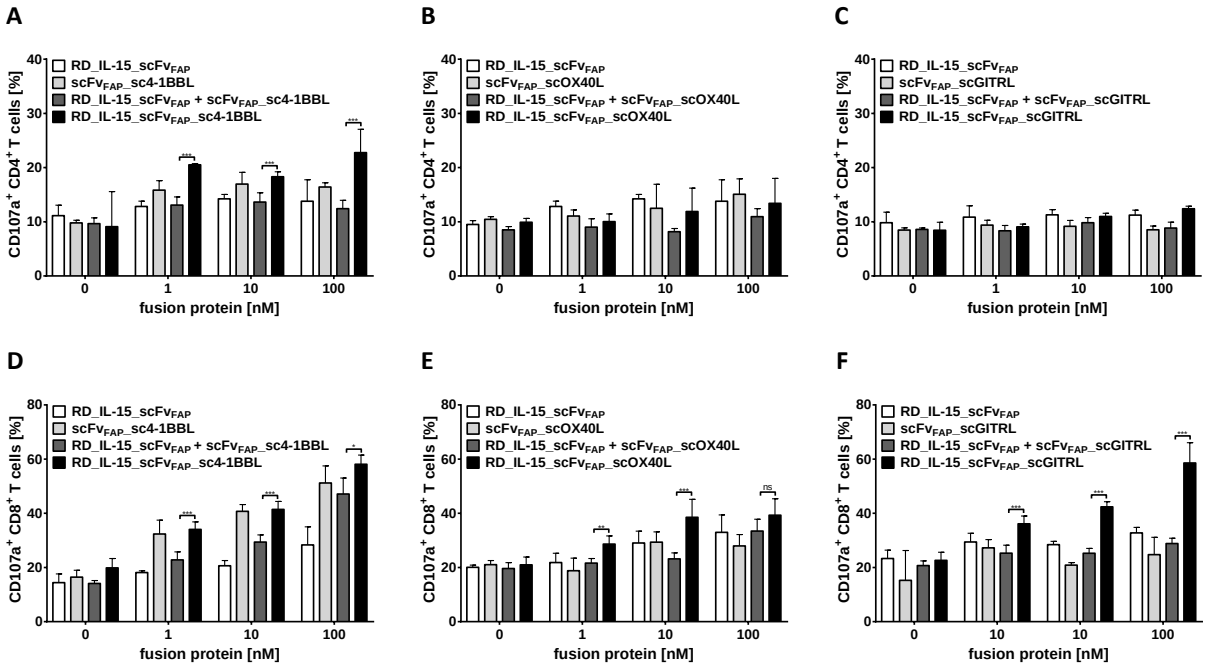

Figure 19: Effect of targeted bi-and trifunctional antibody-fusion proteins on the cytotoxic potential of $CD4^+$ and $CD8^+$ T cells. B16-FAP cells were cocultured with PBMCs, a suboptimal concentration of a cross-linked anti-CD3 mAb and targeted fusion proteins. After 5 days, PBMCs were transferred to fresh B16-FAP cells and incubated in presence of a bispecific antibody (scDbFAPxCD3) retargeting T cells to the target cells. After 6 h, degranulation of **A-C** $CD4^+$ T cells ($CD4^+$ $CD107a^+$) and **D-F** $CD8^+$ T cells ($CD8^+$ $CD107a^+$) was determined using flow cytometry. Mean ± SD, Blockshift, n=3, one-way ANOVA, Tukey's post hoc test, $^{***}p<0.001$, $^{**}p<0.01$, $^{*}p<0.05$.

4.3.7.3 Influence of the trifunctional fusion proteins on the activation of regulatory T cells

While IL-2 has the ability to activate regulatory T cells, IL-15 has shown to be less efficient in expanding regulatory T cells (Vang et al. 2008). Therefore, the trifunctional fusion proteins were assessed for their potential to stimulate regulatory T cells (T_{regs}) and T_{helper} cells. Freshly isolated T_{regs} ($CD3^+CD4^+CD25^+$) from PBMCs were activated by the anti-CD3 mAb but to a lower extent than the fraction of T_{helper} cells ($CD3^+CD4^+CD25^-$). Addition of the trifunctional fusion proteins showed an enhancing effect on the expression of the activation marker CD69 on T_{helper} cells but not on T_{regs} (Figure 20A).

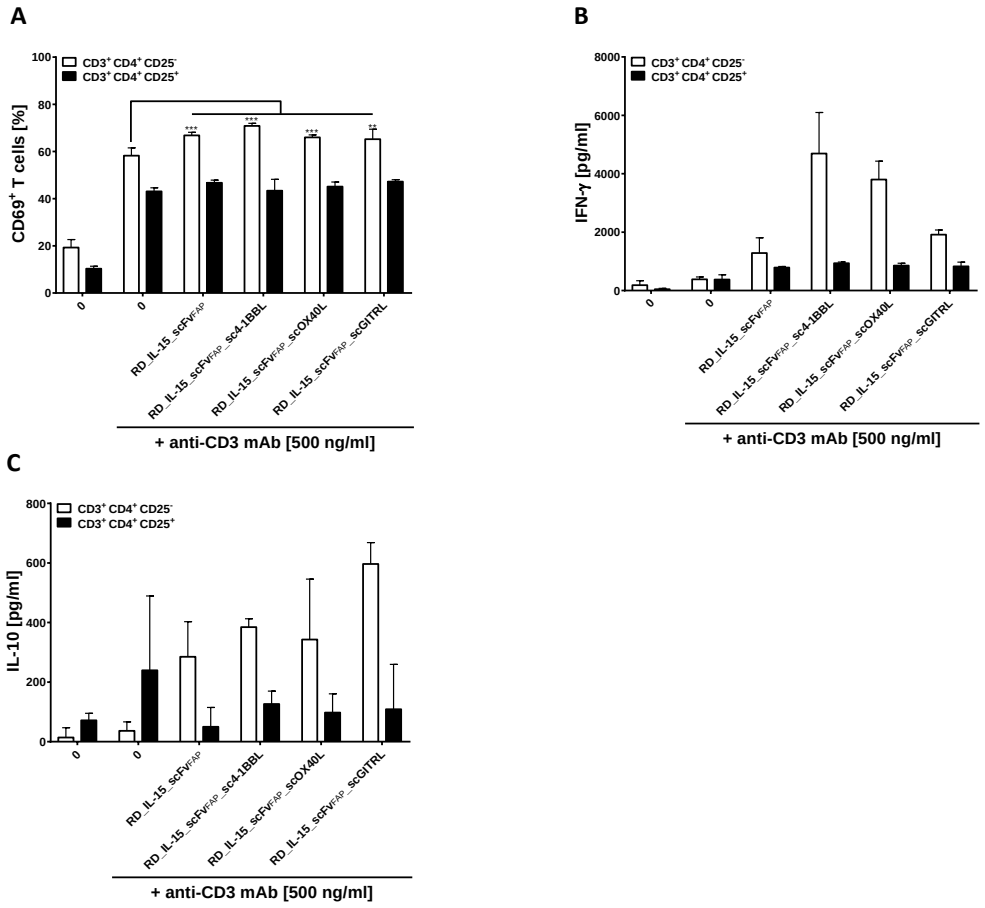

Figure 20: Effect of targeted trifunctional antibody-fusion proteins on regulatory T cells. B16-FAP cells were cocultured with freshly isolated $CD3^+$ $CD4^+$ $CD25^-$ T_{eff} cells or $CD3^+$ $CD4^+$ $CD25^+$ T_{reg} cells in presence of 90 nM targeted fusion proteins and 500 ng/ml of a cross-linked anti-CD3 mAb. After 24 h activation was measured by **A** CD69 via flow cytometry and **B** IFN-γ and **C** IL-10 release was measured in sandwich-ELISA. Mean ± SD, Blockshift, n=3.

Regarding IFN-γ release, costimulation with the trifunctional fusion proteins only showed a slightly higher amount of released IFN-γ for the T_{regs} compared to treatment with the anti-CD3 mAb alone (Figure 20B). To a much higher extent, the trifunctional fusion proteins were able to induce IFN-γ release of the T_{helper} cell fraction. Similar results were obtained for the release of IL-10, where the trifunctional fusion proteins showed a strong enhancement on

the T_{helper} cells (Figure 20C). Thus, the trifunctional fusion proteins had low or no stimulatory effect on T_{regs} compared to T_{helper} cells regarding CD69 expression, IFN-γ release and IL-10 secretion.

4.3.8 Antitumor activity of RD_IL-15_scFv$_{FAP}$_mscGITRL in syngeneic mouse models

RD_IL-15_scFv$_{FAP}$_scGITRL proved to be a promising candidate due to strong stimulatory potential on the proliferation of $CD8^+$ T cells and NK cells and its potential to enhance the cytotoxic potential of $CD8^+$ T cells. Thus, a trifunctional fusion protein incorporating the mouse homologous of scGITRL (aa 49-173) was generated for further *in vivo* studies. In contrast to human GITRL, murine GITRL is reported to present as a dimer (Chattopadhyay et al. 2008). Therefore, human scGITRL was replaced by a mouse scGITRL composed of only two extracellular domains instead of three. Thus, scFv$_{FAP}$_mscGITRL and RD_IL-15_scFv$_{FAP}$_mscGITRL were generated. The glycine-serine linker connecting the extracellular domain of mscGITRL was composed of $(GGGS)_5$. Additionally, an analogues trifunctional fusion protein targeting CEA was generated (RD_IL-15_scFv$_{CEA}$_mscGITRL). The antigen CEA is not present in the mouse, therefore, the generated trifunctional fusion protein serves as a control for the evaluation of the influence of targeting on the antitumor effect.

4.3.8.1 Biochemical characterization of the fusion proteins with mouse GITRL

All novel fusion proteins for the *in vivo* tumor mouse models were produced in HEK293-6E cells and purified using immobilized metal affinity chromatography (IMAC) with yields of 4-25 mg/l. Protein purity was confirmed in SDS-PAGE analysis under reducing (R) and non-reducing (NR) conditions revealing bands corresponding to the monomer for RD_IL-15_scFv$_{FAP}$_mscGITRL (87 kDa), RD_IL-15_scFv$_{FAP}$ (53 kDa) (Figure 21A) and RD_IL-15_scFv$_{CEA}$_mscGITRL (79 kDa) (Figure 21B). correlating to the calculated molecular masses of 81.4, 51.4 and 81.4 kDa, respectively. ScFv$_{FAP}$_mscGITRL with a calculated molecular mass of 57.4 kDa showed double bands of approximately 57 kDa and 53 KDa. One major peak in size exclusion chromatography representing monomeric molecules and additional minor fractions were observed to a similar degree for all GITRL fusion proteins (Figure 21C). While RD_IL-15_scFv$_{FAP}$ only showed a small minor peak pointing towards dimer formation, higher dimer formation was observed for the bi- and trifunctional fusion proteins with mGITRL. Similar amounts of multimers were observed for the two trifunctional fusion proteins. The biochemical properties are summarized in Table 10.

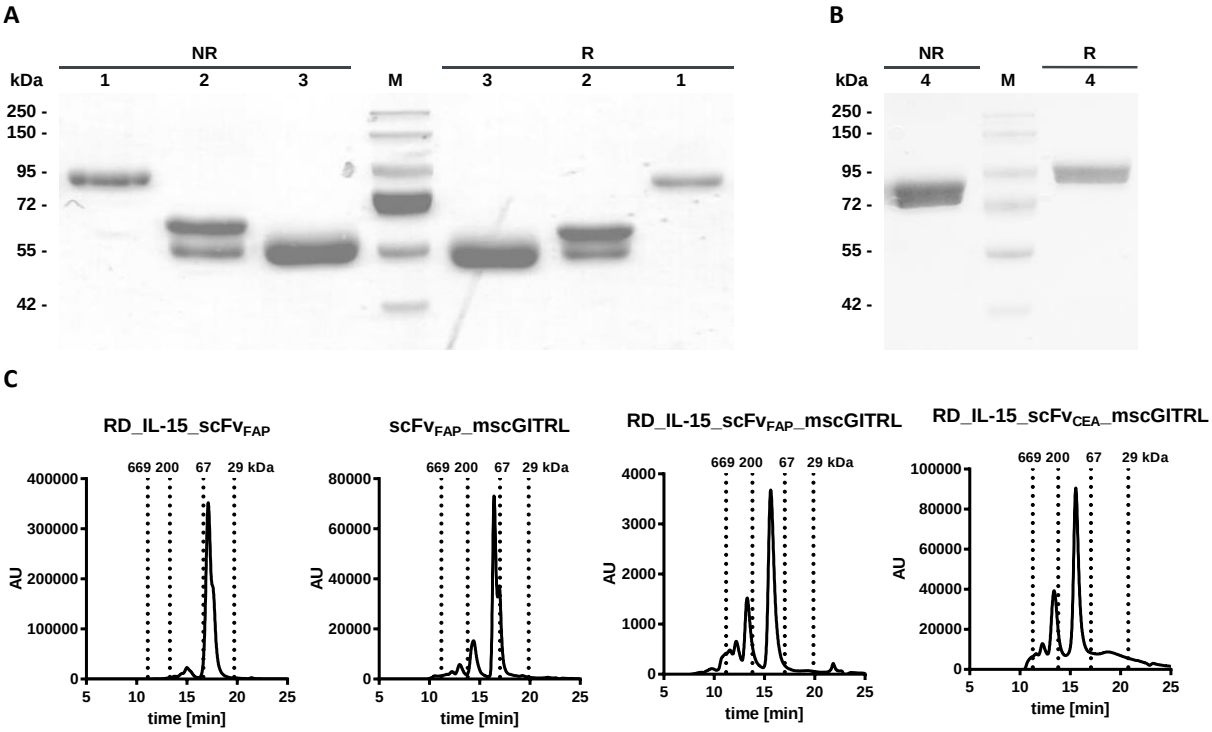

Figure 21: Biochemical characterization of bi- and trifunctional fusion proteins with RD_IL-15 and murine scGITRL. SDS-PAGE analysis (12% PAA; 3 µg/lane, Coomassie Brilliant Blue staining) of **A** RD_IL-15_scFv$_{FAP}$_mscGITRL (1), scFv$_{FAP}$_mscGITRL (2), RD_IL-15_scFv$_{FAP}$ (3) and **B** RD_IL-15_scFv$_{CEA}$_mscGITRL (4) was performed under non-reducing (NR) and reducing (R) conditions. M, protein marker. **C** Size exclusion chromatography. Elution times of standard proteins and their corresponding molecular mass [kDa] are indicated as dashed lines.

Table 10: Biochemical characterization of the antibody-fusion proteins for animal studies.

Fusion protein	MW_{calc}* (kDa, monomer)	MW_{PAGE} (kDa, monomer)	MW_{SEC} (kDa)	Yield (mg/l)
RD_IL-15_scFv$_{FAP}$	51.4	53	94	26.4
scFv$_{FAP}$_mscGITRL	57.4	57/53	94.3	3.7
RD_IL-15_scFv$_{FAP}$_mscGITRL	81.4	87	133.8	24.8
RD_IL-15_scFv$_{CEA}$_mscGITRL	81.4	79	132.2	16

* The calculated molecular mass (MW) is based on the amino acid sequence.

4.3.8.2 Antibody-mediated binding and IL-15 activity of the fusion proteins with mouse scGITRL

Binding of the antibody-fusion proteins targeting FAP was determined on B16-FAP cells (Figure 22A), while binding of the CEA-targeting RD_IL-15_scFv$_{CEA}$_mscGITRL was evaluated on LS174T cells (Figure 22B), using anti-His-PE as a detection system. All FAP-directed fusion proteins bound to B16-FAP cells with EC_{50} values of 0.6±0.04 nM for RD_IL-15_scFv$_{FAP}$, 1.8±0.8 nM for RD_IL-15_ scFv$_{FAP}$_mscGITRL and 0.9±0.09 nM for scFv$_{FAP}$_mscGITRL. The

CEA-directed version of the trifunctional fusion protein bound to LS174T cells with an EC_{50} value of 12.7±2.4 nM. Binding of mscGITRL to its receptor mGITR was confirmed in in ELISA where recombinant FAP-Flag was immobilized and bound antibody-fusion protein was detected using mGITR-Fc and anti-Fc-HRP (Figure 22C).

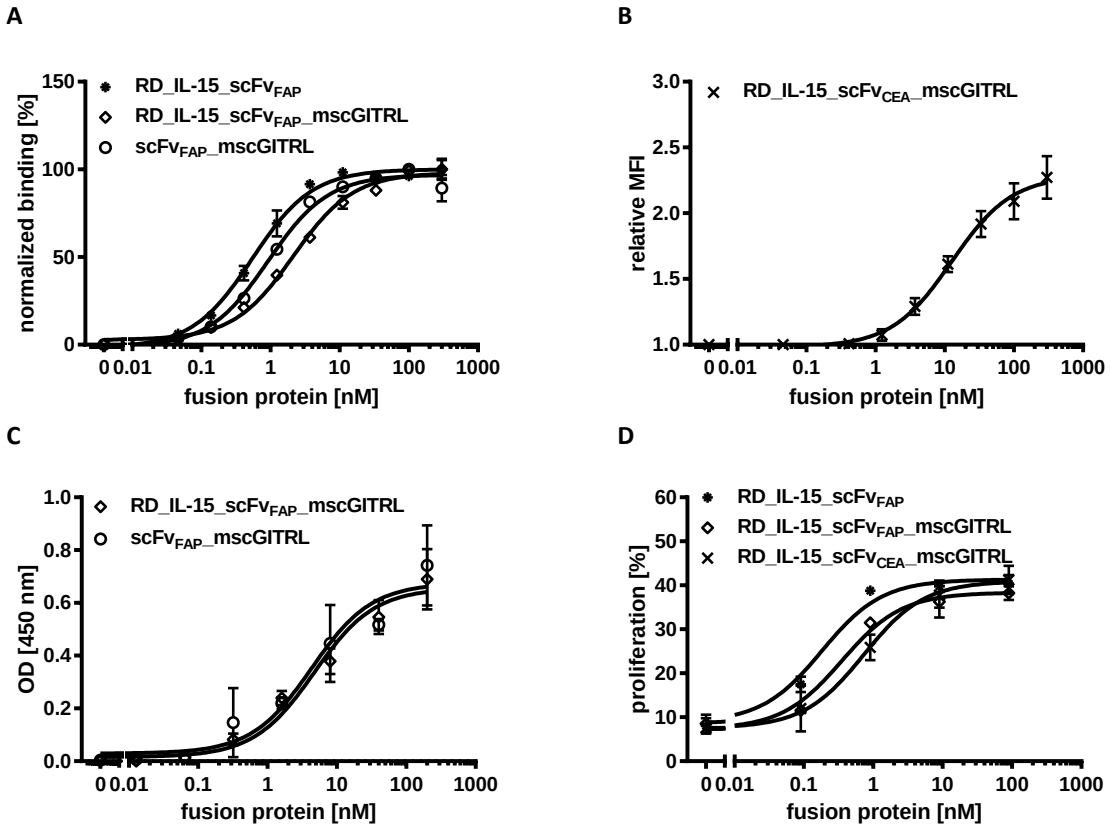

Figure 22: Functional characterization of the fusion proteins to be used in the *in vivo* mouse model. Binding analysis of FAP-directed **A** and CEA-directed **B** antibody-fusion proteins by flow cytometry. **A** B16-FAP and **B** LS174T cells were incubated with a serial dilution of the fusion proteins and bound protein was detected via anti-His-PE mAb. **C** Binding of mscGITRL to its receptor mGITR was determined in ELISA, measuring binding to immobilized FAP and detecting bound fusion protein via mGITR-Fc (5 µg/ml)/anti-huFc-HRP. **D** Cytokine activity on PBMC proliferation. PBMCs were incubated with fusion proteins in absence of target cells. Proliferation of CFSE-labeled PBMCs was determined after 6 days via flow cytometry. Mean ± SD, n=3.

Analysis of binding in ELISA revealed almost identical binding properties for scFv$_{FAP}$_mscGITRL (EC_{50} 3.7±3.5 nM) and RD_IL-15_scFv$_{FAP}$_mscGITRL (EC_{50} 4.9±2.9 nM). IL-15 activity of the fusion proteins was determined by proliferation induction of human PBMCs in absence of target cells (Figure 22D). RD_IL-15_scFv$_{FAP}$ was able to induce proliferation of PBMCs with an EC_{50} value of 0.18±0.02 nM, while the two trifunctional fusion proteins RD_IL-15_scFv$_{FAP}$_mscGITRL (EC_{50} 0.36±0.06 nM) and RD_IL-15_scFv$_{CEA}$_mscGITRL (EC_{50} 0.7±0.2 nM) showed similar proliferative effects. In summary, the fusion proteins were able to bind their target and the RD_IL-15 as well as the mscGITRL units showed functionality in terms of proliferation induction and receptor binding, respectively.

4.3.8.3 Antitumor activity of RD_IL-15_scFv$_{FAP}$_mscGITRL in syngeneic lung tumor model

Therapeutic antitumor potential of the trifunctional antibody-fusion protein with mscGITRL was investigated *in vivo* using a syngeneic lung tumor model in C57BL/6 mice. B16-FAP cells were injected i.v. into C57BL/6 mice, which received 0.2 nmol fusion protein or PBS as a control on day 1, 2 and 10 post tumor cell injection. Mice were sacrificed on day 21, lungs removed and tumors counted (Figure 23A).

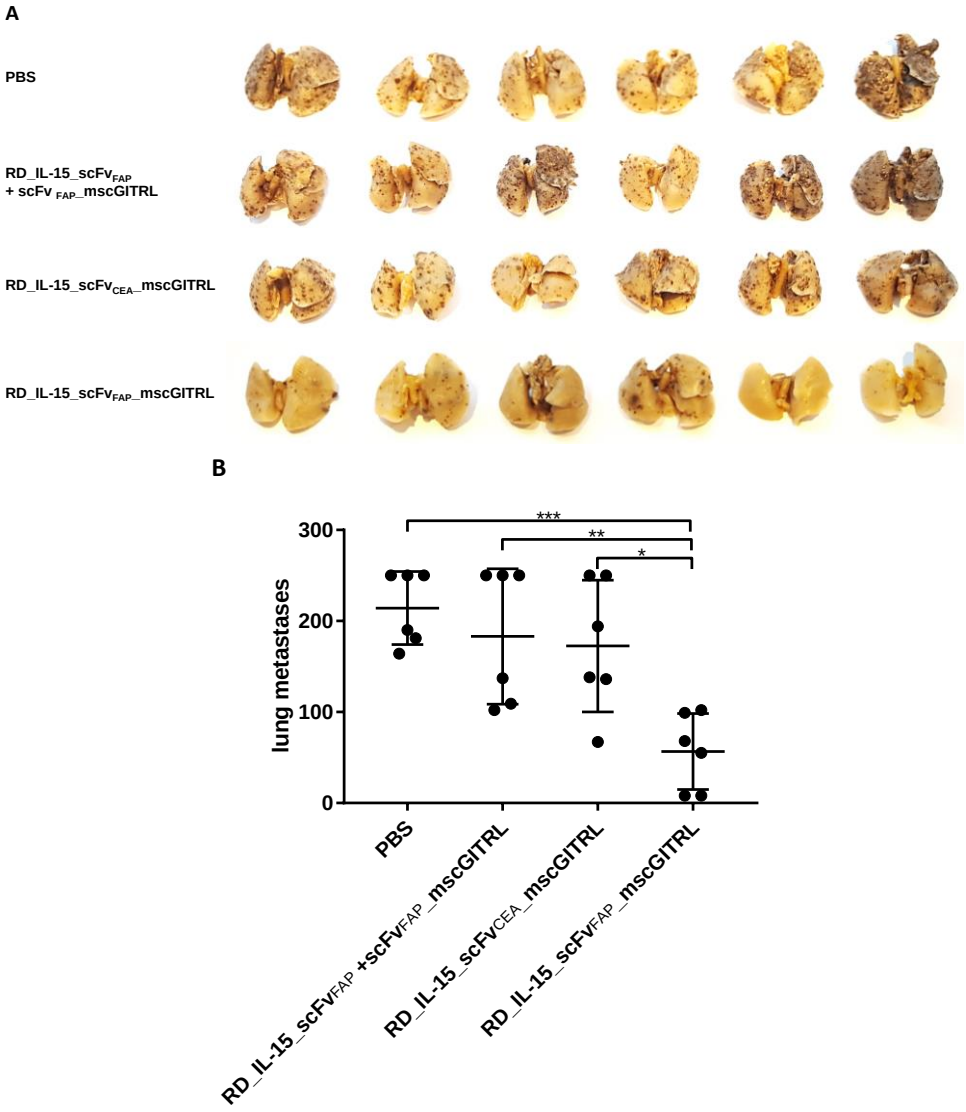

Figure 23: Antitumoral activity of bi- and trifunctional fusion protein in a syngeneic lung metastases tumor mouse model. 8.5x10^5 B16-FAP cells were injected (i.v.) into female C57BL/6 mice. Treatment with 0.2 nmol/day RD_IL-15_scFv$_{FAP}$_mscGITRL, RD_IL-15_scFv$_{CEA}$_mscGITRL, RD_IL-15_scFv$_{FAP}$ + scFv$_{FAP}$_mscGITRL or PBS was performed on day 1, 2 and 10 post tumor cell injection. After sacrificing the mice on day 21 **A** lungs were removed, fixed and **B** tumors on the lung counted. Mean ± SD, n=6 mice/group, one-way ANOVA, Tukey's post hoc test, ***p<0.001, **p<0.01, *p<0.05.

Administration of the trifunctional antibody-fusion protein lead to stronger antitumor effect (approximately 70%) compared to the combination of the respective bifunctional fusion proteins or the PBS group (approximately 74%). Moreover, the trifunctional fusion protein

targeting CEA, which is not expressed in mice, showed less efficacy compared to RD_IL-15_scFv$_{FAP}$_mscGITRL and a similar number of metastases compared to the combination of the two bifunctional fusion proteins. These observations confirms the important role of targeting of the trifunctional fusion protein for the antitumor effect and the beneficial effect of the trifunctional fusion protein compared to the combination of the two bifunctional fusion proteins (Figure 23B).

4.3.8.4 Antitumor activity of RD_IL-15_scFv$_{FAP}$_mscGITRL in a syngeneic solid tumor model

Additionally, the antitumor potential of RD_IL-15_scFv$_{FAP}$_mscGITRL and RD_IL-15_scFv$_{FAP}$ was analyzed in a solid tumor model in C57BL/6 mice. Here, B16-FAP cells were injected into both flanks of C57BL/6 mice. Mice were treated early after tumor cell inoculation (day 1, 2) and later once the tumors became visible (day 10-15, 18). Overall, treatment with RD_IL-15_scFv$_{FAP}$ or RD_IL-15_scFv$_{FAP}$_mscGITRL did not lead to a significant reduction of tumor burden compared to the PBS control (Figure 24A and B) but a tendency for tumor growth delay was observed for groups treated with RD_IL-15_scFv$_{FAP}$_mscGITRL or RD_IL-15_scFv$_{FAP}$. At a very early time point of tumor development (day 12) RD_IL-15_scFv$_{FAP}$_mscGITRL was shown to delay tumor outgrowth significantly. Later on day 17, also RD_IL-15_scFv$_{FAP}$ shortly delayed the tumor growth, nevertheless after that until the final day of the experiment (day 21), no statistically significant differences between the groups could be detected anymore (Figure 24C).

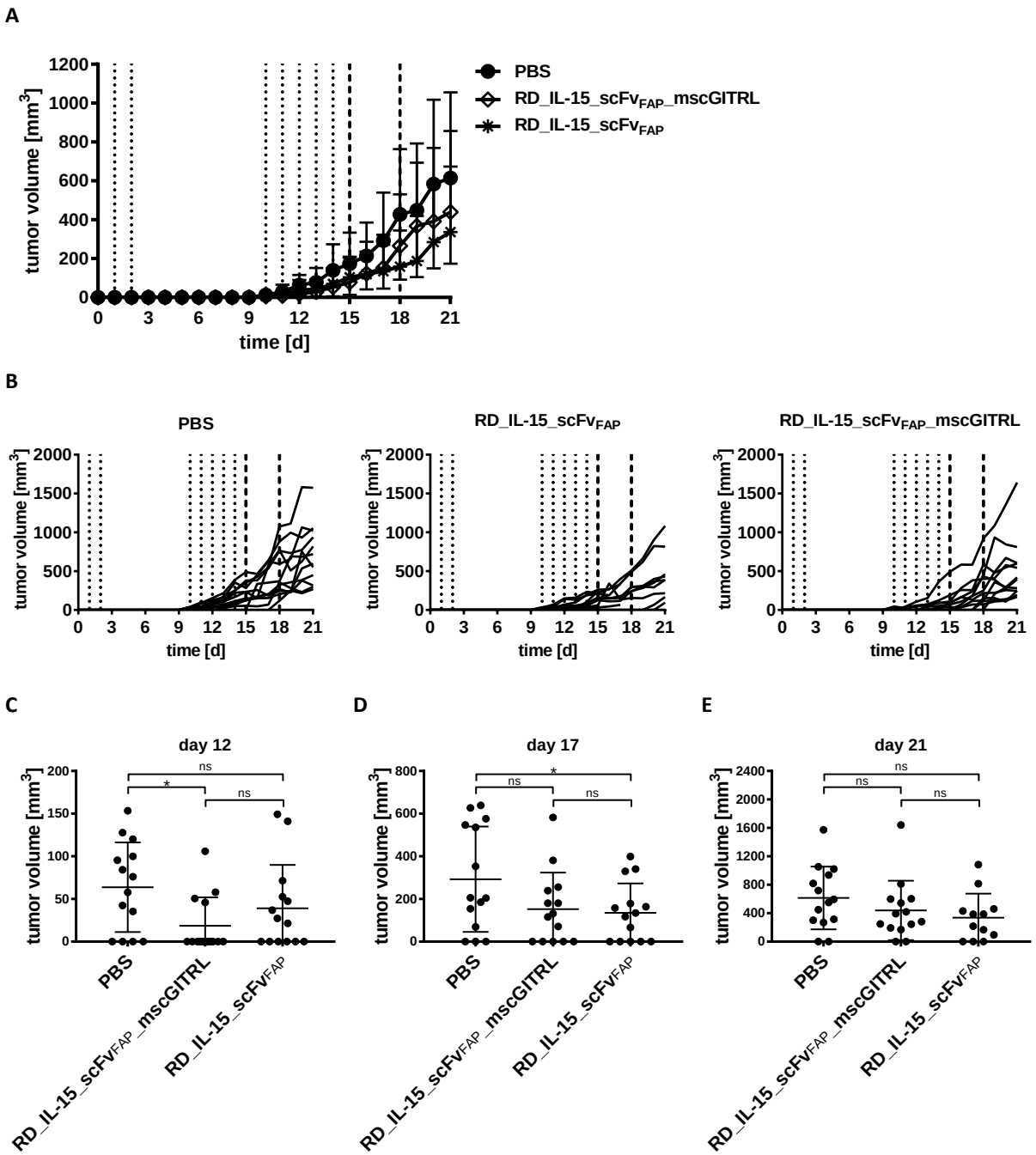

Figure 24: *In vivo* activity of RD_IL-15_scFv$_{FAP}$_mscGITRL in a syngeneic solid tumor mouse model. Tumor growth inhibition is shown **A** indicating the average tumor volume/group, **B** depicting the individual tumor growth /group over time and **C** indicating the individual tumor volume/group at day 12, 17 and 21. 5x10^5 B16-FAP cells were injected (s.c.) into both flanks of C57BL/6 mice. Treatment with RD_IL-15_scFv$_{FAP}$_mscGITRL, RD_IL-15_scFv$_{FAP}$ or PBS was performed on day 1, 2, 10-14 (0.2 nmol, dotted lines) and day 15 and 18 (0.4 nmol, dashed lines). post tumor cell injection. Tumor volume was measured each day. Mean ± SD, n=6 mice/group, unpaired t-test, *p<0.05.

On day 21 mice were sacrificed, tumors removed and analyzed for immune cell infiltration. For this purpose, tumors of each treatment group were pooled according to their size (2-4 tumors in each case). Then, tumors were dissociated and the number of infiltrating leucocytes, in particular T cell (CD3$^+$, CD4$^+$, CD8$^+$, T$_{regs}$) (Figure 25B-D,F) and NK cell (Figure 25E) per grams of tumor was analyzed via flow cytometry. Analysis of immune cell

infiltration did not reveal a significant difference between the control and the treatment groups. Furthermore, there was no correlation between the amount of infiltrated immune cells and the tumor volume.

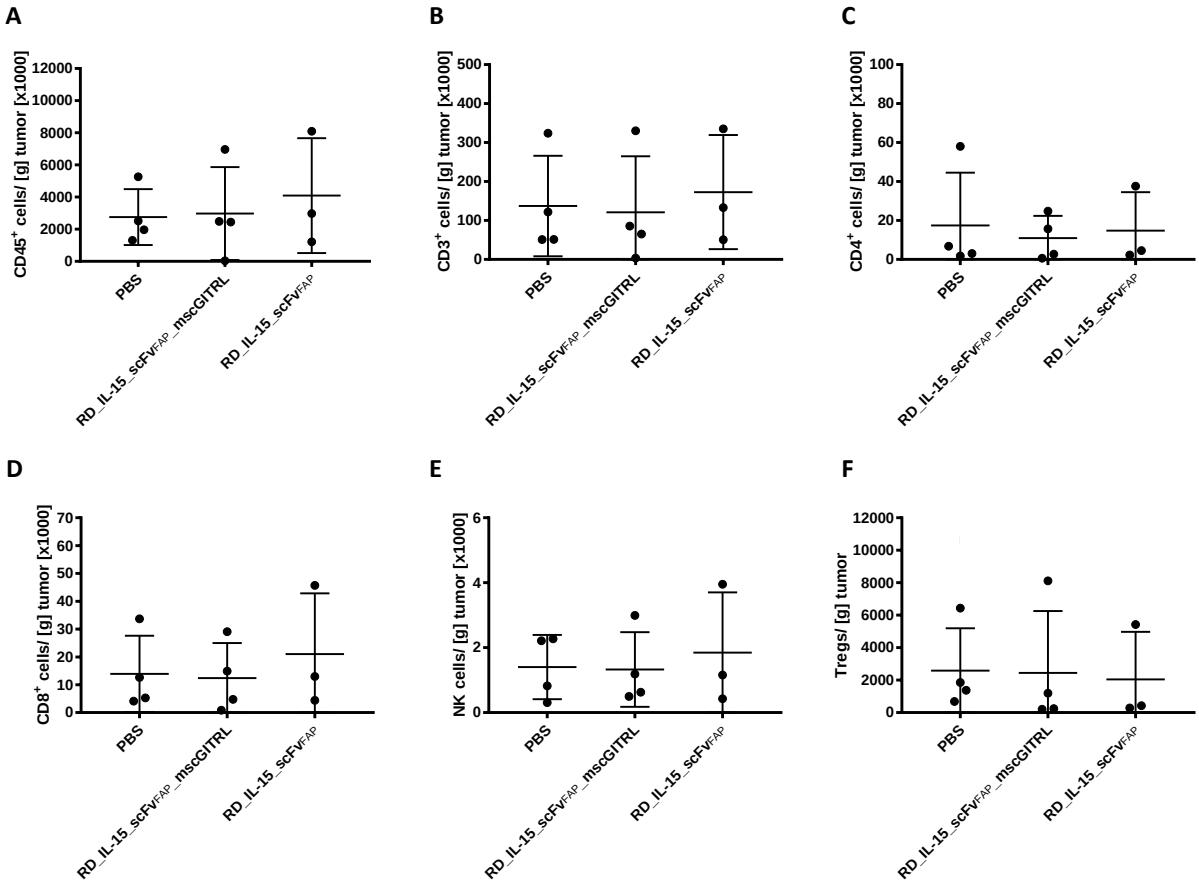

Figure 25: **Analysis of immune cell infiltration into solid tumors after fusion protein treatment.** $5x10^5$ B16-FAP cells were injected into each flank of female C57BL/6 mice (day 0). Treatment with RD_IL-15_scFv$_{FAP}$_mscGITRL, RD_IL-15_scFv$_{FAP}$ or PBS was performed on day 1, 2, 10-14 (0.2 nmol) and day 15 and 18 (0.4 nmol). On day 21 mice were sacrificed, tumors removed, grouped according to their tumor volume (2-4 tumors each group), dissociated and **A** leucocyte ($CD45^+$) **B** T cells($CD3^+$) **C** $CD3^+CD4^+$ T cell **D** $CD3^+CD8^+$ T cell, **E** NK cell ($CD3^-CD94^+$) and **F** regulatory T cell ($CD3^+CD4^+CD25^+$ $FoxP3^+$) infiltration was determined using flow cytometry.

Although treatment with RD_IL-15_scFv$_{FAP}$ or RD_IL-15_scFv$_{FAP}$_mscGITRL did not show an increase in tumor infiltrating immune cells, an effect on the immune cells in the spleen was observed (Figure 26). Here, analysis showed a significant increase of NK cells in spleens of mice treated with RD_IL-15_scFv$_{FAP}$_mscGITRL compared to the PBS group (Figure 26D). Statistic significant enhancement of T cells could not be determined.

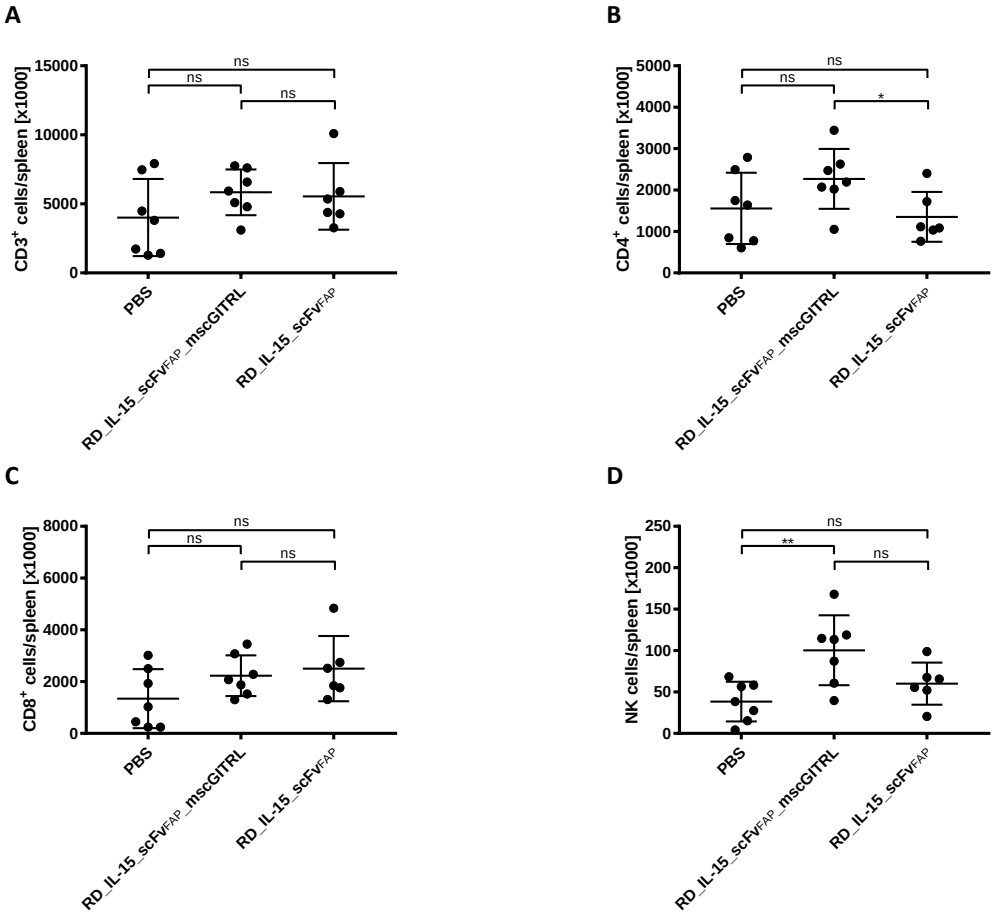

Figure 26: Analysis of immune cells in the spleen. 5x10^5 B16-FAP cells were injected into both flanks of female C57BL/6 mice. Treatment with RD_IL-15_scFv$_{FAP}$_mscGITRL, RD_IL-15_scFv$_{FAP}$ or PBS was performed on day 1, 2, 10-14 (0.2 nmol) and day 15 and 18 (0.4 nmol). post tumor cell injection. On day 21 mice were sacrificed, spleens removed, dissociated and **A** CD3$^+$, **B** CD3$^+$CD4$^+$, **C** CD3$^+$CD8$^+$ T cell and **D** NK cell (CD3$^-$CD94$^+$) infiltration was determined using flow cytometry. one-way ANOVA, Tukey's post hoc test, ***p<0.001, **p<0.01, *p<0.05.

RD_IL-15_scFv$_{FAP}$_scGITRL has shown a significant antitumor effect in the lung tumor model. Consequently, RD_IL-15_scFv$_{FAP}$_scGITRL proved to be a promising candidate for cancer immunotherapy and the trifunctional antibody-format potentially evolves as an interesting platform for further development.

4.4 EGFR-directed trifunctional antibody-fusion proteins for the enhancement of ADCC

The trifunctional antibody-fusion protein platform was further validated by introducing a targeting moiety directed against the epidermal growth factor receptor (EGFR). Here, the fusion proteins RD_IL-15_scFv$_{FAP}$, scFv$_{FAP}$_sc4-1BBL and RD_IL-15scFv$_{FAP}$_sc4-1BBL served as a template, exchanging the scFv$_{FAP}$ for scFv$_{EGFR}$, whereby the scFv$_{EGFR}$ corresponds to a humanized version of Cetuximab (mAb C225, (Goldstein et al. 1995)) provided by Prof. R. Kontermann.

4.4.1 Biochemical properties

RD_IL-15_scFv$_{EGFR}$, scFv$_{EGFR}$_sc4-1BBL and RD_IL-15scFv$_{EGFR}$_sc4-1BBL were transiently produced in HEK-2936E cells and purified by IMAC. All molecules were produced with yields in a range of 5-30 mg/l. SDS-PAGE analysis under reducing (R) and non-reducing conditions (NR) confirmed purity and integrity of all three fusion proteins targeting EGFR (Figure 27A).

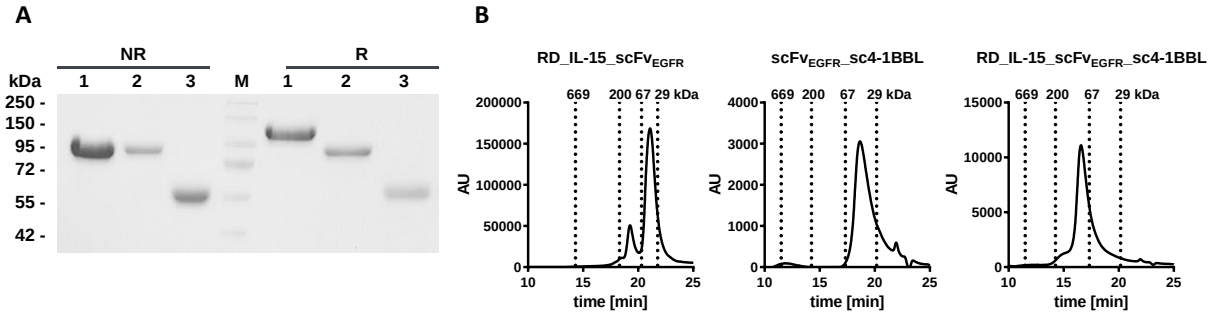

Figure 27: Biochemical characterization of EGFR-directed antibody-fusion proteins with sc4-1BBL. SDS-PAGE analysis (12% PAA; 3 µg/lane, Coomassie Brilliant Blue staining) of **A** RD_IL-15_scFv$_{EGFR}$_sc4-1BBL (1), scFv$_{EGFR}$_sc4-1BBL (2) and RD_IL-15_scFv$_{EGFR}$ (3) was performed under non-reducing (NR) and reducing (R) conditions. M, protein marker**. B** Size exclusion chromatography was used to investigate the proteins under native conditions. Elution times of standard proteins and their corresponding molecular mass [kDa] are indicated as dashed lines.

The apparent molecular mass determined from the SDS-PAGE for RD_IL-15_scFv$_{EGFR}$ (approximately 53 kDa), scFv$_{EGFR}$_sc4-1BBL (approximately 80 kDa) and RD_IL-15_scFv$_{EGFR}$_sc4-1BBL (approximately 97 kDa) correlated with the calculated molecular mass of 50.9 kDa, 88.5 kDa and 111.7 kDa, respectively. Size exclusion chromatography showed that all three proteins eluted as one predominant peak of slightly lower sizes than their calculated molecular weight (Figure 27B). While a small amount of higher molecular species was observed for RD_IL-15_scFv$_{EGFR}$, the two fusion proteins incorporating 4-1BBL did not show such dimer formation. All evaluated characteristics of the bi-and trifunctional antibody-fusion proteins targeting EGFR were summarized in Table 11.

Table 11: Characterization of bi- and trifunctional fusion proteins targeting EGFR.

Fusion protein	MW_{calc} * (kDa, monomer)	MW_{PAGE} # (kDa, monomer)	MW_{SEC} (kDa)	Yield (mg/l)
RD_IL-15_scFv$_{EGFR}$	50.9	53	34	30.2
scFv$_{EGFR}$_sc4-1BBL	88.5	80	50	4.75
RD_IL-15_scFv$_{EGFR}$_sc4-1BBL	111.7	97	98	8.35

* The calculated molecular mass (MW) is based on the amino acid sequence.
# The molecular mass calculated from the SDS-PAGE was only determined from reducing conditions.

4.4.2 Binding properties

The binding capacity to EGFR as well as the ability of sc4-1BBL incorporated in the fusion proteins to bind to the receptor 4-1BB-Fc was evaluated by flow cytometry. All three fusion proteins showed binding to EGFR expressing SKBR-3 cells. Simultaneous binding of the incorporated 4-1BBL to the receptor 4-1BB was shown using 4-1BB-Fc and anti-Fc-PE as a detection system (Figure 28A, upper panel).

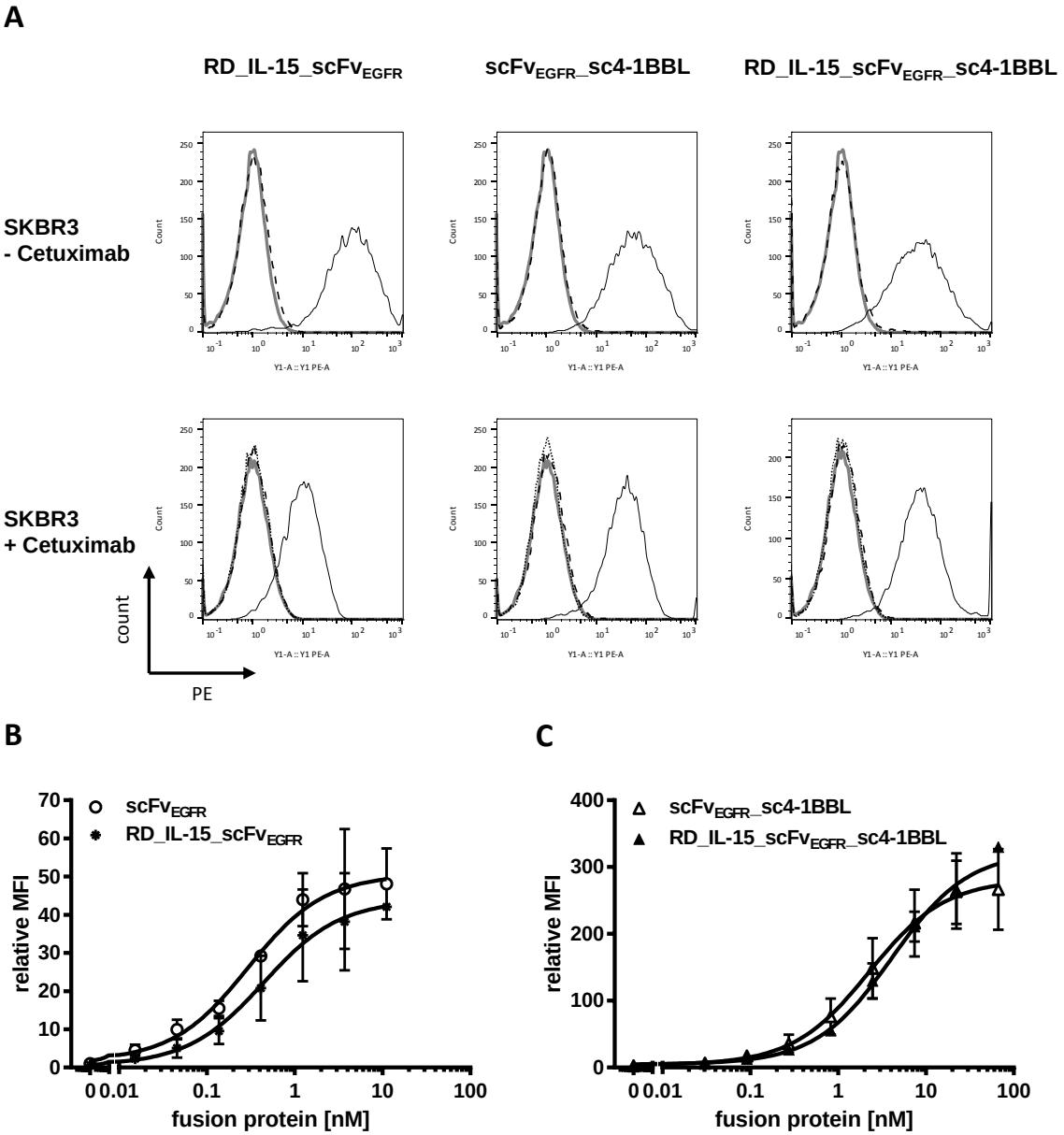

Figure 28: Binding properties of fusion proteins targeting EGFR. A Bifunctional binding analysis by flow cytometry. Fusion proteins (40 nM) were incubated with EGFR$^+$ (SKBR-3) cells (upper panel). To block the binding of the antibody moiety to EGFR, cells were preincubated with a 200-fold molar excess of Cetuximab prior to addition of the antibody-fusion protein (lower panel). Antibody-mediated binding was detected via ligand-receptor interaction, using recombinant 4-1BB-Fc (5 µg/ml), detection was performed by anti-human Fc-PE mAb (upper panel) or anti-His-PE (lower panel). Thick grey line, cells only; dashed black line, detection system; dotted line, fusion protein + Cetuximab; black line, fusion protein. **B and C** Antibody-mediated binding analyzed by flow cytometry. SKBR-3 cells were incubated with fusion proteins followed by detection via **B** anti-His-PE mAb or **C** anti-4-1BB-PE. Mean ± SD, n=3.

When SKBR-3 cells were preincubated with a 200-fold molar excess of Cetuximab, binding of fusion proteins was blocked, proving specific binding of the fusion proteins to EGFR (Figure 28A, lower panel). RD_IL-15_scFv$_{EGFR}$ (EC_{50} 0.17±0.02 nM) demonstrated similar binding compared to scFv$_{EGFR}$ (EC_{50} 0.19±0.04 nM) (Figure 28B), whereas the two fusion proteins scFv$_{EGFR}$_sc4-1BBL (EC_{50} 1.3±0.4 nM) and RD_IL-15_scFv$_{EGFR}$_4-1BBL (EC_{50} 1.7±0.7 nM) showed similar lower binding (Figure 28C). Thus, all fusion proteins showed the capability to specifically bind to EGFR expressing tumor cells (SKBR-3) and to simultaneously bind to the receptor 4-1BB.

4.4.3 IL-15 activity

Activity of the RD_IL-15 in the fusion proteins was determined via the induction of proliferation of CTLL-2 cells (Figure 29A). RD_IL-15_scFv$_{EGFR}$ (EC_{50} 4.6±4.0 nM) as well as RD_IL-15_scFv$_{EGFR}$_sc4-1BBL (EC_{50} 7.2±6.7 nM) showed the ability to induce CTLL-2 proliferation in a concentration dependent manner. In addition, RD_IL-15_scFv$_{EGFR}$_sc4-1BBL showed two times lower activity on PBMC proliferation (EC_{50} 1.9±0.005 nM) compared to RD_IL-15_scFv$_{EGFR}$ (EC_{50} 0.8±0.3 nM) (Figure 29B). This observation was in accordance with the results obtained with the FAP-directed trifunctional fusion proteins, indicating that the IL-15 activity is not enhanced by the sc4-1BBL component in soluble form.

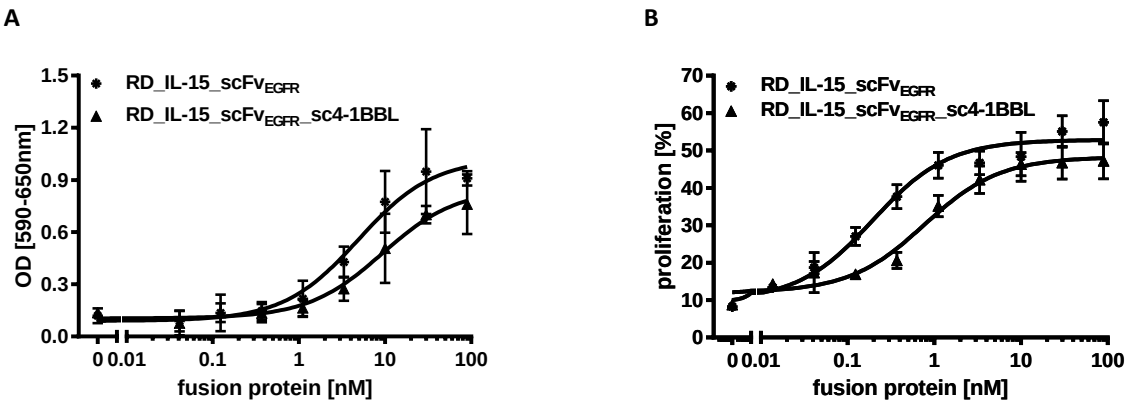

Figure 29: Effect of non-targeted trifunctional fusion proteins on the proliferation of CTLL-2 cells and PBMCs. **A** Previously starved CTLL-2 cells were incubated with fusion proteins. After 72 h, proliferation was assessed in MTT assay. **B** PBMCs were incubated with fusion proteins in absence of target cells. Proliferation of CFSE-labeled PBMCs was determined after 6 days via flow cytometry. Mean ± SD, n=3.

4.4.4 Targeting-mediated activity on T cells

The activity of targeted fusion proteins was determined in a coculture assay with SKBR-3 cells ($EGFR^+$) and PBMCs in presence of an anti-CD3 mAb in suboptimal concertation. Measuring IFN-γ release, the trifunctional fusion protein showed the strongest enhancement effect compared to the corresponding bifunctional fusion proteins (Figure 30A). In terms of T cell proliferation, the trifunctional fusion protein was in general more effective than RD_IL-15_$scFv_{EGFR}$, but less effective than $scFv_{EGFR}$_sc4-1BBL on $CD4^+$ and $CD8^+$ T cells (Figure 30C and D). In general, all novel fusion proteins targeting EGFR have shown costimulatory activity.

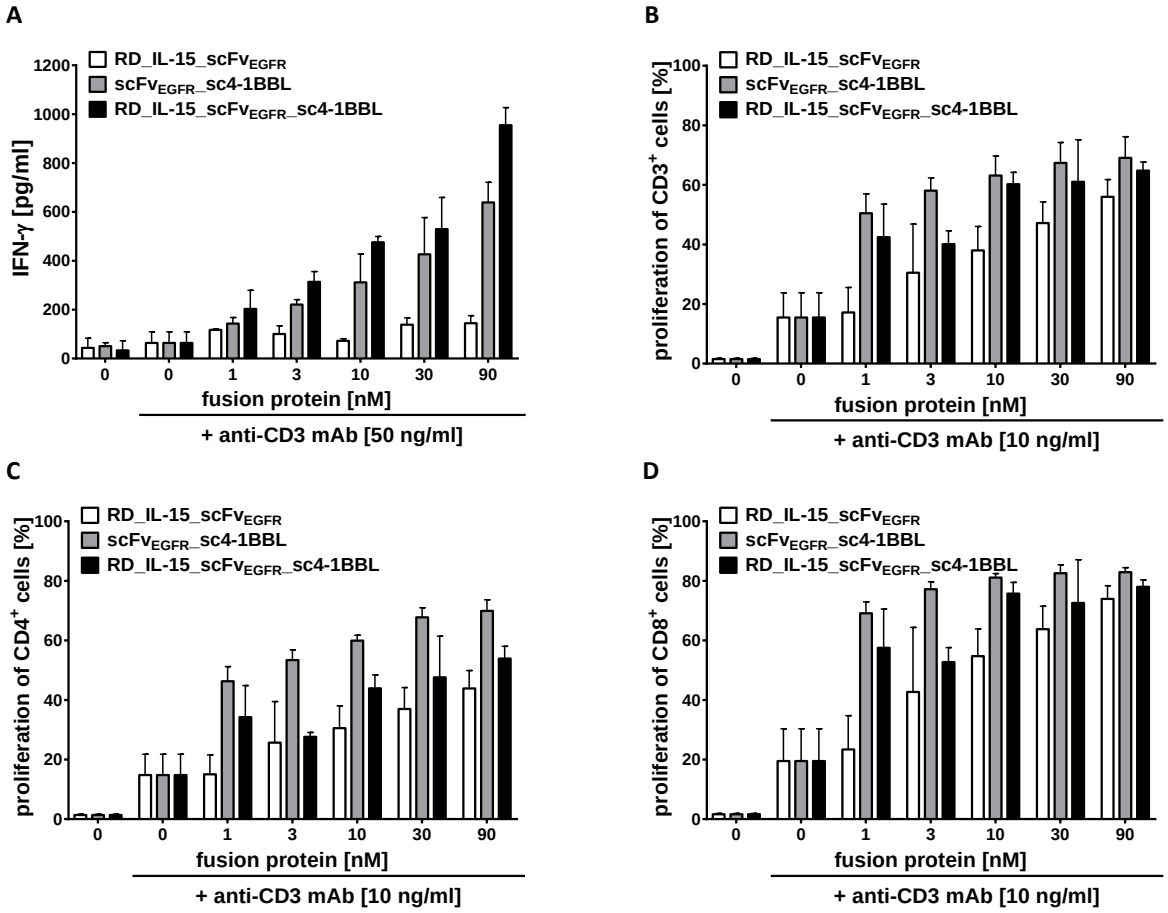

Figure 30: Targeted fusion protein mediated enhancement of T cell stimulation. SKBR-3 cells were cocultured with PBMCs, a suboptimal concentration of a cross-linked anti-CD3 mAb and targeted fusion proteins. **A** After 48 hours IFN-γ release was measured in sandwich- ELISA. **B-D** After 6 days the proliferation of **B** $CD3^+$ T cells, **C** $CD3^+CD4^+$ T cells and **D** $CD3^+$ $CD8^+$ T cells was determined by CFSE dilution in flow cytometry. Mean ± SD, Blockshift, n=3.

4.4.5 Targeting-mediated activity on NK cells

The set of fusion proteins targeting EGFR was developed for the enhancement of antibody-dependent cellular cytotoxicity (ADCC) by NK cells. Therefore, the influence of targeted fusion proteins on NK cell proliferation was determined in a coculture assay with SKBR-3 cells and PBMCs. In presence of an anti-CD3 mAb, the proliferative effect of the fusion proteins on NK cells is supported by cytokine release of T cells. Here, RD_IL-15_scFv$_{EGFR}$_sc4-1BBL showed highest effect on NK cells proliferation at higher concentrations (30, 90 nM). Whereas, in lower concentrations (1, 3, 10 nM) the trifunctional fusion proteins showed similar effect as scFv$_{EGFR}$_sc4-1BBL (Figure 31A). In presence of anti-CD3 mAb, T cell stimulation leads to IL-2 release supporting the stimulation of NK cells. Therefore, the effect of the fusion proteins on NK cells was additionally assessed in absence of anti-CD3 mAb. In contrast, the trifunctional fusion protein mediated higher effects at lower concentration (10 nM) compared to the two bifunctional fusion proteins. At higher concentrations (30, 90 nM), RD_IL-15_scFv$_{EGFR}$ and RD_IL-15_scFv$_{EGFR}$_sc4-1BBL revealed similar proliferative effects, while scFv$_{EGFR}$_sc4-1BBL fell behind (Figure 31B). These findings led to the assumption, that the combination of IL-15 and sc4-1BBL in one trifunctional fusion protein has a beneficial effect on proliferation of NK cells.

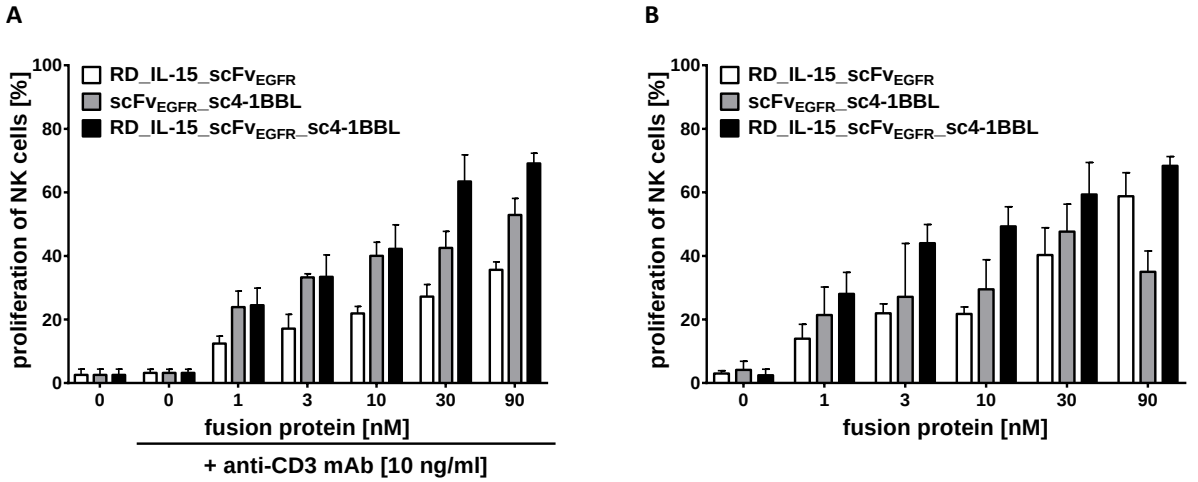

Figure 31: Fusion protein mediated stimulation of proliferation of NK cells. Proliferation of NK cells mediated by targeted fusion proteins was determined either in **A** presence or **B** in absence of a cross-linked anti-CD3 mAb. After 6 days the proliferation of NK cells ($CD3^-$ $CD56^+$) was determined by CFSE dilution in flow cytometry. Mean ± SD, Blockshift, n=3.

4.4.6 Influence of fusion proteins directed against EGFR on antibody-mediated cellular cytotoxicity (ADCC)

Trastuzumab was the first monoclonal antibody targeting HER2 approved for clinical use acting by binding the extracellular domain of HER2 and exhibiting therapeutic efficacy in HER2 overexpressing metastatic and early stage breast cancer. One mechanism of action of Trastuzumab is the antibody-dependent cellular cytotoxicity (ADCC) (Gennari et al. 2004; Cooley et al. 1999; Lewis et al. 1993). Upon exposure to IgG-coated target cells subjected to antibody-dependent cellular cytotoxicity (ADCC), 4-1BB becomes expressed on NK cells (Navabi et al. 2015). Therefore, the fusion proteins targeting EGFR were combined with a Trastuzumab to investigate the potential of the trifunctional fusion protein to enhance the Trastuzumab-induced ADCC of NK cells. SKBR-3 cells (Her-2^+ and $EGFR^+$) with targeted fusion proteins (100 nM) were incubated with a serial dilution of Trastuzumab in presence of PBMCs. After 24 hours, cell viability of target cells (MTT) and cytotoxic potential of NK cells (degranulation, flow cytometry) was determined.

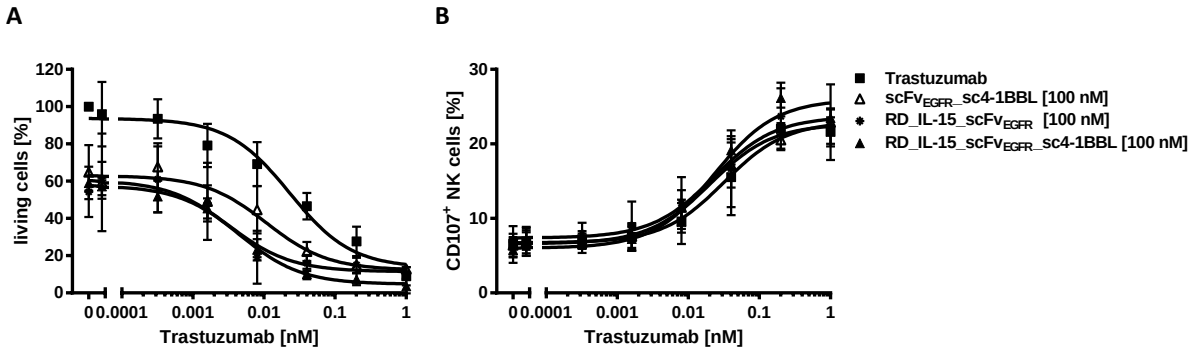

Figure 32: Fusion protein mediated enhancement on ADCC of Trastuzumab. EGFR and Her-2 positive cells (SKBR-3) were cocultured with PBMCs (5% NK cells) in presence of target-bound fusion protein [100 nM] and a serial dilution of Trastuzumab. After 24h **A** ADCC was determined by measuring cell viability in MTT assay and **B** Cytotoxic potential of NK cells was determined by measuring CD107a expression in flow cytometry. Mean ± SD, n=3.

Trastuzumab mediated ADCC in a concentration dependent manner, and all three fusion proteins were able to enhance Trastuzumab-mediated ADCC. In terms of target cell (SKBR-3) viability, RD_IL-15_$scFv_{EGFR}$ (EC_{50} 0.004±0.003 nM) and RD_IL-15_$scFv_{EGFR}$_sc4-1BBL (EC_{50} 0.005±0.002 nM) showed a similar enhancement effect on tumor cell killing, whereas $scFv_{EGFR}$_sc4-1BBL (EC_{50} 0.01±0.006 nM) was less effective (Figure 32A). However in terms of measuring degranulation of NK cells, the effect of Trastuzumab was not further enhanced by the fusion proteins (Figure 32B). 4-1BBL has shown to be active in terms of NK cell-mediated

tumor cell killing in the bifunctional fusion protein, but this effect could not be further enhanced by combining 4-1BBL with IL-15 in the trifunctional fusion protein.

Due to the ability to activated NK cells in terms of proliferation and their Trastuzumab-mediated ADCC enhancing properties, the trifunctional fusion protein with IL-15 and sc4-1BBL provides a suitable platform for further development.

5 Discussion

Using antibody-fusion proteins to modulate the immune system has become a growing field in current research. In the present study, second generation IL-15-based trifunctional fusion proteins have been generated. In comparison to the first generation, IL-15-based trifunctional fusion proteins comprising one targeting moiety (scFv), one RD_IL-15 unit and one effector moiety (4-1BBL) in the single chain format have shown beneficial costimulatory effects. Furthermore, IL-15-based trifunctional fusion proteins were generated incorporating other members of the TNF superfamily (OX40L and GITRL). All trifunctional fusion proteins were stable and costimulatory active, i.e. enhancing the activation of different immune cell subsets. Furthermore, antitumor potential of the trifunctional fusion proteins with 4-1BBL and GITRL was shown by reducing tumor burden in a mouse model *in vivo*. In a last step, an IL-15-based trifunctional fusion protein with sc4-1BBL and a targeting moiety directed against EGFR was generated. The EGFR-targeting fusion protein manifested the ability of NK cell activation and enhanced ADCC mediated by the clinically approved monoclonal antibody Trastuzumab.

5.1 Improving antibody-fusion proteins by introducing the TNFSFL in the single-chain format

The homotrimeric scFv-TNFSFL fusion proteins have been extensively studied. Here, fusion of the TNFSF ligands 4-1BBL, OX40L and GITRL to a scFv lead to targeting-dependent costimulatory activity (Sapski et al. 2017; Kermer et al. 2014; Hornig et al. 2013; Hornig et al. 2012).

The specific assembly of scFv-TNFSFL is mediated by the extracellular TNF homology domain of the TNF superfamily member forming trimers in a non-covalent fashion (Bodmer et al. 2002). Accordingly, ligand-receptor interaction occurs in a 3:3 ratio resulting in receptor clustering and signaling. While other members of the TNF superfamily, e.g. TNF, FasL and TRAIL, present themselves in a tightly packed bell-shaped form, the costimulatory members reveal different structural properties. Despite the typical length of the THD in 4-1BBL, it forms a planar three-bladed propeller shape, whereas OX40L and GITRL have a shorter TNF homology domain leading to a blooming flower-like shape. To date, a single-chain version, i.e. the genetic fusion of three extracellular domains on one polypeptide chain, has been reported to prevent ligand dissociation and therefore stabilized intramolecular

homotrimerization resulting in increased biological activity of TNF (Krippner-Heidenreich et al. 2008), TRAIL (Siegemund et al. 2016; Schneider et al. 2010) and TNFSF ligands (Fellermeier-Kopf et al. 2018; Fellermeier et al. 2016). Especially GITRL was expected to benefit from stabilization by the single-chain format, as human GITRL is described to show only loose trimeric assembly and a dynamic monomer-trimer (Chattopadhyay et al. 2007) or dimer-trimer (Zhou et al. 2008) equilibrium due to substantially smaller intersubunit interfaces with correspondingly fewer contacts between the interacting protomers compared to other TNF superfamily ligands (Chattopadhyay et al. 2009).

In this study, the single-chain version of 4-1BBL, OX40L and GITRL incorporated in bi-and trifunctional fusion proteins have been evaluated. In the generation process of the single-chain format, the length of the linkers connecting the extracellular domains of the costimulatory ligand has to be carefully chosen to support their naturally occurring trimerization. The information about the distance between N- and C-terminus of adjoining subunits in the trimeric structure derived from crystal structure data (Won et al. 2010; Chattopadhyay et al. 2008; Chattopadhyay et al. 2007; Compaan and Hymowitz 2006). In this study, all fusion proteins incorporating the costimulatory ligand in the single-chain format showed the ability to bind their respective receptors, leading to the assumption of correct linker length and thereby correct assembly of the costimulatory ligands. Fusion of sc4-1BBL, scOX40L or scGITRL to $scFv_{FAP}$ or RD_IL-15_$scFv_{FAP}$ did not hamper receptor-ligand interaction of the costimulatory ligands, further validating the single-chain format as a suitable platform for the generation of antibody-fusion proteins. However, lower antibody valency in the single-chain format (antibody-ligand ration 1:1) compared to the homotrimeric format (antibody-ligand ration 3:1) led to reduced antibody binding capacities. Thus, the bifunctional fusion protein in the single-chain format ($scFv_{FAP}$_sc4-1BBL) showed reduced binding compared to the homotrimeric format ($scFv_{FAP}$_4-1BBL) but similar binding compared to the single $scFv_{FAP}$ alone. Similar results were obtained for the trifunctional fusion proteins in the single-chain (RD_IL-15_$scFv_{FAP}$_sc4-1BBL) and homotrimeric format (RD_IL-15_$scFv_{FAP}$_4-1BBL), where reduced binding for RD_IL-15_$scFv_{FAP}$_sc4-1BBL was observed. In contrast, bifunctional fusion proteins with 4-1BBL and OX40L in the single-chain format, but targeting EpCAM or CLD4/6 have either shown similar or even reduced binding compared to the respective scFv alone (Fellermeier et al. 2016). Here, accessibility of the

epitope was potentially hampered upon fusion of the antibody moiety to a costimulatory ligand, which resulted in reduced binding capacity.

Lower antibody valency of $scFv_{FAP}$_sc4-1BBL led to reduced antigen binding capacity in comparison to $scFv_{FAP}$_4-1BBL. Nevertheless, in a targeted setting, monomeric $scFv_{FAP}$_sc4-1BBL showed significantly improved capacity to enhance T cell proliferation and an even more distinct improvement in terms of IFN-γ release of PBMCs compared to homotrimeric $scFv_{FAP}$_4-1BBL (Figure 5). This was not only shown for the bifunctional but also for the trifunctional fusion proteins, where targeted RD_IL-15_$scFv_{FAP}$_sc4-1BBL showed superior costimulatory effects on PBMCs compared to RD_IL-15_$scFv_{FAP}$_4-1BBL (Figure 8). These findings indicate improved bioactivity for the fusion proteins with sc4-1BBL. In the single-chain format, naturally occurring trimerization of the TNFSF ligand presumably is stabilized by covalent linkage of the extracellular domains. According to the current model of TNFSF receptor activation, TNF superfamily ligand-receptor interaction leads to the trimerization of the receptor and further to the formation of ligand-receptor complex clustering (Chattopadhyay et al. 2009). In the context of an antibody-fusion protein, receptor trimerization and clustering can be achieved by cell surface presentation of the trimeric TNF superfamily ligand, mimicked by targeting to a cell surface or oligomerization of soluble ligands (Wajant 2015). Support of trimeric ligand formation through the single-chain format positively influenced ligand-receptor complex clustering while targeting the fusion protein to the tumor cell with one scFv unit is sufficient for membrane presentation of the TNFSF ligand.

It has to be taken into account, that increased costimulatory activity of the bi- and trifunctional fusion proteins with a scTNFSFL could also potentially result from oligomerization in soluble form. Soluble 4-1BBL, OX40L and GITRL are hardly active but can potentially regain their activity by molecular crosslinking. In this study, it was observed that the bifunctional fusion protein $scFv_{FAP}$_sc4-1BBL induced an effect on PBMC proliferation in a soluble form without target cells (Figure 5). In contrast, costimulatory activity of $scFv_{FAP}$_4-1BBL only occurred in a targeted setting, in accordance with former data (Hornig et al. 2012). Compared to the latter, $scFv_{FAP}$_sc4-1BBL showed a small oligomeric fraction in size exclusion chromatography. The oligomeric fraction probably occur due to dimer formation of the scFv which has been described for other scFvs (Arndt et al. 1998). These findings lead to the assumption that spontaneous oligomerization of the scTNFSFL mediated by the scFv

could potentially cause targeting-independent activation of the respective receptor. Thus, differences in the tendency for dimer-formation of scFvs influence oligomersation of the scTNFSFL and therefore potentially targeting-independent activity of the fusion protein. High effects on PBMC proliferation in absence of target cells was observed for bifunctional fusion proteins targeting EpCAM ($scFv_{EpCAM}$_sc4-1BBL and $scFv_{EpCAM}$_4-1BBL) (Fellermeier et al. 2016). Size exclusion chromatography also revealed a dimeric fraction for the bifunctional fusion protein $scFv_{EpCAM}$_scOX40L (Fellermeier et al. 2016). Interestingly, $scFv_{EpCAM}$_scOX40L did not show targeting-independent costimulation of T cells, indicating differences in the influence of the oligomerization state on the activity of different TNFSF members. Due to variations observed for different scFvs and different TNFSF ligands, the targeting moiety as well as the TNFSF ligand have to be chosen carefully. Importantly, independent of the oligomeric state, costimulatory activity of the $scFv_{FAP}$_sc4-1BBL fusion protein was only observed in presence of the anti-CD3 mAb-mediated primary stimulus, indicating a strictly costimulatory nature without any supra-agonistic activity.

In addition to advantageous functional effects, high serum stability for bifunctional fusion proteins in the single-chain format has been observed. Similar results have also been reported for scTNF compared to wild-type TNF (Krippner-Heidenreich et al. 2008), for $scFv_{EpCAM}$_sc4-1BBL compared to $scFv_{EpCAM}$_4-1BBL and $scFv_{EpCAM}$_scOX40L compared to $scFv_{EpCAM}$_OX40L (Fellermeier et al. 2016).

In summary, introduction of the TNF superfamily member 4-1BBL in the single-chain format led to stabilization of the functional unit in the fusion proteins with enhanced costimulatory activity albeit reduced antibody binding capacity.

5.2 Combination of IL-15 and TNF superfamily members 4-1BBL, OX40L and GITRL in trifunctional fusion proteins

In this study, the strong effects of RD_IL-15 were further enhanced when combined with ligands of the TNF superfamily. Previous studies have shown that fusion of IL-15 to the extended sushi domain combined with a targeting moiety (scFv) results in a functional molecule successfully inducing T cell response *in vitro* and reduction of tumor burden in a B16 mouse model (Kermer et al. 2012). In further development, RD_IL-15_$scFv_{FAP}$ was fused to the TNF superfamily member 4-1BBL resulting in a trifunctional fusion protein further enhancing the advantageous features of RD_IL-15_$scFv_{FAP}$ in terms of T cell proliferation and antitumor response (Kermer et al. 2014). Several combinatorial approaches incorporating

two monomeric cytokines in one polypeptide have been described, e.g. the fusion of IL-12 and IL-2 to several antibody fragments resulting in different combinations of the latter (Gillies et al. 2002). The fusion protein scFv_IL-12_Fc_IL-2 has been shown to activate resting T cells and NK cells as well as to induce tumor regression in a mouse tumor model (Jahn et al. 2012). Durable complete responses in mice with WEHI-161 sarcomas have been observed for the dual-cytokine fusion protein, consisting of an antibody moiety targeting fibronectin fused to IL-2 and TNF (Luca et al. 2017). Based on the homotrimeric trifunctional fusion protein by Kermer et al. (2014), a novel trifunctional fusion protein was generated in this study, incorporating the ligand of the TNF superfamily in the single-chain format. Similar to the bifunctional fusion proteins in the homotrimeric and single chain format, introduction of 4-1BBL in the single-chain format led to reduced antibody avidity of the molecule and therefore reduced scFv-mediated binding to target cells. Interestingly, higher avidity in terms of IL-15 for the homotrimeric trifunctional fusion proteins did not show any further advantageous effects compared to RD_IL-15_scFv$_{FAP}$_sc4-1BBL. Accordingly, studies on other antibody-fusion protein formats showed that bivalent IgG-IL-15_RD and monovalent IL-15_RD induced proliferation of Kit225 cells to a similar extend (Vincent et al. 2014). Fusion of 4-1BBL or sc4-1BBL to RD_IL-15_scFv$_{FAP}$ did not enhance but rather inhibit the IL-15 activity of the non-targeted trifunctional fusion protein, indicating inactivity of the costimulatory ligand in solution. Activity of the costimulatory ligand could only be observed in the targeted setting where cell surface expression is mimicked by antibody-mediated binding. This observation is consistent with previous studies on scFv_4-1BBL (Müller et al. 2008a) and scFv_OX40L (Müller et al. 2008b). Lower antibody valency in the single-chain format did not translate into lower ligand activity, leading to the assumption that cell surface presentation of the ligand by a single antigen-binding unit was sufficient. The presence of redundant scFv units might sterically interfere with optimal presentation of the ligand, explaining the improved activity of the trifunctional fusion protein with the TNFSF ligand in the single-chain format.

In the present study, additional trifunctional fusion proteins with the TNF superfamily members OX40L and GITRL in the single-chain format were generated based on the promising results for the trifunctional fusion protein incorporating 4-1BBL in the single-chain format. Strong immune stimulation and a combinatory benefit were observed for the trifunctional fusion proteins in the targeted setting. The combination of the respective

bifunctional fusion proteins was less effective, presumably due to antibody-mediated competition for the same target on the cell surface. Additionally, all trifunctional fusion proteins exceeded the costimulatory effect of to the respective bifunctional fusion protein. Thus, targeting IL-15 and ligands of the TNF superfamily simultaneously to the tumor cell resulted in stimulation of different immune cell subsets, where the effect was dependent on the TNFSFL-cytokine combination. In this study, the trifunctional fusion protein incorporating IL-15 and 4-1BBL showed strong impact on proliferation as well as on the cytotoxic potential of $CD8^+$ T cells (Figure 18 and 19). Under physiological conditions, 4-1BBL and IL-15 play an important role in the maintenance of $CD8^+$ T cell memory. Here, IL-15 induces the expression of 4-1BB on $CD8^+$ effector memory T cells which are then maintained by 4-1BBL stimulation (Pulle et al. 2006). Additionally, elevated expression of 4-1BB was observed on tumor-reactive tumor-infiltrating lymphocytes following incubation with IL-15 and IL-7 (Ye et al. 2014). Interestingly, RD_IL-15_$scFv_{FAP}$_sc4-1BBL did not only show strong impact on the cytotoxic potential of $CD8^+$ T cells, but also on the degranulation of $CD4^+$ T cells (Figure 19). Several studies have reported that $CD4^+$ T cells are powerful antitumor effector cells and can outperform $CD8^+$ T cells (Perez-Diez et al. 2007), i.e. $CD4^+$ T cells kill melanoma cells *in vitro* when recognizing a peptide presented by the tumor cell in the context of HLA class II antigen (Brady et al. 2000). OX40 engagement in the context of chemotherapy-induced lymphopenia has been reported to induce a $CD4^+$ T cell population characterized by secretion of Th1 and Th2 cytokines and thereby eradicating very advanced melanomas in mice (Hirschhorn-Cymerman et al. 2012) and Qui et al. identified a costimulatory pathway (OX40, 4-1BB) and an intracellular mechanism relying on eomesodermin inducing both antigen-specific and bystander cytotoxic $CD4^+$ T cells (Qui et al. 2011).

Furthermore, $scFv_{FAP}$_scOX40L and $scFv_{FAP}$_scGITRL highly benefited from fusion to RD_IL-15 represented by a 2- (RD_IL-15_$scFv_{FAP}$_scOX40L) to 3- fold (RD_IL-15_$scFv_{FAP}$_scGITRL) increase in T cell proliferation (Figure 15). Interestingly, scGITRL only displayed very low activity in the bifunctional fusion protein while the trifunctional fusion protein with scGITRL demonstrated strong activity enhancing the proliferation of $CD8^+$ T cells and the cytotoxic potential of $CD8^+$ T cells. In line with this, GITR expression on $CD8^+$ memory T cells has been observed to be induced upon exposure to IL-15 (Sabbagh et al. 2007). Furthermore, IL-15 as well as GITRL have shown the potential to induce the proliferation and enhance the cytotoxic potential of $CD8^+$ T cells (Robinson and Schluns 2017; Clouthier and Watts 2014).

IL-15 has been reported to enhance the recovery of cytotoxic T lymphocyte activity without losing their specificity and favoring the expansion of $CD8^+$ T_{CM} cells (Daudt et al. 2008). Additionally, transferred $CD8^+$ T cells into IL-15 transgenic mice showed high CTL activity and expression of granzyme B compared to IL-15 knockout mice (Yajima et al. 2005). GITR stimulation was found to enhance cytotoxicity and IFN-γ secretion in a T cell transfer setting (Imai et al. 2009). Modulation of GITR has revealed compelling antitumor activity which is attributed to both its costimulatory role on $CD4^+$ and $CD8^+$ T cells (Côté et al. 2011; Zhou et al. 2007) as well as inhibition or depletion of intratumoral regulatory T cells (Coe et al. 2010; Cohen et al. 2010; Ko et al. 2005). Hence, a trifunctional fusion protein combining IL-15 and GITRL is of great potential, regarding the promotion of an antitumor immune response.

For further evaluation of the costimulatory potential of the trifunctional fusion proteins not only mechanisms at the molecular level but also the immune cell type distribution has to be taken into account. Various studies in colon carcinoma have reported the correlation between high number of memory ($CD45RO^+$) lymphocytes and a high overall survival along with low tumor recurrence (Pagès et al. 2009; Pagès et al. 2005), hypothesizing that a long lasting antitumor capacity and trafficking properties of memory T cells play a central role in control of tumor recurrence (Galon et al. 2006; Xiang et al. 1999). Memory T cells can be further divided in central memory (T_{CM}) and effector memory (T_{EM}) (Sallusto et al. 1999), whereby central memory T cells have been described to traffic to lymphoid tissue and have a higher proliferative capacity (Klebanoff et al. 2005) compared to effector memory T cells, localizing in peripheral tissue and developing effector functions more rapidly (Manjunath et al. 2001). In the present study, T_{EM} cells were strongly responsive to treatment with RD_IL-15_$scFv_{FAP}$_sc4-1BBL, whereby the effect was clearly dominant on $CD8^+$ T_{EM} cells (Figure 17). Similar results were obtained with the bifunctional fusion protein $scFv_{FAP}$_sc4-1BBL in the present study as well as with $scFv_{EDG}$_4-1BBL in the combination with a bispecific antibody (Sapski et al. 2017). Influenza infection of 4-1BBL-deficient mice revealed a role for 4-1BBL in controlling influenza specific effector-memory T cell numbers in the primary response (Tan et al. 2000; Tan et al. 1999), validated by the finding that 4-1BBL is important in antigen-independent (Zhu et al. 2007; Pulle et al. 2006) as well as antigen-dependent (Wiethe et al. 2003) maintenance of $CD8^+$ T cell memory and the ability of 4-1BBL to promote antitumor effector/memory $CD8^+$ T cells in a poorly immunogenic mouse model in combination with an PD-1 antagonist (Chen et al. 2015). Taken together, these studies further elucidate the

potent effects of 4-1BBL on memory T cells. Regarding $CD4^+$ T_{EM} cells, RD_IL-15_$scFv_{FAP}$_scOX40L mediated highest responsiveness represented in high proliferation rate of all $CD4^+$ T cell subpopulations as well as in a clear shift of the population towards $CD4^+$ T_{EM} cells (Figure 17). Again, similar effects have been observed for the bifunctional fusion protein incorporating scOX40L. In line with the present results, Sapski et al. (2017) showed that combined costimulation with OX40L increases the impact on $CD4^+$ T cell subsets. Consistently, the OX40L-Fc fusion protein MEDI6383 mediates proliferation of $CD4^+$ and $CD8^+$ central and effector memory T cells in the peripheral blood of non-human primates (Oberst et al. 2018). RD_IL-15_$scFv_{FAP}$_scGITRL mediated high proliferation of $CD4^+$ and $CD8^+$ T cell (Figure 18) and enhanced the cytotoxic potential of $CD8^+$ T cell (Figure 19). In line with these findings, a study by Snell et al. (2012) postulates the IL-15 dependent upregulation of GITR on memory $CD8^+$ T cells.

The antitumoral activity of the trifunctional fusion proteins was assessed in a B16 lung tumor and a subcutaneous model in immunocompetent C57BL/6 mice. The mouse homolog RD_IL-15_$scFv_{FAP}$_mscGITRL significantly reduced the tumor burden in the lungs (Figure 23). This observation is supported by several studies using the B16 mouse melanoma model describing persistent antitumor responses for targeting GITRL like the rejection of B16 melanoma tumors mediated via the agonistic mAb DTA-1 (Côté et al. 2011; Ramirez-Montagut et al. 2006; Turk et al. 2004). Furthermore, the antitumor potential of GITR agonism in the B16 mouse model was shown in a DC-based vaccination setting, where DCs expressed an agonistic mAb directed against CTLA-4 in combination with and anti-GITR mAb or soluble GITRL (Pruitt et al. 2011). In a tumor model in colon carcinoma, it was shown that treatment with Fc-mGITRL reduced tumor growth and enhanced survival (Hu et al. 2008). Treatment with the non-targeted trifunctional fusion protein RD_IL-15_$scFv_{CEA}$_mscGITRL or the combination of the two bifunctional fusion proteins did not result in reduced tumor formation. These results indicate that target binding mimicking membrane-presentation of the TNFSF and simultaneous presentation of the components IL-15 and TNFSFL play an important role in the effect of the trifunctional fusion protein.

In the subcutaneous syngeneic mouse model a delay of tumor growth for RD_IL-15_$scFv_{FAP}$_mscGITRL and RD_IL-15_$scFv_{FAP}$ was detected (Figure 24). On day 12 after tumor cell injection, treatment with the trifunctional fusion protein showed significantly lower tumor burden in comparison to the PBS group. Unfortunately, on day 21 no significant

difference was observed for the trifunctional fusion protein compared to the bifunctional fusion protein or the PBS group (Figure 24). B16 melanoma cells are known to be poorly immunogenic (Zeiser et al. 2012). Thus, using a more immunogenic mouse model for evaluating the effect of the trifunctional fusion proteins possibly results not only in tumor growth delay but overall tumor reduction.

Regarding the effect on immune cells in the spleen of the mice, treatment with RD_IL-15_scFv$_{FAP}$_mscGITRL led to a significant increase of NK cells (Figure 26). Unfortunately, no significant differences were observed in terms of immune cell infiltration into the tumors (Figure 25). This finding indicates that the fusion proteins either cannot penetrate the tumor or the amount of fusion protein reaching the tumor site is too low to mediate an antitumor effect. Tumor size, vascularization, composition of the extracellular matrix and molecule size are affecting tumor penetration of an antibody or a fusion protein (Beckman et al. 2007). Monoclonal antibodies with a size of approximately 150 kDa have shown the ability to penetrate tumors (Olabiran et al. 1994; Myrdal and Foster 1994; Kwok et al. 1988) .Thus, the low effect of the fusion proteins in this tumor model cannot be explicitly attributed to the size of the fusion proteins. To further elucidate the properties of the trifunctional fusion protein in terms of tumor localization and penetration, the pharmacokinetical properties, bioavailability and biodistribution have to be further assessed.

5.3 Bi- and trifunctional fusion proteins with IL-15 and sc4-1BBL enhance ADCC

Targeting HER2 in antibody-based antitumor therapy has been subject of various studies (Pondé et al. 2018; Di Modica et al. 2017). Trastuzumab was the first monoclonal antibody targeting HER2 approved for clinical use acting by binding the extracellular domain of HER2 and exhibiting therapeutic efficacy in HER2 overexpressing metastatic and early stage breast cancer. However, patients with HER2-positiv tumors only showed a low response rate to Trastuzumab therapy and intrinsic resistance mechanisms evolved upon Trastuzumab monotherapy (Vogel et al. 2002; Cobleigh et al. 1999; Baselga et al. 1996). In contrast, combination therapy of Trastuzumab along with small molecule inhibitors (Hanusch et al. 2015; Baselga et al. 2012; Maira et al. 2012) or chemotherapy (Esteva et al. 2002; Seidman et al. 2001; Slamon et al. 2001) provide a beneficial therapeutic effect. One mechanism of action of Trastuzumab is the antibody-dependent cellular cytotoxicity (ADCC) (Gennari et al. 2004; Cooley et al. 1999; Lewis et al. 1993) which was shown to be further enhanced by

combination of Trastuzumab with IL-2 treatment (Repka et al. 2003). Additionally, in a preclinical study the synergistic effect of antibodies against PD-1 and 4-1BB in combination with Trastuzumab have been observed (Stagg et al. 2011).

ADCC is mediated by NK cells upon binding of the antibody Fc portion to FcγR (Wallace et al. 1994). According to the concept of Kohrt et al. (2014), the monoclonal antibody localizes at the tumor site and activates surrounding NK cells vial the Fc-FcγR interaction, increasing expression of the costimulatory receptor 4-1BB on NK cells. The fusion protein with 4-1BBL could then further enhance the activated NK cell's ability to kill mAb-coated tumor cells. Upregulation of 4-1BB on NK cells has also been shown upon stimulation with IL-15 (Navabi et al. 2015) supporting the rational of combining 4-1BBL and IL-15 in one fusion protein to stimulate NK cells. A K562 feeder cell line expressing MICA, 4-1BB and IL-15 was reported to be sufficient in NK cell expansion and promote NK cell activation, proliferation, IFN-γ production and cytotoxicity (Gong et al. 2010) and *ex vivo* activation of NK cells with 4-1BBL and IL-15 revealed a clinical effect in hematological malignancies in combination with chemotherapy (Vela et al. 2018) further stressing the potent effects on NK cells mediated by the combination of IL-15 and 4-1BBL. In this study, ADCC mediated by Trastuzumab was further enhanced by the combination with the fusion proteins consisting of 4-1BBL and IL-15, whereby the trifunctional fusion and the bifunctional fusion protein RD_IL-15_scFv$_{EGFR}$ showed highest improvement compared to scFv$_{EGFR}$_sc4-1BBL (Figure 32). Several studies have shown the beneficial effect of IL-15, 4-1BB targeting or their combination in the enhancement of ADCC. Synergistic effects have been reported for Trastuzumab and an anti-4-1BB mAb (Kohrt et al. 2012; Stagg et al. 2011) and Trastuzumab with IL-15 (Wege et al. 2017). Additionally, IL-15 and 4-1BB agonism have revealed synergistic effects in combination with other monoclonal antibodies, e.g. Cetuximab (Srivastava et al. 2017; Kohrt et al. 2014).

In the present study, no significant difference was observed between the bifunctional fusion protein RD_IL-15_scFv$_{EGFR}$ and the trifunctional fusion protein regarding the enhancement of ADCC and in terms of enhanced cytotoxic potential of NK cells. These findings led to the assumption, that under the present conditions 4-1BBL in the trifunctional fusion protein did not contribute to the enhancement of NK cell-mediated ADCC. Time shifted application of Trastuzumab and the trifunctional fusion protein might be required to adapt the strategy to the timing of 4-1BB receptor expression. Fc-FcγR interaction was shown to induce the

upregulation of 4-1BB on NK cells in a time dependent manner, peaking at 24 hours (Kohrt et al. 2014; Lin et al. 2008). Accordingly, preactivation of NK cells via Fc-FcγR interaction and addition of the trifunctional fusion protein after 24h could potentially lead to more efficient enhancement of NK cell-mediated ADCC. A similar approach was pursued by Kohrt et al. (2014) where PBMCs were first cultured with Cetuximab and irradiated EGFR-expressing tumor cells for 24h followed by incubation of the preactivated, purified NK cells with EGFR-expressing tumor cells and an anti-4-1BBL mAb.

As one of the first monoclonal antibodies targeting EGFR, Cetuximab was approved by the FDA for the treatment of colorectal and head and neck cancer in 2004. Hence, the clinically validated target EGFR was chosen for the fusion proteins enhancing ADCC, mediated by the clinically used monoclonal antibody Trastuzumab. Upon changing the antibody moiety from $scFv_{FAP}$ to $scFv_{EGFR}$, all components of the trifunctional fusion protein retained their function, reflected in EGFR binding, CTLL-2 proliferation in a non-targeted setting and T cell stimulation of targeted fusion proteins. Thus, the trifunctional fusion protein platform is not only applicable for different TNFSF ligands but additionally for different targets.

5.4 Conclusion and outlook

In this study, the IL-15 based trifunctional fusion protein with 4-1BBL in the single-chain format showed similar T cell stimulation in a non-targeted setting, even improved capacity to enhance T cell stimulation when target bound and a clear antitumor effect in a lung tumor mouse model in comparison to the homotrimeric fusion protein. Furthermore, OX40L and GITRL were successfully incorporated into the novel trifunctional fusion protein single-chain format demonstrating stable protein configuration. Advantageous costimulatory properties were observed for the trifunctional fusion proteins in comparison to the combination of the respective bifunctional fusion proteins. RD_IL-15_$scFv_{FAP}$_scGITRL showed to be especially potent in enhancing the cytotoxic potential of $CD8^+$ T cells and enhancing the proliferation of $CD4^+$ T cells. A syngeneic lung tumor mouse model revealed a strong, targeting-dependent antitumor response for RD_IL-15_$scFv_{FAP}$_scGITRL. Additionally, strong enhancement of monoclonal antibody-mediated ADCC was observed for the trifunctional fusion protein RD_IL-15_$scFv_{EGFR}$_sc4-1BBL.

One strategy to further improve the activity of the trifunctional fusion proteins at the tumor site would be the combination with other immune-modulatory strategies including vaccination to enhance the frequency of tumor-specific T cells (Deumelandt et al. 2018;

Kobayashi et al. 2015; Bartkowiak et al. 2015; Zhu et al. 2015; Ganguly et al. 2010) or the combination with immune checkpoint inhibitors, e.g. anti-PD-1 (Villarreal et al. 2017; Messenheimer et al. 2017; Horton et al. 2015; Shindo et al. 2015; Lu et al. 2014) or anti-CTLA-4 (Pedroza-Gonzalez et al. 2015; Redmond et al. 2014; Curran et al. 2011) monoclonal antibodies possibly leading to a synergistic effect and further enhancement of the immune response at the tumor site.

Immunostimulatory approaches bear the risk of excessive activation of the immune system potentially leading to a cytokine release syndrome, like that observed during phase I studies with the anti-CD28 mAb TGN1412 (Suntharalingam et al. 2006). In contrast to the supra-agonistic monoclonal antibody TGN1412, the fusion proteins used in this study are costimulatory molecules incorporating ligands of the TNF superfamily which are only active upon target binding of the fusion protein. Therefore, no systemic activation of immune cells leading to severe side effects is expected. Latent side effects have been associated with high dose rIL-15 therapy such as hypotension, thrombocytopenia, liver injury and fever (Conlon et al. 2015). In contrast to rhIL-15, RD_IL-15 in the trifunctional fusion proteins used in the present study is expected to show reduced side effects due to their tumor-directed targeting moiety focusing the effect of the fusion protein and thereby IL-15 to the tumor site. Stimulation with trifunctional fusion proteins offer a promising alternative to agonistic antibodies or rIL-15 as they are at lower risk for systemic toxicity due to their tumor-directed targeting moiety. Nevertheless, further studies concerning the safety and tolerability of the trifunctional fusion proteins have to be conducted.

By establishing the trifunctional fusion proteins combining IL-15 with the single-chain TNFSF ligands into novel immunostimulatory tumor-targeted fusion proteins, this study adds a valuable contribution to the field of cancer immunotherapy. The trifunctional fusion proteins elicit strong stimulatory activity on T cells and NK cells and their modular composition potentially enables the implementation of various combinations of TNFSF ligands and cytokines to enhance the immune cell response at the tumor site. Immunotherapeutic molecules in the format of trifunctional fusion proteins combining targeting, cytokines and a TNFSFL in the single chain format are of future therapeutic relevance providing a platform with versatile opportunities for further development.

6 Publication bibliography

Aaronson, S. (1991): Growth factors and cancer. *Science* 254 (5035), pp. 1146–1153.

Acharya, Pinak S.; Zukas, Alicia; Chandan, Vishal; Katzenstein, Anna-Luise A.; Puré, Ellen (2006): Fibroblast activation protein: a serine protease expressed at the remodeling interface in idiopathic pulmonary fibrosis. *Human pathology* 37 (3), pp. 352–360.

Adams, Jerry L.; Smothers, James; Srinivasan, Roopa; Hoos, Axel (2015): Big opportunities for small molecules in immuno-oncology. *Nature reviews. Drug discovery* 14 (9), pp. 603–622.

Aertgeerts, Kathleen; Levin, Irena; Shi, Lihong; Snell, Gyorgy P.; Jennings, Andy; Prasad, G. Sridhar et al. (2005): Structural and kinetic analysis of the substrate specificity of human fibroblast activation protein alpha. *The Journal of biological chemistry* 280 (20), pp. 19441–19444.

Akhmetzyanova, Ilseyar; Zelinskyy, Gennadiy; Littwitz-Salomon, Elisabeth; Malyshkina, Anna; Dietze, Kirsten K.; Streeck, Hendrik et al. (2016): CD137 Agonist Therapy Can Reprogram Regulatory T Cells into Cytotoxic CD4+ T Cells with Antitumor Activity. *Journal of immunology (Baltimore, Md. : 1950)* 196 (1), pp. 484–492.

Alderson, M. R.; Smith, C. A.; Tough, T. W.; Davis-Smith, T.; Armitage, R. J.; Falk, B. et al. (1994): Molecular and biological characterization of human 4-1BB and its ligand. *European journal of immunology* 24 (9), pp. 2219–2227.

Arndt, K. M.; Müller, K. M.; Plückthun, A. (1998): Factors influencing the dimer to monomer transition of an antibody single-chain Fv fragment. *Biochemistry* 37 (37), pp. 12918–12926.

Atkins, M. B.; Lotze, M. T.; Dutcher, J. P.; Fisher, R. I.; Weiss, G.; Margolin, K. et al. (1999): High-dose recombinant interleukin 2 therapy for patients with metastatic melanoma: analysis of 270 patients treated between 1985 and 1993. *Journal of clinical oncology : official journal of the American Society of Clinical Oncology* 17 (7), pp. 2105–2116.

Balkwill, F.; Mantovani, A. (2001): Inflammation and cancer: back to Virchow? *The Lancet* 357 (9255), pp. 539–545.

Bartkowiak, Todd; Singh, Shailbala; Yang, Guojun; Galvan, Gloria; Haria, Dhwani; Ai, Midan et al. (2015): Unique potential of 4-1BB agonist antibody to promote durable regression of HPV+ tumors when combined with an E6/E7 peptide vaccine. *Proceedings of the National Academy of Sciences of the United States of America* 112 (38), E5290-9.

Baselga, J.; Tripathy, D.; Mendelsohn, J.; Baughman, S.; Benz, C. C.; Dantis, L. et al. (1996): Phase II study of weekly intravenous recombinant humanized anti-p185HER2 monoclonal antibody in patients with HER2/neu-overexpressing metastatic breast cancer. *Journal of clinical oncology : official journal of the American Society of Clinical Oncology* 14 (3), pp. 737–744.

Baselga, José; Bradbury, Ian; Eidtmann, Holger; Di Cosimo, Serena; Azambuja, Evandro de; Aura, Claudia et al. (2012): Lapatinib with trastuzumab for HER2-positive early breast

cancer (NeoALTTO): a randomised, open-label, multicentre, phase 3 trial. *Lancet (London, England)* 379 (9816), pp. 633–640.

Baum, P. R.; Gayle, R. B.; Ramsdell, F.; Srinivasan, S.; Sorensen, R. A.; Watson, M. L. et al. (1994): Molecular characterization of murine and human OX40/OX40 ligand systems: identification of a human OX40 ligand as the HTLV-1-regulated protein gp34. *The EMBO journal* 13 (17), pp. 3992–4001.

Baumann, Ralf; Yousefi, Shida; Simon, Dagmar; Russmann, Stefan; Mueller, Christoph; Simon, Hans-Uwe (2004): Functional expression of CD134 by neutrophils. *European journal of immunology* 34 (8), pp. 2268–2275.

Beckman, Robert A.; Weiner, Louis M.; Davis, Hugh M. (2007): Antibody constructs in cancer therapy: protein engineering strategies to improve exposure in solid tumors. *Cancer* 109 (2), pp. 170–179.

Becknell, Brian; Caligiuri, Michael A. (2005): Interleukin-2, interleukin-15, and their roles in human natural killer cells. *Advances in immunology* 86, pp. 209–239.

Bersanelli, Melissa; Buti, Sebastiano; Camisa, Roberta; Brighenti, Matteo; Lazzarelli, Silvia; Mazza, Giancarlo; Passalacqua, Rodolfo (2014): Gefitinib plus interleukin-2 in advanced non-small cell lung cancer patients previously treated with chemotherapy. *Cancers* 6 (4), pp. 2035–2048.

Bessard, Anne; Solé, Véronique; Bouchaud, Grégory; Quéméner, Agnès; Jacques, Yannick (2009): High antitumor activity of RLI, an interleukin-15 (IL-15)-IL-15 receptor alpha fusion protein, in metastatic melanoma and colorectal cancer. *Molecular cancer therapeutics* 8 (9), pp. 2736–2745.

Bird, R.; Hardman, K.; Jacobson, J.; Johnson, S.; Kaufman, B.; Lee, S. et al. (1988): Single-chain antigen-binding proteins. *Science* 242 (4877), pp. 423–426.

Bodmer, Jean-Luc; Schneider, Pascal; Tschopp, Jürg (2002): The molecular architecture of the TNF superfamily. *Trends in biochemical sciences* 27 (1), pp. 19–26.

Bossen, Claudia; Ingold, Karine; Tardivel, Aubry; Bodmer, Jean-Luc; Gaide, Olivier; Hertig, Sylvie et al. (2006): Interactions of tumor necrosis factor (TNF) and TNF receptor family members in the mouse and human. *The Journal of biological chemistry* 281 (20), pp. 13964–13971.

Brady, M. S.; Lee, F.; Petrie, H.; Eckels, D. D.; Lee, J. S. (2000): CD4(+) T cells kill HLA-class-II-antigen-positive melanoma cells presenting peptide in vitro. *Cancer immunology, immunotherapy : CII* 48 (11), pp. 621–626.

Brocks, B.; Garin-Chesa, P.; Behrle, E.; Park, J. E.; Rettig, W. J.; Pfizenmaier, K.; Moosmayer, D. (2001): Species-crossreactive scFv against the tumor stroma marker "fibroblast activation protein" selected by phage display from an immunized FAP-/- knock-out mouse. *Molecular medicine (Cambridge, Mass.)* 7 (7), pp. 461–469.

Butterfield, Lisa H. (2015): Cancer vaccines. *BMJ (Clinical research ed.)* 350, h988.

Callahan, Margaret K.; Kluger, Harriet; Postow, Michael A.; Segal, Neil H.; Lesokhin, Alexander; Atkins, Michael B. et al. (2018): Nivolumab Plus Ipilimumab in Patients With Advanced Melanoma: Updated Survival, Response, and Safety Data in a Phase I Dose-Escalation Study. *Journal of clinical oncology : official journal of the American Society of Clinical Oncology* 36 (4), pp. 391–398.

Carswell, E. A.; Old, L. J.; Kassel, R. L.; Green, S.; Fiore, N.; Williamson, B. (1975): An endotoxin-induced serum factor that causes necrosis of tumors. *Proceedings of the National Academy of Sciences of the United States of America* 72 (9), pp. 3666–3670.

Castillo, Eliseo F.; Schluns, Kimberly S. (2012): Regulating the immune system via IL-15 transpresentation. *Cytokine* 59 (3), pp. 479–490.

Chattopadhyay, Kausik; Lazar-Molnar, Eszter; Yan, Qingrong; Rubinstein, Rotem; Zhan, Chenyang; Vigdorovich, Vladimir et al. (2009): Sequence, structure, function, immunity: structural genomics of costimulation. *Immunological reviews* 229 (1), pp. 356–386.

Chattopadhyay, Kausik; Ramagopal, Udupi A.; Brenowitz, Michael; Nathenson, Stanley G.; Almo, Steven C. (2008): Evolution of GITRL immune function: murine GITRL exhibits unique structural and biochemical properties within the TNF superfamily. *Proceedings of the National Academy of Sciences of the United States of America* 105 (2), pp. 635–640.

Chattopadhyay, Kausik; Ramagopal, Udupi A.; Mukhopadhaya, Arunika; Malashkevich, Vladimir N.; Dilorenzo, Teresa P.; Brenowitz, Michael et al. (2007): Assembly and structural properties of glucocorticoid-induced TNF receptor ligand: Implications for function. *Proceedings of the National Academy of Sciences of the United States of America* 104 (49), pp. 19452–19457.

Chen, Shihao; Lee, Li-Fen; Fisher, Timothy S.; Jessen, Bart; Elliott, Mark; Evering, Winston et al. (2015): Combination of 4-1BB agonist and PD-1 antagonist promotes antitumor effector/memory CD8 T cells in a poorly immunogenic tumor model. *Cancer immunology research* 3 (2), pp. 149–160.

Chen, Xi-Lin; Bobbala, Diwakar; Cepero Donates, Yuneivy; Mayhue, Marian; Ilangumaran, Subburaj; Ramanathan, Sheela (2014): IL-15 trans-presentation regulates homeostasis of CD4(+) T lymphocytes. *Cellular & molecular immunology* 11 (4), pp. 387–397.

Cherkassky, Leonid; Morello, Aurore; Villena-Vargas, Jonathan; Feng, Yang; Dimitrov, Dimiter S.; Jones, David R. et al. (2016): Human CAR T cells with cell-intrinsic PD-1 checkpoint blockade resist tumor-mediated inhibition. *The Journal of clinical investigation* 126 (8), pp. 3130–3144.

Clouthier, Derek L.; Watts, Tania H. (2014): Cell-specific and context-dependent effects of GITR in cancer, autoimmunity, and infection. *Cytokine & growth factor reviews* 25 (2), pp. 91–106.

Cobleigh, M. A.; Vogel, C. L.; Tripathy, D.; Robert, N. J.; Scholl, S.; Fehrenbacher, L. et al. (1999): Multinational study of the efficacy and safety of humanized anti-HER2 monoclonal antibody in women who have HER2-overexpressing metastatic breast cancer that has progressed after chemotherapy for metastatic disease. *Journal of*

clinical oncology : official journal of the American Society of Clinical Oncology 17 (9), pp. 2639–2648.

Coe, David; Begom, Shaima; Addey, Caroline; White, Matthew; Dyson, Julian; Chai, Jian-Guo (2010): Depletion of regulatory T cells by anti-GITR mAb as a novel mechanism for cancer immunotherapy. *Cancer immunology, immunotherapy : CII* 59 (9), pp. 1367–1377.

Cohen, Adam D.; Schaer, David A.; Liu, Cailian; Li, Yanyun; Hirschhorn-Cymmerman, Daniel; Kim, Soo Chong et al. (2010): Agonist anti-GITR monoclonal antibody induces melanoma tumor immunity in mice by altering regulatory T cell stability and intra-tumor accumulation. *PloS one* 5 (5), e10436.

Cohen, Steven J.; Alpaugh, R. Katherine; Palazzo, Irma; Meropol, Neal J.; Rogatko, André; Xu, Zhiheng et al. (2008): Fibroblast activation protein and its relationship to clinical outcome in pancreatic adenocarcinoma. *Pancreas* 37 (2), pp. 154–158.

Coley, W. B. (1910): The Treatment of Inoperable Sarcoma by Bacterial Toxins (the Mixed Toxins of the Streptococcus erysipelas and the Bacillus prodigiosus). *Proceedings of the Royal Society of Medicine* 3 (Surg Sect), pp. 1–48.

Compaan, Deanne M.; Hymowitz, Sarah G. (2006): The crystal structure of the costimulatory OX40-OX40L complex. *Structure (London, England : 1993)* 14 (8), pp. 1321–1330.

Conlon, Kevin C.; Lugli, Enrico; Welles, Hugh C.; Rosenberg, Steven A.; Fojo, Antonio Tito; Morris, John C. et al. (2015): Redistribution, hyperproliferation, activation of natural killer cells and CD8 T cells, and cytokine production during first-in-human clinical trial of recombinant human interleukin-15 in patients with cancer. *Journal of clinical oncology : official journal of the American Society of Clinical Oncology* 33 (1), pp. 74–82.

Cooley, S.; Burns, L. J.; Repka, T.; Miller, J. S. (1999): Natural killer cell cytotoxicity of breast cancer targets is enhanced by two distinct mechanisms of antibody-dependent cellular cytotoxicity against LFA-3 and HER2/neu. *Experimental hematology* 27 (10), pp. 1533–1541.

Côté, Anik L.; Zhang, Peisheng; O'Sullivan, Jeremy A.; Jacobs, Valerie L.; Clemis, Carli R.; Sakaguchi, Shimon et al. (2011): Stimulation of the glucocorticoid-induced TNF receptor family-related receptor on CD8 T cells induces protective and high-avidity T cell responses to tumor-specific antigens. *Journal of immunology (Baltimore, Md. : 1950)* 186 (1), pp. 275–283.

Curran, Michael A.; Kim, Myoungjoo; Montalvo, Welby; Al-Shamkhani, Aymen; Allison, James P. (2011): Combination CTLA-4 blockade and 4-1BB activation enhances tumor rejection by increasing T-cell infiltration, proliferation, and cytokine production. *PloS one* 6 (4), e19499.

Daudt, Liane; Maccario, Rita; Locatelli, Franco; Turin, Ilaria; Silla, Lucia; Montini, Enrica et al. (2008): Interleukin-15 favors the expansion of central memory CD8+ T cells in ex vivo generated, antileukemia human cytotoxic T lymphocyte lines. *Journal of immunotherapy (Hagerstown, Md. : 1997)* 31 (4), pp. 385–393.

DeBenedette, M. A.; Shahinian, A.; Mak, T. W.; Watts, T. H. (1997): Costimulation of CD28- T lymphocytes by 4-1BB ligand. *Journal of immunology (Baltimore, Md. : 1950)* 158 (2), pp. 551–559.

DeBenedette, M. A.; Wen, T.; Bachmann, M. F.; Ohashi, P. S.; Barber, B. H.; Stocking, K. L. et al. (1999): Analysis of 4-1BB ligand (4-1BBL)-deficient mice and of mice lacking both 4-1BBL and CD28 reveals a role for 4-1BBL in skin allograft rejection and in the cytotoxic T cell response to influenza virus. *Journal of immunology (Baltimore, Md. : 1950)* 163 (9), pp. 4833–4841.

Deumelandt, Katrin; Platten, Michael; Ochs, Katharina (2018): Synergy of vaccination and agonist OX40 treatment-toward a mechanism-driven combination of glioma immunotherapy. *Neuro-oncology* 20 (1), pp. 4–5.

Dhupkar, Pooja; Gordon, Nancy (2017): Interleukin-2: Old and New Approaches to Enhance Immune-Therapeutic Efficacy. *Advances in experimental medicine and biology* 995, pp. 33–51.

Di Modica, Martina; Tagliabue, Elda; Triulzi, Tiziana (2017): Predicting the Efficacy of HER2-Targeted Therapies: A Look at the Host. *Disease markers* 2017, p. 7849108.

Dixon, J. F.; Law, J. L.; Favero, J. J. (1989): Activation of human T lymphocytes by crosslinking of anti-CD3 monoclonal antibodies. *Journal of leukocyte biology* 46 (3), pp. 214–220.

D'Souza, Warren N.; Lefrançois, Leo (2003): IL-2 is not required for the initiation of CD8 T cell cycling but sustains expansion. *Journal of immunology (Baltimore, Md. : 1950)* 171 (11), pp. 5727–5735.

Dubois, Sigrid; Mariner, Jennifer; Waldmann, Thomas A.; Tagaya, Yutaka (2002): IL-15Ralpha recycles and presents IL-15 In trans to neighboring cells. *Immunity* 17 (5), pp. 537–547.

Dubois, Sigrid; Patel, Hiral J.; Zhang, Meili; Waldmann, Thomas A.; Müller, Jürgen R. (2008): Preassociation of IL-15 with IL-15R alpha-IgG1-Fc enhances its activity on proliferation of NK and CD8+/CD44high T cells and its antitumor action. *Journal of immunology (Baltimore, Md. : 1950)* 180 (4), pp. 2099–2106.

Durham, Nick M.; Holoweckyj, Nick; MacGill, Randall S.; McGlinchey, Kelly; Leow, Ching Ching; Robbins, Scott H. (2017): GITR ligand fusion protein agonist enhances the tumor antigen-specific CD8 T-cell response and leads to long-lasting memory. *Journal for immunotherapy of cancer* 5, p. 47.

Dustin, Michael L. (2014): The immunological synapse. *Cancer immunology research* 2 (11), pp. 1023–1033.

Esteva, Francisco J.; Valero, Vicente; Booser, Daniel; Guerra, Laura T.; Murray, James L.; Pusztai, Lajos et al. (2002): Phase II study of weekly docetaxel and trastuzumab for patients with HER-2-overexpressing metastatic breast cancer. *Journal of clinical oncology : official journal of the American Society of Clinical Oncology* 20 (7), pp. 1800–1808.

Fellermeier, Sina; Beha, Nadine; Meyer, Jan-Erik; Ring, Sarah; Bader, Stefan; Kontermann, Roland E.; Müller, Dafne (2016): Advancing targeted co-stimulation with antibody-fusion

proteins by introducing TNF superfamily members in a single-chain format. *Oncoimmunology* 5 (11), e1238540.

Fellermeier-Kopf, Sina; Gieseke, Friederike; Sahin, Ugur; Müller, Dafne; Pfizenmaier, Klaus; Kontermann, Roland E. (2018): Duokines: a novel class of dual-acting co-stimulatory molecules acting in cis or trans. *Oncoimmunology*, pp. 1–10.

Fischer, Eliane; Chaitanya, Krishna; Wüest, Thomas; Wadle, Andreas; Scott, Andrew M.; van den Broek, Maries et al. (2012): Radioimmunotherapy of fibroblast activation protein positive tumors by rapidly internalizing antibodies. *Clinical cancer research : an official journal of the American Association for Cancer Research* 18 (22), pp. 6208–6218.

Floros, Theofanis; Tarhini, Ahmad A. (2015): Anticancer Cytokines: Biology and Clinical Effects of Interferon-α2, Interleukin (IL)-2, IL-15, IL-21, and IL-12. *Seminars in oncology* 42 (4), pp. 539–548.

Franke, T. F.; Kaplan, D. R.; Cantley, L. C. (1997): PI3K: downstream AKTion blocks apoptosis. *Cell* 88 (4), pp. 435–437.

Friedmann, M. C.; Migone, T. S.; Russell, S. M.; Leonard, W. J. (1996): Different interleukin 2 receptor beta-chain tyrosines couple to at least two signaling pathways and synergistically mediate interleukin 2-induced proliferation. *Proceedings of the National Academy of Sciences of the United States of America* 93 (5), pp. 2077–2082.

Fromm, George; Silva, Suresh de; Giffin, Louise; Xu, Xin; Rose, Jason; Schreiber, Taylor H. (2016): Gp96-Ig/Costimulator (OX40L, ICOSL, or 4-1BBL) Combination Vaccine Improves T-cell Priming and Enhances Immunity, Memory, and Tumor Elimination. *Cancer immunology research* 4 (9), pp. 766–778.

Fujita, Tomoko; Kambe, Naotomo; Uchiyama, Takashi; Hori, Toshiyuki (2006): Type I interferons attenuate T cell activating functions of human mast cells by decreasing TNF-alpha production and OX40 ligand expression while increasing IL-10 production. *Journal of clinical immunology* 26 (6), pp. 512–518.

Gaffen, S. L. (2001): Signaling domains of the interleukin 2 receptor. *Cytokine* 14 (2), pp. 63–77.

Galon, Jérôme; Costes, Anne; Sanchez-Cabo, Fatima; Kirilovsky, Amos; Mlecnik, Bernhard; Lagorce-Pagès, Christine et al. (2006): Type, density, and location of immune cells within human colorectal tumors predict clinical outcome. *Science* 313 (5795), pp. 1960–1964.

Ganguly, Sumita; Liu, Jinyan; Pillai, Vinod B.; Mittler, Robert S.; Amara, Rama Rao (2010): Adjuvantive effects of anti-4-1BB agonist Ab and 4-1BBL DNA for a HIV-1 Gag DNA vaccine: different effects on cellular and humoral immunity. *Vaccine* 28 (5), pp. 1300–1309.

Garin-Chesa, P.; Old, L. J.; Rettig, W. J. (1990): Cell surface glycoprotein of reactive stromal fibroblasts as a potential antibody target in human epithelial cancers. *Proceedings of the National Academy of Sciences of the United States of America* 87 (18), pp. 7235–7239.

Gedeon, Patrick C.; Schaller, Teilo H.; Chitneni, Satish K.; Choi, Bryan D.; Kuan, Chien-Tsun; Suryadevara, Carter M. et al. (2018): A Rationally Designed Fully Human EGFRvIII:CD3-

Targeted Bispecific Antibody Redirects Human T Cells to Treat Patient-derived Intracerebral Malignant Glioma. *Clinical cancer research : an official journal of the American Association for Cancer Research*.

Gennari, Roberto; Menard, Sylvie; Fagnoni, Francesco; Ponchio, Luisa; Scelsi, Mario; Tagliabue, Elda et al. (2004): Pilot study of the mechanism of action of preoperative trastuzumab in patients with primary operable breast tumors overexpressing HER2. *Clinical cancer research : an official journal of the American Association for Cancer Research* 10 (17), pp. 5650–5655.

Gillies, Stephen D.; Lan, Yan; Brunkhorst, Bea; Wong, Wai-Keung; Li, Yue; Lo, Kin-Ming (2002): Bi-functional cytokine fusion proteins for gene therapy and antibody-targeted treatment of cancer. *Cancer immunology, immunotherapy : CII* 51 (8), pp. 449–460.

Goebeler, Maria-Elisabeth; Knop, Stefan; Viardot, Andreas; Kufer, Peter; Topp, Max S.; Einsele, Hermann et al. (2016): Bispecific T-Cell Engager (BiTE) Antibody Construct Blinatumomab for the Treatment of Patients With Relapsed/Refractory Non-Hodgkin Lymphoma: Final Results From a Phase I Study. *Journal of clinical oncology : official journal of the American Society of Clinical Oncology* 34 (10), pp. 1104–1111.

Goldstein, N. I.; Prewett, M.; Zuklys, K.; Rockwell, P.; Mendelsohn, J. (1995): Biological efficacy of a chimeric antibody to the epidermal growth factor receptor in a human tumor xenograft model. *Clinical cancer research : an official journal of the American Association for Cancer Research* 1 (11), pp. 1311–1318.

Gong, W.; Xiao, W.; Hu, M.; Weng, X.; Qian, L.; Pan, X.; Ji, M. (2010): Ex vivo expansion of natural killer cells with high cytotoxicity by K562 cells modified to co-express major histocompatibility complex class I chain-related protein A, 4-1BB ligand, and interleukin-15. *Tissue antigens* 76 (6), pp. 467–475.

Gordon, J.; MacLean, L. D. (1965): A lymphocyte-stimulating factor produced in vitro. *Nature* 208 (5012), pp. 795–796.

Goscinski, Mariusz Adam; Suo, Zhenhe; Flørenes, Vivi Ann; Vlatkovic, Ljiljana; Nesland, Jahn Marthin; Giercksky, Karl-Erik (2008): FAP-alpha and uPA show different expression patterns in premalignant and malignant esophageal lesions. *Ultrastructural pathology* 32 (3), pp. 89–96.

Grabstein, K. H.; Eisenman, J.; Shanebeck, K.; Rauch, C.; Srinivasan, S.; Fung, V. et al. (1994): Cloning of a T cell growth factor that interacts with the beta chain of the interleukin-2 receptor. *Science* 264 (5161), pp. 965–968.

Grotendorst, G. R.; Soma, Y.; Takehara, K.; Charette, M. (1989): EGF and TGF-alpha are potent chemoattractants for endothelial cells and EGF-like peptides are present at sites of tissue regeneration. *Journal of cellular physiology* 139 (3), pp. 617–623.

Guo, Yin; Luan, Liming; Rabacal, Whitney; Bohannon, Julia K.; Fensterheim, Benjamin A.; Hernandez, Antonio; Sherwood, Edward R. (2015): IL-15 Superagonist-Mediated Immunotoxicity: Role of NK Cells and IFN-γ. *Journal of immunology (Baltimore, Md. : 1950)* 195 (5), pp. 2353–2364.

Gurney, A. L.; Marsters, S. A.; Huang, R. M.; Pitti, R. M.; Mark, D. T.; Baldwin, D. T. et al. (1999): Identification of a new member of the tumor necrosis factor family and its receptor, a human ortholog of mouse GITR. *Current biology : CB* 9 (4), pp. 215–218.

Han, Jianfeng; Chu, Jianhong; Keung Chan, Wing; Zhang, Jianying; Wang, Youwei; Cohen, Justus B. et al. (2015): CAR-Engineered NK Cells Targeting Wild-Type EGFR and EGFRvIII Enhance Killing of Glioblastoma and Patient-Derived Glioblastoma Stem Cells. *Scientific reports* 5, p. 11483.

Hanusch, Claus; Schneeweiss, Andreas; Loibl, Sibylle; Untch, Michael; Paepke, Stefan; Kümmel, Sherko et al. (2015): Dual Blockade with AFatinib and Trastuzumab as NEoadjuvant Treatment for Patients with Locally Advanced or Operable Breast Cancer Receiving Taxane-Anthracycline Containing Chemotherapy-DAFNE (GBG-70). *Clinical cancer research : an official journal of the American Association for Cancer Research* 21 (13), pp. 2924–2931.

Harbury, P. B.; Zhang, T.; Kim, P. S.; Alber, T. (1993): A switch between two-, three-, and four-stranded coiled coils in GCN4 leucine zipper mutants. *Science* 262 (5138), pp. 1401–1407.

Harwood, Seandean Lykke; Alvarez-Cienfuegos, Ana; Nuñez-Prado, Natalia; Compte, Marta; Hernández-Pérez, Sara; Merino, Nekane et al. (2017): ATTACK, a novel bispecific T cell-recruiting antibody with trivalent EGFR binding and monovalent CD3 binding for cancer immunotherapy. *Oncoimmunology* 7 (1), e1377874.

Hazan, Rachel B.; Norton, Larry (1998): The Epidermal Growth Factor Receptor Modulates the Interaction of E-cadherin with the Actin Cytoskeleton. *The Journal of biological chemistry* 273 (15), pp. 9078–9084.

Hirschhorn-Cymerman, Daniel; Budhu, Sadna; Kitano, Shigehisa; Liu, Cailian; Zhao, Feng; Zhong, Hong et al. (2012): Induction of tumoricidal function in CD4+ T cells is associated with concomitant memory and terminally differentiated phenotype. *The Journal of experimental medicine* 209 (11), pp. 2113–2126.

Hirschhorn-Cymerman, Daniel; Rizzuto, Gabrielle A.; Merghoub, Taha; Cohen, Adam D.; Avogadri, Francesca; Lesokhin, Alexander M. et al. (2009): OX40 engagement and chemotherapy combination provides potent antitumor immunity with concomitant regulatory T cell apoptosis. *The Journal of experimental medicine* 206 (5), pp. 1103–1116.

Hodi, F. Stephen; O'Day, Steven J.; McDermott, David F.; Weber, Robert W.; Sosman, Jeffrey A.; Haanen, John B. et al. (2010): Improved survival with ipilimumab in patients with metastatic melanoma. *The New England journal of medicine* 363 (8), pp. 711–723.

Hofheinz, R-D; al-Batran, S-E; Hartmann, F.; Hartung, G.; Jäger, D.; Renner, C. et al. (2003): Stromal antigen targeting by a humanised monoclonal antibody: an early phase II trial of sibrotuzumab in patients with metastatic colorectal cancer. *Onkologie* 26 (1), pp. 44–48.

Hornig, Nora; Kermer, Vanessa; Frey, Katharina; Diebolder, Philipp; Kontermann, Roland E.; Müller, Dafne (2012): Combination of a bispecific antibody and costimulatory antibody-

ligand fusion proteins for targeted cancer immunotherapy. *Journal of immunotherapy (Hagerstown, Md. : 1997)* 35 (5), pp. 418–429.

Hornig, Nora; Reinhardt, Katharina; Kermer, Vanessa; Kontermann, Roland E.; Müller, Dafne (2013): Evaluating combinations of costimulatory antibody-ligand fusion proteins for targeted cancer immunotherapy. *Cancer immunology, immunotherapy : CII* 62 (8), pp. 1369–1380.

Horton, Brendan; Williams, Jason B.; Spranger, Stefani; Gajewski, Thomas F. (2015): Agonist anti-4-1BB plus neutralizing anti-CTLA-4 or -PD-L1 synergize to promote tumor regression by rescuing dying dysfunctional CD8+ T cells within the tumor microenvironment. *Journal for immunotherapy of cancer* 3 (Suppl 2), O10.

Hsu, Wei-Chuan; Cheng, Chu-Nian; Lee, Te-Wei; Hwang, Jeng-Jong (2015): Cytotoxic Effects of PEGylated Anti-EGFR Immunoliposomes Combined with Doxorubicin and Rhenium-188 Against Cancer Cells. *Anticancer research* 35 (9), pp. 4777–4788.

Hu, Peisheng; Arias, Robyn S.; Sadun, Rebecca E.; Nien, Yu-Chih; Zhang, Nan; Sabzevari, Helen et al. (2008): Construction and preclinical characterization of Fc-mGITRL for the immunotherapy of cancer. *Clinical cancer research : an official journal of the American Association for Cancer Research* 14 (2), pp. 579–588.

Huber, Margit A.; Kraut, Norbert; Park, John E.; Schubert, Roland D.; Rettig, Wolfgang J.; Peter, Ralf U.; Garin-Chesa, Pilar (2003): Fibroblast activation protein: differential expression and serine protease activity in reactive stromal fibroblasts of melanocytic skin tumors. *The Journal of investigative dermatology* 120 (2), pp. 182–188.

Huntington, Nicholas D.; Legrand, Nicolas; Alves, Nuno L.; Jaron, Barbara; Weijer, Kees; Plet, Ariane et al. (2009): IL-15 trans-presentation promotes human NK cell development and differentiation in vivo. *The Journal of experimental medicine* 206 (1), pp. 25–34.

Imai, Naoko; Ikeda, Hiroaki; Tawara, Isao; Wang, Linan; Wang, Lijie; Nishikawa, Hiroyoshi et al. (2009): Glucocorticoid-induced tumor necrosis factor receptor stimulation enhances the multifunctionality of adoptively transferred tumor antigen-specific CD8+ T cells with tumor regression. *Cancer science* 100 (7), pp. 1317–1325.

Ito, Tomoki; Wang, Yui-Hsi; Duramad, Omar; Hori, Toshiyuki; Delespesse, Guy J.; Watanabe, Norihiko et al. (2005): TSLP-activated dendritic cells induce an inflammatory T helper type 2 cell response through OX40 ligand. *The Journal of experimental medicine* 202 (9), pp. 1213–1223.

Jahn, Tobias; Zuther, Martin; Friedrichs, Björn; Heuser, Claudia; Guhlke, Stefan; Abken, Hinrich; Hombach, Andreas A. (2012): An IL12-IL2-antibody fusion protein targeting Hodgkin's lymphoma cells potentiates activation of NK and T cells for an anti-tumor attack. *PloS one* 7 (9), e44482.

Jakobisiak, Marek; Golab, Jakub; Lasek, Witold (2011): Interleukin 15 as a promising candidate for tumor immunotherapy. *Cytokine & growth factor reviews* 22 (2), pp. 99–108.

Jenkins, M. K.; Taylor, P. S.; Norton, S. D.; Urdahl, K. B. (1991): CD28 delivers a costimulatory signal involved in antigen-specific IL-2 production by human T cells. *Journal of immunology (Baltimore, Md. : 1950)* 147 (8), pp. 2461–2466.

Karulf, Matthew; Kelly, Ann; Weinberg, Andrew D.; Gold, Jeffrey A. (2010): OX40 ligand regulates inflammation and mortality in the innate immune response to sepsis. *Journal of immunology (Baltimore, Md. : 1950)* 185 (8), pp. 4856–4862.

Kaufman, Howard L.; Ruby, Carl E.; Hughes, Tasha; Slingluff, Craig L. (2014): Current status of granulocyte-macrophage colony-stimulating factor in the immunotherapy of melanoma. *Journal for immunotherapy of cancer* 2, p. 11.

Kermer, Vanessa; Baum, Volker; Hornig, Nora; Kontermann, Roland E.; Müller, Dafne (2012): An antibody fusion protein for cancer immunotherapy mimicking IL-15 trans-presentation at the tumor site. *Molecular cancer therapeutics* 11 (6), pp. 1279–1288.

Kermer, Vanessa; Hornig, Nora; Harder, Markus; Bondarieva, Anastasiia; Kontermann, Roland E.; Müller, Dafne (2014): Combining antibody-directed presentation of IL-15 and 4-1BBL in a trifunctional fusion protein for cancer immunotherapy. *Molecular cancer therapeutics* 13 (1), pp. 112–121.

Kim, Hyoung Pyo; Imbert, Jean; Leonard, Warren J. (2006): Both integrated and differential regulation of components of the IL-2/IL-2 receptor system. *Cytokine & growth factor reviews* 17 (5), pp. 349–366.

Kjaergaard, J.; Tanaka, J.; Kim, J. A.; Rothchild, K.; Weinberg, A.; Shu, S. (2000): Therapeutic efficacy of OX-40 receptor antibody depends on tumor immunogenicity and anatomic site of tumor growth. *Cancer research* 60 (19), pp. 5514–5521.

Klebanoff, Christopher A.; Gattinoni, Luca; Torabi-Parizi, Parizad; Kerstann, Keith; Cardones, Adela R.; Finkelstein, Steven E. et al. (2005): Central memory self/tumor-reactive CD8+ T cells confer superior antitumor immunity compared with effector memory T cells. *Proceedings of the National Academy of Sciences of the United States of America* 102 (27), pp. 9571–9576.

Ko, Kuibeom; Yamazaki, Sayuri; Nakamura, Kyoko; Nishioka, Tomohisa; Hirota, Keiji; Yamaguchi, Tomoyuki et al. (2005): Treatment of advanced tumors with agonistic anti-GITR mAb and its effects on tumor-infiltrating Foxp3+CD25+CD4+ regulatory T cells. *The Journal of experimental medicine* 202 (7), pp. 885–891.

Kobayashi, Takumi; Doff, Brianna L.; Rearden, Rory C.; Leggatt, Graham R.; Mattarollo, Stephen R. (2015): NKT cell-targeted vaccination plus anti-4-1BB antibody generates persistent CD8 T cell immunity against B cell lymphoma. *Oncoimmunology* 4 (3), e990793.

Köhler, G.; Milstein, C. (2005): Continuous cultures of fused cells secreting antibody of predefined specificity. 1975. *Journal of immunology (Baltimore, Md. : 1950)* 174 (5), pp. 2453–2455.

Kohrt, Holbrook E.; Colevas, A. Dimitrios; Houot, Roch; Weiskopf, Kipp; Goldstein, Matthew J.; Lund, Peder et al. (2014): Targeting CD137 enhances the efficacy of cetuximab. *The Journal of clinical investigation* 124 (6), pp. 2668–2682.

Kohrt, Holbrook E.; Houot, Roch; Goldstein, Matthew J.; Weiskopf, Kipp; Alizadeh, Ash A.; Brody, Josh et al. (2011): CD137 stimulation enhances the antilymphoma activity of anti-CD20 antibodies. *Blood* 117 (8), pp. 2423–2432.

Kohrt, Holbrook E.; Houot, Roch; Weiskopf, Kipp; Goldstein, Matthew J.; Scheeren, Ferenc; Czerwinski, Debra et al. (2012): Stimulation of natural killer cells with a CD137-specific antibody enhances trastuzumab efficacy in xenotransplant models of breast cancer. *The Journal of clinical investigation* 122 (3), pp. 1066–1075.

König, R.; Huang, L. Y.; Germain, R. N. (1992): MHC class II interaction with CD4 mediated by a region analogous to the MHC class I binding site for CD8. *Nature* 356 (6372), pp. 796–798.

Kontermann, Roland E. (2012): Antibody-cytokine fusion proteins. *Archives of biochemistry and biophysics* 526 (2), pp. 194–205.

Koon, Henry B.; Shepard, Dale Randall; Merghoub, Taha; Schaer, David A.; Sirard, Cynthia A.; Wolchok, Jedd D. (2016): First-in-human phase 1 single-dose study of TRX-518, an anti-human glucocorticoid-induced tumor necrosis factor receptor (GITR) monoclonal antibody in adults with advanced solid tumors. *Journal of clinical oncology : official journal of the American Society of Clinical Oncology* 34 (15_suppl), p. 3017.

Krausz, Ludovic Tibor; Bianchini, Rodolfo; Ronchetti, Simona; Fettucciari, Katia; Nocentini, Giuseppe; Riccardi, Carlo (2007): GITR-GITRL system, a novel player in shock and inflammation. *TheScientificWorldJournal* 7, pp. 533–566.

Krippner-Heidenreich, Anja; Grunwald, Ingo; Zimmermann, Gudrun; Kühnle, Marie; Gerspach, Jeannette; Sterns, Theobald et al. (2008): Single-chain TNF, a TNF derivative with enhanced stability and antitumoral activity. *Journal of immunology (Baltimore, Md. : 1950)* 180 (12), pp. 8176–8183.

Krishnamurthy, Anuradha; Jimeno, Antonio (2018): Bispecific antibodies for cancer therapy: A review. *Pharmacology & therapeutics* 185, pp. 122–134.

Kwok, C. S.; Cole, S. E.; Liao, S. K. (1988): Uptake kinetics of monoclonal antibodies by human malignant melanoma multicell spheroids. *Cancer research* 48 (7), pp. 1856–1863.

Kwon, B. S.; Weissman, S. M. (1989): cDNA sequences of two inducible T-cell genes. *Proceedings of the National Academy of Sciences of the United States of America* 86 (6), pp. 1963–1967.

Lafferty, K. J.; Prowse, S. J.; Simeonovic, C. J.; Warren, H. S. (1983): Immunobiology of tissue transplantation: a return to the passenger leukocyte concept. *Annual review of immunology* 1, pp. 143–173.

Lafreniere, R.; Rosenberg, S. A. (1985): Successful immunotherapy of murine experimental hepatic metastases with lymphokine-activated killer cells and recombinant interleukin 2. *Cancer research* 45 (8), pp. 3735–3741.

Lai, Chester; August, Suzannah; Albibas, Amel; Behar, Ramnik; Cho, Shin-Young; Polak, Marta E. et al. (2016): OX40+ Regulatory T Cells in Cutaneous Squamous Cell Carcinoma Suppress Effector T-Cell Responses and Associate with Metastatic Potential. *Clinical*

cancer research : an official journal of the American Association for Cancer Research 22 (16), pp. 4236–4248.

Lee, Seung-Joo; Myers, Lara; Muralimohan, Guruprasaadh; Dai, Jie; Qiao, Yi; Li, Zihai et al. (2004): 4-1BB and OX40 dual costimulation synergistically stimulate primary specific CD8 T cells for robust effector function. *Journal of immunology (Baltimore, Md. : 1950)* 173 (5), pp. 3002–3012.

Leonard, W. J. (2001): Cytokines and immunodeficiency diseases. *Nature reviews. Immunology* 1 (3), pp. 200–208.

Leonard, W. J.; Depper, J. M.; Crabtree, G. R.; Rudikoff, S.; Pumphrey, J.; Robb, R. J. et al. (1984): Molecular cloning and expression of cDNAs for the human interleukin-2 receptor. *Nature* 311 (5987), pp. 626–631.

Leonard, Warren J.; Spolski, Rosanne (2005): Interleukin-21: a modulator of lymphoid proliferation, apoptosis and differentiation. *Nature reviews. Immunology* 5 (9), pp. 688–698.

Lewis, G. D.; Figari, I.; Fendly, B.; Wong, W. L.; Carter, P.; Gorman, C.; Shepard, H. M. (1993): Differential responses of human tumor cell lines to anti-p185HER2 monoclonal antibodies. *Cancer immunology, immunotherapy : CII* 37 (4), pp. 255–263.

Leyland, Rebecca; Watkins, Amanda; Mulgrew, Kathy A.; Holoweckyj, Nicholas; Bamber, Lisa; Tigue, Natalie J. et al. (2017): A Novel Murine GITR Ligand Fusion Protein Induces Antitumor Activity as a Monotherapy That Is Further Enhanced in Combination with an OX40 Agonist. *Clinical cancer research : an official journal of the American Association for Cancer Research* 23 (13), pp. 3416–3427.

Lin, J. X.; Leonard, W. J. (2000): The role of Stat5a and Stat5b in signaling by IL-2 family cytokines. *Oncogene* 19 (21), pp. 2566–2576.

Lin, Wei; Voskens, Caroline J.; Zhang, Xiaoyu; Schindler, Daniel G.; Wood, Aaron; Burch, Erin et al. (2008): Fc-dependent expression of CD137 on human NK cells: insights into "agonistic" effects of anti-CD137 monoclonal antibodies. *Blood* 112 (3), pp. 699–707.

Linē, A.; Stengrēvics, A.; Slucka, Z.; Li, G.; Jankevics, E.; Rees, R. C. (2002): Serological identification and expression analysis of gastric cancer-associated genes. *British journal of cancer* 86 (11), pp. 1824–1830.

Linsley, P. S.; Brady, W.; Urnes, M.; Grosmaire, L. S.; Damle, N. K.; Ledbetter, J. A. (1991): CTLA-4 is a second receptor for the B cell activation antigen B7. *The Journal of experimental medicine* 174 (3), pp. 561–569.

Linsley, P. S.; Clark, E. A.; Ledbetter, J. A. (1990): T-cell antigen CD28 mediates adhesion with B cells by interacting with activation antigen B7/BB-1. *Proceedings of the National Academy of Sciences of the United States of America* 87 (13), pp. 5031–5035.

Lodolce, James P.; Burkett, Patrick R.; Koka, Rima M.; Boone, David L.; Ma, Averil (2002): Regulation of lymphoid homeostasis by interleukin-15. *Cytokine & growth factor reviews* 13 (6), pp. 429–439.

Lu, Lei; Xu, Xiaobing; Zhang, Bin; Zhang, Rongsheng; Ji, Hongzan; Wang, Xuan (2014): Combined PD-1 blockade and GITR triggering induce a potent antitumor immunity in murine cancer models and synergizes with chemotherapeutic drugs. *Journal of translational medicine* 12, p. 36.

Luca, Roberto de; Soltermann, Alex; Pretto, Francesca; Pemberton-Ross, Catherine; Pellegrini, Giovanni; Wulhfard, Sarah; Neri, Dario (2017): Potency-matched Dual Cytokine-Antibody Fusion Proteins for Cancer Therapy. *Molecular cancer therapeutics* 16 (11), pp. 2442–2451.

Lucas, Mathias; Schachterle, William; Oberle, Karin; Aichele, Peter; Diefenbach, Andreas (2007): Dendritic cells prime natural killer cells by trans-presenting interleukin 15. *Immunity* 26 (4), pp. 503–517.

Lum, Lawrence G.; Choi, Minsig; Thakur, Archana; Deol, Abhinav; Fields, Kristie; Tomaszewski, Elyse et al. (2015): Five advanced pancreatic cancer patients in a Phase I study of anti-CD3 x anti-EGFR bispecific antibody armed activated T cells (BATS). *Journal for immunotherapy of cancer* 3 (Suppl 2), P55.

Lutterbuese, Ralf; Raum, Tobias; Kischel, Roman; Hoffmann, Patrick; Mangold, Susanne; Rattel, Benno et al. (2010): T cell-engaging BiTE antibodies specific for EGFR potently eliminate KRAS- and BRAF-mutated colorectal cancer cells. *Proceedings of the National Academy of Sciences of the United States of America* 107 (28), pp. 12605–12610.

Ma, Pan; He, Qiang; Li, Wei; Li, Xianliang; Han, Huamin; Jin, Mengmeng et al. (2015): Anti-CD3 x EGFR bispecific antibody redirects cytokine-induced killer cells to glioblastoma in vitro and in vivo. *Oncology reports* 34 (5), pp. 2567–2575.

Magis, Cedrik; van der Sloot, Almer M.; Serrano, Luis; Notredame, Cedric (2012): An improved understanding of TNFL/TNFR interactions using structure-based classifications. *Trends in biochemical sciences* 37 (9), pp. 353–363.

Maira, Sauveur-Michel; Pecchi, Sabina; Huang, Alan; Burger, Matthew; Knapp, Mark; Sterker, Dario et al. (2012): Identification and characterization of NVP-BKM120, an orally available pan-class I PI3-kinase inhibitor. *Molecular cancer therapeutics* 11 (2), pp. 317–328.

Malek, Thomas R.; Castro, Iris (2010): Interleukin-2 receptor signaling: at the interface between tolerance and immunity. *Immunity* 33 (2), pp. 153–165.

Mallett, S.; Fossum, S.; Barclay, A. N. (1990): Characterization of the MRC OX40 antigen of activated CD4 positive T lymphocytes--a molecule related to nerve growth factor receptor. *The EMBO journal* 9 (4), pp. 1063–1068.

Mamot, Christoph; Ritschard, Reto; Wicki, Andreas; Stehle, Gregor; Dieterle, Thomas; Bubendorf, Lukas et al. (2012): Tolerability, safety, pharmacokinetics, and efficacy of doxorubicin-loaded anti-EGFR immunoliposomes in advanced solid tumours: a phase 1 dose-escalation study. *The Lancet. Oncology* 13 (12), pp. 1234–1241.

Manjunath, N.; Shankar, P.; Wan, J.; Weninger, W.; Crowley, M. A.; Hieshima, K. et al. (2001): Effector differentiation is not prerequisite for generation of memory cytotoxic T lymphocytes. *The Journal of clinical investigation* 108 (6), pp. 871–878.

Manzo, Teresa; Heslop, Helen E.; Rooney, Cliona M. (2015): Antigen-specific T cell therapies for cancer. *Human molecular genetics* 24 (R1), R67-73.

Marks-Konczalik, J.; Dubois, S.; Losi, J. M.; Sabzevari, H.; Yamada, N.; Feigenbaum, L. et al. (2000): IL-2-induced activation-induced cell death is inhibited in IL-15 transgenic mice. *Proceedings of the National Academy of Sciences of the United States of America* 97 (21), pp. 11445–11450.

Mathew, S.; Scanlan, M. J.; Mohan Raj, B. K.; Murty, V. V.; Garin-Chesa, P.; Old, L. J. et al. (1995): The gene for fibroblast activation protein alpha (FAP), a putative cell surface-bound serine protease expressed in cancer stroma and wound healing, maps to chromosome band 2q23. *Genomics* 25 (1), pp. 335–337.

Mathios, Dimitrios; Park, Chul-Kee; Marcus, Warren D.; Alter, Sarah; Rhode, Peter R.; Jeng, Emily K. et al. (2016): Therapeutic administration of IL-15 superagonist complex ALT-803 leads to long-term survival and durable antitumor immune response in a murine glioblastoma model. *International journal of cancer* 138 (1), pp. 187–194.

Maude, Shannon L.; Laetsch, Theodore W.; Buechner, Jochen; Rives, Susana; Boyer, Michael; Bittencourt, Henrique et al. (2018): Tisagenlecleucel in Children and Young Adults with B-Cell Lymphoblastic Leukemia. *The New England journal of medicine* 378 (5), pp. 439–448.

McHugh, Rebecca S.; Whitters, Matthew J.; Piccirillo, Ciriaco A.; Young, Deborah A.; Shevach, Ethan M.; Collins, Mary; Byrne, Michael C. (2002): CD4(+)CD25(+) immunoregulatory T cells: gene expression analysis reveals a functional role for the glucocorticoid-induced TNF receptor. *Immunity* 16 (2), pp. 311–323.

McNamara, James O.; Kolonias, Despina; Pastor, Fernando; Mittler, Robert S.; Chen, Lieping; Giangrande, Paloma H. et al. (2008): Multivalent 4-1BB binding aptamers costimulate CD8+ T cells and inhibit tumor growth in mice. *The Journal of clinical investigation* 118 (1), pp. 376–386.

Melero, I.; Shuford, W. W.; Newby, S. A.; Aruffo, A.; Ledbetter, J. A.; Hellström, K. E. et al. (1997): Monoclonal antibodies against the 4-1BB T-cell activation molecule eradicate established tumors. *Nature medicine* 3 (6), pp. 682–685.

Meseck, Marcia; Huang, Tiangui; Ma, Ge; Wang, George; Chen, Shu-Hsia; Woo, Savio L. C. (2011): A functional recombinant human 4-1BB ligand for immune costimulatory therapy of cancer. *Journal of immunotherapy (Hagerstown, Md. : 1997)* 34 (2), pp. 175–182.

Messenheimer, David J.; Jensen, Shawn M.; Afentoulis, Michael E.; Wegmann, Keith W.; Feng, Zipei; Friedman, David J. et al. (2017): Timing of PD-1 Blockade Is Critical to Effective Combination Immunotherapy with Anti-OX40. *Clinical cancer research : an official journal of the American Association for Cancer Research* 23 (20), pp. 6165–6177.

Miller, J. F.; Mitchell, G. F.; Weiss, N. S. (1967): Cellular basis of the immunological defects in thymectomized mice. *Nature* 214 (5092), pp. 992–997.

Mølgaard, Kasper; Harwood, Seandean L.; Compte, Marta; Merino, Nekane; Bonet, Jaume; Alvarez-Cienfuegos, Ana et al. (2018): Bispecific light T-cell engagers for gene-based

immunotherapy of epidermal growth factor receptor (EGFR)-positive malignancies. *Cancer immunology, immunotherapy : CII*.

Morillon, Y. Maurice; Hammond, Scott A.; Durham, Nicholas M.; Schlom, Jeffrey; Greiner, John W. (2017): Enhanced immunotherapy by combining a vaccine with a novel murine GITR ligand fusion protein. *Oncotarget* 8 (43), pp. 73469–73482.

Morishima, Chihiro; McNeel, Douglas G.; Patel, Manish R.; Kohrt, Holbrook E.; Waldmann, Thomas A.; Thompson, John A. et al. (2015): CITN11-02 interim trial results: subcutaneous administration of recombinant human IL-15 (rhIL-15) is associated with expansion of peripheral blood CD56+ NK cells and CD8+ T cells. *Journal for immunotherapy of cancer* 3 (Suppl 2), P203.

Morris, Nicholas P.; Peters, Carmen; Montler, Ryan; Hu, Hong-Ming; Curti, Brendan D.; Urba, Walter J.; Weinberg, Andrew D. (2007): Development and characterization of recombinant human Fc:OX40L fusion protein linked via a coiled-coil trimerization domain. *Molecular Immunology* 44 (12), pp. 3112–3121.

Mortier, Erwan; Quéméner, Agnès; Vusio, Patricia; Lorenzen, Inken; Boublik, Yvan; Grötzinger, Joachim et al. (2006): Soluble interleukin-15 receptor alpha (IL-15R alpha)-sushi as a selective and potent agonist of IL-15 action through IL-15R beta/gamma. Hyperagonist IL-15 x IL-15R alpha fusion proteins. *The Journal of biological chemistry* 281 (3), pp. 1612–1619.

Mueller, D. L.; Jenkins, M. K.; Schwartz, R. H. (1989): Clonal expansion versus functional clonal inactivation: a costimulatory signalling pathway determines the outcome of T cell antigen receptor occupancy. *Annual review of immunology* 7, pp. 445–480.

Müller, Dafne (2015): Antibody fusions with immunomodulatory proteins for cancer therapy. *Pharmacology & therapeutics* 154, pp. 57–66.

Müller, Dafne; Frey, Katharina; Kontermann, Roland E. (2008a): A novel antibody-4-1BBL fusion protein for targeted costimulation in cancer immunotherapy. *Journal of immunotherapy (Hagerstown, Md. : 1997)* 31 (8), pp. 714–722.

Müller, Dafne; Kontermann, Roland E. (2010): Bispecific antibodies for cancer immunotherapy: Current perspectives. *BioDrugs : clinical immunotherapeutics, biopharmaceuticals and gene therapy* 24 (2), pp. 89–98.

Müller, Nicole; Wyzgol, Agnes; Münkel, Sabine; Pfizenmaier, Klaus; Wajant, Harald (2008b): Activity of soluble OX40 ligand is enhanced by oligomerization and cell surface immobilization. *The FEBS journal* 275 (9), pp. 2296–2304.

Murata, Satoshi; Ladle, Brian H.; Kim, Peter S.; Lutz, Eric R.; Wolpoe, Matthew E.; Ivie, Susan E. et al. (2006): OX40 costimulation synergizes with GM-CSF whole-cell vaccination to overcome established CD8+ T cell tolerance to an endogenous tumor antigen. *Journal of immunology (Baltimore, Md. : 1950)* 176 (2), pp. 974–983.

Murphy, Katherine A.; Lechner, Melissa G.; Popescu, Flavia E.; Bedi, Jessica; Decker, Stacy A.; Hu, Peisheng et al. (2012): An in vivo immunotherapy screen of costimulatory molecules identifies Fc-OX40L as a potent reagent for the treatment of established murine

gliomas. *Clinical cancer research : an official journal of the American Association for Cancer Research* 18 (17), pp. 4657–4668.

Myrdal, S.; Foster, M. (1994): Time-resolved confocal analysis of antibody penetration into living, solid tumor spheroids. *Scanning* 16 (3), pp. 155–167.

Navabi, Shadi sadat; Doroudchi, Mehrnoosh; Tashnizi, Ahmad Hosseini; Habibagahi, Mojtaba (2015): Natural Killer Cell Functional Activity After 4-1BB Costimulation. *Inflammation* 38 (3), pp. 1181–1190.

Nelson, B. H.; Willerford, D. M. (1998): Biology of the interleukin-2 receptor. *Advances in immunology* 70, pp. 1–81.

Nestle, F. O.; Alijagic, S.; Gilliet, M.; Sun, Y.; Grabbe, S.; Dummer, R. et al. (1998): Vaccination of melanoma patients with peptide- or tumor lysate-pulsed dendritic cells. *Nature medicine* 4 (3), pp. 328–332.

Niedermeyer, J.; Kriz, M.; Hilberg, F.; Garin-Chesa, P.; Bamberger, U.; Lenter, M. C. et al. (2000): Targeted disruption of mouse fibroblast activation protein. *Molecular and cellular biology* 20 (3), pp. 1089–1094.

Niu, Liguo; Strahotin, Simona; Hewes, Becker; Zhang, Benyue; Zhang, Yuanyuan; Archer, David et al. (2007): Cytokine-mediated disruption of lymphocyte trafficking, hemopoiesis, and induction of lymphopenia, anemia, and thrombocytopenia in anti-CD137-treated mice. *Journal of immunology (Baltimore, Md. : 1950)* 178 (7), pp. 4194–4213.

Nocentini, G.; Giunchi, L.; Ronchetti, S.; Krausz, L. T.; Bartoli, A.; Moraca, R. et al. (1997): A new member of the tumor necrosis factor/nerve growth factor receptor family inhibits T cell receptor-induced apoptosis. *Proceedings of the National Academy of Sciences of the United States of America* 94 (12), pp. 6216–6221.

Oberst, Michael D.; Augé, Catherine; Morris, Chad; Kentner, Stacy; Mulgrew, Kathy; McGlinchey, Kelly et al. (2018): Potent Immune Modulation by MEDI6383, an Engineered Human OX40 Ligand IgG4P Fc Fusion Protein. *Molecular cancer therapeutics* 17 (5), pp. 1024–1038.

Ohshima, Y.; Tanaka, Y.; Tozawa, H.; Takahashi, Y.; Maliszewski, C.; Delespesse, G. (1997): Expression and function of OX40 ligand on human dendritic cells. *Journal of immunology (Baltimore, Md. : 1950)* 159 (8), pp. 3838–3848.

Ohteki, T.; Suzue, K.; Maki, C.; Ota, T.; Koyasu, S. (2001): Critical role of IL-15-IL-15R for antigen-presenting cell functions in the innate immune response. *Nature immunology* 2 (12), pp. 1138–1143.

Olabiran, Y.; Ledermann, J. A.; Marston, N. J.; Boxer, G. M.; Hicks, R.; Souhami, R. L. et al. (1994): The selection of antibodies for targeted therapy of small-cell lung cancer (SCLC) using a human tumour spheroid model to compare the uptake of cluster 1 and cluster w4 antibodies. *British journal of cancer* 69 (2), pp. 247–252.

Ostermann, Elinborg; Garin-Chesa, Pilar; Heider, Karl Heinz; Kalat, Milena; Lamche, Herbert; Puri, Christina et al. (2008): Effective immunoconjugate therapy in cancer models

targeting a serine protease of tumor fibroblasts. *Clinical cancer research : an official journal of the American Association for Cancer Research* 14 (14), pp. 4584–4592.

Pagès, Franck; Berger, Anne; Camus, Matthieu; Sanchez-Cabo, Fatima; Costes, Anne; Molidor, Robert et al. (2005): Effector memory T cells, early metastasis, and survival in colorectal cancer. *The New England journal of medicine* 353 (25), pp. 2654–2666.

Pagès, Franck; Kirilovsky, Amos; Mlecnik, Bernhard; Asslaber, Martin; Tosolini, Marie; Bindea, Gabriela et al. (2009): In situ cytotoxic and memory T cells predict outcome in patients with early-stage colorectal cancer. *Journal of clinical oncology : official journal of the American Society of Clinical Oncology* 27 (35), pp. 5944–5951.

Paterson, D.; Jefferies, W.; Green, J.; Brandon, M.; Corthesy, P.; Puklavec, M.; Williams, A. (1987): Antigens of activated rat T lymphocytes including a molecule of 50,000 Mr detected only on CD4 positive T blasts. *Molecular Immunology* 24 (12), pp. 1281–1290.

Pedroza-Gonzalez, Alexander; Zhou, Guoying; Singh, Simar Pal; Boor, Patrick Pc; Pan, Qiuwei; Grunhagen, Dirk et al. (2015): GITR engagement in combination with CTLA-4 blockade completely abrogates immunosuppression mediated by human liver tumor-derived regulatory T cells ex vivo. *Oncoimmunology* 4 (12), e1051297.

Perez-Diez, Ainhoa; Joncker, Nathalie T.; Choi, Kyungho; Chan, William F. N.; Anderson, Colin C.; Lantz, Olivier; Matzinger, Polly (2007): CD4 cells can be more efficient at tumor rejection than CD8 cells. *Blood* 109 (12), pp. 5346–5354.

Pollok, K. E.; Kim, Y. J.; Zhou, Z.; Hurtado, J.; Kim, K. K.; Pickard, R. T.; Kwon, B. S. (1993): Inducible T cell antigen 4-1BB. Analysis of expression and function. *Journal of immunology (Baltimore, Md. : 1950)* 150 (3), pp. 771–781.

Pondé, Noam; Brandão, Mariana; El-Hachem, Georges; Werbrouck, Emilie; Piccart, Martine (2018): Treatment of advanced HER2-positive breast cancer: 2018 and beyond. *Cancer treatment reviews* 67, pp. 10–20.

Pruitt, Scott K.; Boczkowski, David; Rosa, Nicole de; Haley, N. Rebecca; Morse, Michael A.; Tyler, Douglas S. et al. (2011): Enhancement of anti-tumor immunity through local modulation of CTLA-4 and GITR by dendritic cells. *European journal of immunology* 41 (12), pp. 3553–3563.

Pulle, Gayle; Vidric, Mariana; Watts, Tania H. (2006): IL-15-dependent induction of 4-1BB promotes antigen-independent CD8 memory T cell survival. *Journal of immunology (Baltimore, Md. : 1950)* 176 (5), pp. 2739–2748.

Qui, Harry Z.; Hagymasi, Adam T.; Bandyopadhyay, Suman; St Rose, Marie-Clare; Ramanarasimhaiah, Raghunath; Ménoret, Antoine et al. (2011): CD134 plus CD137 dual costimulation induces Eomesodermin in CD4 T cells to program cytotoxic Th1 differentiation. *Journal of immunology (Baltimore, Md. : 1950)* 187 (7), pp. 3555–3564.

Quill, H.; Schwartz, R. H. (1987): Stimulation of normal inducer T cell clones with antigen presented by purified Ia molecules in planar lipid membranes: specific induction of a long-lived state of proliferative nonresponsiveness. *Journal of immunology (Baltimore, Md. : 1950)* 138 (11), pp. 3704–3712.

Rabu, Catherine; Quéméner, Agnès; Jacques, Yannick; Echasserieau, Klara; Vusio, Patricia; Lang, François (2005): Production of recombinant human trimeric CD137L (4-1BBL). Cross-linking is essential to its T cell co-stimulation activity. *The Journal of biological chemistry* 280 (50), pp. 41472–41481.

Ramirez-Montagut, Teresa; Chow, Andrew; Hirschhorn-Cymerman, Daniel; Terwey, Theis H.; Kochman, Adam A.; Lu, Sydney et al. (2006): Glucocorticoid-induced TNF receptor family related gene activation overcomes tolerance/ignorance to melanoma differentiation antigens and enhances antitumor immunity. *Journal of immunology (Baltimore, Md. : 1950)* 176 (11), pp. 6434–6442.

Redmond, William L.; Gough, Michael J.; Weinberg, Andrew D. (2009): Ligation of the OX40 co-stimulatory receptor reverses self-Ag and tumor-induced CD8 T-cell anergy in vivo. *European journal of immunology* 39 (8), pp. 2184–2194.

Redmond, William L.; Linch, Stefanie N.; Kasiewicz, Melissa J. (2014): Combined targeting of costimulatory (OX40) and coinhibitory (CTLA-4) pathways elicits potent effector T cells capable of driving robust antitumor immunity. *Cancer immunology research* 2 (2), pp. 142–153.

Redmond, William L.; Triplett, Todd; Floyd, Kevin; Weinberg, Andrew D. (2012): Dual anti-OX40/IL-2 therapy augments tumor immunotherapy via IL-2R-mediated regulation of OX40 expression. *PloS one* 7 (4), e34467.

Repka, Tanya; Chiorean, Elena G.; Gay, Juliette; Herwig, Katherine E.; Kohl, Virginia K.; Yee, Douglas; Miller, Jeffrey S. (2003): Trastuzumab and interleukin-2 in HER2-positive metastatic breast cancer: a pilot study. *Clinical cancer research : an official journal of the American Association for Cancer Research* 9 (7), pp. 2440–2446.

Reusch, Ursula; Sundaram, Magesh; Davol, Pamela A.; Olson, Sarah D.; Davis, James B.; Demel, Kurt et al. (2006): Anti-CD3 x anti-epidermal growth factor receptor (EGFR) bispecific antibody redirects T-cell cytolytic activity to EGFR-positive cancers in vitro and in an animal model. *Clinical cancer research : an official journal of the American Association for Cancer Research* 12 (1), pp. 183–190.

Robert, Caroline; Ribas, Antoni; Wolchok, Jedd D.; Hodi, F. Stephen; Hamid, Omid; Kefford, Richard et al. (2014): Anti-programmed-death-receptor-1 treatment with pembrolizumab in ipilimumab-refractory advanced melanoma: a randomised dose-comparison cohort of a phase 1 trial. *The Lancet* 384 (9948), pp. 1109–1117.

Robert, Caroline; Thomas, Luc; Bondarenko, Igor; O'Day, Steven; Weber, Jeffrey; Garbe, Claus et al. (2011): Ipilimumab plus dacarbazine for previously untreated metastatic melanoma. *The New England journal of medicine* 364 (26), pp. 2517–2526.

Robinson, Tanya O.; Schluns, Kimberly S. (2017): The potential and promise of IL-15 in immuno-oncogenic therapies. *Immunology letters* 190, pp. 159–168.

Rochman, Yrina; Spolski, Rosanne; Leonard, Warren J. (2009): New insights into the regulation of T cells by gamma(c) family cytokines. *Nature reviews. Immunology* 9 (7), pp. 480–490.

Ronchetti, Simona; Zollo, Ornella; Bruscoli, Stefano; Agostini, Massimiliano; Bianchini, Rodolfo; Nocentini, Giuseppe et al. (2004): GITR, a member of the TNF receptor superfamily, is costimulatory to mouse T lymphocyte subpopulations. *European journal of immunology* 34 (3), pp. 613–622.

Rosario, Maximillian; Liu, Bai; Kong, Lin; Collins, Lynne I.; Schneider, Stephanie E.; Chen, Xiaoyue et al. (2016): The IL-15-Based ALT-803 Complex Enhances FcγRIIIa-Triggered NK Cell Responses and In Vivo Clearance of B Cell Lymphomas. *Clinical cancer research : an official journal of the American Association for Cancer Research* 22 (3), pp. 596–608.

Rosenberg, Steven A. (2014): IL-2: the first effective immunotherapy for human cancer. *Journal of immunology (Baltimore, Md. : 1950)* 192 (12), pp. 5451–5458.

Rubinstein, Mark P.; Kovar, Marek; Purton, Jared F.; Cho, Jae-Ho; Boyman, Onur; Surh, Charles D.; Sprent, Jonathan (2006): Converting IL-15 to a superagonist by binding to soluble IL-15R{alpha}. *Proceedings of the National Academy of Sciences of the United States of America* 103 (24), pp. 9166–9171.

Sabbagh, Laurent; Snell, Laura M.; Watts, Tania H. (2007): TNF family ligands define niches for T cell memory. *Trends in immunology* 28 (8), pp. 333–339.

Saito, Takashi; Yokosuka, Tadashi; Hashimoto-Tane, Akiko (2010): Dynamic regulation of T cell activation and co-stimulation through TCR-microclusters. *FEBS Letters* 584 (24), pp. 4865–4871.

Sakaguchi, Shimon; Yamaguchi, Tomoyuki; Nomura, Takashi; Ono, Masahiro (2008): Regulatory T cells and immune tolerance. *Cell* 133 (5), pp. 775–787.

Sallusto, F.; Lenig, D.; Förster, R.; Lipp, M.; Lanzavecchia, A. (1999): Two subsets of memory T lymphocytes with distinct homing potentials and effector functions. *Nature* 401 (6754), pp. 708–712.

Sapski, Sabrina; Beha, Nadine; Kontermann, Roland; Müller, Dafne (2017): Tumor-targeted costimulation with antibody-fusion proteins improves bispecific antibody-mediated immune response in presence of immunosuppressive factors. *Oncoimmunology* 6 (12), e1361594.

Sato, J. D.; Kawamoto, T.; Le, A. D.; Mendelsohn, J.; Polikoff, J.; Sato, G. H. (1983): Biological effects in vitro of monoclonal antibodies to human epidermal growth factor receptors. *Molecular biology & medicine* 1 (5), pp. 511–529.

Schabowsky, Rich-Henry; Elpek, Kutlu G.; Madireddi, Shravan; Sharma, Rajesh K.; Yolcu, Esma S.; Bandura-Morgan, Laura et al. (2009): A novel form of 4-1BBL has better immunomodulatory activity than an agonistic anti-4-1BB Ab without Ab-associated severe toxicity. *Vaccine* 28 (2), pp. 512–522.

Schneider, B.; Münkel, S.; Krippner-Heidenreich, A.; Grunwald, I.; Wels, W. S.; Wajant, H. et al. (2010): Potent antitumoral activity of TRAIL through generation of tumor-targeted single-chain fusion proteins. *Cell Death Dis* 1, e68.

Schwartzentruber, Douglas J.; Lawson, David H.; Richards, Jon M.; Conry, Robert M.; Miller, Donald M.; Treisman, Jonathan et al. (2011): gp100 peptide vaccine and interleukin-2 in

patients with advanced melanoma. *The New England journal of medicine* 364 (22), pp. 2119–2127.

Scott, Andrew M.; Wiseman, Greg; Welt, Sydney; Adjei, Alex; Lee, Fook-Thean; Hopkins, Wendie et al. (2003): A Phase I dose-escalation study of sibrotuzumab in patients with advanced or metastatic fibroblast activation protein-positive cancer. *Clinical cancer research : an official journal of the American Association for Cancer Research* 9 (5), pp. 1639–1647.

Segal, Neil H.; Logan, Theodore F.; Hodi, F. Stephen; McDermott, David; Melero, Ignacio; Hamid, Omid et al. (2017): Results from an Integrated Safety Analysis of Urelumab, an Agonist Anti-CD137 Monoclonal Antibody. *Clinical cancer research : an official journal of the American Association for Cancer Research* 23 (8), pp. 1929–1936.

Seidman, A. D.; Fornier, M. N.; Esteva, F. J.; Tan, L.; Kaptain, S.; Bach, A. et al. (2001): Weekly trastuzumab and paclitaxel therapy for metastatic breast cancer with analysis of efficacy by HER2 immunophenotype and gene amplification. *Journal of clinical oncology : official journal of the American Society of Clinical Oncology* 19 (10), pp. 2587–2595.

Serghides, L.; Bukczynski, J.; Wen, T.; Wang, C.; Routy, J.-P.; Boulassel, M.-R. et al. (2005): Evaluation of OX40 Ligand as a Costimulator of Human Antiviral Memory CD8 T Cell Responses: Comparison with B7.1 and 4-1BBL. *Journal of immunology (Baltimore, Md. : 1950)* 175 (10), pp. 6368–6377.

Sharon, M.; Klausner, R.; Cullen, B.; Chizzonite, R.; Leonard, W. (1986): Novel interleukin-2 receptor subunit detected by cross-linking under high-affinity conditions. *Science* 234 (4778), pp. 859–863.

Shindo, Yoshitaro; Yoshimura, Kiyoshi; Kuramasu, Atsuo; Watanabe, Yusaku; Ito, Hideaki; Kondo, Tomoko et al. (2015): Combination immunotherapy with 4-1BB activation and PD-1 blockade enhances antitumor efficacy in a mouse model of subcutaneous tumor. *Anticancer research* 35 (1), pp. 129–136.

Shively, J. E.; Beatty, J. D. (1985): CEA-related antigens: molecular biology and clinical significance. *Critical reviews in oncology/hematology* 2 (4), pp. 355–399.

Siegemund, Martin; Seifert, Oliver; Zarani, Maria; Džinić, Tamara; Leo, Valentino de; Göttsch, Doris et al. (2016): An optimized antibody-single-chain TRAIL fusion protein for cancer therapy. *mAbs* 8 (5), pp. 879–891.

Silke, J.; Brink, R. (2010): Regulation of TNFRSF and innate immune signalling complexes by TRAFs and cIAPs. *Cell death and differentiation* 17 (1), pp. 35–45.

Slamon, D. J.; Leyland-Jones, B.; Shak, S.; Fuchs, H.; Paton, V.; Bajamonde, A. et al. (2001): Use of chemotherapy plus a monoclonal antibody against HER2 for metastatic breast cancer that overexpresses HER2. *The New England journal of medicine* 344 (11), pp. 783–792.

Srivastava, Raghvendra M.; Trivedi, Sumita; Concha-Benavente, Fernando; Gibson, Sandra P.; Reeder, Carly; Ferrone, Soldano; Ferris, Robert L. (2017): CD137 Stimulation Enhances Cetuximab-Induced Natural Killer: Dendritic Cell Priming of Antitumor T-Cell Immunity in

Patients with Head and Neck Cancer. *Clinical cancer research : an official journal of the American Association for Cancer Research* 23 (3), pp. 707–716.

Stagg, John; Loi, Sherene; Divisekera, Upulie; Ngiow, Shin Foong; Duret, Helene; Yagita, Hideo et al. (2011): Anti-ErbB-2 mAb therapy requires type I and II interferons and synergizes with anti-PD-1 or anti-CD137 mAb therapy. *Proceedings of the National Academy of Sciences of the United States of America* 108 (17), pp. 7142–7147.

Stoklasek, Thomas A.; Schluns, Kimberly S.; Lefrançois, Leo (2006): Combined IL-15/IL-15Ralpha immunotherapy maximizes IL-15 activity in vivo. *Journal of immunology (Baltimore, Md. : 1950)* 177 (9), pp. 6072–6080.

Suntharalingam, Ganesh; Perry, Meghan R.; Ward, Stephen; Brett, Stephen J.; Castello-Cortes, Andrew; Brunner, Michael D.; Panoskaltsis, Nicki (2006): Cytokine storm in a phase 1 trial of the anti-CD28 monoclonal antibody TGN1412. *The New England journal of medicine* 355 (10), pp. 1018–1028.

Suvas, Susmit; Kim, Bumseok; Sarangi, Pranita P.; Tone, Masahide; Waldmann, Herman; Rouse, Barry T. (2005): In vivo kinetics of GITR and GITR ligand expression and their functional significance in regulating viral immunopathology. *Journal of virology* 79 (18), pp. 11935–11942.

Takeshita, T.; Asao, H.; Ohtani, K.; Ishii, N.; Kumaki, S.; Tanaka, N. et al. (1992): Cloning of the gamma chain of the human IL-2 receptor. *Science* 257 (5068), pp. 379–382.

Tan, J. T.; Whitmire, J. K.; Ahmed, R.; Pearson, T. C.; Larsen, C. P. (1999): 4-1BB ligand, a member of the TNF family, is important for the generation of antiviral CD8 T cell responses. *Journal of immunology (Baltimore, Md. : 1950)* 163 (9), pp. 4859–4868.

Tan, J. T.; Whitmire, J. K.; Murali-Krishna, K.; Ahmed, R.; Altman, J. D.; Mittler, R. S. et al. (2000): 4-1BB costimulation is required for protective anti-viral immunity after peptide vaccination. *Journal of immunology (Baltimore, Md. : 1950)* 164 (5), pp. 2320–2325.

Thaysen-Andersen, M.; Chertova, E.; Bergamaschi, C.; Moh, E. S. X.; Chertov, O.; Roser, J. et al. (2016): Recombinant human heterodimeric IL-15 complex displays extensive and reproducible N- and O-linked glycosylation. *Glycoconjugate journal* 33 (3), pp. 417–433.

Tigue, Natalie J.; Bamber, Lisa; Andrews, John; Ireland, Samantha; Hair, James; Carter, Edward et al. (2017): MEDI1873, a potent, stabilized hexameric agonist of human GITR with regulatory T-cell targeting potential. *Oncoimmunology* 6 (3), e1280645.

Turk, Mary Jo; Guevara-Patiño, José A.; Rizzuto, Gabrielle A.; Engelhorn, Manuel E.; Sakaguchi, Shimon; Houghton, Alan N. (2004): Concomitant tumor immunity to a poorly immunogenic melanoma is prevented by regulatory T cells. *The Journal of experimental medicine* 200 (6), pp. 771–782.

Turnert, Timothy; Chen, Philip; Goodly, Lyndon J.; NWells, Alan (1996): EGF receptor signaling enhances in vivo invasiveness of DU-145 human prostate carcinoma cells. *Clin Exp Metast* 14 (4), pp. 409–418.

Uberall, I.; Kolár, Z.; Trojanec, R.; Berkovcová, J.; Hajdúch, M. (2008): The status and role of ErbB receptors in human cancer. *Experimental and molecular pathology* 84 (2), pp. 79–89.

van der Bruggen, P.; Traversari, C.; Chomez, P.; Lurquin, C.; Plaen, E. de; van den Eynde, B. et al. (1991): A gene encoding an antigen recognized by cytolytic T lymphocytes on a human melanoma. *Science* 254 (5038), pp. 1643–1647.

Vang, K. B.; Yang, J.; Mahmud, S. A.; Burchill, M. A.; Vegoe, A. L.; Farrar, M. A. (2008): IL-2, -7, and -15, but Not Thymic Stromal Lymphopoeitin, Redundantly Govern CD4+Foxp3+ Regulatory T Cell Development. *Journal of immunology (Baltimore, Md. : 1950)* 181 (5), pp. 3285–3290.

Vela, M.; Corral, D.; Carrasco, P.; Fernández, L.; Valentín, J.; González, B. et al. (2018): Haploidentical IL-15/41BBL activated and expanded natural killer cell infusion therapy after salvage chemotherapy in children with relapsed and refractory leukemia. *Cancer letters* 422, pp. 107–117.

Verbeek, Bianca S.; Adriaansen-Slot, Sabrina S.; Vroom, Thea M.; Beckers, Thomas; Rijksen, Gert (1998): Overexpression of EGFR and c-erbB2 causes enhanced cell migration in human breast cancer cells and NIH3T3 fibroblasts. *FEBS Letters* 425 (1), pp. 145–150.

Vigneron, Nathalie (2015): Human Tumor Antigens and Cancer Immunotherapy. *BioMed research international* 2015, p. 948501.

Villarreal, Daniel O.; Chin, Diana; Smith, Melissa A.; Luistro, Leopoldo L.; Snyder, Linda A. (2017): Combination GITR targeting/PD-1 blockade with vaccination drives robust antigen-specific antitumor immunity. *Oncotarget* 8 (24), pp. 39117–39130.

Vinay, D. S.; Kwon, B. S. (1998): Role of 4-1BB in immune responses. *Seminars in immunology* 10 (6), pp. 481–489.

Vinay, Dass S.; Kwon, Byoung S. (2011): 4-1BB signaling beyond T cells. *Cellular & molecular immunology* 8 (4), pp. 281–284.

Vincent, Marie; Bessard, Anne; Cochonneau, Denis; Teppaz, Géraldine; Solé, Véronique; Maillasson, Mike et al. (2013): Tumor targeting of the IL-15 superagonist RLI by an anti-GD2 antibody strongly enhances its antitumor potency. *International journal of cancer* 133 (3), pp. 757–765.

Vincent, Marie; Teppaz, Géraldine; Lajoie, Laurie; Solé, Véronique; Bessard, Anne; Maillasson, Mike et al. (2014): Highly potent anti-CD20-RLI immunocytokine targeting established human B lymphoma in SCID mouse. *mAbs* 6 (4), pp. 1026–1037.

Vogel, Charles L.; Cobleigh, Melody A.; Tripathy, Debu; Gutheil, John C.; Harris, Lyndsay N.; Fehrenbacher, Louis et al. (2002): Efficacy and safety of trastuzumab as a single agent in first-line treatment of HER2-overexpressing metastatic breast cancer. *Journal of clinical oncology : official journal of the American Society of Clinical Oncology* 20 (3), pp. 719–726.

Wajant, H. (2015): Principles of antibody-mediated TNF receptor activation. *Cell death and differentiation* 22 (11), pp. 1727–1741.

Waldmann, Thomas A. (2017): Cytokines in Cancer Immunotherapy. *Cold Spring Harbor perspectives in biology*.

Wallace, P. K.; Howell, A. L.; Fanger, M. W. (1994): Role of Fc gamma receptors in cancer and infectious disease. *Journal of leukocyte biology* 55 (6), pp. 816–826.

Wang, Xin Maggie; Yao, Tsun-Wen; Nadvi, Naveed A.; Osborne, Brenna; McCaughan, Geoffrey W.; Gorrell, Mark D. (2008): Fibroblast activation protein and chronic liver disease. *Frontiers in bioscience : a journal and virtual library* 13, pp. 3168–3180.

Wang, Xinquan; Rickert, Mathias; Garcia, K. Christopher (2005): Structure of the quaternary complex of interleukin-2 with its alpha, beta, and gammac receptors. *Science* 310 (5751), pp. 1159–1163.

Watts, Tania H. (2005): TNF/TNFR family members in costimulation of T cell responses. *Annual review of immunology* 23, pp. 23–68.

Wege, Anja K.; Weber, Florian; Kroemer, Alexander; Ortmann, Olaf; Nimmerjahn, Falk; Brockhoff, Gero (2017): IL-15 enhances the anti-tumor activity of trastuzumab against breast cancer cells but causes fatal side effects in humanized tumor mice (HTM). *Oncotarget* 8 (2), pp. 2731–2744.

Weinberg, A. D.; Rivera, M. M.; Prell, R.; Morris, A.; Ramstad, T.; Vetto, J. T. et al. (2000): Engagement of the OX-40 receptor in vivo enhances antitumor immunity. *Journal of immunology (Baltimore, Md. : 1950)* 164 (4), pp. 2160–2169.

Welt, S.; Divgi, C. R.; Scott, A. M.; Garin-Chesa, P.; Finn, R. D.; Graham, M. et al. (1994): Antibody targeting in metastatic colon cancer: a phase I study of monoclonal antibody F19 against a cell-surface protein of reactive tumor stromal fibroblasts. *Journal of clinical oncology : official journal of the American Society of Clinical Oncology* 12 (6), pp. 1193–1203.

Wiethe, Carsten; Dittmar, Kurt; Doan, Tracy; Lindenmaier, Werner; Tindle, Robert (2003): Provision of 4-1BB ligand enhances effector and memory CTL responses generated by immunization with dendritic cells expressing a human tumor-associated antigen. *Journal of immunology (Baltimore, Md. : 1950)* 170 (6), pp. 2912–2922.

Willoughby, Jane E.; Kerr, Jonathan P.; Rogel, Anne; Taraban, Vadim Y.; Buchan, Sarah L.; Johnson, Peter W. M.; Al-Shamkhani, Aymen (2014): Differential impact of CD27 and 4-1BB costimulation on effector and memory CD8 T cell generation following peptide immunization. *Journal of immunology (Baltimore, Md. : 1950)* 193 (1), pp. 244–251.

Won, Eun-Young; Cha, Kiweon; Byun, Jung-Sue; Kim, Dong-Uk; Shin, Sumi; Ahn, Byungchan et al. (2010): The structure of the trimer of human 4-1BB ligand is unique among members of the tumor necrosis factor superfamily. *The Journal of biological chemistry* 285 (12), pp. 9202–9210.

Wu, Zhongfu; Xu, Yibing (2010): IL-15R alpha-IgG1-Fc enhances IL-2 and IL-15 anti-tumor action through NK and CD8+ T cells proliferation and activation. *Journal of molecular cell biology* 2 (4), pp. 217–222.

Xiang, R.; Lode, H. N.; Gillies, S. D.; Reisfeld, R. A. (1999): T cell memory against colon carcinoma is long-lived in the absence of antigen. *Journal of immunology (Baltimore, Md. : 1950)* 163 (7), pp. 3676–3683.

Xu, Wenxin; Jones, Monica; Liu, Bai; Zhu, Xiaoyun; Johnson, Christopher B.; Edwards, Ana C. et al. (2013): Efficacy and mechanism-of-action of a novel superagonist interleukin-15: interleukin-15 receptor αSu/Fc fusion complex in syngeneic murine models of multiple myeloma. *Cancer research* 73 (10), pp. 3075–3086.

Yajima, Toshiki; Nishimura, Hitoshi; Sad, Subash; Shen, Hao; Kuwano, Hiroyuki; Yoshikai, Yasunobu (2005): A novel role of IL-15 in early activation of memory CD8+ CTL after reinfection. *Journal of immunology (Baltimore, Md. : 1950)* 174 (6), pp. 3590–3597.

Ye, Qunrui; Song, De-Gang; Poussin, Mathilde; Yamamoto, Tori; Best, Andrew; Li, Chunsheng et al. (2014): CD137 accurately identifies and enriches for naturally occurring tumor-reactive T cells in tumor. *Clinical cancer research : an official journal of the American Association for Cancer Research* 20 (1), pp. 44–55.

Zhang, X.; Sun, S.; Hwang, I.; Tough, D. F.; Sprent, J. (1998): Potent and selective stimulation of memory-phenotype CD8+ T cells in vivo by IL-15. *Immunity* 8 (5), pp. 591–599.

Zhou, Pengfei; L'italien, Lawrence; Hodges, Douglas; Schebye, Xiao Min (2007): Pivotal roles of CD4+ effector T cells in mediating agonistic anti-GITR mAb-induced-immune activation and tumor immunity in CT26 tumors. *Journal of immunology (Baltimore, Md. : 1950)* 179 (11), pp. 7365–7375.

Zhou, Zhaocai; Song, Xiaomin; Berezov, Alan; Zhang, Geng; Li, Yanjing; Zhang, Hongtao et al. (2008): Human glucocorticoid-induced TNF receptor ligand regulates its signaling activity through multiple oligomerization states. *Proceedings of the National Academy of Sciences of the United States of America* 105 (14), pp. 5465–5470.

Zhu, Anqing; Sha, Huizi; Su, Shu; Chen, Fangjun; Wei, Jia; Meng, Fanyan et al. (2018): Bispecific tumor-penetrating protein anti-EGFR-iRGD efficiently enhances the infiltration of lymphocytes in gastric cancer. *American journal of cancer research* 8 (1), pp. 91–105.

Zhu, Li X.; Davoodi, Michael; Srivastava, Minu K.; Kachroo, Puja; Lee, Jay M.; St John, Maie et al. (2015): GITR agonist enhances vaccination responses in lung cancer. *Oncoimmunology* 4 (4), e992237.

Zhu, Yuwen; Yao, Sheng; Chen, Lieping (2011): Cell surface signaling molecules in the control of immune responses: a tide model. *Immunity* 34 (4), pp. 466–478.

Zhu, Yuwen; Zhu, Gefeng; Luo, Liqun; Flies, Andrew S.; Chen, Lieping (2007): CD137 stimulation delivers an antigen-independent growth signal for T lymphocytes with memory phenotype. *Blood* 109 (11), pp. 4882–4889.

7 Sequences

7.1 scFv$_{FAP}$_scTNFSFL

```
   1  atg gag aca gac aca ctc ctg cta tgg gta ctg ctg ctc tgg gtt cca ggt
      >>.....................Igkappa leader.........................>
        m   e   t   d   t   l   l   l   w   v   l   l   l   w   v   p   g

                             SfiI
                        -----------+-----
  52  tcc act ggt gac gcg gcc cag ccg gcc atg gcc cag gtg cag ctg aag cag
      >...........>> Igkappa leader
        s   t   g   d
                                                >>.......VH_FAP.........>
                                                  q   v   q   l   k   q

 103  tct gga gct gaa ctg gtg aaa ccc ggg gca tca gtg aag ctg tcc tgc aag
      >.............................VH_FAP.............................>
        s   g   a   e   l   v   k   p   g   a   s   v   k   l   s   c   k

 154  act tct ggc tac acc ttc act gaa aat att ata cac tgg gta aag cag agg
      >.............................VH_FAP.............................>
        t   s   g   y   t   f   t   e   n   i   i   h   w   v   k   q   r

 205  tct ggg cag ggt ctt gag tgg att ggg tgg ttt cac cct gga agt ggt agt
      >.............................VH_FAP.............................>
        s   g   q   g   l   e   w   i   g   w   f   h   p   g   s   g   s

 256  ata aag tac aat gag aaa ttc aag gac aag gcc aca ttg act gcg gac aaa
      >.............................VH_FAP.............................>
        i   k   y   n   e   k   f   k   d   k   a   t   l   t   a   d   k

 307  tcc tcc agc aca gtc tat atg gag ctt agt aga ttg aca tct gaa gac tct
      >.............................VH_FAP.............................>
        s   s   s   t   v   y   m   e   l   s   r   l   t   s   e   d   s

 358  gcg gtc tat ttc tgt gca aga cac gga gga act ggg cga gga gct atg gac
      >.............................VH_FAP.............................>
        a   v   y   f   c   a   r   h   g   g   t   g   r   g   a   m   d

                                              XhoI
                                           --+-----
 409  tac tgg ggt caa gga acc tca gtc acc gtc tcg agt ggt gga ggc ggt tca
      >.....................VH_FAP.....................>>
        y   w   g   q   g   t   s   v   t   v   s   s
                                                  >>....linker......>
                                                    g   g   g   g   s

 460  ggc gga ggt ggc tct ggc ggt agt gca caa att ctg atg acc cag tct cct
      >...........linker...........>>
        g   g   g   g   s   g   g   s
                                        >>...........VL_FAP.............>
                                          q   i   l   m   t   q   s   p

 511  gct tcc tca gtt gta tct ctg ggg cag agg gcc acc atc tca tgc agg gcc
      >.............................VL_FAP.............................>
        a   s   s   v   v   s   l   g   q   r   a   t   i   s   c   r   a

 562  agc aaa agt gtc agt aca tct gcc tat agt tat atg cac tgg tac caa cag
      >.............................VL_FAP.............................>
        s   k   s   v   s   t   s   a   y   s   y   m   h   w   y   q   q
```

```
613  aaa cca gga cag cca ccc aaa ctc ctc atc tat ctt gca tcc aac cta gaa
     >.............................VL(FAP).............................>
       k   p   g   q   p   p   k   l   l   i   y   l   a   s   n   l   e

664  tct ggg gtc cct ccc agg ttc agt ggc agt ggg tct ggg aca gac ttc acc
     >.............................VL(FAP).............................>
       s   g   v   p   p   r   f   s   g   s   g   s   g   t   d   f   t

715  ctc aac atc cac cct gtg gag gag gag gat gct gca acc tat tac tgt cag
     >.............................VL(FAP).............................>
       l   n   i   h   p   v   e   e   e   d   a   a   t   y   y   c   q

766  cac agt agg gag ctt ccg tac acg ttc gga ggg ggg acc aag ctg gaa ata
     >.............................VL(FAP).............................>
       h   s   r   e   l   p   y   t   f   g   g   g   t   k   l   e   i

               NotI                                              BamHI
           --+-------                                          -+-----
817  aaa cgg gcg gcc gca cat cat cac cat cac cac ggc gga ggt gga tcc tct
     >....>> VL(FAP)        >>......His tag......>>
       k   r                h   h   h   h   h   h

                          EcoRI
                         -+-----
868  aga  ... ...  ... ... tga gaa ttc
          >>..scTNFSFL..>>
```

7.2 RD_IL-15_scFv$_{FAP}$_scTNFSFL

```
       1  atg gag aca gac aca ctc ctg cta tgg gta ctg ctg ctc tgg gtt cca
ggt
      >>.........................Igkappa leader.........................>
        m   e   t   d   t   l   l   l   w   v   l   l   l   w   v   p   g

                                SfiI
                          ------------+-----
  52  tcc act ggt gac gcg gcc cag ccg gcc atc acc tgc cct ccc cct atg tcc
      >............>> Igkappa leader
        s   t   g   d
                                        >>......RD (aa 31-107).........>
                                          i   t   c   p   p   p   m   s

 103  gtg gag cac gcc gac atc tgg gtg aag tcc tac tcc ctg tac tcc aga gag
      >.........................RD (aa 31-107).........................>
        v   e   h   a   d   i   w   v   k   s   y   s   l   y   s   r   e

 154  cgg tac atc tgc aac tcc ggc ttc aag cgg aag gcc ggc acc tcc tcc ctg
      >.........................RD (aa 31-107).........................>
        r   y   i   c   n   s   g   f   k   r   k   a   g   t   s   s   l

 205  acc gag tgc gtg ctg aac aag gcc acc aac gtg gcc cac tgg acc acc cct
      >.........................RD (aa 31-107).........................>
        t   e   c   v   l   n   k   a   t   n   v   a   h   w   t   t   p



 256  tcc ctg aag tgc atc cgg gac cct gcc ctg gtg cat cag cgg cct gca cct
      >.........................RD (aa 31-107).........................>
        s   l   k   c   i   r   d   p   a   l   v   h   q   r   p   a   p
```

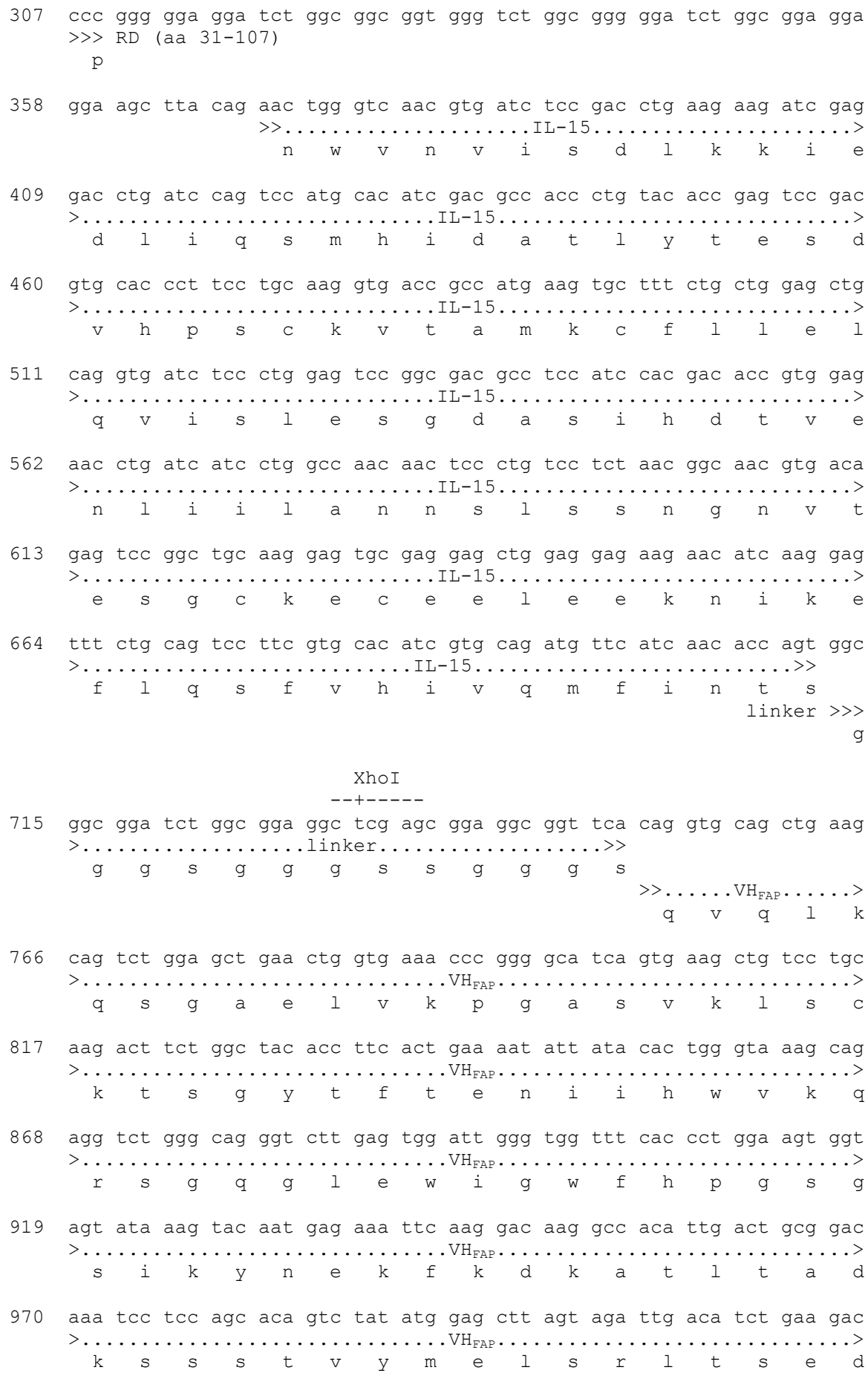
307 ccc ggg gga gga tct ggc ggc ggt ggg tct ggc ggg gga tct ggc gga gga
>>> RD (aa 31-107)
p
358 gga agc tta cag aac tgg gtc aac gtg atc tcc gac ctg aag aag atc gag
>>.....IL-15.....>
n w v n v i s d l k k i e
409 gac ctg atc cag tcc atg cac atc gac gcc acc ctg tac acc gag tcc gac
>.....IL-15.....>
d l i q s m h i d a t l y t e s d
460 gtg cac cct tcc tgc aag gtg acc gcc atg aag tgc ttt ctg ctg gag ctg
>.....IL-15.....>
v h p s c k v t a m k c f l l e l
511 cag gtg atc tcc ctg gag tcc ggc gac gcc tcc atc cac gac acc gtg gag
>.....IL-15.....>
q v i s l e s g d a s i h d t v e
562 aac ctg atc atc ctg gcc aac aac tcc ctg tcc tct aac ggc aac gtg aca
>.....IL-15.....>
n l i i l a n n s l s s n g n v t
613 gag tcc ggc tgc aag gag tgc gag gag ctg gag gag aag aac atc aag gag
>.....IL-15.....>
e s g c k e c e e l e e k n i k e
664 ttt ctg cag tcc ttc gtg cac atc gtg cag atg ttc atc aac acc agt ggc
>.....IL-15.....>>
f l q s f v h i v q m f i n t s
linker >>>
g
XhoI
--+-----
715 ggc gga tct ggc gga ggc tcg agc gga ggc ggt tca cag gtg cag ctg aag
>.....linker.....>>
g g s g g g s s g g g s
>>.....VHFAP.....>
q v q l k
766 cag tct gga gct gaa ctg gtg aaa ccc ggg gca tca gtg aag ctg tcc tgc
>.....VHFAP.....>
q s g a e l v k p g a s v k l s c
817 aag act tct ggc tac acc ttc act gaa aat att ata cac tgg gta aag cag
>.....VHFAP.....>
k t s g y t f t e n i i h w v k q
868 agg tct ggg cag ggt ctt gag tgg att ggg tgg ttt cac cct gga agt ggt
>.....VHFAP.....>
r s g q g l e w i g w f h p g s g
919 agt ata aag tac aat gag aaa ttc aag gac aag gcc aca ttg act gcg gac
>.....VHFAP.....>
s i k y n e k f k d k a t l t a d
970 aaa tcc tcc agc aca gtc tat atg gag ctt agt aga ttg aca tct gaa gac
>.....VHFAP.....>
k s s s t v y m e l s r l t s e d

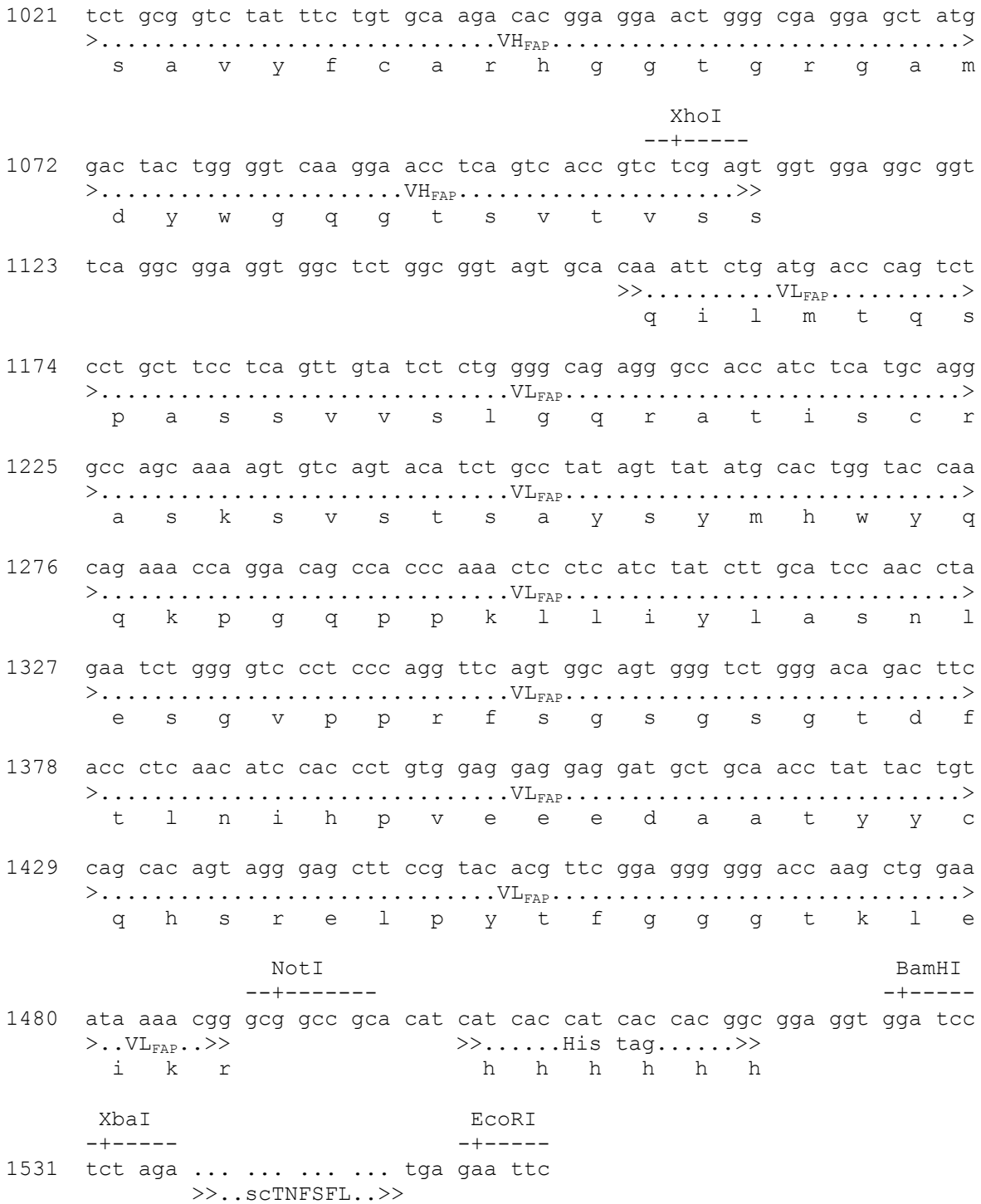
1021 tct gcg gtc tat ttc tgt gca aga cac gga gga act ggg cga gga gct atg
>.....VHFAP.....>
s a v y f c a r h g g t g r g a m
XhoI
--+-----
1072 gac tac tgg ggt caa gga acc tca gtc acc gtc tcg agt ggt gga ggc ggt
>.....VHFAP.....>>
d y w g q g t s v t v s s
1123 tca ggc gga ggt ggc tct ggc ggt agt gca caa att ctg atg acc cag tct
>>.....VLFAP.....>
q i l m t q s
1174 cct gct tcc tca gtt gta tct ctg ggg cag agg gcc acc atc tca tgc agg
>.....VLFAP.....>
p a s s v v s l g q r a t i s c r
1225 gcc agc aaa agt gtc agt aca tct gcc tat agt tat atg cac tgg tac caa
>.....VLFAP.....>
a s k s v s t s a y s y m h w y q
1276 cag aaa cca gga cag cca ccc aaa ctc ctc atc tat ctt gca tcc aac cta
>.....VLFAP.....>
q k p g q p p k l l i y l a s n l
1327 gaa tct ggg gtc cct ccc agg ttc agt ggc agt ggg tct ggg aca gac ttc
>.....VLFAP.....>
e s g v p p r f s g s g s g t d f
1378 acc ctc aac atc cac cct gtg gag gag gag gat gct gca acc tat tac tgt
>.....VLFAP.....>
t l n i h p v e e e d a a t y y c
1429 cag cac agt agg gag ctt ccg tac acg ttc gga ggg ggg acc aag ctg gaa
>.....VLFAP.....>
q h s r e l p y t f g g g t k l e
NotI
--+-------
BamHI
-+-----
1480 ata aaa cgg gcg gcc gca cat cat cac cat cac cac ggc gga ggt gga tcc
>..VLFAP..>>
>>.....His tag.....>>
i k r
h h h h h h
XbaI
-+-----
EcoRI
-+-----
1531 tct aga ... ... tga gaa ttc
>>..scTNFSFL..>>

7.3 sc4-1BBL

```
                XbaI
               -+-----
      BamHI
     -+-----
   1 gga tcc tct aga gag gga ccc gag ctg agc ccc gat gat cct gct gga ctg
               >>.................4-1BBL (aa 71-254).................>
                 r   e   g   p   e   l   s   p   d   d   p   a   g   l

  52 ctg gac ctg cgg cag ggc atg ttt gct cag ctg gtg gcc cag aac gtg ctg
     >.......................4-1BBL (aa 71-254).......................>
       l   d   l   r   q   g   m   f   a   q   l   v   a   q   n   v   l

 103 ctg atc gat ggc ccc ctg agc tgg tac agc gat cct gga ctg gct ggc gtg
     >.......................4-1BBL (aa 71-254).......................>
       l   i   d   g   p   l   s   w   y   s   d   p   g   l   a   g   v

 154 tca ctg aca ggc ggc ctg agc tac aaa gag gac acc aaa gaa ctg gtg gtg
     >.......................4-1BBL (aa 71-254).......................>
       s   l   t   g   g   l   s   y   k   e   d   t   k   e   l   v   v

 205 gcc aag gcc ggc gtg tac tac gtg ttc ttt cag ctg gaa ctg cgg aga gtg
     >.......................4-1BBL (aa 71-254).......................>
       a   k   a   g   v   y   y   v   f   f   q   l   e   l   r   r   v

 256 gtg gcc ggc gaa gga tct ggc tct gtg tct ctg gcc ctg cat ctg cag cct
     >.......................4-1BBL (aa 71-254).......................>
       v   a   g   e   g   s   g   s   v   s   l   a   l   h   l   q   p

 307 ctg aga agc gct gct ggc gct gca gct ctg gca ctg aca gtg gat ctg cct
     >.......................4-1BBL (aa 71-254).......................>
       l   r   s   a   a   g   a   a   a   l   a   l   t   v   d   l   p

 358 cct gcc agc tcc gag gcc aga aac agc gca ttc ggg ttt caa ggc agg ctg
     >.......................4-1BBL (aa 71-254).......................>
       p   a   s   s   e   a   r   n   s   a   f   g   f   q   g   r   l

 409 ctg cac ctg tct gcc ggc cag agg ctg gga gtg cat ctg cac aca gag gcc
     >.......................4-1BBL (aa 71-254).......................>
       l   h   l   s   a   g   q   r   l   g   v   h   l   h   t   e   a

 460 agg gct aga cac gcc tgg cag ctg aca cag ggc gct aca gtg ctg ggc ctg
     >.......................4-1BBL (aa 71-254).......................>
       r   a   r   h   a   w   q   l   t   q   g   a   t   v   l   g   l

 511 ttc aga gtg acc ccc gag att cca gcc ggc ctg cct tct cca aga agc gaa
     >.......................4-1BBL (aa 71-254).......................>>
       f   r   v   t   p   e   i   p   a   g   l   p   s   p   r   s   e

                                       BamHI
                                      -+-----
 562 ggc ggc gga gga agc gga ggc gga gga tcc ggc gga ggg gga tct ggg gga
     >>............................linker..............................>
       g   g   g   g   s   g   g   g   g   s   g   g   g   g   s   g   g

 613 ggc gga tca aga gaa ggc cca gag ctg tcc cct gac gat cca gcc ggg ctg
     >.linker.>>
       g   g   s
                 >>.................4-1BBL (aa 71-254).................>
                   r   e   g   p   e   l   s   p   d   d   p   a   g   l
```

```
664  ctg gat ctg aga cag gga atg ttc gcc cag ctg gtg gct cag aat gtg ctg
     >.....................4-1BBL (aa 71-254).....................>
       l   d   l   r   q   g   m   f   a   q   l   v   a   q   n   v   l

715  ctg att gac gga cct ctg tcc tgg tac tcc gac cca ggg ctg gca ggg gtg
     >.....................4-1BBL (aa 71-254).....................>
       l   i   d   g   p   l   s   w   y   s   d   p   g   l   a   g   v

766  tcc ctg act ggg gga ctg tcc tac aaa gaa gat aca aaa gaa ctg gtg gtg
     >.....................4-1BBL (aa 71-254).....................>
       s   l   t   g   g   l   s   y   k   e   d   t   k   e   l   v   v

817  gct aaa gct ggg gtg tac tat gtg ttt ttt cag ctg gaa ctg agg cgg gtg
     >.....................4-1BBL (aa 71-254).....................>
       a   k   a   g   v   y   y   v   f   f   q   l   e   l   r   r   v

868  gtg gct ggg gag ggc tca gga tct gtg tcc ctg gct ctg cat ctg cag cca
     >.....................4-1BBL (aa 71-254).....................>
       v   a   g   e   g   s   g   s   v   s   l   a   l   h   l   q   p

919  ctg cgc tct gct gct ggc gca gct gca ctg gct ctg act gtg gac ctg cca
     >.....................4-1BBL (aa 71-254).....................>
       l   r   s   a   a   g   a   a   a   l   a   l   t   v   d   l   p

970  cca gcc tct agc gag gct cgg aac tcc gca ttt ggg ttc caa gga cgc ctg
     >.....................4-1BBL (aa 71-254).....................>
       p   a   s   s   e   a   r   n   s   a   f   g   f   q   g   r   l

1021 ctg cat ctg agc gcc gga cag cgc ctg gga gtg cat ctg cat act gaa gcc
     >.....................4-1BBL (aa 71-254).....................>
       l   h   l   s   a   g   q   r   l   g   v   h   l   h   t   e   a

1072 aga gcc cgg cat gct tgg cag ctg acc cag ggg gca act gtg ctg gga ctg
     >.....................4-1BBL (aa 71-254).....................>
       r   a   r   h   a   w   q   l   t   q   g   a   t   v   l   g   l

1123 ttt cgc gtg aca cct gag atc cct gcc gga ctg cca agc cct aga tca gaa
     >.....................4-1BBL (aa 71-254).....................>>
       f   r   v   t   p   e   i   p   a   g   l   p   s   p   r   s   e

1174 ggg ggg gga ggc tct ggc gga ggc ggc tcc gga ggg ggc gga tct ggc ggg
     >>..........................linker............................>
       g   g   g   g   s   g   g   g   g   s   g   g   g   g   s   g   g

1225 gga ggc agt aga gaa gga cct gaa ctg tct ccc gat gac ccc gca gga ctg
     >.linker.>>
       g   g   s
                 >>.............4-1BBL (aa 71-254).................>
                   r   e   g   p   e   l   s   p   d   d   p   a   g   l

1276 ctg gac ctg aga cag ggc atg ttc gca cag ctg gtg gcc cag aat gtg ctg
     >.....................4-1BBL (aa 71-254).....................>
       l   d   l   r   q   g   m   f   a   q   l   v   a   q   n   v   l

1327 ctg atc gac ggg cca ctg agt tgg tat tcc gat ccc ggc ctg gcc ggc gtg
     >.....................4-1BBL (aa 71-254).....................>
       l   i   d   g   p   l   s   w   y   s   d   p   g   l   a   g   v

1378 tcc ctg acc ggc gga ctg agt tac aaa gag gat aca aaa gaa ctg gtg gtg
     >.....................4-1BBL (aa 71-254).....................>
       s   l   t   g   g   l   s   y   k   e   d   t   k   e   l   v   v
```

```
1429  gca aag gca ggg gtg tac tat gtg ttc ttt cag ctg gaa ctg aga agg gtg
      >.....................4-1BBL (aa 71-254).....................>
        a   k   a   g   v   y   y   v   f   f   q   l   e   l   r   r   v

1480  gtg gcc ggc gag gga agc gga tca gtg tca ctg gca ctg cat ctg cag ccc
      >.....................4-1BBL (aa 71-254).....................>
        v   a   g   e   g   s   g   s   v   s   l   a   l   h   l   q   p

1531  ctg aga tca gct gca ggg gcc gct gcc ctg gcc ctg acc gtg gat ctg ccc
      >.....................4-1BBL (aa 71-254).....................>
        l   r   s   a   a   g   a   a   a   l   a   l   t   v   d   l   p

1582  cca gct tct tct gag gcc cgg aat agt gca ttc ggg ttt caa gga cgc ctg
      >.....................4-1BBL (aa 71-254).....................>
        p   a   s   s   e   a   r   n   s   a   f   g   f   q   g   r   l

1633  ctg cac ctg tcc gct gga cag aga ctg gga gtg cat ctg cat acc gag gct
      >.....................4-1BBL (aa 71-254).....................>
        l   h   l   s   a   g   q   r   l   g   v   h   l   h   t   e   a

1684  cgc gcc aga cat gca tgg cag ctg aca cag ggc gca acc gtg ctg gga ctg
      >.....................4-1BBL (aa 71-254).....................>
        r   a   r   h   a   w   q   l   t   q   g   a   t   v   l   g   l

1735  ttt aga gtg act cca gaa atc ccc gct ggc ctg cct agc cct cgg agc gaa
      >.....................4-1BBL (aa 71-254).....................>>
        f   r   v   t   p   e   i   p   a   g   l   p   s   p   r   s   e

          EcoRI
        -+-----
1786  tga gaa ttc
```

7.4 scOX40L

```
                XbaI
              -+-----
       BamHI
     -+-----
   1  gga tcc tct aga cag gtg tcc cac aga tac ccc aga atc cag agc atc aag
                    >>.............OX40L (aa 51-183).............>
                      q   v   s   h   r   y   p   r   i   q   s   i   k

  52  gtg cag ttc acc gag tac aag aaa gag aag ggc ttc atc ctg acc agc cag
      >.....................OX40L (aa 51-183).....................>
        v   q   f   t   e   y   k   k   e   k   g   f   i   l   t   s   q

 103  aaa gag gac gag atc atg aag gtg cag aac aac agc gtg atc atc aac tgc
      >.....................OX40L (aa 51-183).....................>
        k   e   d   e   i   m   k   v   q   n   n   s   v   i   i   n   c

 154  gac ggc ttc tac ctg atc agc ctg aag ggc tac ttc agc cag gaa gtg aac
      >.....................OX40L (aa 51-183).....................>
        d   g   f   y   l   i   s   l   k   g   y   f   s   q   e   v   n

 205  atc agc ctg cac tac cag aag gac gag gaa ccc ctg ttc cag ctg aag aaa
      >.....................OX40L (aa 51-183).....................>
        i   s   l   h   y   q   k   d   e   e   p   l   f   q   l   k   k
```

```
256  gtg cgg agc gtg aac agc ctg atg gtg gcc agc ctg acc tac aag gac aag
     >.....................OX40L (aa 51-183).....................>
       v   r   s   v   n   s   l   m   v   a   s   l   t   y   k   d   k

307  gtg tac ctg aac gtg acc acc gac aac acc agc ctg gac gac ttc cac gtg
     >.....................OX40L (aa 51-183).....................>
       v   y   l   n   v   t   t   d   n   t   s   l   d   d   f   h   v

358  aac ggc ggc gag ctg atc ctg att cac cag aac ccc ggc gag ttc tgc gtg
     >.....................OX40L (aa 51-183).....................>
       n   g   g   e   l   i   l   i   h   q   n   p   g   e   f   c   v

                  BamHI
                 -+-----
409  ctg ggc gga gga tcc ggc gga gga cag gtg tca cat cgg tat cct aga atc
     >>> OX40L (aa 51-183)
       l
         >>........linker.........>>
           g   g   g   s   g   g   g
                                    >>.......OX40L (aa 51-183).........>
                                      q   v   s   h   r   y   p   r   i

460  cag tct att aag gtg cag ttt aca gag tat aag aaa gaa aaa ggc ttt att
     >.....................OX40L (aa 51-183).....................>
       q   s   i   k   v   q   f   t   e   y   k   k   e   k   g   f   i

511  ctg act tcc cag aaa gaa gat gag att atg aag gtg cag aac aat tcc gtg
     >.....................OX40L (aa 51-183).....................>
       l   t   s   q   k   e   d   e   i   m   k   v   q   n   n   s   v

562  att atc aat tgt gat ggg ttt tat ctg atc tcc ctg aaa gga tac ttt agt
     >.....................OX40L (aa 51-183).....................>
       i   i   n   c   d   g   f   y   l   i   s   l   k   g   y   f   s

613  cag gaa gtg aat att tct ctg cac tat cag aaa gat gaa gaa cct ctg ttc
     >.....................OX40L (aa 51-183).....................>
       q   e   v   n   i   s   l   h   y   q   k   d   e   e   p   l   f

664  cag ctg aaa aaa gtg cgc tcc gtg aac tct ctg atg gtg gct tcc ctg aca
     >.....................OX40L (aa 51-183).....................>
       q   l   k   k   v   r   s   v   n   s   l   m   v   a   s   l   t

715  tac aaa gac aaa gtg tat ctg aat gtg aca aca gat aat acc tcc ctg gat
     >.....................OX40L (aa 51-183).....................>
       y   k   d   k   v   y   l   n   v   t   t   d   n   t   s   l   d

766  gat ttc cat gtg aat ggg ggg gaa ctg att ctg atc cat cag aat cct ggg
     >.....................OX40L (aa 51-183).....................>
       d   f   h   v   n   g   g   e   l   i   l   i   h   q   n   p   g

817  gaa ttt tgt gtg ctg gga ggc ggc tcc gga ggc ggc cag gtg tcc cat agg
     >..............>> OX40L (aa 51-183)
       e   f   c   v   l
                       >>........linker.........>>
                         g   g   g   s   g   g   g
                                 OX40L (aa 51-183) >>..............>
                                                     q   v   s   h   r

868  tat ccc cgc att cag tcc atc aaa gtg cag ttt act gag tac aaa aaa gag
     >.....................OX40L (aa 51-183).....................>
       y   p   r   i   q   s   i   k   v   q   f   t   e   y   k   k   e
```

```
 919  aaa gga ttc att ctg acc tct cag aaa gag gac gaa att atg aag gtg cag
      >.....................OX40L (aa 51-183).....................>
        k   g   f   i   l   t   s   q   k   e   d   e   i   m   k   v   q

 970  aac aac tct gtg atc att aac tgt gat gga ttc tat ctg att agt ctg aaa
      >.....................OX40L (aa 51-183).....................>
        n   n   s   v   i   i   n   c   d   g   f   y   l   i   s   l   k

1021  gga tat ttc agc cag gaa gtg aac att tcc ctg cat tac cag aag gat gaa
      >.....................OX40L (aa 51-183).....................>
        g   y   f   s   q   e   v   n   i   s   l   h   y   q   k   d   e

1072  gaa cca ctg ttc cag ctg aag aaa gtg cgc tct gtg aat agt ctg atg gtg
      >.....................OX40L (aa 51-183).....................>
        e   p   l   f   q   l   k   k   v   r   s   v   n   s   l   m   v

1123  gcc tct ctg act tat aag gat aag gtg tac ctg aat gtg aca act gac aat
      >.....................OX40L (aa 51-183).....................>
        a   s   l   t   y   k   d   k   v   y   l   n   v   t   t   d   n

1174  act tct ctg gac gac ttt cat gtg aac ggg gga gag ctg att ctg atc cac
      >.....................OX40L (aa 51-183).....................>
        t   s   l   d   d   f   h   v   n   g   g   e   l   i   l   i   h

                                                  EcoRI
                                                 -+-----
1225  cag aat cca ggc gag ttc tgt gtg ctg tga gaa ttc g
      >........OX40L (aa 51-183).......>>
        q   n   p   g   e   f   c   v   l
```

7.5 scGITRL

```
                XbaI
              -+-----
       BamHI
      -+-----
   1  gga tcc tct aga cag ctg gaa acc gcc aaa gaa ccc tgc atg gcc aag ttc
                    >>.............hGITRL (aa 72-199).............>
                      q   l   e   t   a   k   e   p   c   m   a   k   f

  52  ggc ccc ctg cct agc aag tgg cag atg gcc tct agc gag ccc ccc tgc gtg
      >.....................hGITRL (aa 72-199).....................>
        g   p   l   p   s   k   w   q   m   a   s   s   e   p   p   c   v

 103  aac aag gtg tcc gac tgg aag ctg gaa atc ctg cag aac ggc ctg tac ctg
      >.....................hGITRL (aa 72-199).....................>
        n   k   v   s   d   w   k   l   e   i   l   q   n   g   l   y   l

 154  atc tac ggc cag gtg gcc ccc aac gcc aac tac aac gat gtg gcc ccc ttc
      >.....................hGITRL (aa 72-199).....................>
        i   y   g   q   v   a   p   n   a   n   y   n   d   v   a   p   f

 205  gaa gtg cgg ctg tac aag aac aag gac atg atc cag acc ctg acc aac aag
      >.....................hGITRL (aa 72-199).....................>
        e   v   r   l   y   k   n   k   d   m   i   q   t   l   t   n   k

 256  agc aag atc cag aac gtg ggc ggc acc tac gag ctg cac gtg ggc gat acc
      >.....................hGITRL (aa 72-199).....................>
        s   k   i   q   n   v   g   g   t   y   e   l   h   v   g   d   t
```

```
307  atc gac ctg atc ttc aac agc gag cac cag gtg ctg aag aac aac acc tac
     >.....................hGITRL (aa 72-199).....................>
       i   d   l   i   f   n   s   e   h   q   v   l   k   n   n   t   y

                                                                 BamHI
                                                                 -+-----
358  tgg ggc atc atc ctg ctg gcc aac ccc cag ttc atc agc gga gga tcc ggc
     >.............hGITRL (aa 72-199).............>>
       w   g   i   i   l   l   a   n   p   q   f   i   s
                                                     >>..linker....>
                                                       g   g   s   g

409  gga ggc gga tct ggc ggc cag ctg gaa aca gct aaa gaa cct tgt atg gct
     >......linker......>>
       g   g   g   s   g   g
                           >>.........hGITRL (aa 72-199).............>
                             q   l   e   t   a   k   e   p   c   m   a

460  aaa ttt ggg cct ctg ccc tcc aaa tgg cag atg gca agc agc gag cct cct
     >.....................hGITRL (aa 72-199).....................>
       k   f   g   p   l   p   s   k   w   q   m   a   s   s   e   p   p

511  tgt gtg aac aaa gtg tct gat tgg aaa ctg gaa atc ctg cag aat ggg ctg
     >.....................hGITRL (aa 72-199).....................>
       c   v   n   k   v   s   d   w   k   l   e   i   l   q   n   g   l

562  tat ctg atc tat gga cag gtg gca cct aat gct aat tac aat gac gtg gca
     >.....................hGITRL (aa 72-199).....................>
       y   l   i   y   g   q   v   a   p   n   a   n   y   n   d   v   a

613  cct ttt gaa gtg cgc ctg tat aag aac aaa gat atg att cag aca ctg aca
     >.....................hGITRL (aa 72-199).....................>
       p   f   e   v   r   l   y   k   n   k   d   m   i   q   t   l   t

664  aac aaa tcc aag att cag aat gtg ggg ggg aca tat gaa ctg cat gtg gga
     >.....................hGITRL (aa 72-199).....................>
       n   k   s   k   i   q   n   v   g   g   t   y   e   l   h   v   g

715  gac aca atc gat ctg att ttc aat tcc gaa cat cag gtg ctg aaa aac aat
     >.....................hGITRL (aa 72-199).....................>
       d   t   i   d   l   i   f   n   s   e   h   q   v   l   k   n   n

766  act tat tgg ggg att att ctg ctg gct aat cct cag ttt atc tcc ggc ggc
     >.................hGITRL (aa 72-199).................>>
       t   y   w   g   i   i   l   l   a   n   p   q   f   i   s
                                                       linker >>....>
                                                                 g   g

817  tct ggg ggc gga ggc tcc gga ggg cag ctg gaa act gca aaa gaa cct tgc
     >..........linker..........>>
       s   g   g   g   g   s   g   g
                                 >>......hGITRL (aa 72-199).......>
                                   q   l   e   t   a   k   e   p   c

868  atg gca aag ttt gga cca ctg cct tct aag tgg cag atg gct tcc tcc gag
     >.....................hGITRL (aa 72-199).....................>
       m   a   k   f   g   p   l   p   s   k   w   q   m   a   s   s   e

919  cca cca tgc gtg aac aaa gtg tca gat tgg aag ctg gaa atc ctg cag aat
     >.....................hGITRL (aa 72-199).....................>
       p   p   c   v   n   k   v   s   d   w   k   l   e   i   l   q   n
```

```
 970  gga ctg tac ctg atc tat ggc cag gtg gca cca aat gcc aac tat aac gac
      >.....................hGITRL (aa 72-199).....................>
        g   l   y   l   i   y   g   q   v   a   p   n   a   n   y   n   d

1021  gtg gcc cct ttt gaa gtg cgg ctg tac aaa aac aag gat atg att cag act
      >.....................hGITRL (aa 72-199).....................>
        v   a   p   f   e   v   r   l   y   k   n   k   d   m   i   q   t

1072  ctg act aac aag tca aaa atc cag aat gtg gga gga act tat gag ctg cac
      >.....................hGITRL (aa 72-199).....................>
        l   t   n   k   s   k   i   q   n   v   g   g   t   y   e   l   h

1123  gtg ggg gac act att gat ctg atc ttt aac tct gag cat cag gtg ctg aaa
      >.....................hGITRL (aa 72-199).....................>
        v   g   d   t   i   d   l   i   f   n   s   e   h   q   v   l   k

1174  aac aac aca tac tgg ggg atc att ctg ctg gca aac cca cag ttt att agc
      >.....................hGITRL (aa 72-199).....................>>
        n   n   t   y   w   g   i   i   l   l   a   n   p   q   f   i   s

          EcoRI
        -+-----
1225  tga gaa ttc
```

7.6 msc4-1BBL

```
                XbaI
              -+-----
       BamHI
      -+-----
   1  gga tcc tct aga agg acc gag cca cgg ccc gcc ctc acc atc acc acc agc
                   >>............m4-1BBL (aa 104-309).............>
                     r   t   e   p   r   p   a   l   t   i   t   t   s

  52  cct aac ctg ggc acc aga gag aac aac gcc gac caa gtg acc ccc gtg tcc
      >.....................m4-1BBL (aa 104-309).....................>
        p   n   l   g   t   r   e   n   n   a   d   q   v   t   p   v   s

 103  cac atc ggc tgc cct aac aca aca cag cag ggc agc ccc gtg ttc gcc aag
      >.....................m4-1BBL (aa 104-309).....................>
        h   i   g   c   p   n   t   t   q   q   g   s   p   v   f   a   k

 154  ctg ctg gct aag aac cag gcc agc ctg tgc aac acc acc ctg aac tgg cac
      >.....................m4-1BBL (aa 104-309).....................>
        l   l   a   k   n   q   a   s   l   c   n   t   t   l   n   w   h

 205  agc cag gac ggc gct ggc agc agc tat ctg agc cag ggc ctg aga tac gag
      >.....................m4-1BBL (aa 104-309).....................>
        s   q   d   g   a   g   s   s   y   l   s   q   g   l   r   y   e

 256  gaa gat aag aaa gaa ctg gtg gtg gac agc cct ggc ctg tac tac gtg ttc
      >.....................m4-1BBL (aa 104-309).....................>
        e   d   k   k   e   l   v   v   d   s   p   g   l   y   y   v   f

 307  ctg gaa ctg aag ctg agc ccc acc ttc acc aac acc ggc cac aag gtg cag
      >.....................m4-1BBL (aa 104-309).....................>
        l   e   l   k   l   s   p   t   f   t   n   t   g   h   k   v   q

 358  ggc tgg gtg tca ctg gtg ctg cag gct aag cct cag gtg gac gac ttc gac
      >.....................m4-1BBL (aa 104-309).....................>
        g   w   v   s   l   v   l   q   a   k   p   q   v   d   d   f   d
```

```
409  aac ctg gcc ctg aca gtg gaa ctg ttc ccc tgc agc atg gaa aac aag ctg
     >.....................m4-1BBL (aa 104-309).....................>
       n   l   a   l   t   v   e   l   f   p   c   s   m   e   n   k   l

460  gtg gat aga agc tgg tcc cag ctc ctg ctg ctg aag gct ggc cac aga ctg
     >.....................m4-1BBL (aa 104-309).....................>
       v   d   r   s   w   s   q   l   l   l   l   k   a   g   h   r   l

511  agc gtg ggc ctg agg gct tat ctg cac ggc gcc cag gac gcc tac aga gac
     >.....................m4-1BBL (aa 104-309).....................>
       s   v   g   l   r   a   y   l   h   g   a   q   d   a   y   r   d

562  tgg gag ctg agc tac ccc aac aca acc agc ttc ggc ctg ttc ctc gtg aaa
     >.....................m4-1BBL (aa 104-309).....................>
       w   e   l   s   y   p   n   t   t   s   f   g   l   f   l   v   k

613  cct gat aat ccc tgg gag ggc ggc gga gga agc gga ggc gga ggg tcc ggc
     >.....................>> m4-1BBL (aa 104-309)
       p   d   n   p   w   e
                           >>.................linker..................>
                             g   g   g   g   s   g   g   g   g   s   g

664  gga ggg gga tct ggg gga ggc gga tca aga aca gaa cct aga cct gct ctg
     >.............linker.............>>
       g   g   g   s   g   g   g   g   s
                                       >>...m4-1BBL (aa 104-309).....>
                                         r   t   e   p   r   p   a   l

715  acc atc acc acc agc cct aac ctg ggc acc aga gag aac aac gcc gac caa
     >.....................m4-1BBL (aa 104-309).....................>
       t   i   t   t   s   p   n   l   g   t   r   e   n   n   a   d   q

766  gtg acc ccc gtg tcc cac atc ggc tgc cct aac aca aca cag cag ggc agc
     >.....................m4-1BBL (aa 104-309).....................>
       v   t   p   v   s   h   i   g   c   p   n   t   t   q   q   g   s

817  ccc gtg ttc gcc aag ctg ctg gct aag aac cag gcc agc ctg tgc aac acc
     >.....................m4-1BBL (aa 104-309).....................>
       p   v   f   a   k   l   l   a   k   n   q   a   s   l   c   n   t

868  acc ctg aac tgg cac agc cag gac ggc gct ggc agc agc tat ctg agc cag
     >.....................m4-1BBL (aa 104-309).....................>
       t   l   n   w   h   s   q   d   g   a   g   s   s   y   l   s   q

919  ggc ctg aga tac gag gaa gat aag aaa gaa ctg gtg gtg gac agc cct ggc
     >.....................m4-1BBL (aa 104-309).....................>
       g   l   r   y   e   e   d   k   k   e   l   v   v   d   s   p   g

970  ctg tac tac gtg ttc ctg gaa ctg aag ctg agc ccc acc ttc acc aac acc
     >.....................m4-1BBL (aa 104-309).....................>
       l   y   y   v   f   l   e   l   k   l   s   p   t   f   t   n   t

1021 ggc cac aag gtg cag ggc tgg gtg tca ctg gtg ctg cag gct aag cct cag
     >.....................m4-1BBL (aa 104-309).....................>
       g   h   k   v   q   g   w   v   s   l   v   l   q   a   k   p   q

1072 gtg gac gac ttc gac aac ctg gcc ctg aca gtg gaa ctg ttc ccc tgc agc
     >.....................m4-1BBL (aa 104-309).....................>
       v   d   d   f   d   n   l   a   l   t   v   e   l   f   p   c   s
```

```
1123  atg gaa aac aag ctg gtg gat aga agc tgg tcc cag ctc ctg ctg ctg aag
      >.....................m4-1BBL (aa 104-309).....................>
        m   e   n   k   l   v   d   r   s   w   s   q   l   l   l   l   k

1174  gct ggc cac aga ctg agc gtg ggc ctg agg gct tat ctg cac ggc gcc cag
      >.....................m4-1BBL (aa 104-309).....................>
        a   g   h   r   l   s   v   g   l   r   a   y   l   h   g   a   q

1225  gac gcc tac aga gac tgg gag ctg agc tac ccc aac aca acc agc ttc ggc
      >.....................m4-1BBL (aa 104-309).....................>
        d   a   y   r   d   w   e   l   s   y   p   n   t   t   s   f   g

1276  ctg ttc ctc gtg aaa cct gat aat ccc tgg gag ggg ggg gga ggc tct ggc
      >.........m4-1BBL (aa 104-309).........>>
        l   f   l   v   k   p   d   n   p   w   e
                                              >>......linker........>
                                                g   g   g   g   s   g

1327  gga ggc ggc tcc gga ggg ggc gga tct ggc ggg gga ggc agt aga aca gaa
      >.....................linker.....................>>
        g   g   g   s   g   g   g   g   s   g   g   g   g   s
                                    m4-1BBL(aa 104-309) >>........>
                                                          r   t   e

1378  cct aga cct gct ctg acc atc acc acc agc cct aac ctg ggc acc aga gag
      >.....................m4-1BBL(aa 104-309).....................>
        p   r   p   a   l   t   i   t   t   s   p   n   l   g   t   r   e

1429  aac aac gcc gac caa gtg acc ccc gtg tcc cac atc ggc tgc cct aac aca
      >.....................m4-1BBL(aa 104-309).....................>
        n   n   a   d   q   v   t   p   v   s   h   i   g   c   p   n   t

1480  aca cag cag ggc agc ccc gtg ttc gcc aag ctg ctg gct aag aac cag gcc
      >.....................m4-1BBL(aa 104-309).....................>
        t   q   q   g   s   p   v   f   a   k   l   l   a   k   n   q   a

1531  agc ctg tgc aac acc acc ctg aac tgg cac agc cag gac ggc gct ggc agc
      >.....................m4-1BBL(aa 104-309).....................>
        s   l   c   n   t   t   l   n   w   h   s   q   d   g   a   g   s

1582  agc tat ctg agc cag ggc ctg aga tac gag gaa gat aag aaa gaa ctg gtg
      >.....................m4-1BBL(aa 104-309).....................>
        s   y   l   s   q   g   l   r   y   e   e   d   k   k   e   l   v

1633  gtg gac agc cct ggc ctg tac tac gtg ttc ctg gaa ctg aag ctg agc ccc
      >.....................m4-1BBL(aa 104-309).....................>
        v   d   s   p   g   l   y   y   v   f   l   e   l   k   l   s   p

1684  acc ttc acc aac acc ggc cac aag gtg cag ggc tgg gtg tca ctg gtg ctg
      >.....................m4-1BBL(aa 104-309).....................>
        t   f   t   n   t   g   h   k   v   q   g   w   v   s   l   v   l



1735  cag gct aag cct cag gtg gac gac ttc gac aac ctg gcc ctg aca gtg gaa
      >.....................m4-1BBL(aa 104-309).....................>
        q   a   k   p   q   v   d   d   f   d   n   l   a   l   t   v   e

1786  ctg ttc ccc tgc agc atg gaa aac aag ctg gtg gat aga agc tgg tcc cag
      >.....................m4-1BBL(aa 104-309).....................>
        l   f   p   c   s   m   e   n   k   l   v   d   r   s   w   s   q
```

```
1837  ctc ctg ctg ctg aag gct ggc cac aga ctg agc gtg ggc ctg agg gct tat
      >.....................m4-1BBL(aa 104-309).....................>
        l   l   l   l   k   a   g   h   r   l   s   v   g   l   r   a   y

1888  ctg cac ggc gcc cag gac gcc tac aga gac tgg gag ctg agc tac ccc aac
      >.....................m4-1BBL(aa 104-309).....................>
        l   h   g   a   q   d   a   y   r   d   w   e   l   s   y   p   n

1939  aca acc agc ttc ggc ctg ttc ctc gtc aag ccc gac aac cct tgg gag taa
      >.....................m4-1BBL(aa 104-309).....................>>
        t   t   s   f   g   l   f   l   v   k   p   d   n   p   w   e

       EcoRI
      -+-----
1990  gaa ttc
```

7.7 mscGITRL

```
               XbaI
             -+-----
       BamHI
      -+-----
   1  gga tcc tct aga atc gag agc tgc atg gtc aag ttc gag ctg agc agc agc
                    >>..............mGITRL (aa 49-173).................>
                      i   e   s   c   m   v   k   f   e   l   s   s   s
      >....>> linker
        g   s

  52  aag tgg cac atg acc agc ccc aag ccc cac tgc gtg aac acc acc tcc gac
      >.....................mGITRL (aa 49-173).....................>
        k   w   h   m   t   s   p   k   p   h   c   v   n   t   t   s   d

 103  ggc aag ctg aag atc ctg cag agc ggc acc tac ctg atc tac ggc caa gtg
      >.....................mGITRL (aa 49-173).....................>
        g   k   l   k   i   l   q   s   g   t   y   l   i   y   g   q   v

 154  atc ccc gtg gac aag aag tac atc aag gac aac gcc ccc ttc gtg gtg caa
      >.....................mGITRL (aa 49-173).....................>
        i   p   v   d   k   k   y   i   k   d   n   a   p   f   v   v   q

 205  atc tac aag aaa aac gac gtg ctg cag acc ctg atg aac gac ttc cag atc
      >.....................mGITRL (aa 49-173).....................>
        i   y   k   k   n   d   v   l   q   t   l   m   n   d   f   q   i

 256  ctg ccc atc ggc ggc gtg tac gaa ctg cac gcc ggc gac aac atc tac ctg
      >.....................mGITRL (aa 49-173).....................>
        l   p   i   g   g   v   y   e   l   h   a   g   d   n   i   y   l

 307  aag ttc aac agc aag gac cac atc cag aaa aca aac acc tac tgg ggc atc
      >.....................mGITRL (aa 49-173).....................>
        k   f   n   s   k   d   h   i   q   k   t   n   t   y   w   g   i

                                                                 BamHI
                                                                -+----
 358  atc ctg atg ccc gac ctg ccc ttc atc agc ggc gga gga agt ggc gga gga
      >.........mGITRL (aa 49-173).........>>
        i   l   m   p   d   l   p   f   i   s
                                          >>........linker..........>
                                            g   g   g   s   g   g   g
```

```
409  tcc ggg gga gga tct ggc ggc gga agc gga ggc gga tct atc gag tcc tgc
     >.....................linker.....................>>
       s   g   g   g   s   g   g   g   s   g   g   g   s
                                    mGITRL (aa 49-173) >>.....>
                                                         i   e   s   c

460  atg gtc aaa ttc gaa ctg tcc agc tct aag tgg cat atg act tcc cca aag
     >.....................mGITRL (aa 49-173).....................>
       m   v   k   f   e   l   s   s   s   k   w   h   m   t   s   p   k

511  cct cat tgt gtg aat acc acc agt gat ggg aag ctg aaa att ctg cag tct
     >.....................mGITRL (aa 49-173).....................>
       p   h   c   v   n   t   t   s   d   g   k   l   k   i   l   q   s

562  ggg aca tat ctg atc tat gga caa gtg att cct gtg gat aag aag tat att
     >.....................mGITRL (aa 49-173).....................>
       g   t   y   l   i   y   g   q   v   i   p   v   d   k   k   y   i

613  aag gat aac gct cct ttt gtg gtg caa atc tac aaa aag aat gat gtg ctg
     >.....................mGITRL (aa 49-173).....................>
       k   d   n   a   p   f   v   v   q   i   y   k   k   n   d   v   l

664  cag aca ctg atg aat gat ttt cag att ctg cct att ggg ggg gtg tac gag
     >.....................mGITRL (aa 49-173).....................>
       q   t   l   m   n   d   f   q   i   l   p   i   g   g   v   y   e

715  ctg cat gct ggg gat aat atc tat ctg aaa ttc aat tcc aag gat cat att
     >.....................mGITRL (aa 49-173).....................>
       l   h   a   g   d   n   i   y   l   k   f   n   s   k   d   h   i

766  cag aaa act aat act tat tgg ggg att att ctg atg cct gat ctg cct ttt
     >.....................mGITRL (aa 49-173).....................>
       q   k   t   n   t   y   w   g   i   i   l   m   p   d   l   p   f

                EcoRI
               -+-----
817  atc tcc tga gaa ttc
     >....>> mGITRL (aa 49-173)
       i   s
```

7.8 scFv$_{CEA}$

```
           XhoI
         --+-----
  1  aac cgc tcg agc gga ggc ggt tca cag gtg aaa ctg cag cag tct ggg gca
                                  >>.............VH_CEA.............>
                                    q   v   k   l   q   q   s   g   a

 52  gaa ctt gtg agg tca ggg acc tca gtc aag ttg tcc tgc aca gct tct ggc
     >..............................VH_CEA..............................>
       e   l   v   r   s   g   t   s   v   k   l   s   c   t   a   s   g

103  ttc aac att aaa gac tcc tat atg cac tgg ttg agg cag ggg cct gaa cag
     >..............................VH_CEA..............................>
       f   n   i   k   d   s   y   m   h   w   l   r   q   g   p   e   q

154  ggc ctg gag tgg att gga tgg att gat cct gag aat ggt gat act gaa tat
     >..............................VH_CEA..............................>
       g   l   e   w   i   g   w   i   d   p   e   n   g   d   t   e   y
```

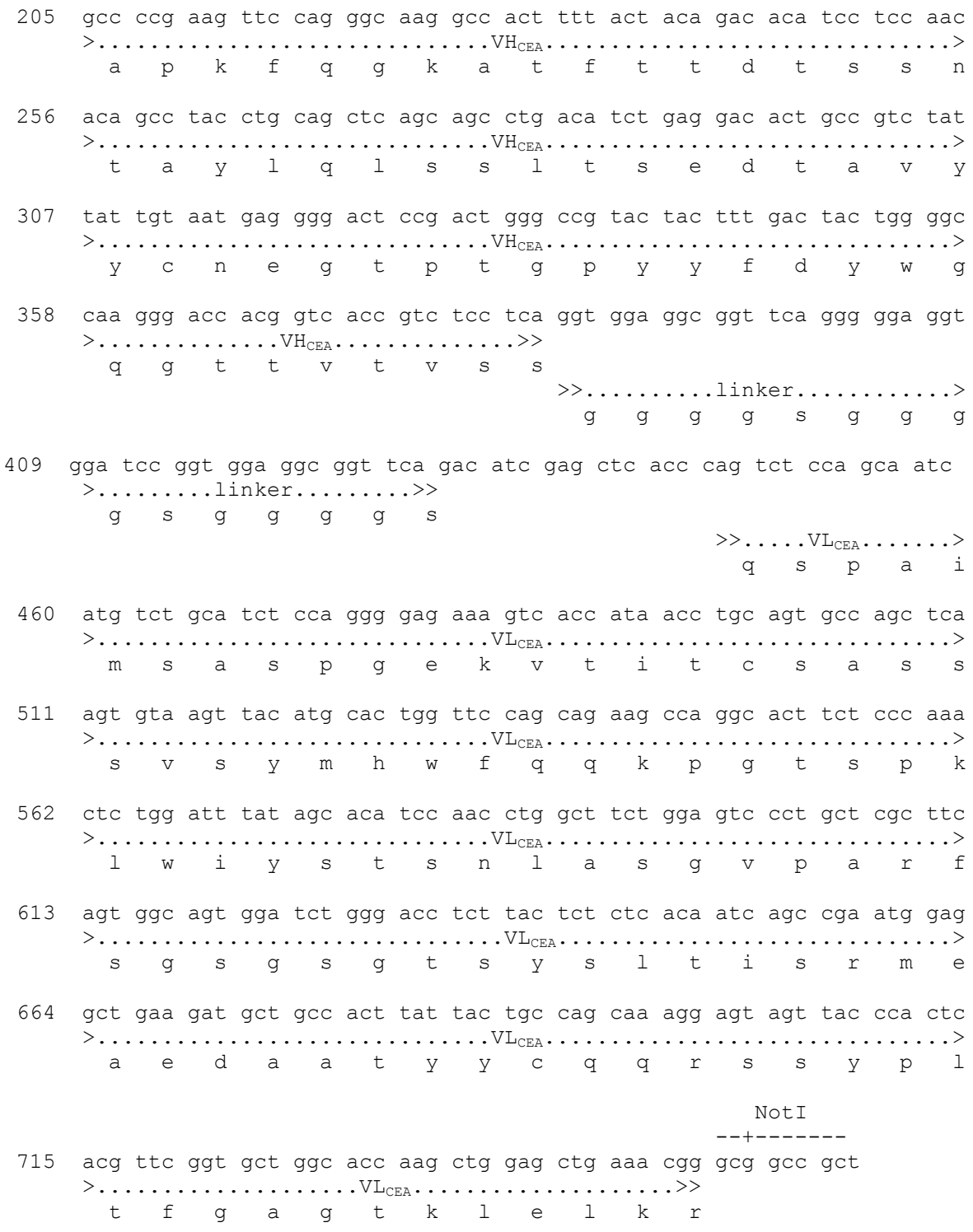
205 gcc ccg aag ttc cag ggc aag gcc act ttt act aca gac aca tcc tcc aac
VHCEA
a p k f q g k a t f t t d t s s n
256 aca gcc tac ctg cag ctc agc agc ctg aca tct gag gac act gcc gtc tat
VHCEA
t a y l q l s s l t s e d t a v y
307 tat tgt aat gag ggg act ccg act ggg ccg tac tac ttt gac tac tgg ggc
VHCEA
y c n e g t p t g p y y f d y w g
358 caa ggg acc acg gtc acc gtc tcc tca ggt gga ggc ggt tca ggg gga ggt
VHCEA
q g t t v t v s s
linker
g g g g s g g g
409 gga tcc ggt gga ggc ggt tca gac atc gag ctc acc cag tct cca gca atc
linker
g s g g g g s
VLCEA
q s p a i
460 atg tct gca tct cca ggg gag aaa gtc acc ata acc tgc agt gcc agc tca
VLCEA
m s a s p g e k v t i t c s a s s
511 agt gta agt tac atg cac tgg ttc cag cag aag cca ggc act tct ccc aaa
VLCEA
s v s y m h w f q q k p g t s p k
562 ctc tgg att tat agc aca tcc aac ctg gct tct gga gtc cct gct cgc ttc
VLCEA
l w i y s t s n l a s g v p a r f
613 agt ggc agt gga tct ggg acc tct tac tct ctc aca atc agc cga atg gag
VLCEA
s g s g s g t s y s l t i s r m e
664 gct gaa gat gct gcc act tat tac tgc cag caa agg agt agt tac cca ctc
VLCEA
a e d a a t y y c q q r s s y p l
NotI
715 acg ttc ggt gct ggc acc aag ctg gag ctg aaa cgg gcg gcc gct
VLCEA
t f g a g t k l e l k r

7.9 scFv$_{EGFR}$

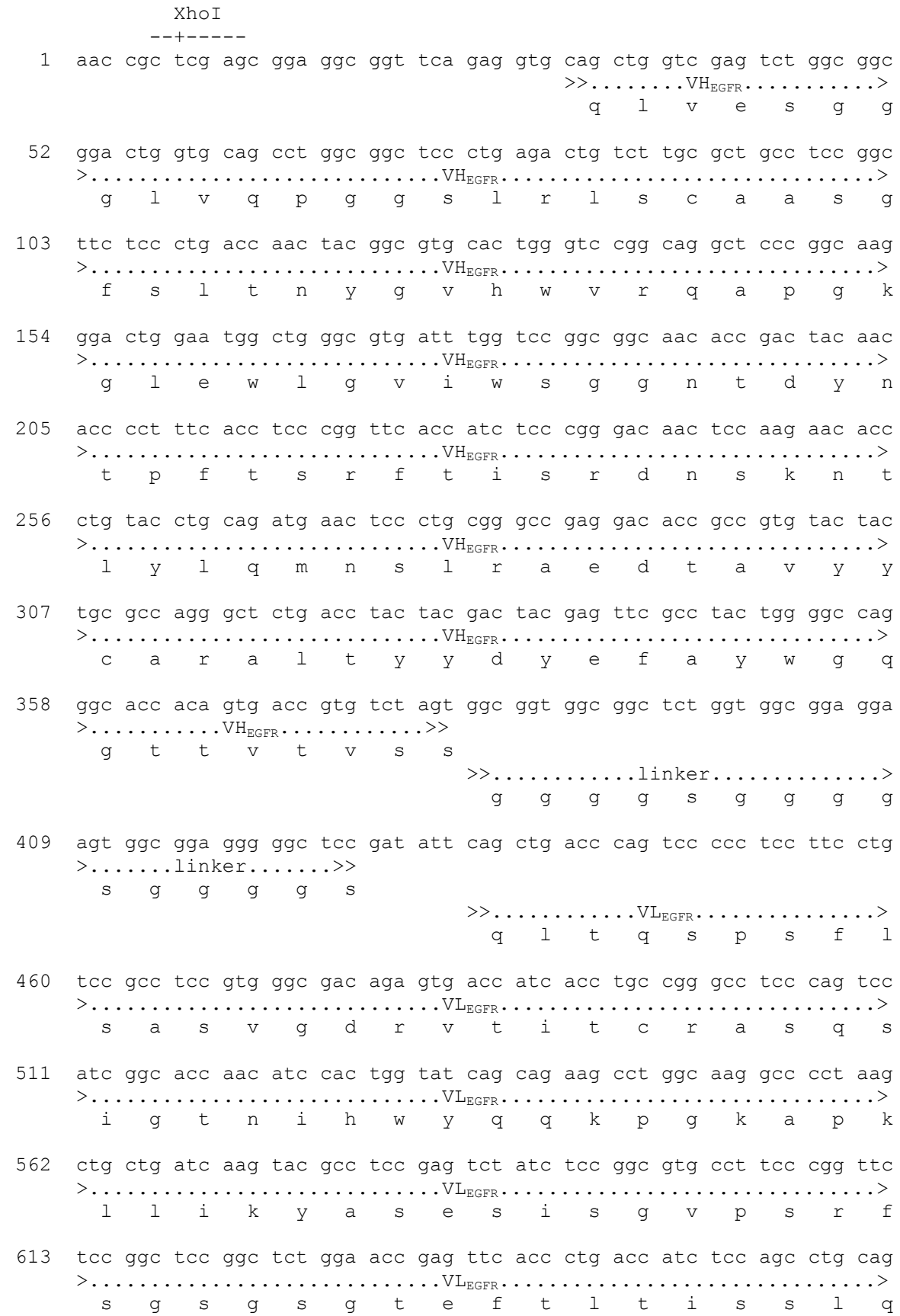

```
664  cct gag gac ttc gcc acc tac tac tgc cag cag aac aac aac tgg cct acc
     >.............................VL_EGFR.................................>
       p   e   d   f   a   t   y   y   c   q   q   n   n   n   w   p   t

                                                          NotI
                                                        --+-------
715  acc ttc ggc gct ggc acc aag ctg gaa atc aag aga gcg gcc gct
     >.................VL_EGFR..................>>
       t   f   g   a   g   t   k   l   e   i   k
```

List of Figures

Figure 1: Common γ-chain receptor family. 13
Figure 2: Costimulatory and co-inhibitory signaling at the immune synapse...... 18
Figure 3: Biochemical characterization of bifunctional antibody-fusion proteins...... 57
Figure 4: Binding properties of antibody-fusion proteins with 4-1BBL analyzed in flow cytometry...... 59
Figure 5: Costimulatory activity of scFv-ligand fusion proteins in target-bound (A) or non-target bound (B) form. 60
Figure 6: Biochemical characterization of trifunctional fusion proteins.. 62
Figure 7: Binding properties of trifunctional fusion proteins. 63
Figure 8: Activity of trifunctional fusion protein in target bound (A and C) or non-target bound (B) form on PBMC proliferation and cytokine release. 64
Figure 9: Characterization of the trifunctional fusion proteins applied in the *in vivo* mouse model. 66
Figure 10: Antitumoral activity of trifunctional fusion protein *in vivo*. 68
Figure 11: Biochemical characterization of bi- and trifunctional fusion proteins with different scTNFSF ligands. 69
Figure 12: Binding properties of bi- and trifunctional antibody-fusion proteins..... 72
Figure 13: Plasma stability of fusion proteins.. 73
Figure 14: Effect of non-targeted trifunctional fusion proteins on proliferation of PBMCs and proliferation of CTLL-2 cells...... 75
Figure 16: Bifunctional fusion protein mediated effect on proliferation and composition of T cell subpopulations...... 76
Figure 17: Trifunctional fusion protein induced effect on proliferation and composition of T cell subpopulations...... 77
Figure 18: Activity of targeted combined bi- and trifunctional antibody-fusion proteins on the proliferation of T cells and NK cells. 79
Figure 19: Effect of targeted bi-and trifunctional antibody-fusion proteins on the cytotoxic potential of $CD4^+$ and $CD8^+$ T cells. 80
Figure 20: Effect of targeted trifunctional antibody-fusion proteins on regulatory T cells. 81
Figure 21: Biochemical characterization of bi- and trifunctional fusion proteins with RD_IL-15 and murine scGITRL.. 83

Figure 22: Functional characterization of the fusion proteins to be used in the *in vivo* mouse model.. 84
Figure 23: Antitumoral activity of bi- and trifunctional fusion protein in a syngeneic lung metastases tumor mouse model. 85
Figure 24: *In vivo* activity of RD_IL-15_scFv$_{FAP}$_mscGITRL in a syngeneic solid tumor mouse model. 87
Figure 25: **Analysis of immune cell infiltration into solid tumors after fusion protein treatment.** 88
Figure 26: Analysis of immune cells in the spleen. 89
Figure 27: Biochemical characterization of EGFR-directed antibody-fusion proteins with sc4-1BBL. 90
Figure 28: Binding properties of fusion proteins targeting EGFR.. 91
Figure 29: Effect of non-targeted trifunctional fusion proteins on the proliferation of CTLL-2 cells and PBMCs. 92
Figure 30: Targeted fusion protein mediated enhancement of T cell stimulation. 93
Figure 31: Fusion protein mediated stimulation of proliferation of NK cells.. 94
Figure 32: Fusion protein mediated enhancement on ADCC of Trastuzumab.. 95

List of Tables

Table 1: Immunomodulatory antibodies for cancer therapy either approved or in ongoing clinical trials. 9

Table 2: Antibodies used in this study. 29

Table 3: Cell lines used in this study. 33

Table 4: Primers for cloning. 36

Table 5: Identification of leucocyte subpopulations. 47

Table 6: Biochemical characterization of the bifunctional antibody-fusion proteins with 4-1BBL. 58

Table 7: Biochemical characterization of the trifunctional antibody-fusion proteins. 62

Table 8: Characterization of trifunctional fusion proteins for *in vivo* study. 67

Table 9: Characterization of bi- and trifunctional fusion proteins with sc4-1BBL, scOX40L and scGITRL. 71

Table 10: Biochemical characterization of the antibody-fusion proteins for animal studies. 83

Table 11: Characterization of bi- and trifunctional fusion proteins targeting EGFR. 90

Declaration

I hereby declare that I performed and wrote this thesis independent from further help or other materials than stated.

Erklärung

Hiermit erkläre ich, dass die vorgelegte Dissertation von mir persönlich und ohne Zuhilfenahme anderer Unterstützung oder Materialien als den angegebenen durchgeführt und geschrieben wurde.

Nadine Beha

Stuttgart den 21.01.2019

Danksagung

Allen voran gilt mein Dank meinem Doktorvater Prof. Dr. Roland Kontermann und meiner Betreuerin PD Dr. Dafne Müller für die allzeit hervorragende Betreuung während meiner Doktorarbeit, die vielen hilfreichen Diskussionen und Anregungen, motivierende Worte, für eure Unterstützung und euer Vertrauen in meine Arbeit. Danke, dass ich in den letzten Jahren Teil dieser beider Forschungsgruppen sein durfte und es immer noch sein darf.

Herzlichen Dank an Prof. Dr. Thomas Kufer für die Übernahme des Zweitgutachtens dieser Arbeit.

Besonderer Dank gilt meinen Kollegen Dr. Oliver Seifert, Dr. Fabian Richter und Alexander Rau sowie allen “Kontermännern” und “Honkies” für die tolle gemeinsame Zeit. Lieber Oli, lieber Fabi, lieber Alex, danke für eure Unterstützung, auch in schwierigen Zeiten. Danke, dass wir in der Vergangenheit ein tolles Team waren und immer noch sind und natürlich für die wundervolle Zeit die wir gemeinsam hatten und sicher noch haben werden. Wir haben uns als Kollegen kennengelernt und sind zu Freunden geworden.
Zudem danke ich Sabrina Sapski und Sarah Ring für die Einarbeitung in die Methoden und die vielen hilfreichen Tipps. Außerdem möchte ich den TAs Nadine Heidel, Elke Gerlach und Doris Göttsch sowie den Tierpflegerinnen Beatrice Reiser und Alexandra Kraske für ihre Unterstützung danken.

An dieser Stelle möchte ich mich bei den wichtigsten Personen bedanken. Danke an meine Eltern. Danke für eure Unterstützung und euren Glauben an mich. Danke an Tanja für 16 wundervolle Jahre Freundschaft in denen du nie den Glauben an mich verloren hast und immer für mich da warst. Der größte Dank geht an den Mann an meiner Seite. Danke Sascha, für deine immerwährende, bedingungslose Unterstützung, für dein Verständnis, deine Geduld und deinen Glauben an mich. Ohne dich würde es diese Arbeit nicht geben.

Conference contributions and publications

Conference contributions, trainings and workshops

10/2018	*European Antibody Congress 2018* | poster presentation
04/2018	3rd *Immuno-Oncology Summit Europe* | poster presentation
05/2016	*15th CIMT Annual Meeting* | poster presentation
03/2016	Training for the handling of laboratory animals (GV-SOLAS, FELASA B)

Publications

2018	Siegemund M, **Beha N**, Müller D. Production, Purification, and Characterization of Antibody-TNF Superfamily Ligand Fusion Proteins. *Methods in molecular biology*. 2018; 1827:351-364.
2017	Sapski S, **Beha N**, Kontermann RE, Müller D. Tumor-targeted costimulation with antibody-fusion proteins improves bispecific antibody-mediated immune response in presence of immunosuppressive factors. *Oncoimmunology*. 2017 Aug 17;6(12):e1361594.
2016	Fellermeier S, **Beha N**, Meyer JE, Ring S, Bader S, Kontermann RE, Müller D. Advancing targeted co-stimulation with antibody-fusion proteins by introducing TNF superfamily members in a single-chain format. *Oncoimmunology*. 2016 Sep 27;5(11): e1238540.